2SGT2019

2nd SEMINAR
ON TRANSPORTATION
GEOTECHNICS

SOIL IMPROVEMENT CHALLENGES ON ALLUVIAL ZONES

28-29 January 2019
Vila Franca de Xira, Portugal

Presentations e-Book

Volume 1

Edited by

Alexandre Pinto, António A. Cristóvão, António Alberto Correia,
António Gomes Correia, Baldomiro Xavier, Eduardo Fortunato,
Isabel Pinto, Jorge Barros, José Luis Antunes,
José Mateus de Brito, José Neves, Madalena Barroso,
Pedro Guedes Melo, Rui Tomásio, Vieira Simões

Organization

Sociedade Portuguesa de Geotecnia

CPGT
Comissão Portugues de Geotecnia nos Transportes

igs Portugal
Comissão Portuguesa de Geossintéticos

vfx Ligações Fortes
CÂMARA MUNICIPAL

Support

ORDEM DOS ENGENHEIROS

LNEC LABORATÓRIO NACIONAL DE ENGENHARIA CIVIL

2nd Seminar on Transportation Geotechnics
28-29 January 2019 | Vila Franca de Xira | Portugal

Soil Improvement Challenges on Alluvial Zones

Volume 1

ISBN 978-989-54038-2-0
DOI: http://doi.org/10.24849/spg.cpgt.2019.02

ORGANIZATION

Sociedade Portuguesa de Geotecnia

Comissão Portuguesa de Geotecnia nos Transportes

Comissão Portuguesa de Geossintéticos

SUPPORT

LABORATÓRIO NACIONAL DE ENGENHARIA CIVIL

ORDEM DOS ENGENHEIROS

SOIL IMPROVEMENT CHALLENGES ON ALLUVIAL ZONES

2nd Seminar on Transportation Geotechnics
28-29 January 2019 | Vila Franca de Xira | Portugal

Venue

Fábrica das Palavras da Biblioteca de Vila Franca de Xira, Portugal

Website

https://cpgtspg.wixsite.com/02sgt2019

Editors

Organized by

Portuguese Commission on Transportation Geotechnics (CPGT)
Portuguese Chapter of International of Geosynthetics Society (IGS Portugal)
Portuguese Geotechnical Society (SPG)
Câmara Municipal de Vila Franca de Xira

SOIL IMPROVEMENT CHALLENGES ON ALLUVIAL ZONES

2nd Seminar on Transportation Geotechnics
28-29 January 2019 | Vila Franca de Xira | Portugal

PRESENTATIONS e-BOOK

Published by
Sociedade Portuguesa de Geotecnia
Laboratório Nacional de Engenharia Civil, Avenida do Brasil, 101, 1700-066 Lisboa, Portugal
Phone: +351.218.443.859
Fax: +351.218.443.021
Email: spg@lnec.pt

Text and design: José Neves
Credits for photo of the cover: Câmara Municipal de Vila Franca de Xira, Portugal

SOIL IMPROVEMENT CHALLENGES ON ALLUVIAL ZONES

2nd Seminar on Transportation Geotechnics
28-29 January 2019 | Vila Franca de Xira | Portugal

PRESENTATIONS e-BOOK

SOIL IMPROVEMENT CHALLENGES ON ALLUVIAL ZONES

2nd Seminar on Transportation Geotechnics
28-29 January 2019 | Vila Franca de Xira | Portugal

PRESENTATIONS e-BOOK

Preface

Significant advances in soil improvement and reinforcement methods are expected in the near future to meet the challenges that the increasingly demanding market poses, in particular as regards both efficiency and speed of control of costs. Regarding the importance of ensuring the best practices in the indispensable soil improvement works, which will certainly be included in the investments planned in the country in transport infrastructures, this seminar intends to present the most recent national and international experience of geotechnical solutions for soil improvement in the field of road, rail, airport and maritime-port infrastructures, focusing on the experience acquired in the execution and observation of work cases in conjunction with recent developments of innovative techniques and with greater sustainability.

The editors
Alexandre Pinto, António A. Cristóvão, António Alberto Correia, António Gomes Correia,
Baldomiro Xavier, Eduardo Fortunato, Isabel Pinto, Jorge Barros, José Luis Antunes,
José Mateus de Brito, José Neves, Madalena Barroso, Pedro Guedes Melo, Rui Tomásio, Vieira Simões

SPONSORS
Gold

Cofra

HUESKER
Ideas. Ingenieros. Innovación.

EP ENGENHARIA - GEOTECNIA

TENCATE GEOSYNTHETICS

GEOSIN GEOSYNTHETICS

Propex GEOSOLUTIONS

RODIO

SPONSORS
Silver

BIU INTERNACIONAL

coba GROUP

DIACLASE

fase ESTUDOS E PROJECTOS, S.A.

Geoárea Consultores de Geotecnia e Ambiente

JET SJ

KELLER

MOTAENGIL ENGENHARIA

nrv | norvia CONSULTORES DE ENGENHARIA, S.A.

QUADRANTE

Santander UNIVERSIDADES

TERRATEST, S.A.

tpf

Seth

TEIXEIRA DUARTE

tgeotecnia na génese da construção

Opening ceremony

Opening ceremony

Audience

Technical exibition

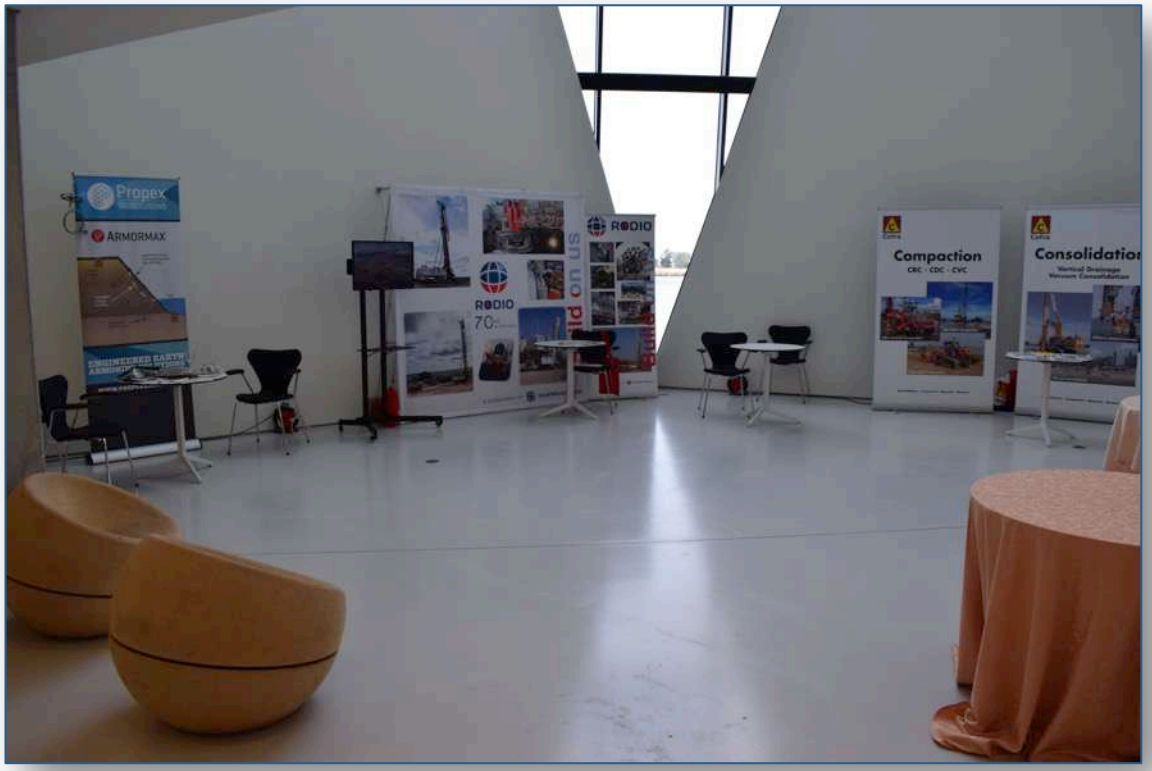

Technical visit

Organizing Committee

CONTENTS

MODULE I - The Problem of Soil Improvement. The Portuguese Experience

I.1 Soft silt-clayey alluvions of Portugal - parameterization for the design of geotechnical structures 17
Elisabete Esteves (ISEP)

I.2 Innovative solutions to mitigate Earthquake Induced soil Liquefaction Damages (EILD) 54
António Viana da Fonseca (FEUP)

I.3 Foundation Strengthening of Stilling Basin 7E of Crestuma-lever Dam 119
Laura Caldeira (LNEC)

I.4 Stabilization of Highway Embankment Over Soft Soils 175
Rui Tomásio, Alexandre Pinto (JETSJ)

I.5 Soil Treatment with Jet-Grouting Associated to Retaining Structures of the Machico-Caniçal Expressway in Madeira Island 199
Carlos Oliveira Baião (TPF); Miguel Menezes Conceição (TPF); Vitória Conceição Rodrigues (TPF); José Mateus de Brito (TPF)

I.6 *Ground improvment solutions at Myriad Sana Vasco da Gama Hotel* 263
João Falcão (TECNASOL)

I.7 Soil improvement by precast driven pile rigid inclusions for embankments on very soft soils 308
Rafael Gil (RODIO)

I.8 Landfills on soft soils. One or two layers of geogrids. Influence modulus of elasticity of the geogrid. Success and failure cases 324
Jesús Ignacio Diego Pereda (U. NAVARRA e HUESKER)

MODULE I
The Problem of Soil Improvement
The Portuguese Experience

ORGANIZATION

Sociedade Portuguesa de Geotecnia

Comissão Portuguesa de Geotecnia nos Transportes

Comissão Portuguesa de Geossintéticos

SUPPORT

LABORATÓRIO NACIONAL DE ENGENHARIA CIVIL

ORDEM DOS ENGENHEIROS

Aluviões Silto-Argilosos Moles de Portugal

Parametrização para o Dimensionamento de Estruturas Geotécnicas

Elisabete Costa Esteves

ISEP, Porto, Portugal

Organização apresentação

- PORQUÊ?
- PROPOSTA DE PARAMETRIZAÇÃO
  - PARÂMETROS FÍSICOS E DE IDENTIFICAÇÃO
  - PARÂMETROS DE COMPRESSIBILIDADE
  - PARÂMETROS DE RESISTÊNCIA

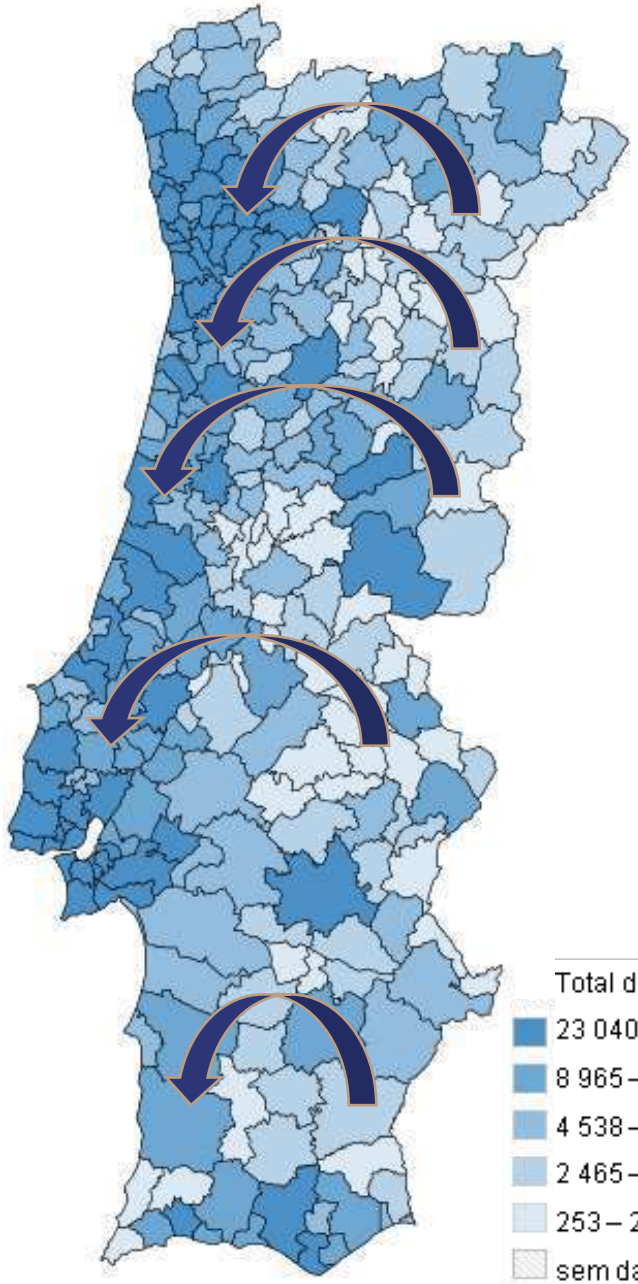

migração das populações do interior para o litoral

aumento da densificação nas áreas litorais urbanas

crescimento desordenado das cidades obriga ao aproveitamento de áreas formadas por vales aluvionares de **baixa resistência**, **elevada compressibilidade** e **comportamento diferido no tempo**

coincidência entre os locais de maior densidade populacional e a ocorrência de depósitos de solos moles - **desafio para a Engenharia Civil**

Formações silto-argilosas brandas formam materiais de fundação suportando infraestruturas de grande importância

Zona 1	Zona 2	Zona 3
		

1.	**Acessos à Ponte Internacional de Valença**	13.	**Linha do Norte**, troço Quintas - Ovar
2.	**Acessos à Ponte de Viana do Castelo**	14.	Ramal **Ferroviário** do Porto de Aveiro
3.	**A11 / IC14, lanço Esposende - Braga**	15.	E.N. 235 – 335, troço Aveiro - Mamodeiro
4.	**IC5 / A7, Fafe**	16.	Escola Básica dos 2º e 3º Ciclos de Pedrulha
5.	**Porto** de mar da Póvoa do Varzim	17.	**A1, lanço Coimbra - Condeixa**
6.	Porto de Leixões	18.	**IC2, lanço Coimbra – Sargento-Mor**
7.	Ampliação do terminal de contentores do Porto de Leixões (**plataforma logística**)	19.	**Acessos à Ponte de Santa Clara sobre o rio Mondego, em Coimbra**
8.	Dique de proteção contra as marés (Baixo Vouga Lagunar)	20.	Ponte **Pedro e Inês sobre o rio Mondego, em Coimbra**
9.	**IP5, troço Aveiro – Albergaria**	21.	Aproveitamento hidroagrícola do Baixo Mondego
10.	**IC1, troço Angeja - Estarreja**	22.	Ponte Europa sobre o rio Mondego em Coimbra
11.	Sistema Multimunicipal de Saneamento da Ria de Aveiro	23.	**IP3, troço Figueira da Foz – S.ta Eulália**
12.	Portucel Cacia – Central Termoelétrica a Biomassa **(unidades industriais)**	24.	Linha do Norte, troço Alfarelos - Soure

Zona 4

Zona 5

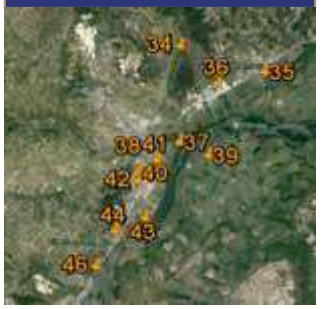

Zona 6

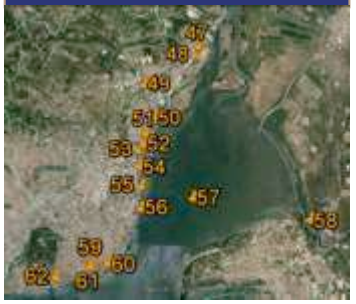

Zona 7

25.	Aproveitamento hidroagrícola do Vale do Lis: reabilitação dos açudes das Saladas	47.	Quinta das Drogas e da Vardelha em Alverca do Ribatejo
26.	Subsistema Carreira do Sistema de Saneamento do Lis	48.	E.T.A.R. de Alverca do Ribatejo
27.	Aproveitamento hidroagrícola do Vale do Lis: reabilitação dos açudes de Arrabalde	49.	**Variante à E.N.10, troço Alverca – EXPO 98**
28.	**E.T.A.R.** de Alcobaça	50.	Valorsul: E.T.A.R.
29.	**A8, troço Caldas da Rainha – Valado de Frades**	51.	E.T.A.R. de S. João da Talha
30.	**IP6 / IC1, troço Peniche – Caldas da Rainha**	52.	**Terminal Ferroviário de Bobadela em Sacavém**
31.	**Linha do Norte, troço Setil - Entroncamento**	53.	**Parque do Oriente de Bobadela**
32.	Ponte Salgueiro Maia em Santarém sobre o rio Tejo	54.	**Aterro Sanitário de Beirolas**
33.	Linha do Norte, troço Azambuja – Vale de Santarém	55.	**Obras da EXPO 98**
34.	A1, troços Vila Franca de Xira – Carregado e Carregado – Aveiras de Cima	56.	**Marina do Parque das Nações**
35.	E.T.A.R. da Azambuja	57.	**Ponte Vasco da Gama sobre o rio Tejo**
36.	Plataforma Logística da Azambuja	58.	**Ponte sobre a Ribeira das Enguias sobre o rio Tejo**
37.	**A10, Ponte da Lezíria sobre o rio Tejo**	59.	Extensão da rede do Metropolitano de Lisboa entre o Rossio e o Cais do Sodré
38.	Central Termoeléctrica do Ribatejo no Carregado	60.	**Terminal de passageiros da Doca do Jardim do Tabaco**
39.	**A10, troço Carregado - Benavente**	61.	**Extensão da rede do Metropolitano de Lisboa entre o Chiado e Santa Apolónia**
40.	Italagro – Indústria de Transformação de Produtos Alimentares, S. A. no Carregado	62.	Porto de Lisboa
41.	**Plataforma Logística Lisboa - Norte**	63.	Extensão da Fábrica do Seixal da Siderurgia Nacional
42.	Estação elevatória de esgotos de Castanheira do Ribatejo	64.	E.T.A.R. do Seixal
43.	Projeto de rega e drenagem da Lezíria Grande de Vila Franca de Xira	65.	Variante Ferroviária de Alcácer do Sal
44.	E.T.A.R. de Vila Franca de Xira	66.	**Ponte de Alcácer do Sal sobre o rio Sado**
45.	**Ponte Marechal Carmona em Vila Franca de Xira sobre o rio Tejo**	67.	**Linha do Sul, variante entre a Estação do Pinheiro e o km 94 da Linha do Sul**
46.	Cimianto – Projeto de selagem da lixeira em Vila Franca de Xira	68.	Terminal do Carvão de Sines

Zona 8

70.	**E.N. 125, variante de Portimão, com Ponte sobre o rio Arade**
71.	Obras da Expo Arade, Portimão
72.	Doca de Olhão
73.	Porto de Mar de Olhão
74.	**Ponte do rio Gilão em Tavira**
75.	Projeto turístico "Verdelago", em Faro **(empreendimentos imobiliários)**
76.	E.T.A.R. de Vila Real de Santo António
77.	**Ponte Internacional de Vila Real de Santo António sobre o rio Guadiana**

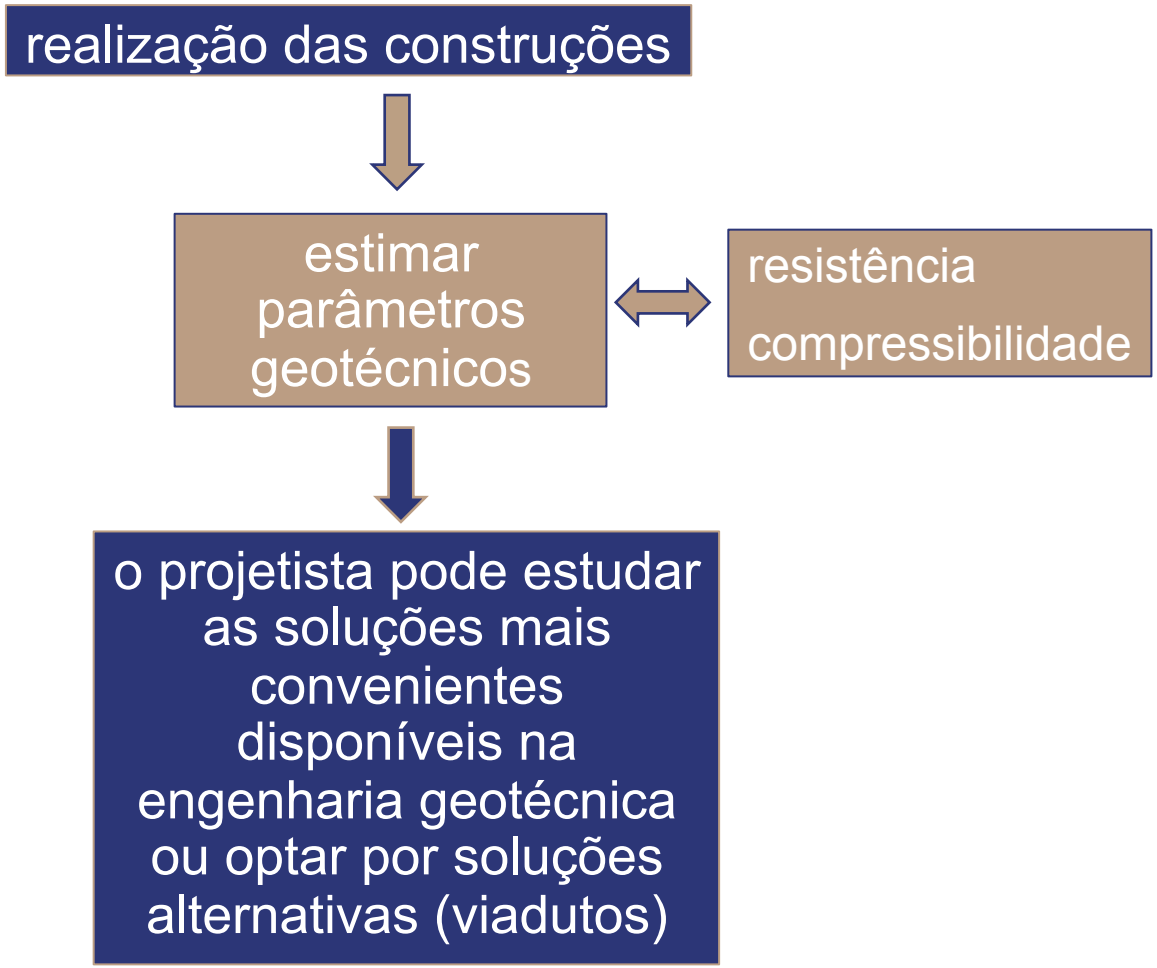
realização das construções
estimar parâmetros geotécnicos
resistência
compressibilidade
o projetista pode estudar as soluções mais convenientes disponíveis na engenharia geotécnica ou optar por soluções alternativas (viadutos)

Tratamento sistemático dos elementos existentes (120 locais)

Resultados de ensaios em laboratório	Resultados de ensaios de campo
Identificação (587 amostras)	DMT (32 ensaios)
Edométricos (290 amostras)	CPTU (14 ensaios)
Triaxiais (146 amostras)	FVT (408 ensaios)

Associação de novos resultados – Campo experimental (Cacia, Aveiro)

PARÂMETROS FÍSICOS E DE IDENTIFICAÇÃO

- Composição granulométrica

Banda de curvas granulométricas que permite situar os aluviões silto-argilosos moles de Portugal

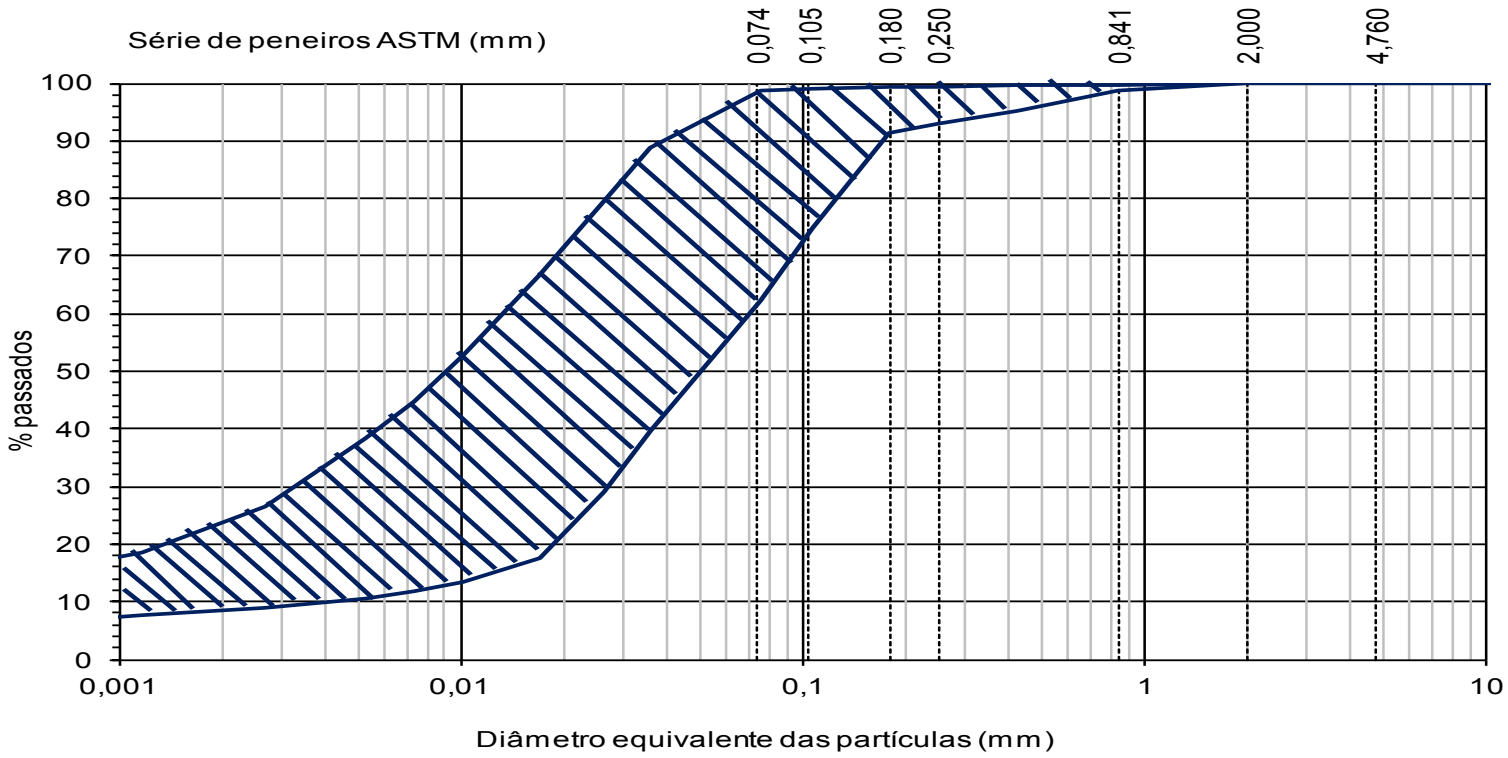

ARGILA	SILTE			AREIA			CASCALHO
	FINO	MÉDIO	GROSSO	FINA	MÉDIA	GROSSA	

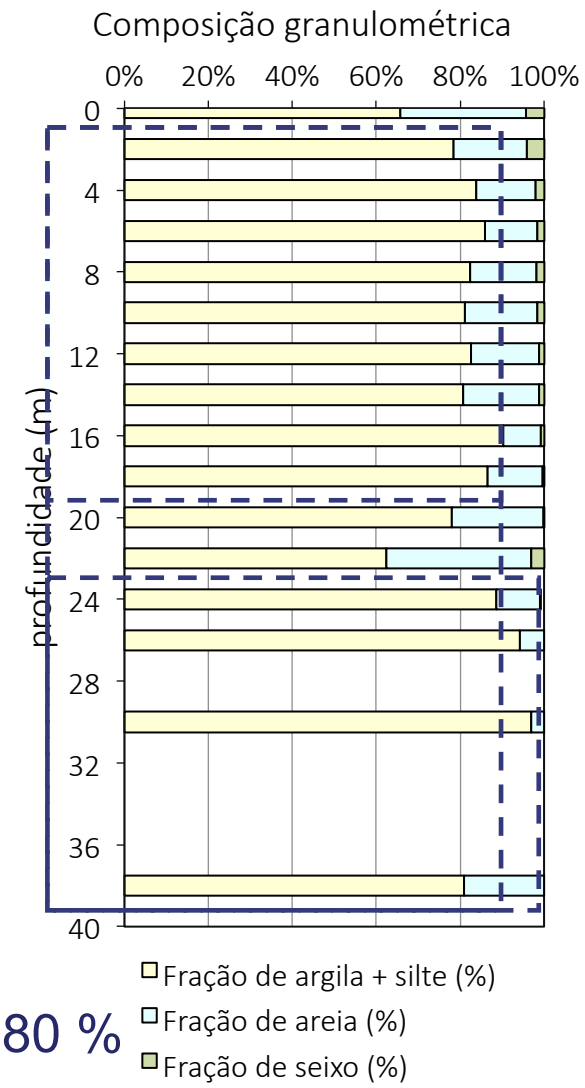

80 %

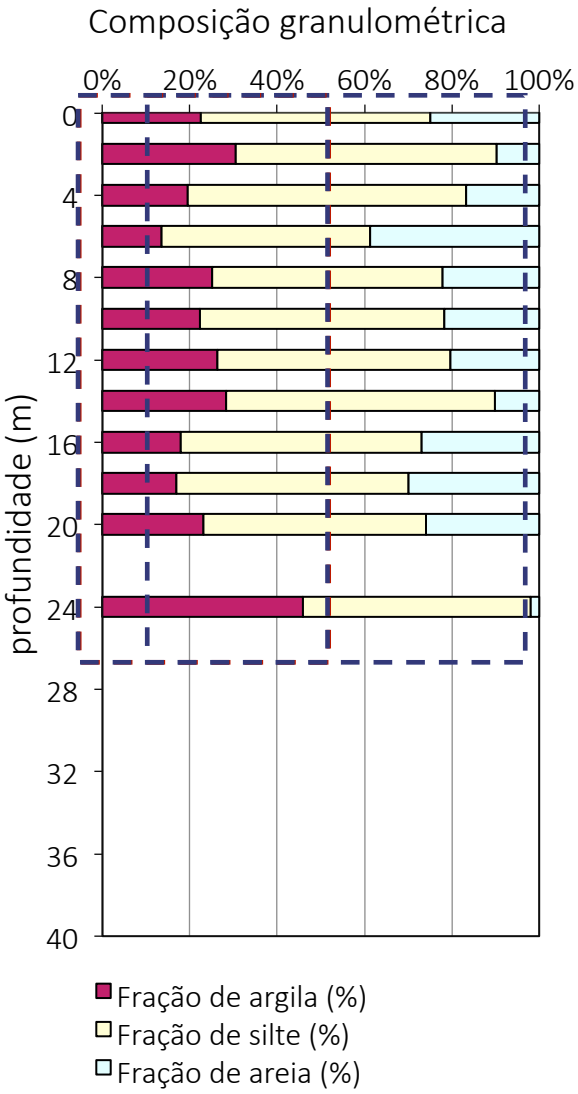

fração argila é
praticamente
(50% e 65 %)

fração fina é predominante

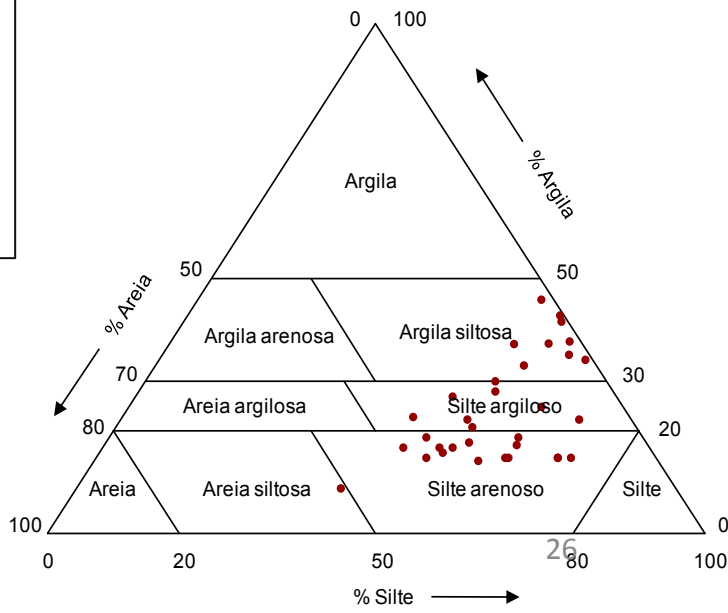

- Teor em Matéria Orgânica

  - elevado (até 13%)
  - variação espacial significativa;
  - valores mais elevados na zona superficial;
  - valores dependentes do processo de determinação de *OM* (perdas por ignição e oxidação húmida)

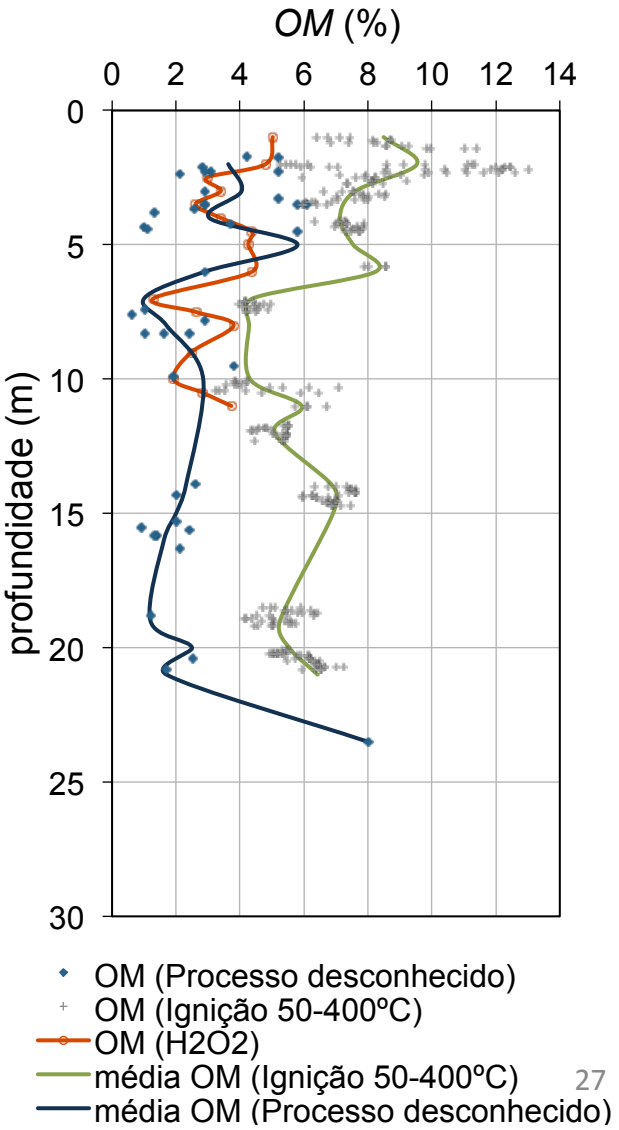

- Limites de Atterberg e Índice de Plasticidade

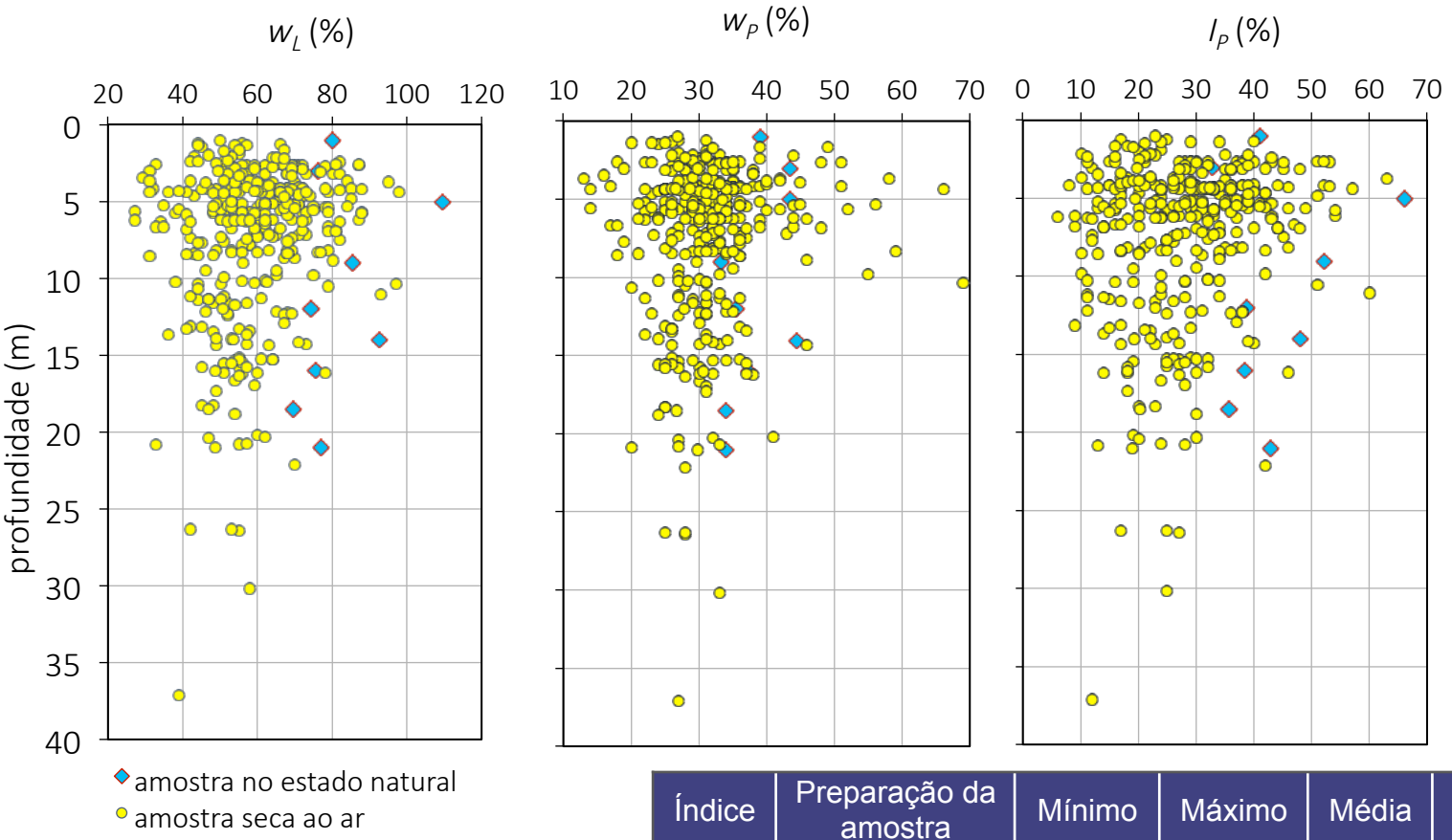

Índice	Preparação da amostra	Mínimo	Máximo	Média	Desvio padrão	Nº ensaios
w_L (%)	Estado natural	70	110	82	12	9
	Seca ao ar	27	98	59	13	361
w_P (%)	Estado natural	33	45	38	5	9
	Seca ao ar	13	69	31	7	360
I_P (%)	Estado natural	33	66	44	10	9
	Seca ao ar	6	63	28	10	360

- Influência *OM* na variabilidade das características físicas e de plasticidade.
- Redução da plasticidade do solo quando sujeito a secagem.
- Os limites de Atterberg e o I_P assumem uma variação expressiva traduzida por um desvio padrão elevado.

- Atividade das Argilas

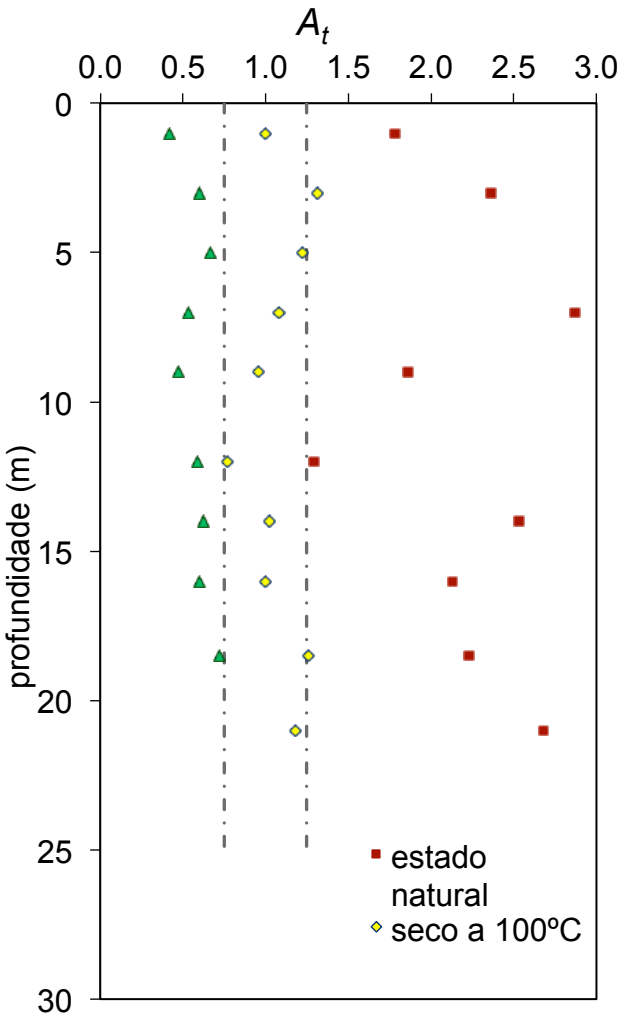

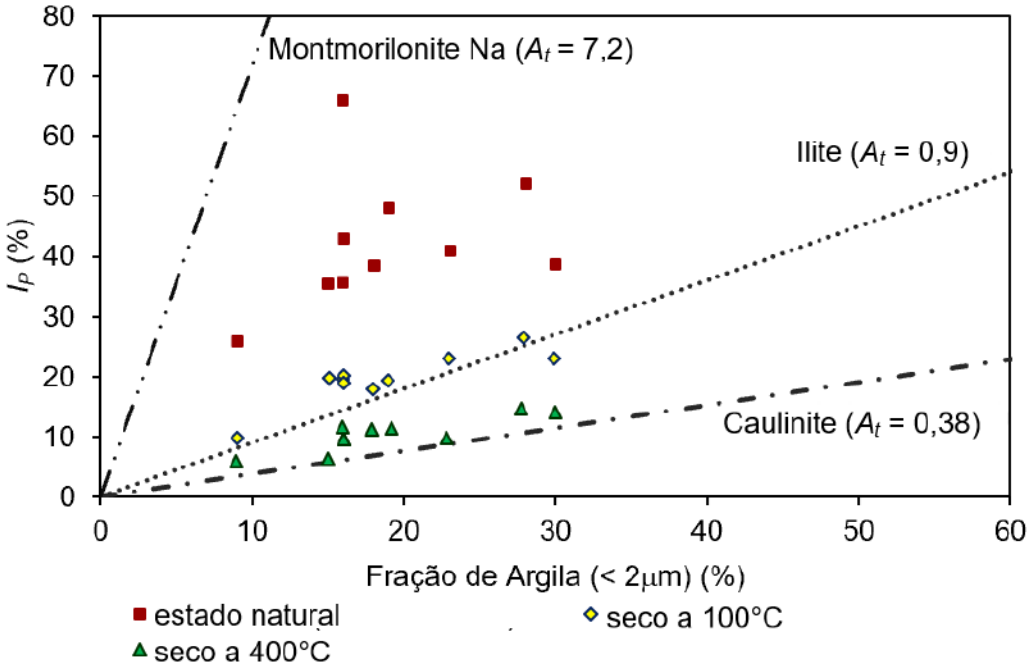

- Maiores atividades ocorrem nas amostras ensaiadas no estado natural.
- Atividade diminui à medida que a secagem reduz a influência da matéria orgânica sobre a plasticidade do solo
- Resultados das amostras secas a 400º fornecem indicação sobre a composição mineralógica da fração argilosa

- Índices Físicos

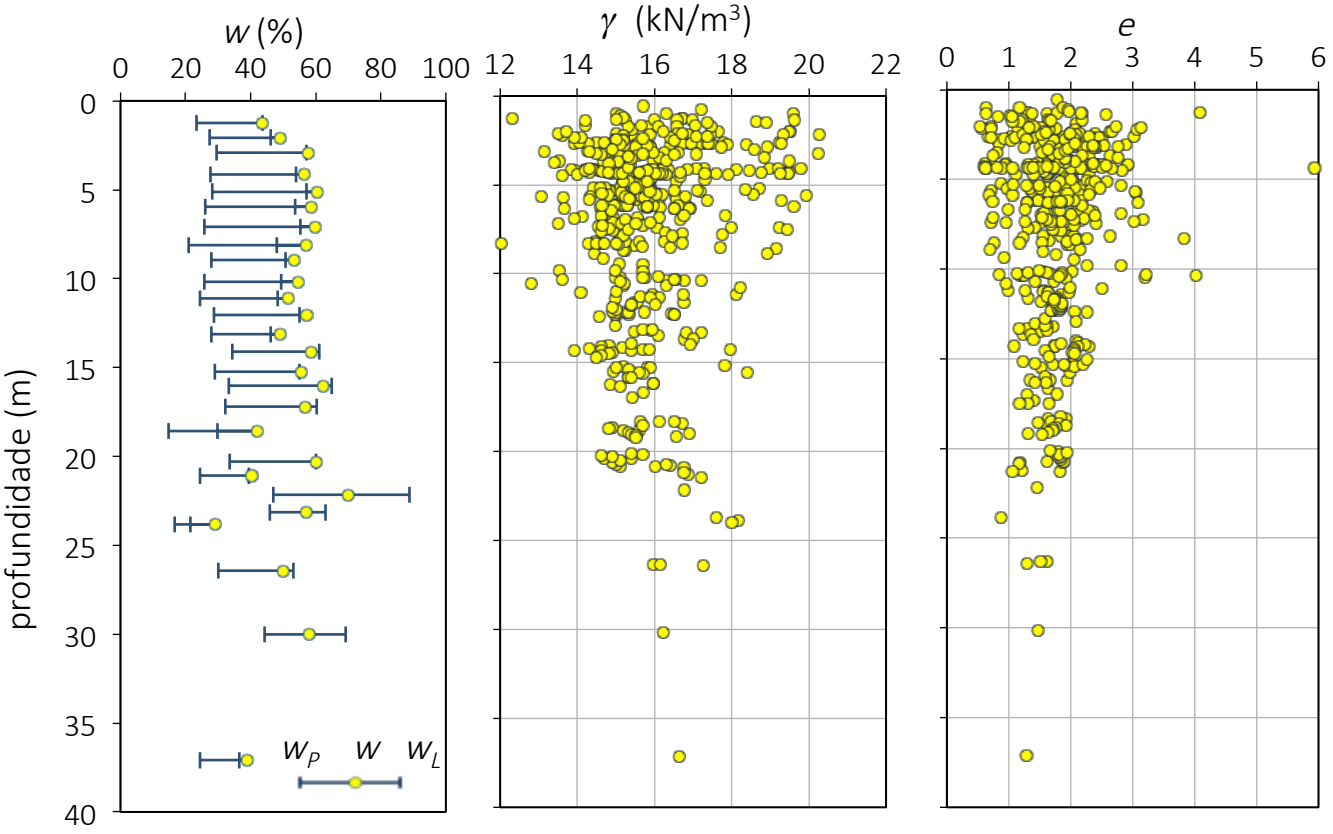

w (%) = 64 ± 17 [n = 461]

w_P (%) = 31 ± 7 [n = 360]

w_L (%) = 59 ± 13 [n = 361]

γ (kN/m³) = 15,9± 1,4 [n = 497]

e = 1,77± 0,56 [n = 509]

teor em água próximo do limite de liquidez

↓

solos muito moles

CLASSIFICAÇÃO DOS SOLOS DE ACORDO COM A CLASSIFICAÇÃO UNIFICADA

Resultados separados considerando a influência da bacia hidrográfica onde as amostras foram recolhidas.

Considerando a bacia hidrográfica com a constituição geológica atualmente aflorante e apenas considerando as argilas provenientes dos minerais argilosos contidos nas rochas aflorantes e dos minerais de neoformação, as bacias hidrográficas foram agrupadas em quatro grupos:

1º. **Rios Cávado, Leça e Guadiana**, com uma contribuição predominante do soco ibérico, de granitos, de rochas metassedimentares xistentas e de minerais argilosos precipitados a partir das soluções aquosas veiculadas pelas redes hidrográficas;

2º. **Rios Vouga e Mondego**, com contribuição mista de rochas hersínicas do soco ibérico e de rochas sedimentares do secundário, de grés, de argilas e de calcários;

3º. **Rios Tejo e Sado**, com contribuição, em posição distal, de rochas granitóides e metassedimentos xistentos e, em posição proximal, de sedimentos areno-argilosos do Terciário;

4º. **Rio Lis, Ribeiras do Oeste e Ribeiras do Algarve**, com predominância de rochas carbonatadas, essencialmente calcários do Jurássico e grés do Cretácico.

CLASSIFICAÇÃO DOS SOLOS DE ACORDO COM A CLASSIFICAÇÃO UNIFICADA

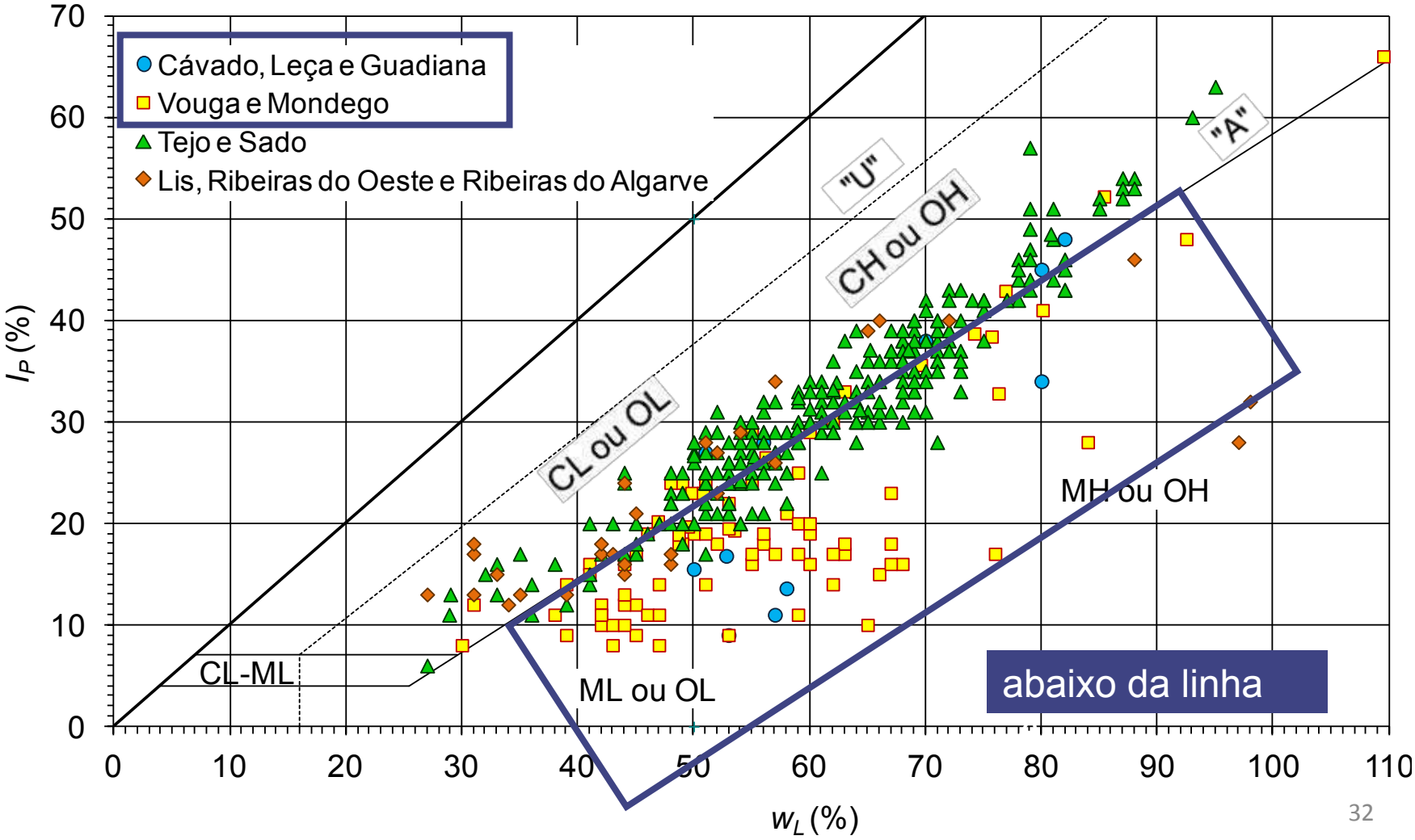

CLASSIFICAÇÃO DOS SOLOS DE ACORDO COM A CLASSIFICAÇÃO UNIFICADA

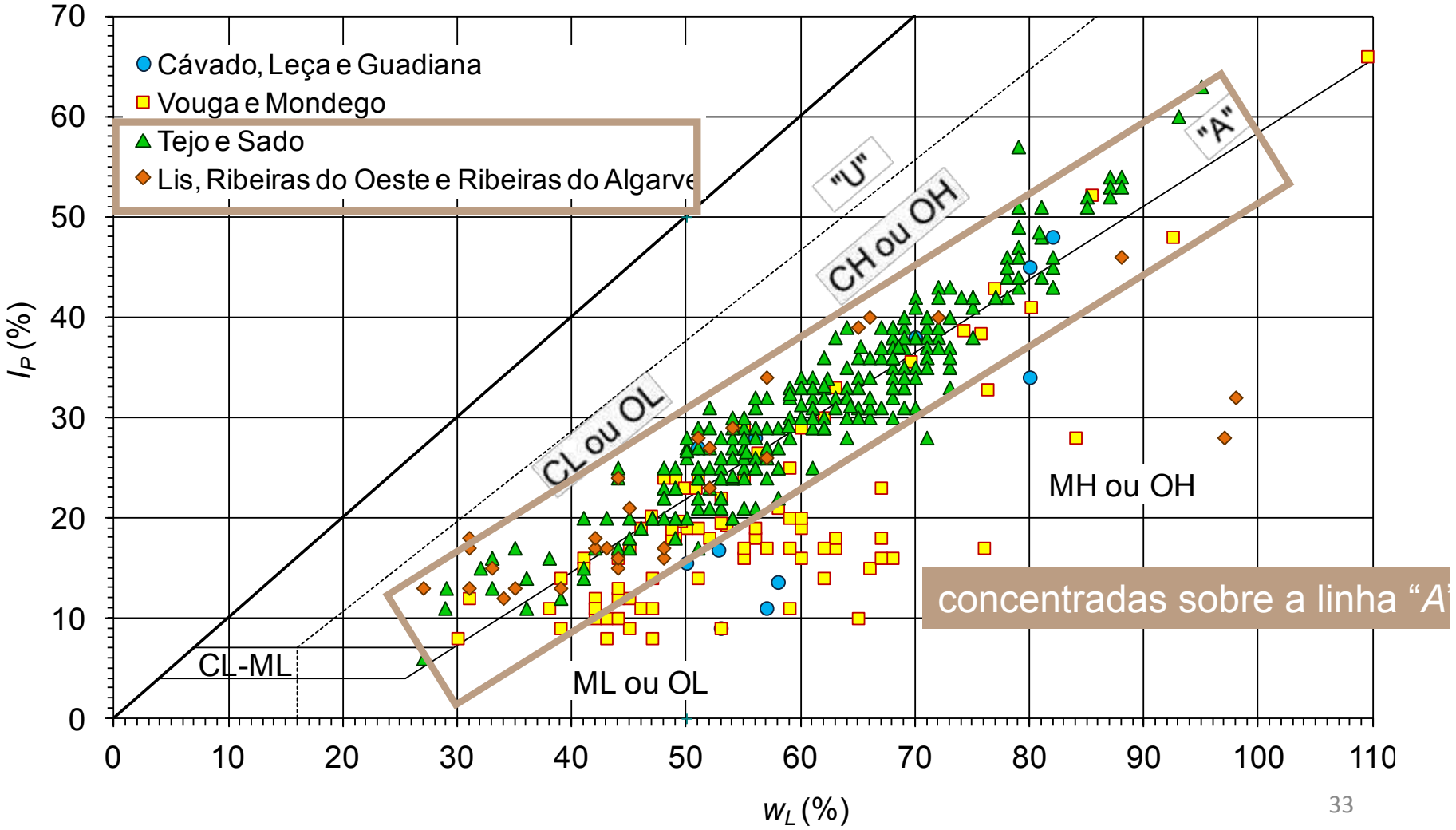

concentradas sobre a linha "*A*"

CLASSIFICAÇÃO DOS SOLOS DE ACORDO COM A CLASSIFICAÇÃO UNIFICADA

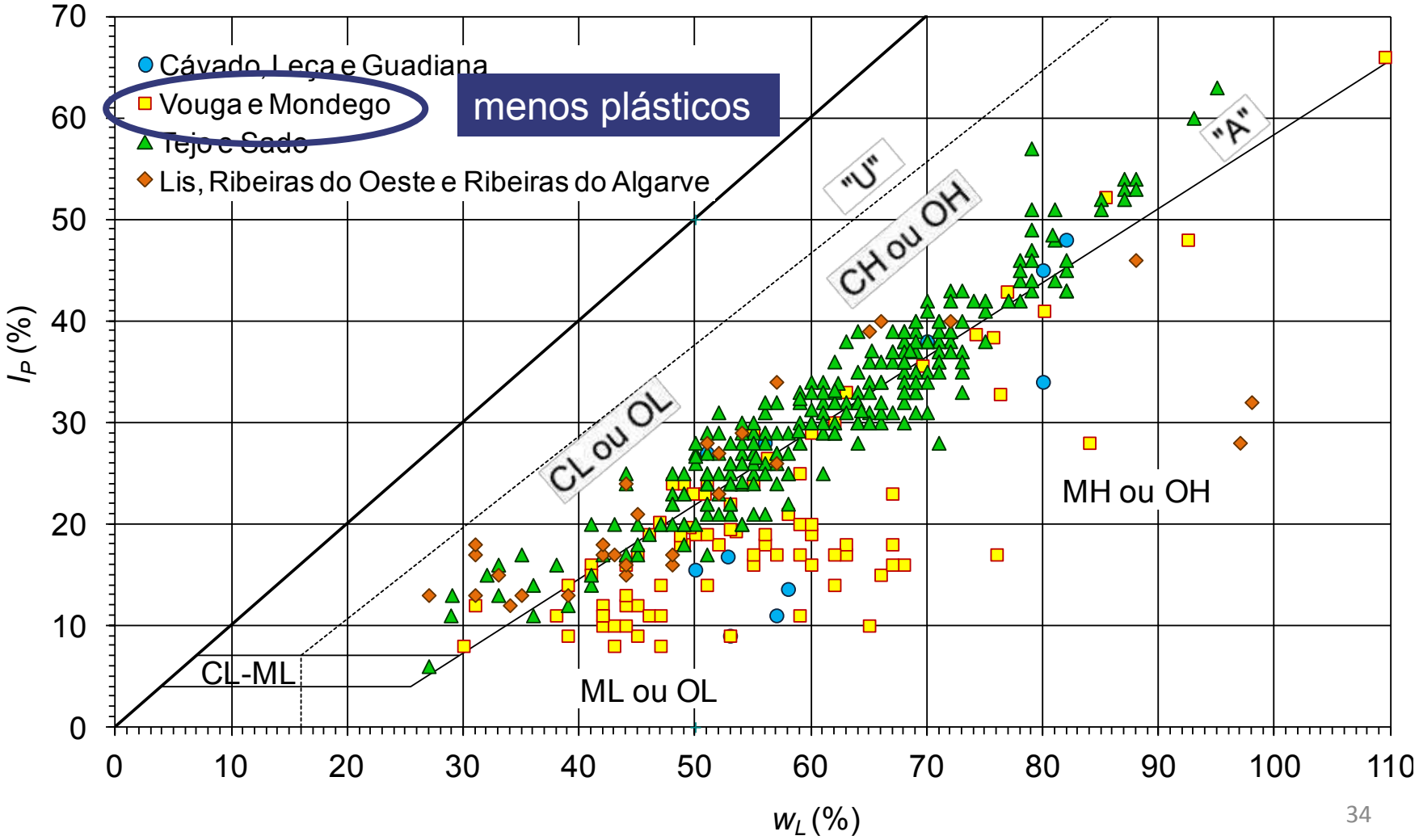

PARÂMETROS COMPRESSIBILIDADE

Parâmetros de compressibilidade, C_c, C_r e C_α

→ Ensaios de laboratório

→ determinação difícil e morosa

Modelos de regressão definidos à custa de parâmetros geotécnicos de fácil determinação

↓

tratamento sistemático de resultados de 290 ensaios **edométricos** → C_c C_r C_α

- R_{OC}

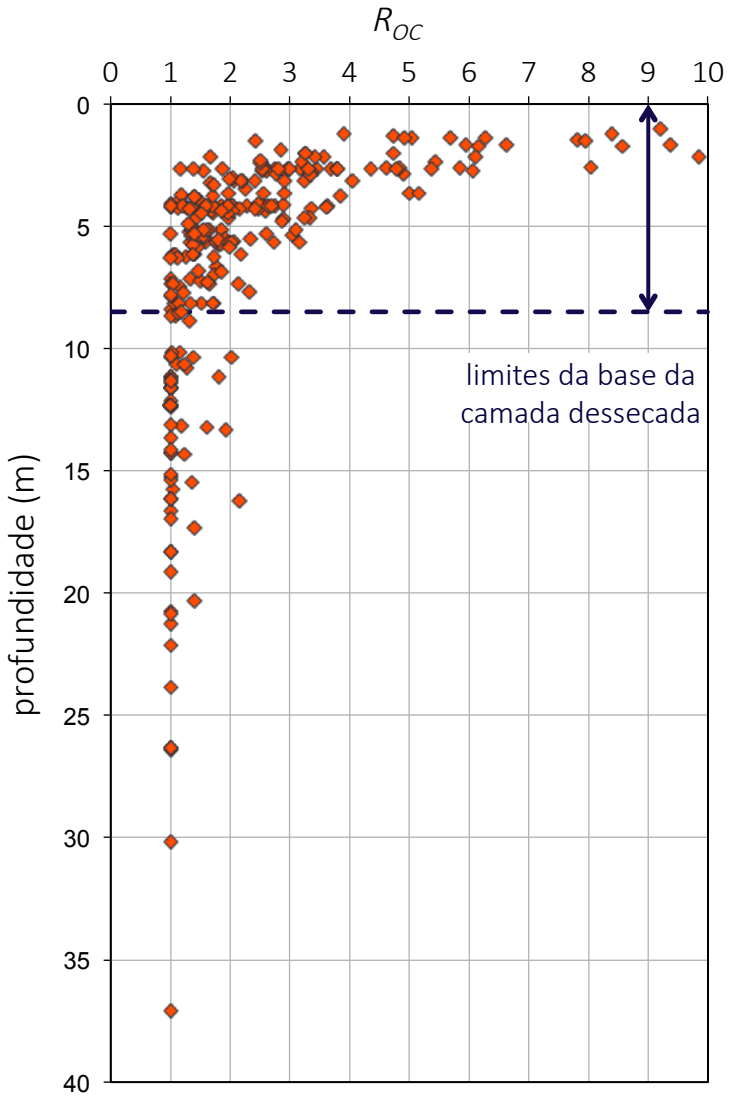

crosta sobreconsolidada por dessecação tem espessura bastante elevada

para profundidades fora da zona de influência desta crosta o depósito apresenta-se normalmente consolidado ou muito levemente sobreconsolidado.

Avaliação dos parâmetros de compressibilidade, C_c, C_r e C_α

Análise estatística preliminar

Análise univariada

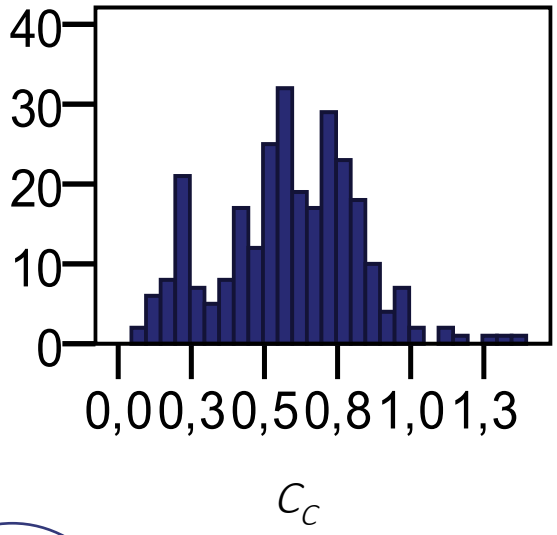

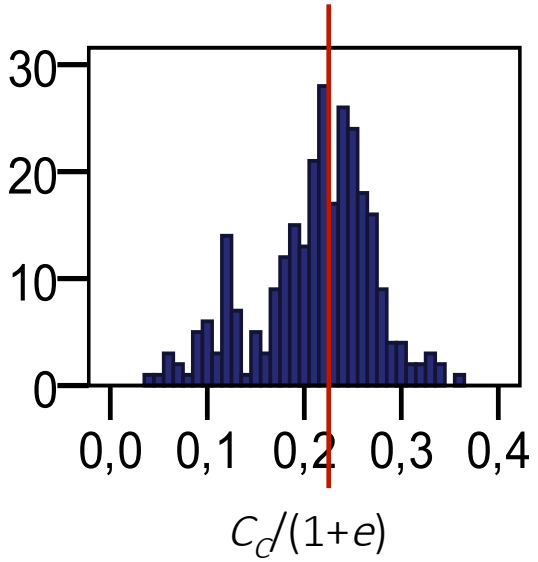

C_c	$C_c/(1+e)$	C_r/C_c
0,58 (± 0,24)	0,22 (± 0,06)	0,14 (± 0,04)
n = 278	n = 241	n = 255

Valor médio (± desvio padrão)
n – número de ensaios

$C_d/(1+e) \approx 0,22$
[desvio padrão reduzido]

Avaliação dos parâmetros de compressibilidade, C_c, C_r e C_α

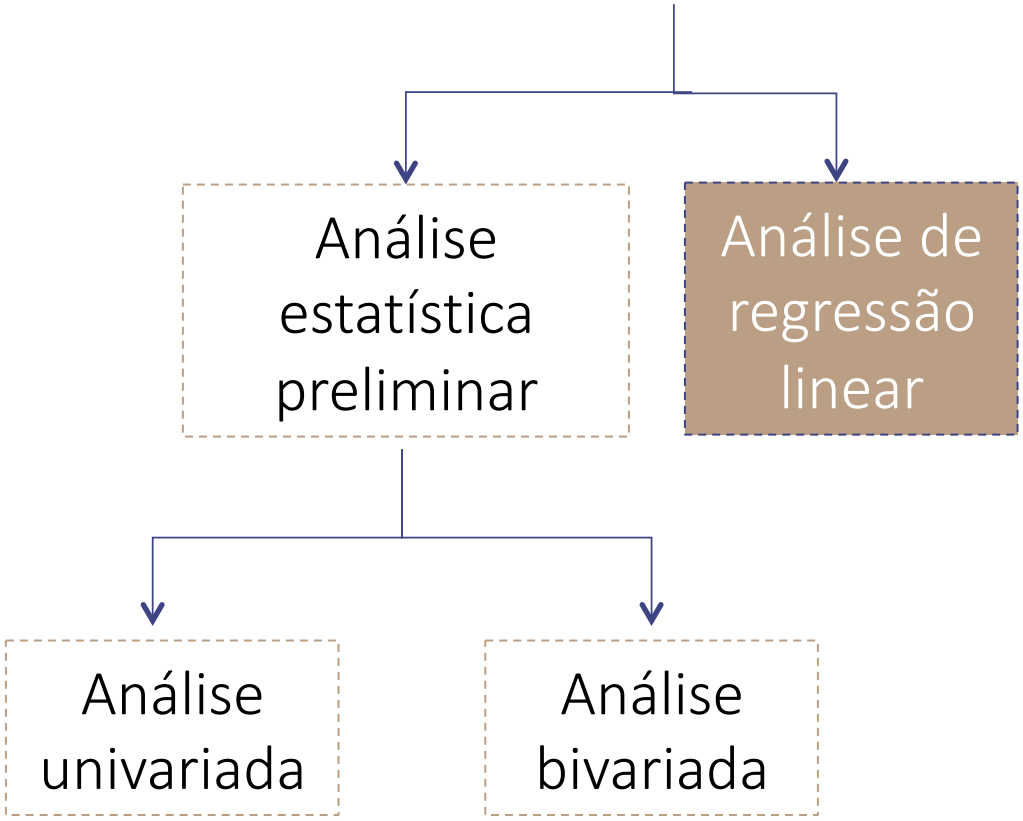

Modelo	variáveis		unidades
	dependente	independentes	
1	C_c	w_L	(%)
2		I_p	(%)
3		w	(%)
4		e	adimensional
5		e	adimensional
		w_L	(%)
6		I_p	(%)
		G_s	adimensional
7		w	(%)
		w_L	(%)
8		e	adimensional
		G_s	adimensional
9		w_L	(%)
		G_s	adimensional
10		e	adimensional
		w	(%)
		w_L	(%)
11	$C_c/(1+e)$	w	(%)
12		C_c	adimensional
13	C_r	w	(%)
14		I_p	(%)

$C_c = f(w)$

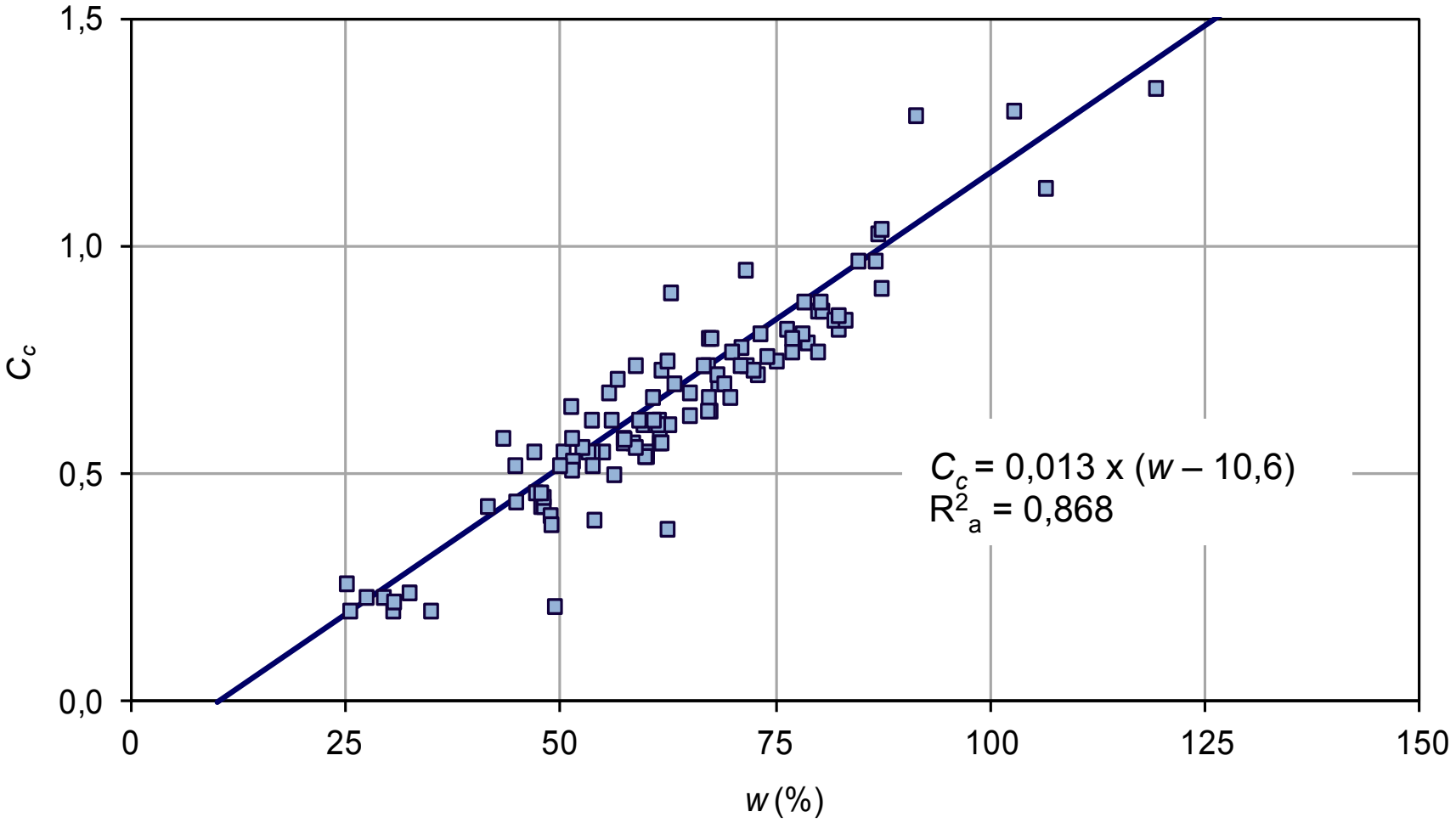

C_c / (1+e) = f(w)

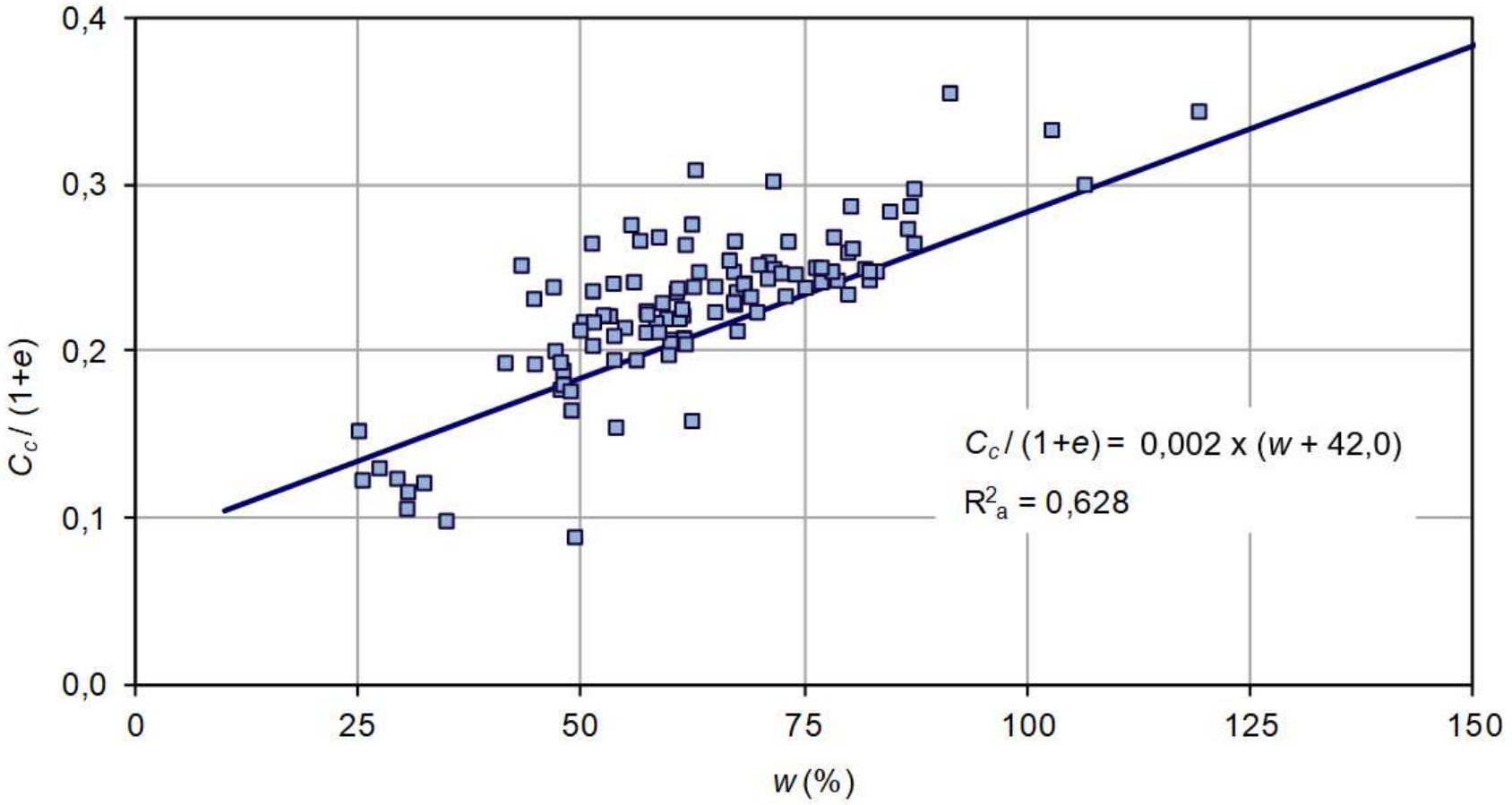
0,4
0,3
0,2
0,1
0,0
C_c / (1+e)
0
25
50
75
100
125
150
w (%)
C_c / (1+e) = 0,002 x (w + 42,0)
R^2_a = 0,628

$C_r = f(C_c)$

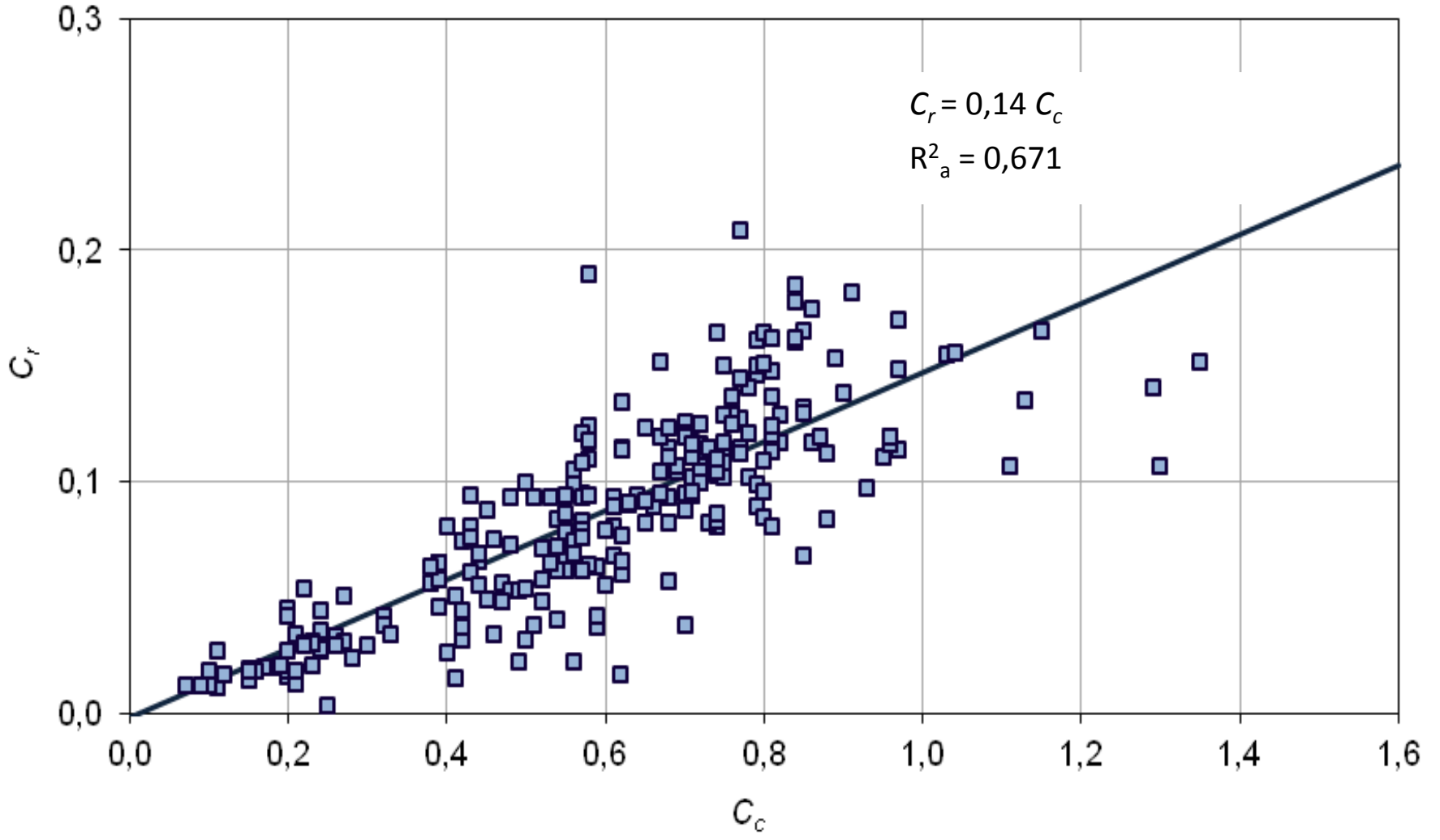

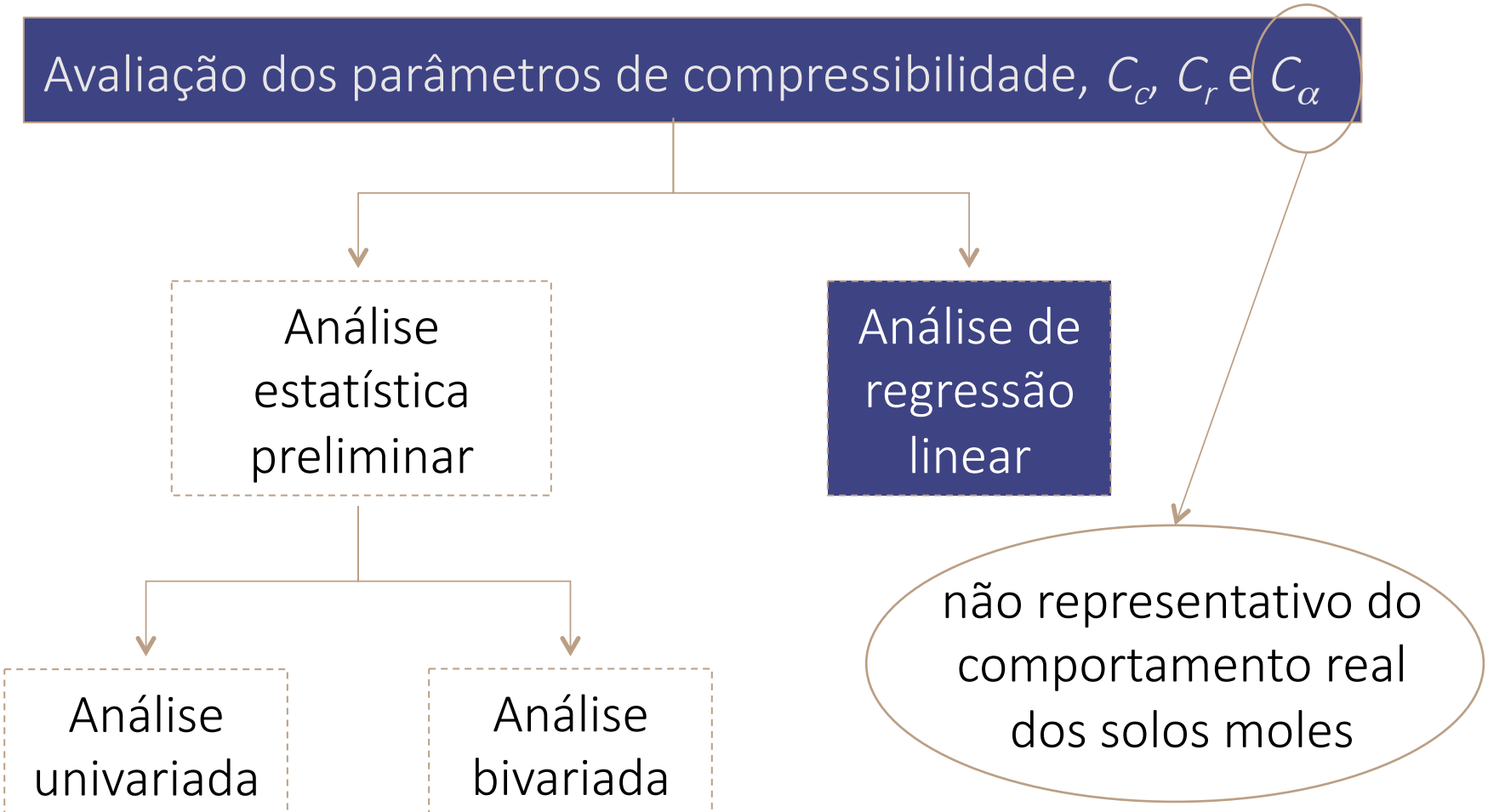
Avaliação dos parâmetros de compressibilidade, C_c, C_r e C_α
Análise estatística preliminar
Análise de regressão linear
Análise univariada
Análise bivariada
não representativo do comportamento real dos solos moles

Resultados dos ensaios de muito longa duração

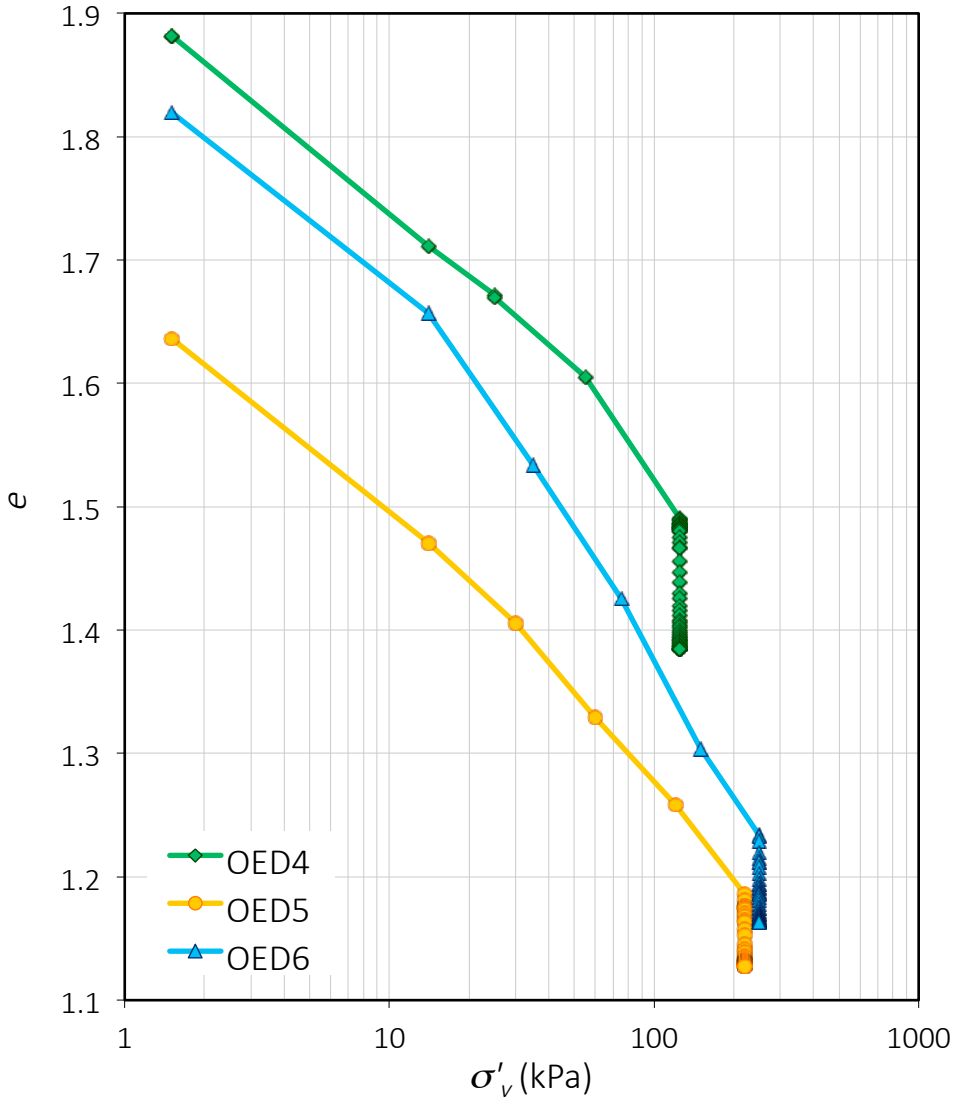

Ensaio	prof. (m)	escalão de carga (kPa)	tempo de aplicação da carga (dias)
OED4	**4,03**	**125**	**629**
OED5	**17,05**	**220**	**626**
OED6	**21,80**	**250**	**626**
OED7	3,80	600	204
OED8	15,80	1000	203
OED9	21,85	1000	203

Tensão constante de σ'_{v0} + 100 kPa (correspondente a um aterro de ± 5m)

Resultados dos ensaios de longa duração

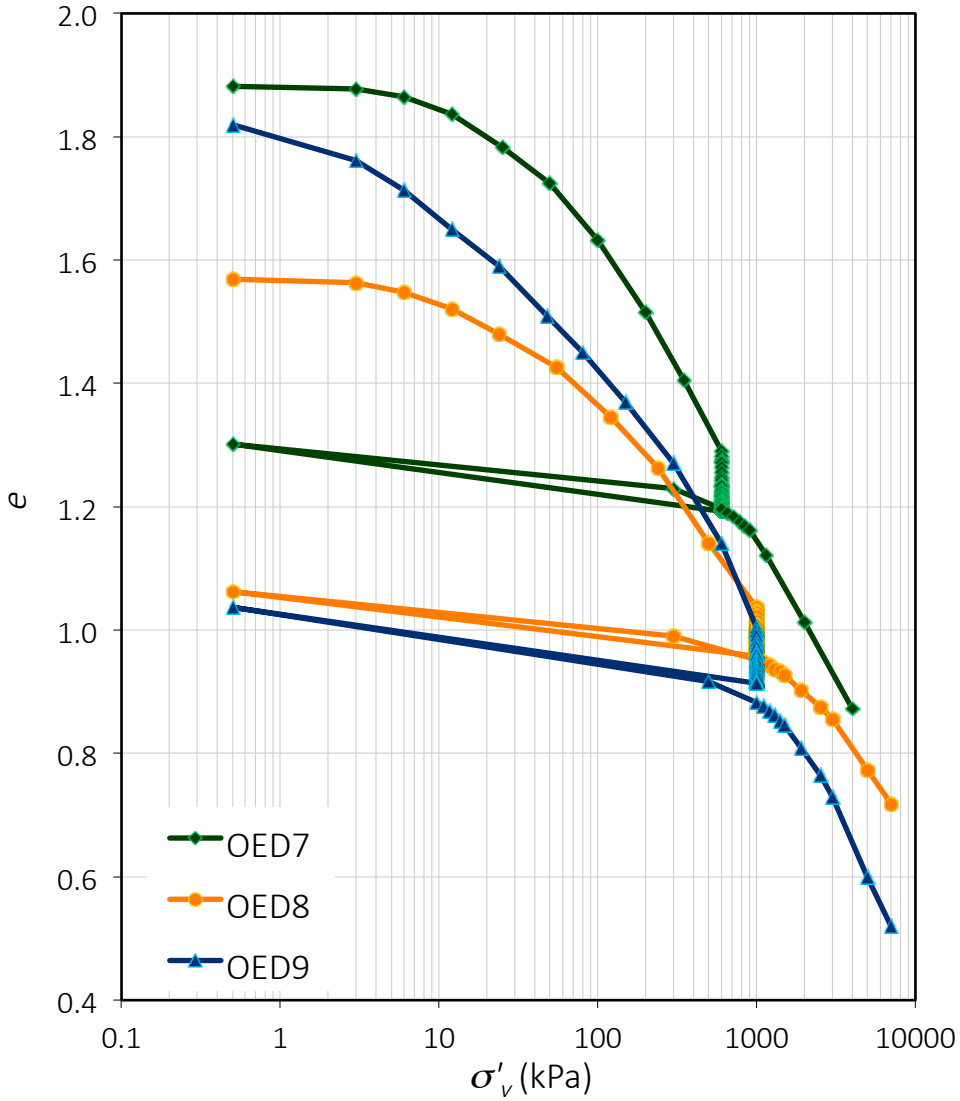

Ensaio	prof. (m)	escalão de carga (kPa)	tempo de aplicação da carga (dias)
OED4	4,03	125	629
OED5	17,05	220	626
OED6	21,80	250	626
OED7	3,80	600	204
OED8	15,80	1000	203
OED9	21,85	1000	203

Tensão constante superior → carregamento no ramo virgem

Coeficiente de consolidação secundária

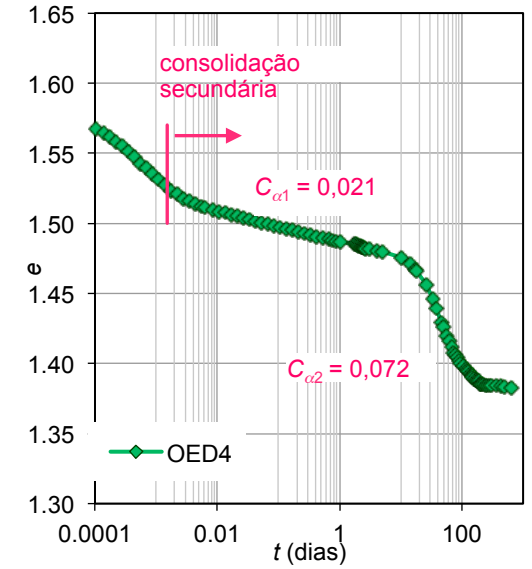

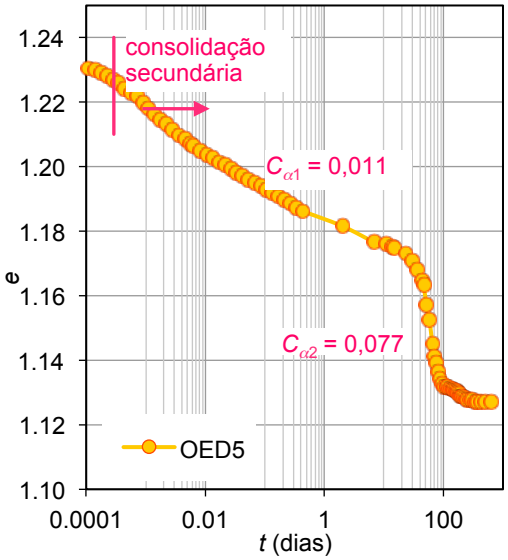

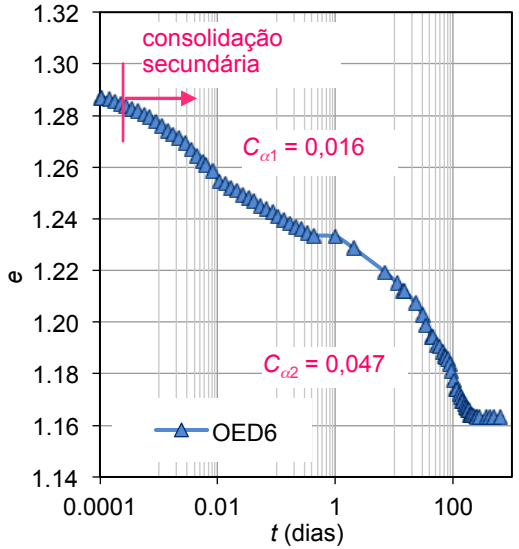

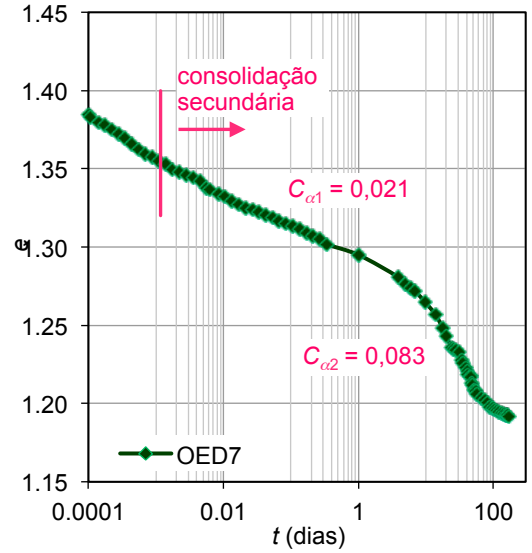

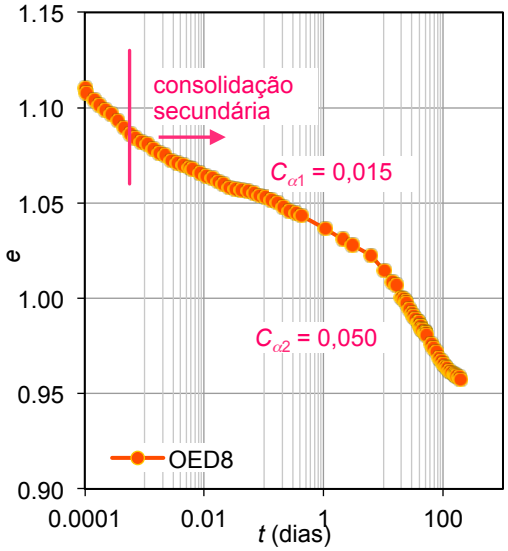

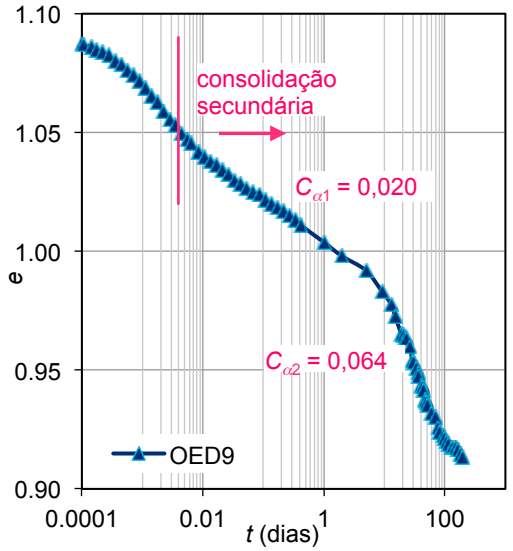

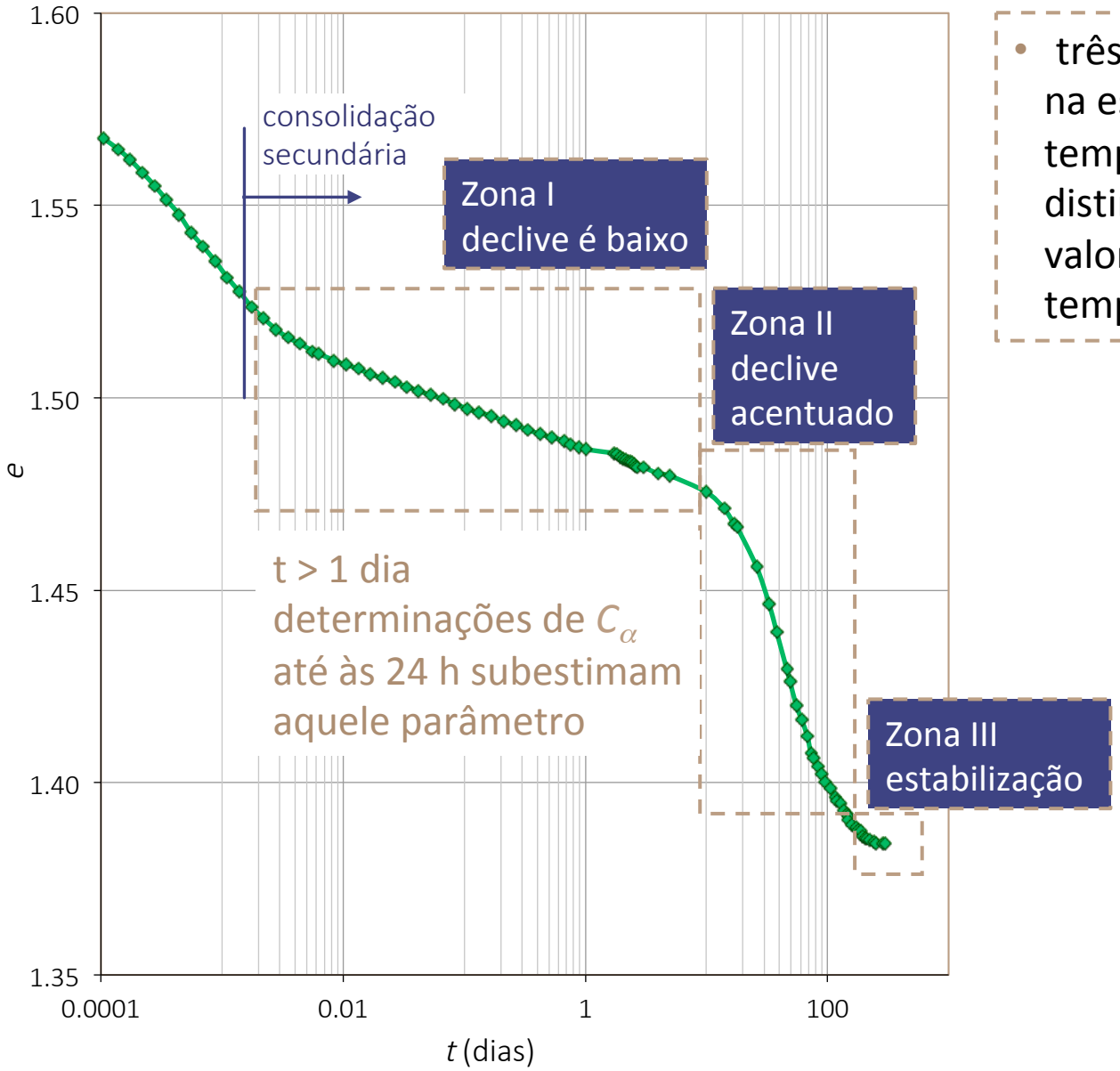

- três zonas de resposta linear na escala semi-logarítmica do tempo, com taxas muito distintas, originando diferentes valores de C_α para diferentes tempos de carregamento

PARÂMETROS RESISTÊNCIA

- Objetivo
  - Envolvente de rotura em tensões efetivas (c', ϕ')
  - Resistência não drenada (c_u)
- Tratamento sistemático de resultados de ensaios:
  - Laboratório: **triaxiais**
    - Critérios de identificação da rotura
      - Máxima tensão de desvio, $(\sigma_1\text{-}\sigma_3)_{máx}$
      - Máxima obliquidade, $(\sigma'_1/\sigma'_3)_{máx}$
      - Máximo excesso de pressão neutra, $\Delta u_{máx}$
  - Campo: **DMT**, **CPTU** e **FVT**

PARÂMETROS DE RESISTÊNCIA EM TENSÕES EFETIVAS

Envolventes de rotura (compressão)

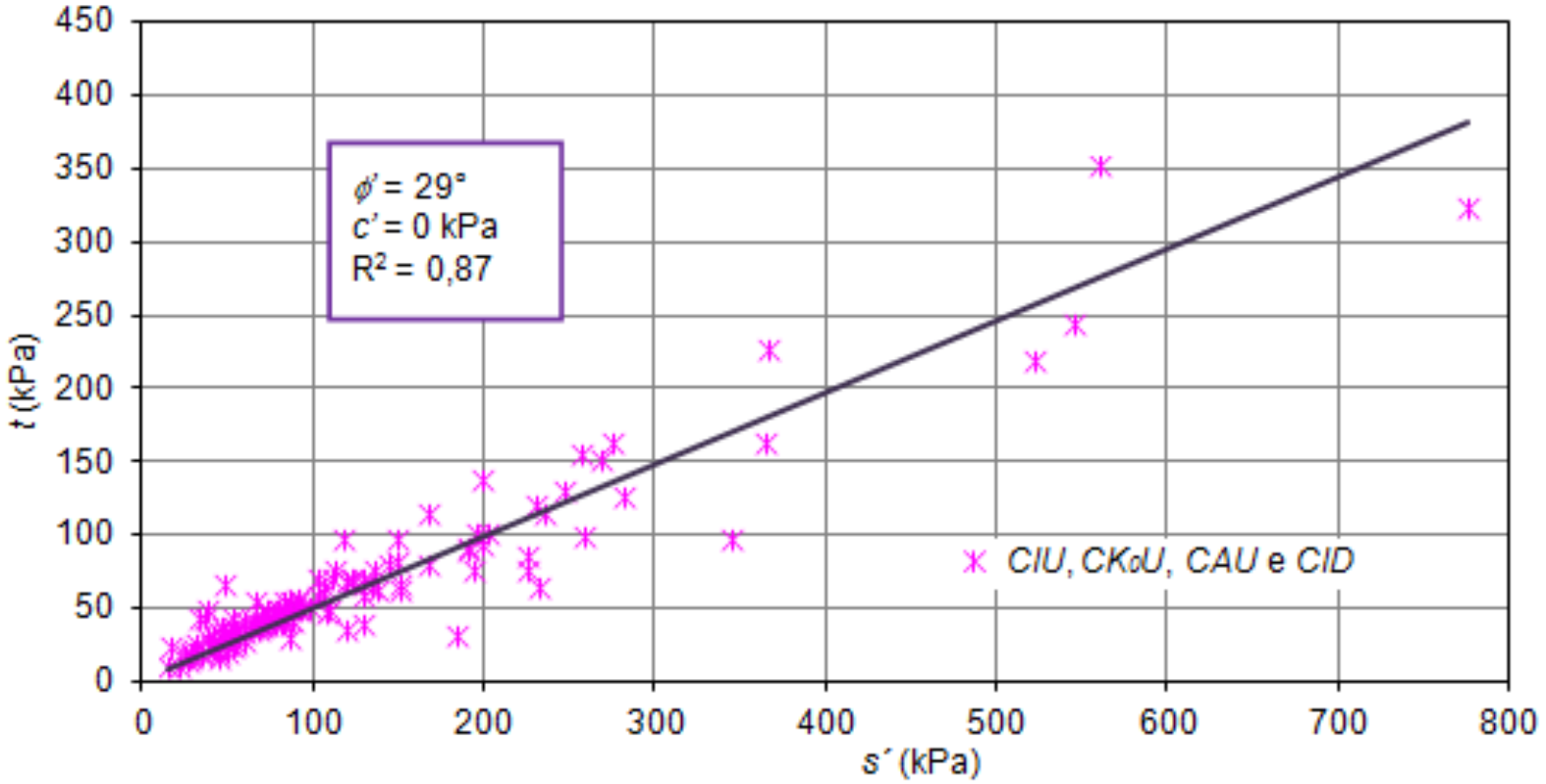

- Ensaios sobre amostras normalmente consolidadas
- Pequenas diferenças entre ensaios CIU, CK_0U, CAU e CID
- Pode assumir-se apenas uma envolvente de rotura em compressão

RESISTÊNCIA NÃO DRENADA

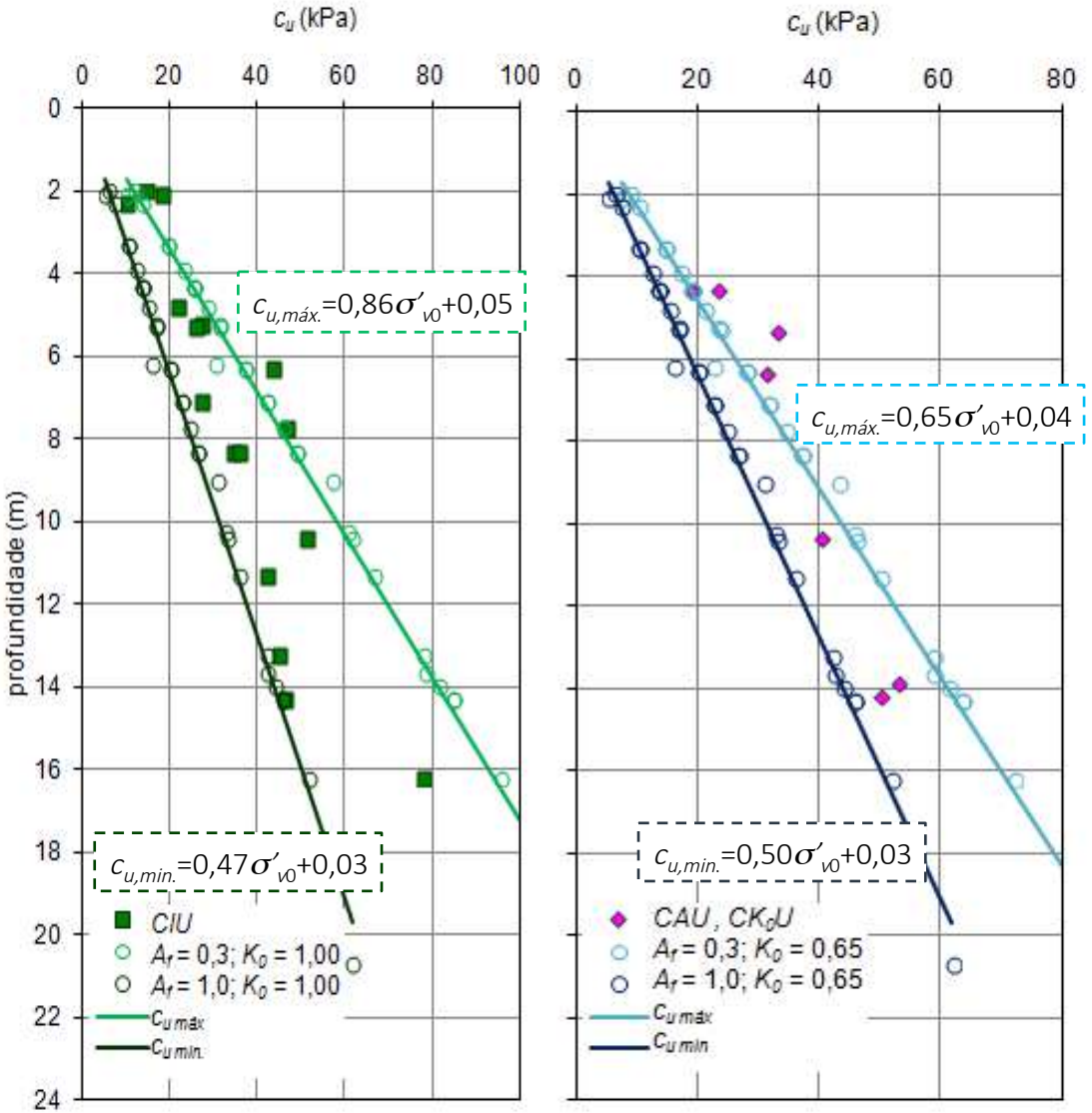

- Definição de $c_u = f(\phi', K_0, A_f)$ para enquadrar os resultados existentes

$$\frac{c_u}{\sigma'_{v0}} = \frac{sen\emptyset'(K_0 + A_f - K_0 A_f)}{1 - sen\emptyset' + 2A_f sen\emptyset'} = f(K_0, A_f, \emptyset')$$

- Balizar pelo parâmetro A_f os limites superior e inferior de c_u *in situ*

c'=0; ϕ'=29º; K_0 =1 (CIU) e K_0 =0,65 (CAU e CK$_0$U) ; A_f ϵ [0,3; 1,0]

que há um bom ajuste entre os valores experimentais ($\sigma'_c \approx \sigma'_{v0}$) e os valores teóricos

- Resistência não drenada

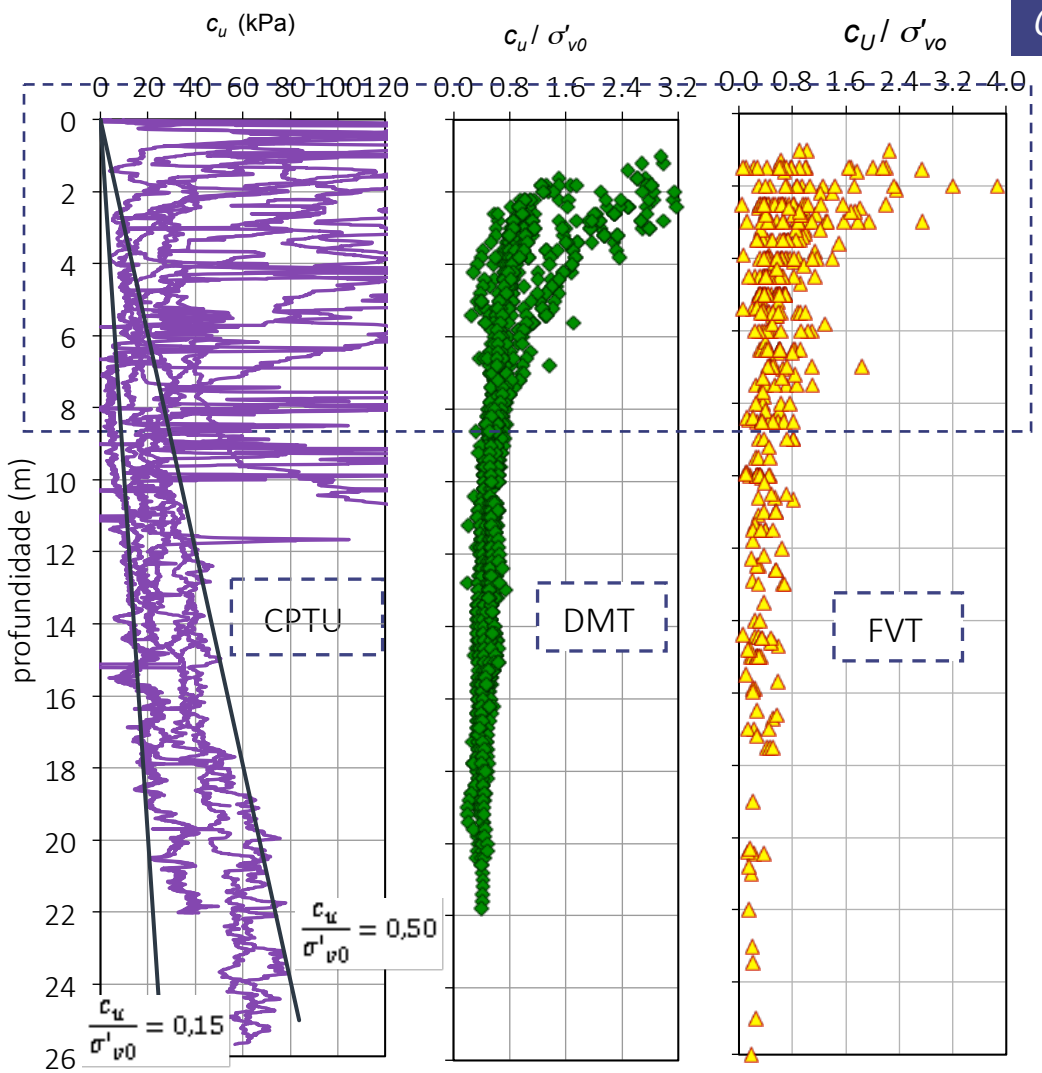

Camada dessecada

sobrestimado

DMT: $0{,}3 < c_u/\sigma'_{v0} < 0{,}7$

CPTU $N_{kt} \approx 12$ $0{,}15 < c_u/\sigma'_{v0} < 0{,}5$

FVT: $0{,}20 < c_u/\sigma'_{v0} < 0{,}5$

Limite superior excessivo explicado, em parte, por pequenas intercalações arenosas, presença de conchas e outros fósseis

AGRADECIMENTOS

Geocontrole

Cenorgeo

Geotest

Mota-Engil

CICCOPN

Instituto Politécnico da Guarda

Laboratório de Geotecnia da FEUP (LabGeo)

Laboratório de Geotecnia e Materiais de Construção (LGMC) do ISEP

OBRIGADA

Elisabete Costa Esteves

ISEP, Porto, Portugal

Innovative solutions to mitigate Earthquake Induced soil Liquefaction Damages (EILD)

António Viana da Fonseca

U.PORTO FEUP FACULDADE DE ENGENHARIA UNIVERSIDADE DO PORTO
Institute of R&D in Structures and Construction
Department of Civil Engineering
CONSTRUCT

Liquefaction Damages - Lifelines

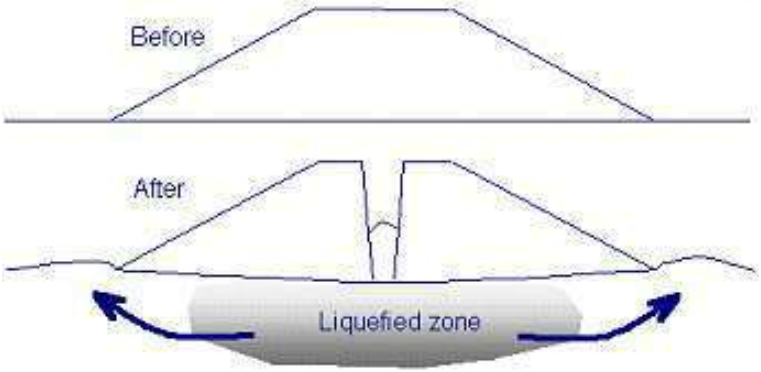

Great East Japan (Tohoku Pacific) Earthquake

Liquefaction Damages - Lifelines

Great East Japan (Tohoku Pacific) Earthquake

Great East Japan (Tohoku Pacific) Earthquake 2011

Liquefaction Damages - Lifelines

Liquefaction Damages - INFRASTRUCTURES

M_w7.8 Kaikoura NZ Earthquake

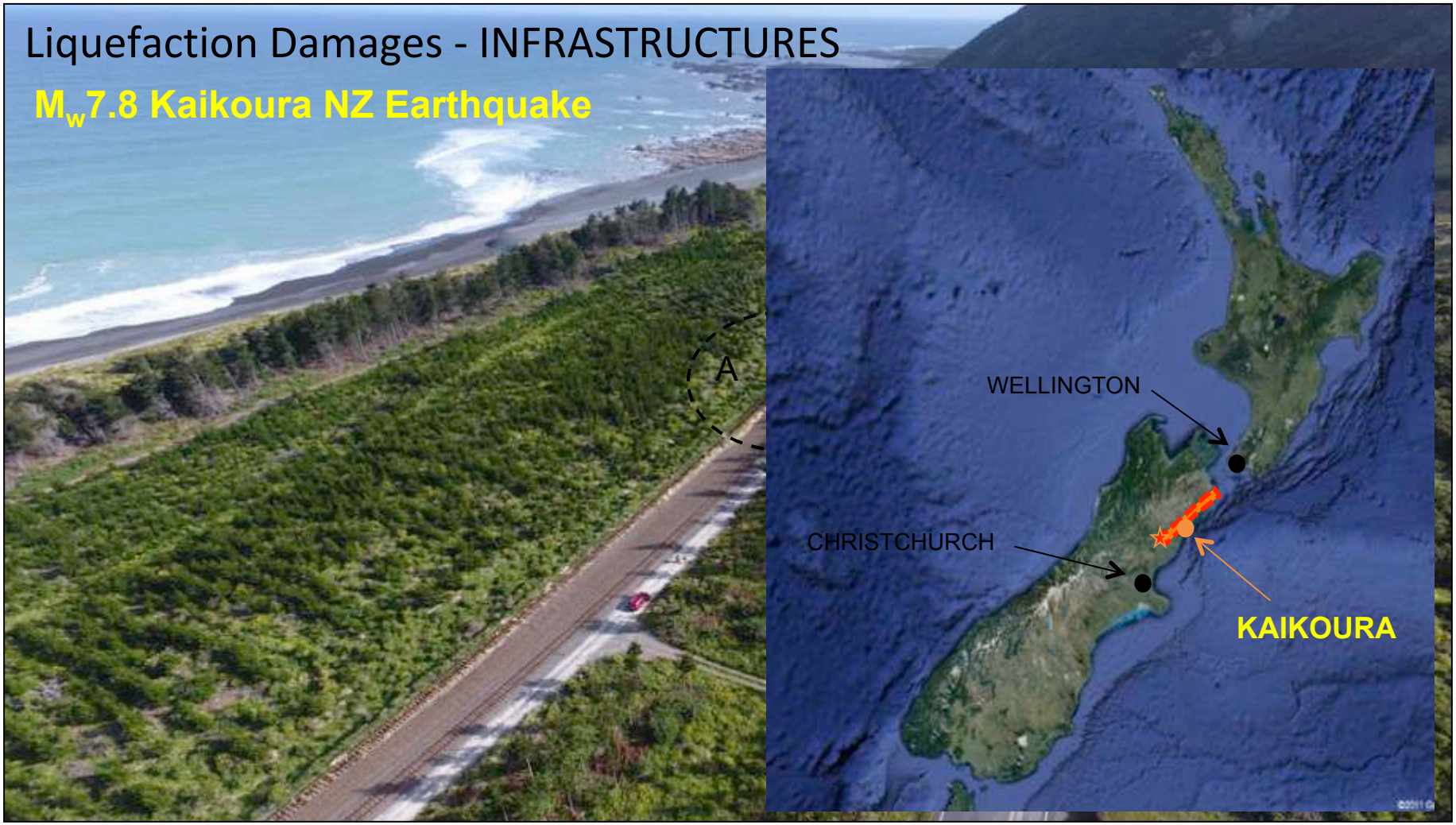

- At least 5 m left-lateral slip and 3 m vertical offset (near the coast)
- Max of up to 6 m vertical offset (inland)

Extensive cracking and residual settlement of river dyke in Katori city, Chiba prefecture, Japan (2011 Great East Japan Earthquake)

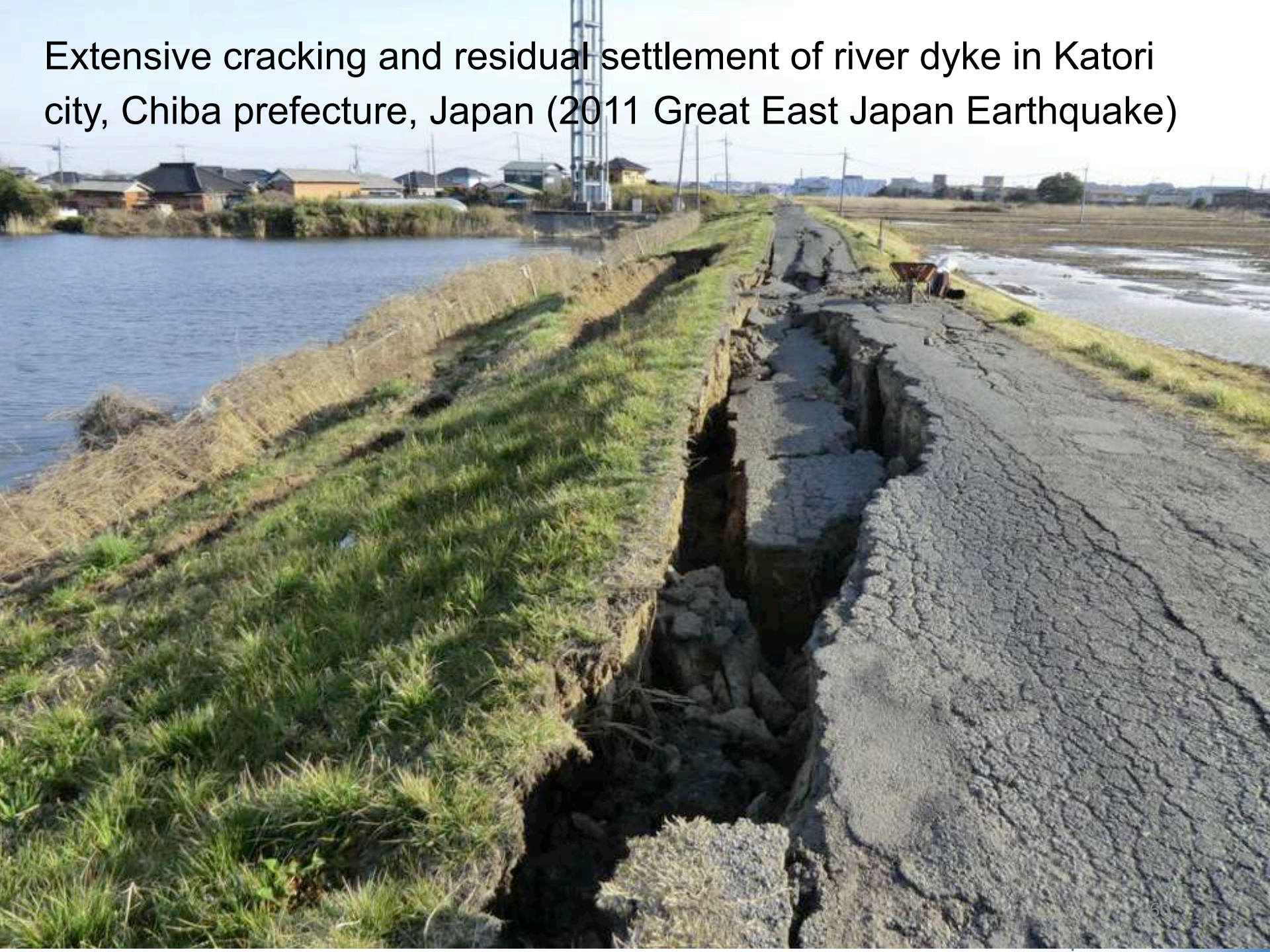

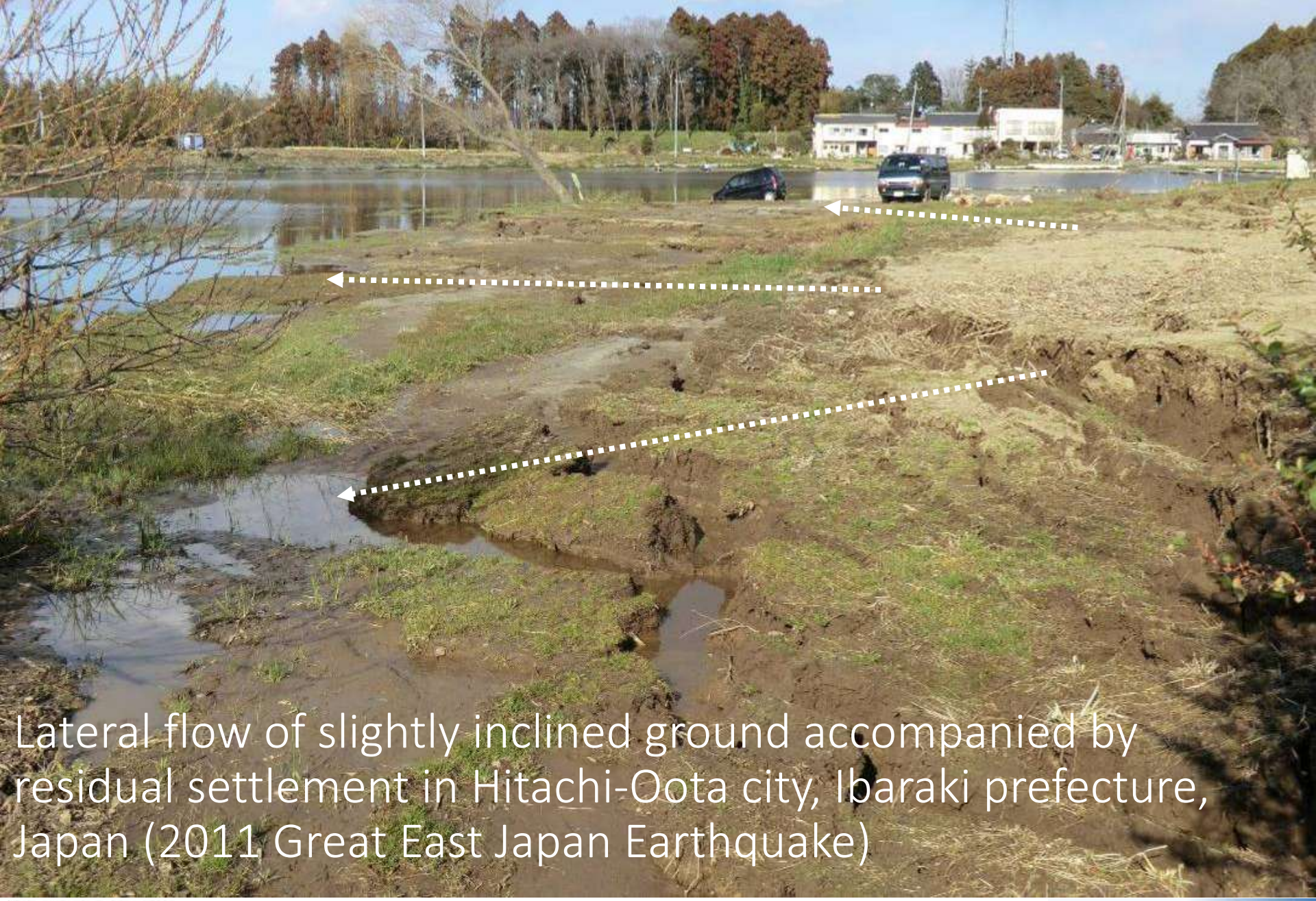

Lateral flow of slightly inclined ground accompanied by residual settlement in Hitachi-Oota city, Ibaraki prefecture, Japan (2011 Great East Japan Earthquake)

liquefACT

[WP2 activities @UPORTO]

LOCALIZED ASSESSMENT OF LIQUEFACTION POTENTIAL (MICROZONATION) AT THE PORTUGUESE EXPERIMENTAL SITE

Low Tagus Valley Site: Benavente and East Vila Franca de Xira

The source of the 1909 Benavente earthquake

Surface evidence of faulting and the historical evidences of liquefied sands

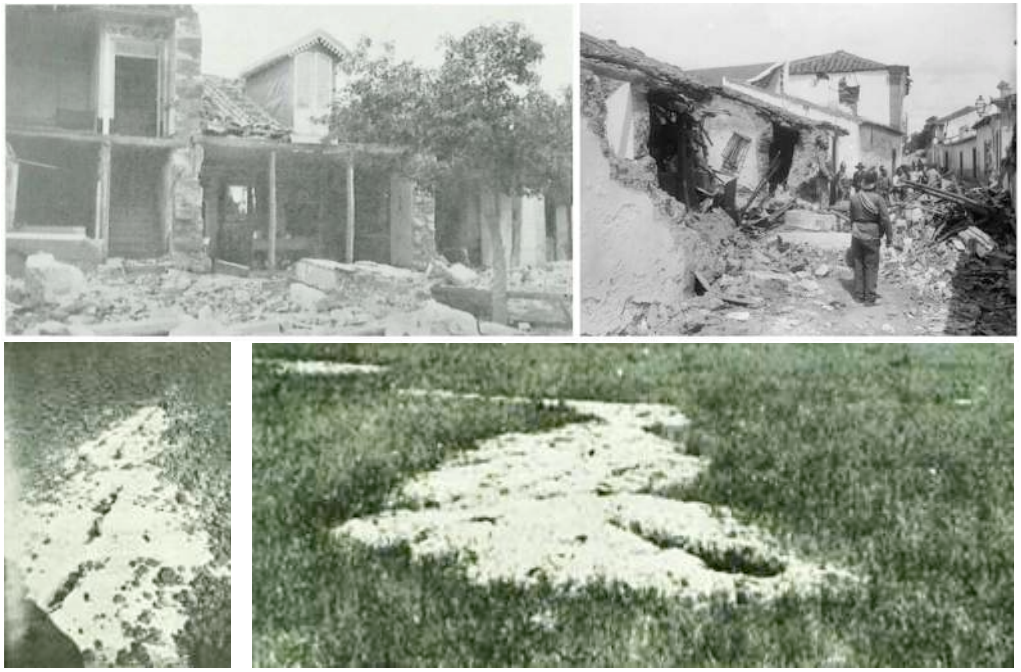

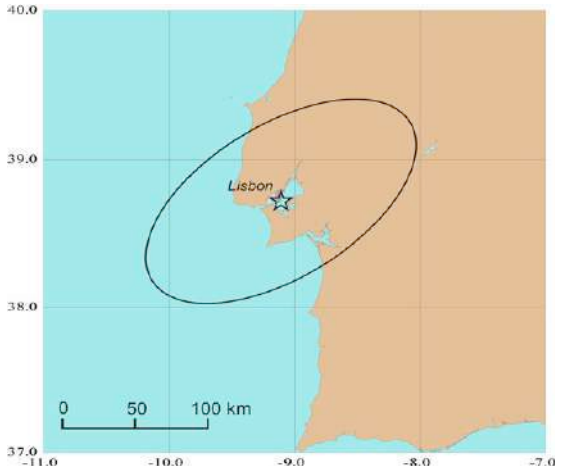

Epicenter location of the 23 April 1909 Benavente earthquake (Cabral et al., 2011)

liquefACT

[WP2 activities @UPORTO]

LOCALIZED ASSESSMENT OF LIQUEFACTION POTENTIAL (MICROZONATION) AT THE PORTUGUESE EXPERIMENTAL SITE

liquefACT

[WP2 activities @UPORTO]

LOCALIZED ASSESSMENT OF LIQUEFACTION POTENTIAL (MICROZONATION) AT THE PORTUGUESE EXPERIMENTAL SITE

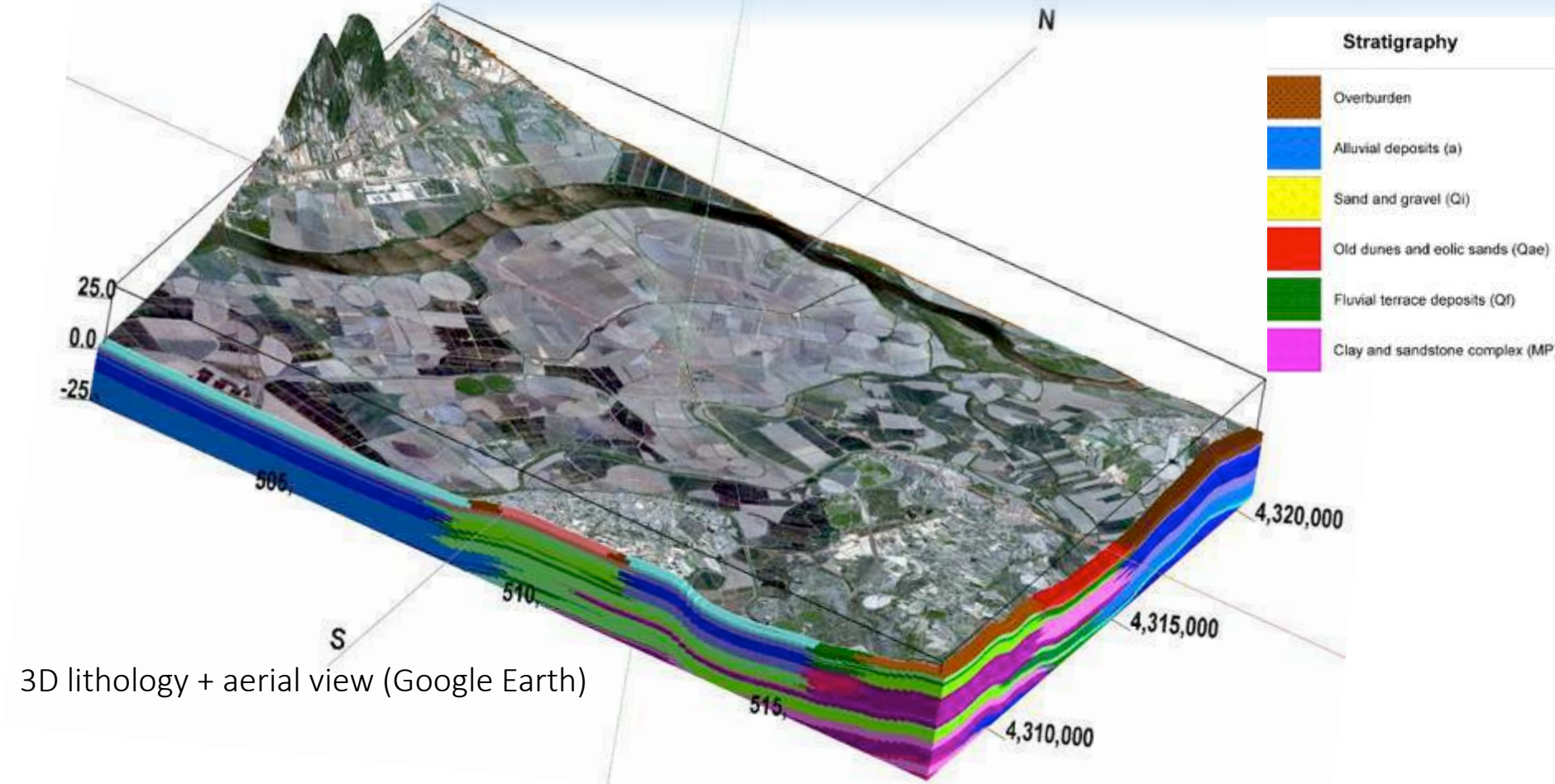

3D lithology + aerial view (Google Earth)

liquefACT

[WP2 activities @UPORTO]

LOCALIZED ASSESSMENT OF LIQUEFACTION POTENTIAL (MICROZONATION) AT THE PORTUGUESE EXPERIMENTAL SITE

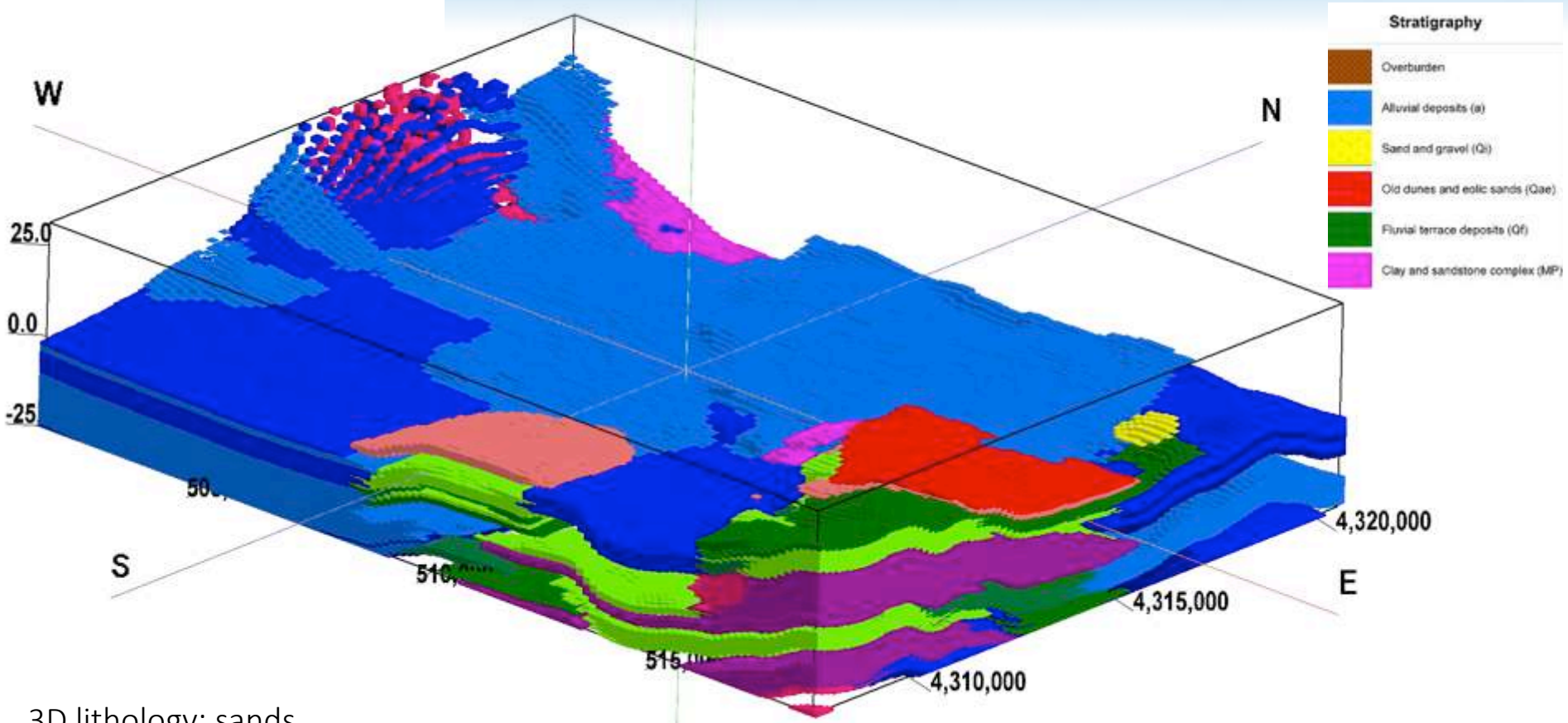

3D lithology: sands

liquefACT

[WP2 activities @UPORTO]

LOCALIZED ASSESSMENT OF LIQUEFACTION POTENTIAL (MICROZONATION) AT THE PORTUGUESE EXPERIMENTAL SITE

EN 1998-1, Eurocode 8/EC8-NA (CEN, 2010)

Factor of safety (Type 1): via SPT

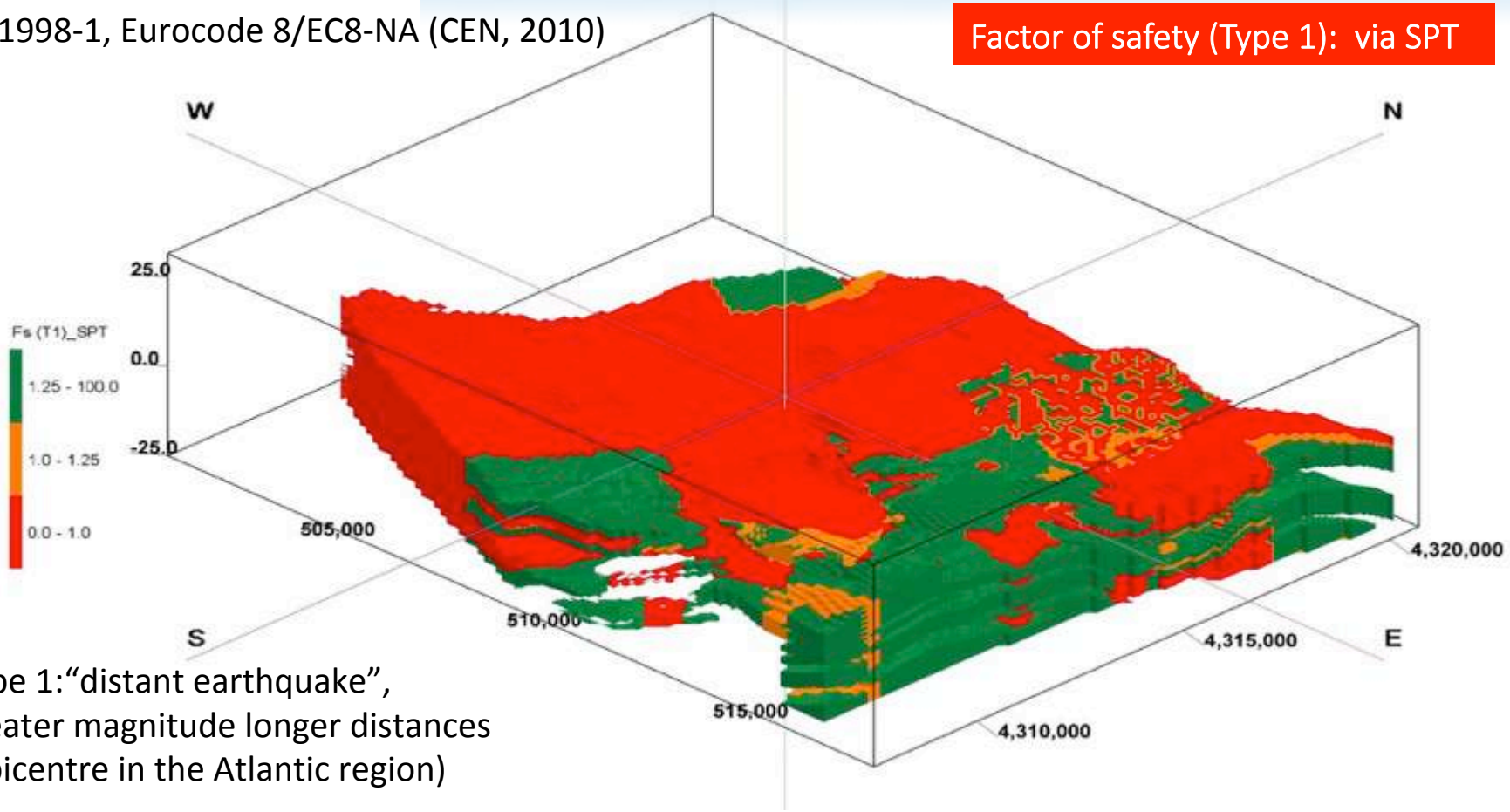

Type 1:"distant earthquake", greater magnitude longer distances (epicentre in the Atlantic region)

liquefACT

[WP2 activities @UPORTO]

LOCALIZED ASSESSMENT OF LIQUEFACTION POTENTIAL (MICROZONATION) AT THE PORTUGUESE EXPERIMENTAL SITE

EN 1998-1, Eurocode 8/EC8-NA (CEN, 2010)

Factor of safety (Type 2): via SPT

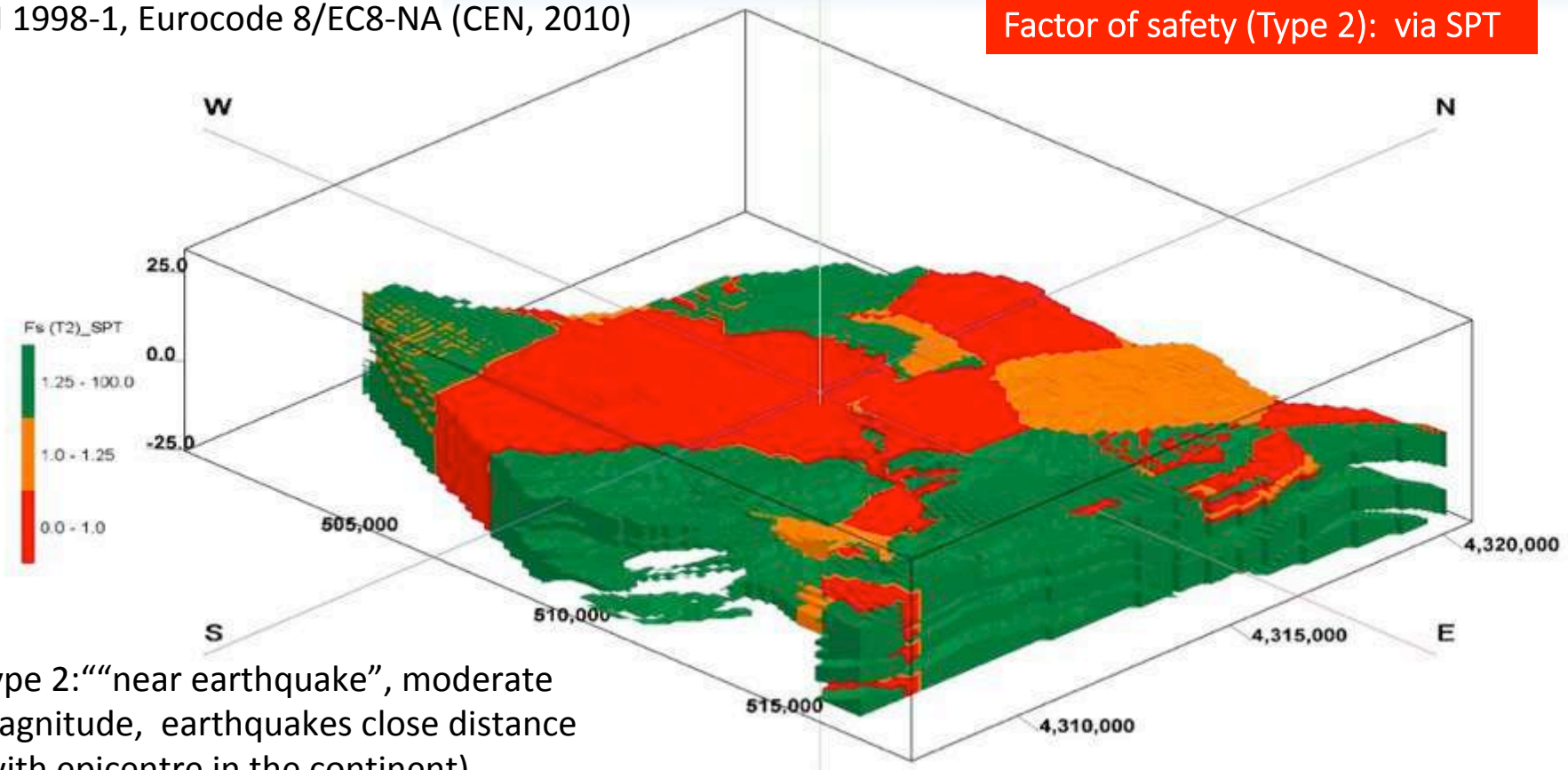

Type 2:““near earthquake”, moderate magnitude, earthquakes close distance (with epicentre in the continent)

Objective: Risk Mitigation R = (H*V)*E

E = Elements subjected to liquefaction risk : CRITICAL INFRASTRUCTURES

- The basic physical and organizational structures and facilities (e.g. **buildings, roads, power supplies**) needed for the operation of a society or enterprise.
- The infrastructure of a country, society or organization consists of the basic facilities such as **transport communications, power supplies,** and **buildings**, which enable it to function.

Pipelines

Public Buildings

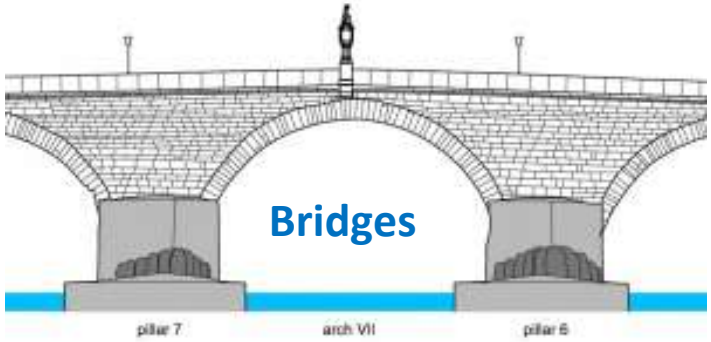

Bridges

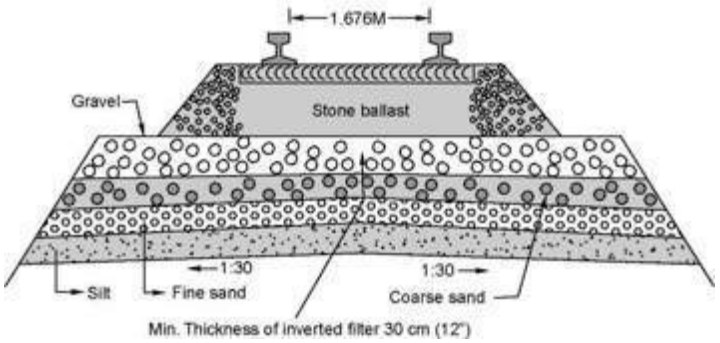

Road & Railway Embankments

NEW and EXISTING INFRASTRUCTURES

GUIDELINES SHOULD BE COMPATIBLE WITH DESIGN EUROCODES (under revision by CEN Technical Comittee 250)

Eurocode 7: Geotechnical design
Eurocode 8: Design of structures for earthquake resistance

- **FOR U.L.S.** $R_D > E_D$ **(Resistance > Effect of Action)**
- **FOR S.L.S.** $E_D < C_D$ **(Effect of Action < its Limiting Value)**

Remediation Technologies should improve resistance R and/or reduce effects E

Note: F is the Action (e.g. earthquake) that produces the **effects E** (**define the effect chain for each typical case**: i.e. exc. pore pressures – seepage – soil strength reduction – deformations – settlements – lateral spreading - global tilting - structural damage, etc.).

Decrease Vulnerabity / Increase Populations Resilience
MITIGATION APROACHES

a) Reduce Soil Susceptibility to Liquefaction

b) Reduce Structures/Infrastrucutres Capacity to withstand liquefaction

From D.O.A. part B

1.4.2.1. Reducing the Site Susceptibility to Liquefaction

The first category includes techniques that improve the liquefaction strength of the soil (***ground improvement techniques***), usually by one or more of the following factors:

1- Densification of the liquefiable soil (to be achieved with any kind of compaction)
2- Stabilization of soil skeleton (to be achieved by different actions)
3- Dissipation of increased excess pore pressure (e.g. by improving drainage capacity)
4- Desaturation of the liquefiable soil

New Zealand Guidelines →

1. Densification
2. Solidification
3. Drainage
4. Reinforcement
5. (Replacement)

Decrease Vulnerabity / Increase Populations Resilience
MITIGATION APROACHES

a) Reduce Soil Susceptibility to Liquefaction
b) Reduce Structures/Infrastrucutres Capacity to withstand liquefaction

From D.O.A. part B

The most common strategies for seismic retrofit of existing structures are:

- restriction or change of use,
- partial demolition and/or mass reduction,
- removal or lessening of existing irregularities and discontinuities,
- addition of new lateral load resisting systems,
- local or global modification of elements and systems,
- seismic demand reduction by means of base isolators or steel dissipating braces.

GUIDELINES WILL CONSIDER ONLY APPROACH

a)

(i.e. where ground improvement can be applied)

CEN Technical Comittee 250

TABLE OF CONTENTS

Tentative…

1. Objective
1.1 Critical Infrastructures
1.2 Liquefaction Risk
1.2 Mitigation Approaches
2. Ground Improvement Techniques
2.1 Densification
2.2 Stabilization
2.3 Drainage
2.4 Desaturation
2.5 Other… ?
3. B.A.T. choice for new & existing infrastructures
3.1 Embankments
3.2 Pipelines
3.3 Bridges
3.4 Buildings
3.5 ….
4. Ground Improvement Design
4.1 Design principles
4.2 Design process
5. Construction control

STANDARD USE OF REMEDIATION TECHNOLOGY AGAINST LIQUEFACTION

Existing codes and guidelines

EUROPE

DESIGN CODES:

Geotechnical Design Eurocode (ongoing revision by TC250/SC7) - *Final Report on Ground improvement by Evolution Group EG 14* (2015)

EXECUTION STANDARDS:

CEN/TC 288 Execution of special geotechnical works

EN 12715:2000 Grouting
EN 12716:2001 Jet grouting
EN 14679:2005 Deep mixing
EN 14731:2005 Ground treatment by deep vibration
EN 15237:2007 Vertical drainage

NEW ZEALAND

GUIDELINES:

Earthquake geotechnical engineering Module 5

Ground improvement of soils prone to liquefaction, NZGS Guidelines (Murashev and Keepa, 2017)

ITALY

GUIDELINES:

Microzonazione sismica - Linee guida per la gestione del territorio in aree interessate da liquefazione (LQ)

APPENDICE A2 – Metodi di mitigazione del rischio dovuto alla liquefazione (Commissione tecnica per la microzonazione sismica, 2017)

JAPAN

Remedial measures against soil liquefaction

From investigation and design to implementation (JGS, 1998)

Geo-hazard during earthquakes and mitigation measures

Lessons and recommendations from the 2011 great east japan earthquake (JGS, 2011)

AVAILABLE TECHNIQUES AND EFFECTS

EFFECTS

TECHNIQUES	REPLACEMENT	DENSIFICATION	CEMENTATION	DRAINAGE	DESATURATION

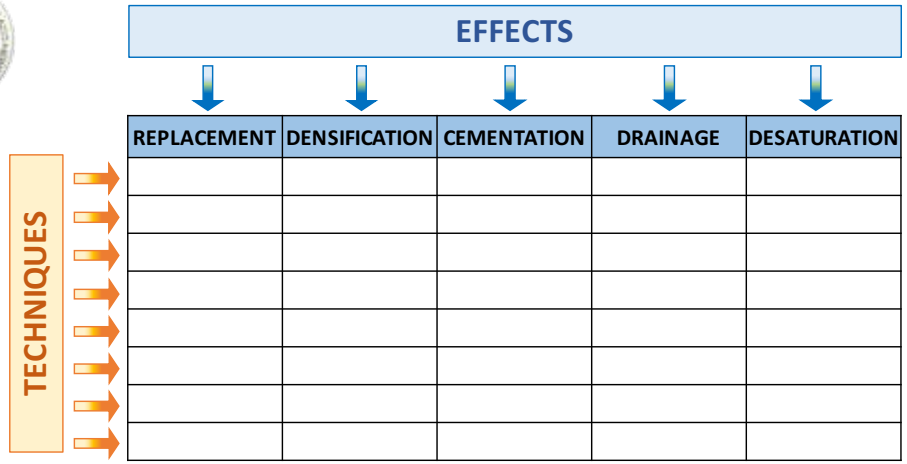

- High Energy Impact Compaction
- Rapid Impact Compaction
- Static/Vibratory Shallow Compaction
- Electric Pulse Compaction
- Blasting
- Compaction Grouting
- Vibro-compaction
- Deep Dynamic Compaction
- Dynamic Replacement
- Deep Soil Mixing
- Stone Columns (Vibro Displacement - Replacement)
- Sand Columns

- Jet Grouting
- Resin Injection
- Permeation Grouting
- Bacteria Permeation
- Earthquake Drains
- Gravity Drains
- Vacuum-pump Drains
- Dewatering
- Dense Gravel Replacement
- Stabilised Soil Replacement
- Surcharging
- Ground Freezing/Heating
- Vacuum Consolidation
- Electro-osmosis
- Granular Stabilisation
- Granular Mixing
- Chemical Stabilisation
- Physical Stabilisation
- Electro-chemical Stabilisation
- Steel/Wood/Concrete Columns
- Geosynthetic Encased Columns
- ……

State of the Art Liquefaction Mitigation Measures

Is EILD counteracted by increasing resistance by itself or is it a risk that can be minimized by reduce pore pressure build up during seismic

- **To increase the safety factor for the liquefaction mechanism**

  Codes (e.g. EC) suggest limit values of FS=CRR/CSR

  Empirical correlations with synthetic parameters available

- **To limit to a tolerable value the reduction in the safety factor for bearing capacity of a structure**

  Analytical tools available

- **To reduce to a tolerable value the induced settlements**

  Analytical tools available

GROUND IMPROVEMENT DESIGN

Design Principles

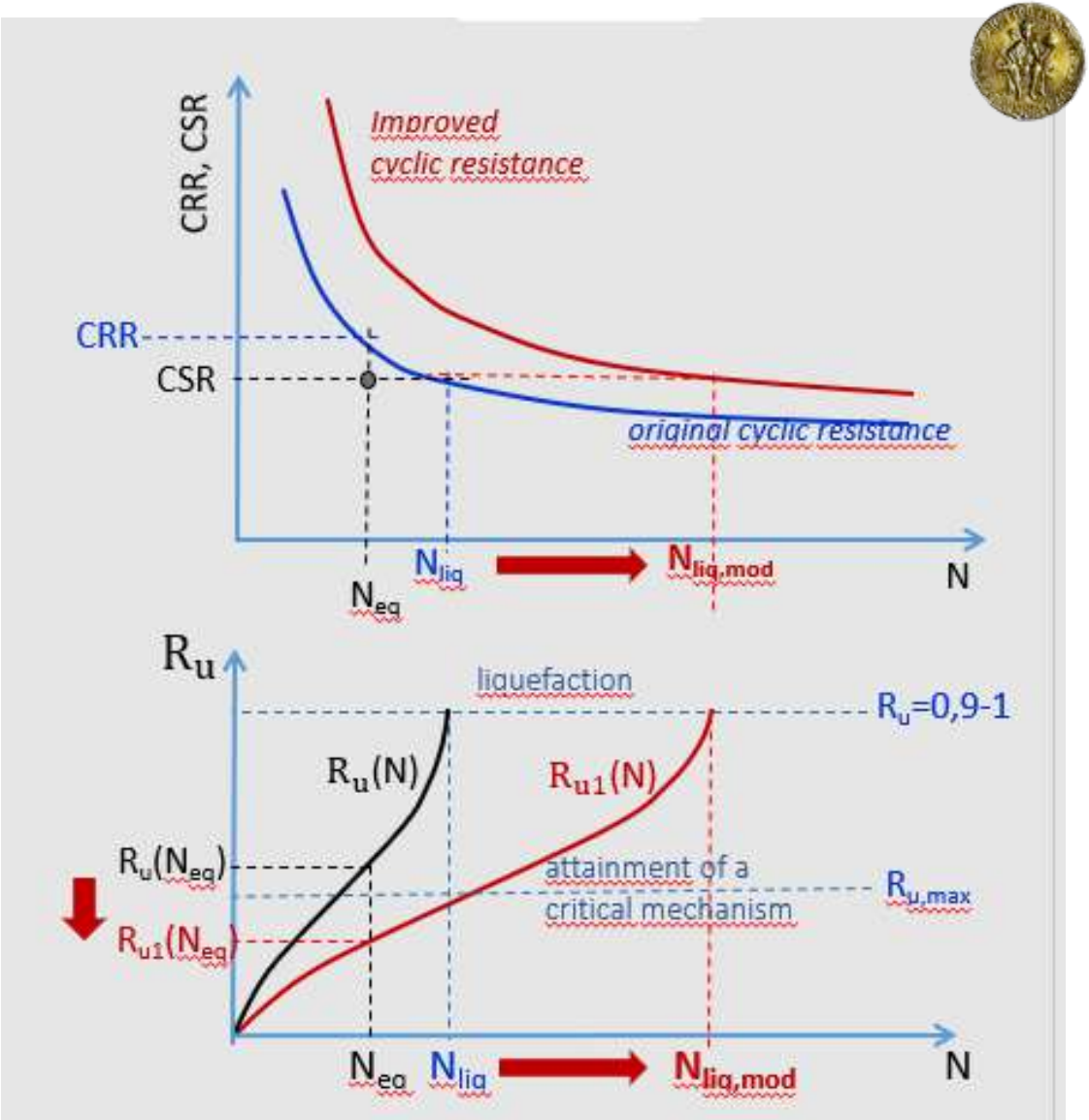

CONSTRUCTION CONTROL

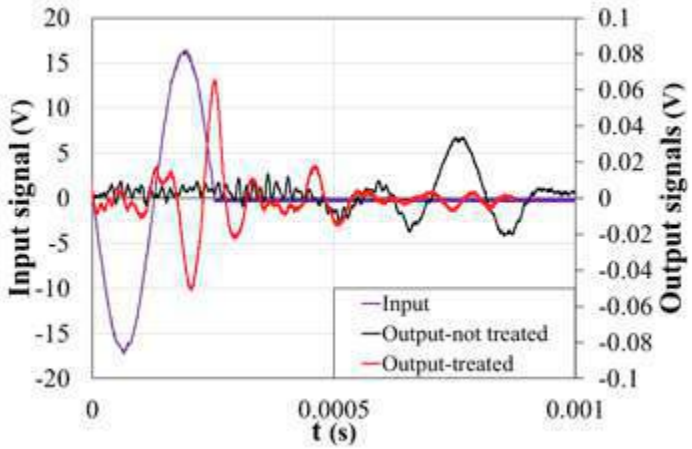

Quality assurance

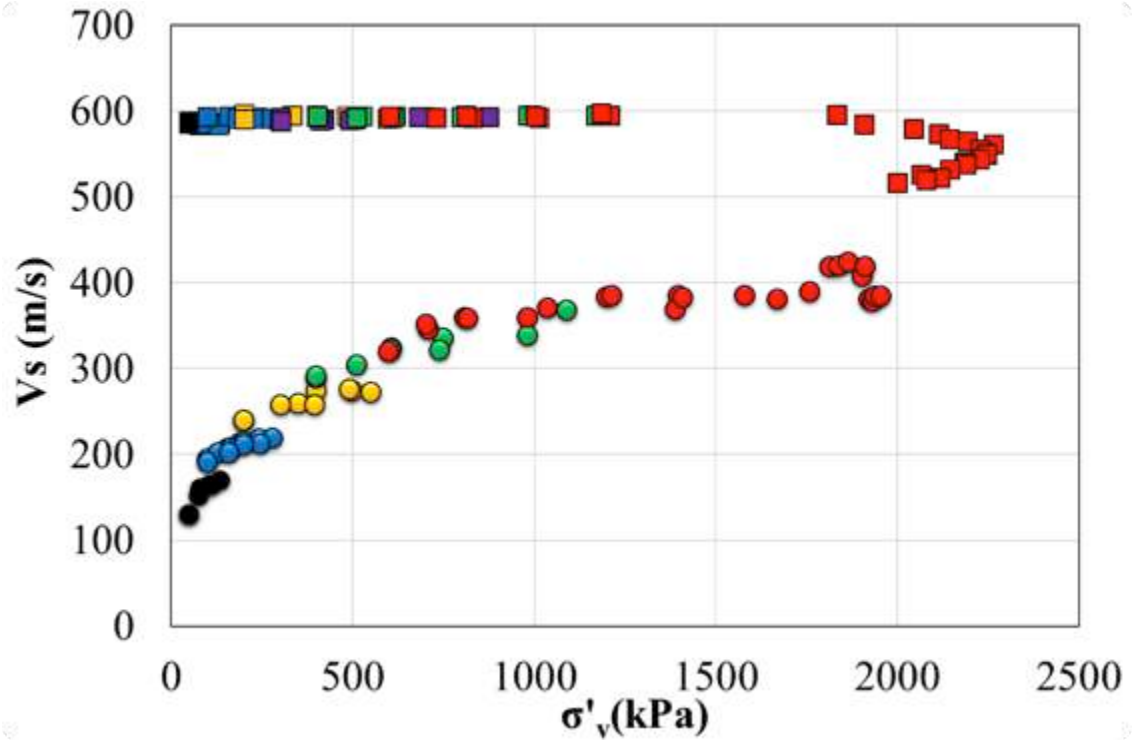

Comparative Analysis of State of the Art Liquefaction Mitigation Measures

Liquefaction mitigation techniques	Lab tests to done and ongoing on untreated/treated soil	ISSUES
Densification	Cyclic simple shear & Triaxial tests Resonant column shear tests	• Choice of design parameters in order to have a homogeneous treatment
Addition of laponite / / colloidal silica	Cyclic simple shear & Triaxial tests Resonant column shear tests	•Long term behaviour •Interaction with ground water •Injection technologies
Low Desaturation	Cyclic simple shear & Triaxial tests Resonant column shear tests	• Lab desaturation techniques •In situ desaturation techniques

Field trials at the selected case study pilot testing site

To demonstrate the possible achievement of up-scaling the proposed technologies, one field trial site will be implemented in Italy by TREVI.

only 2 of 3 technologies

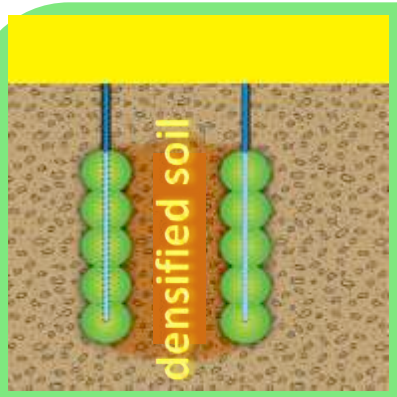

compaction grouting

BLASTING

MEGA-SHAKERS

liquefaction?

induced partial saturation

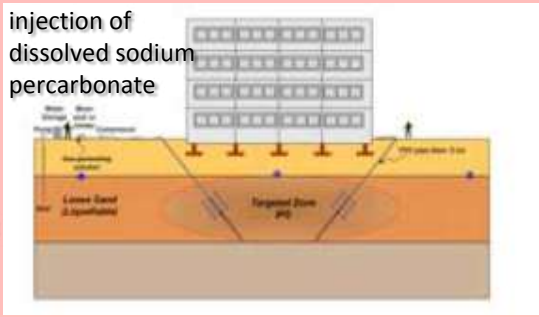

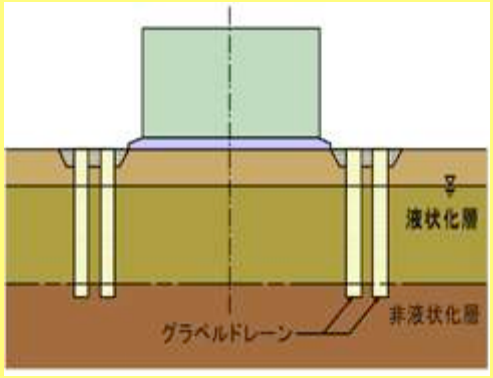

vertical & horizontal drains

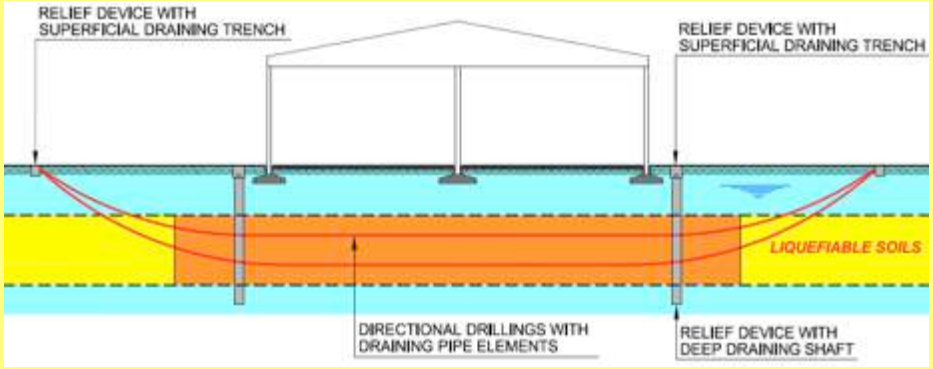

Indução de Saturação Parcial: *Induced Partial Saturation (IPS)*

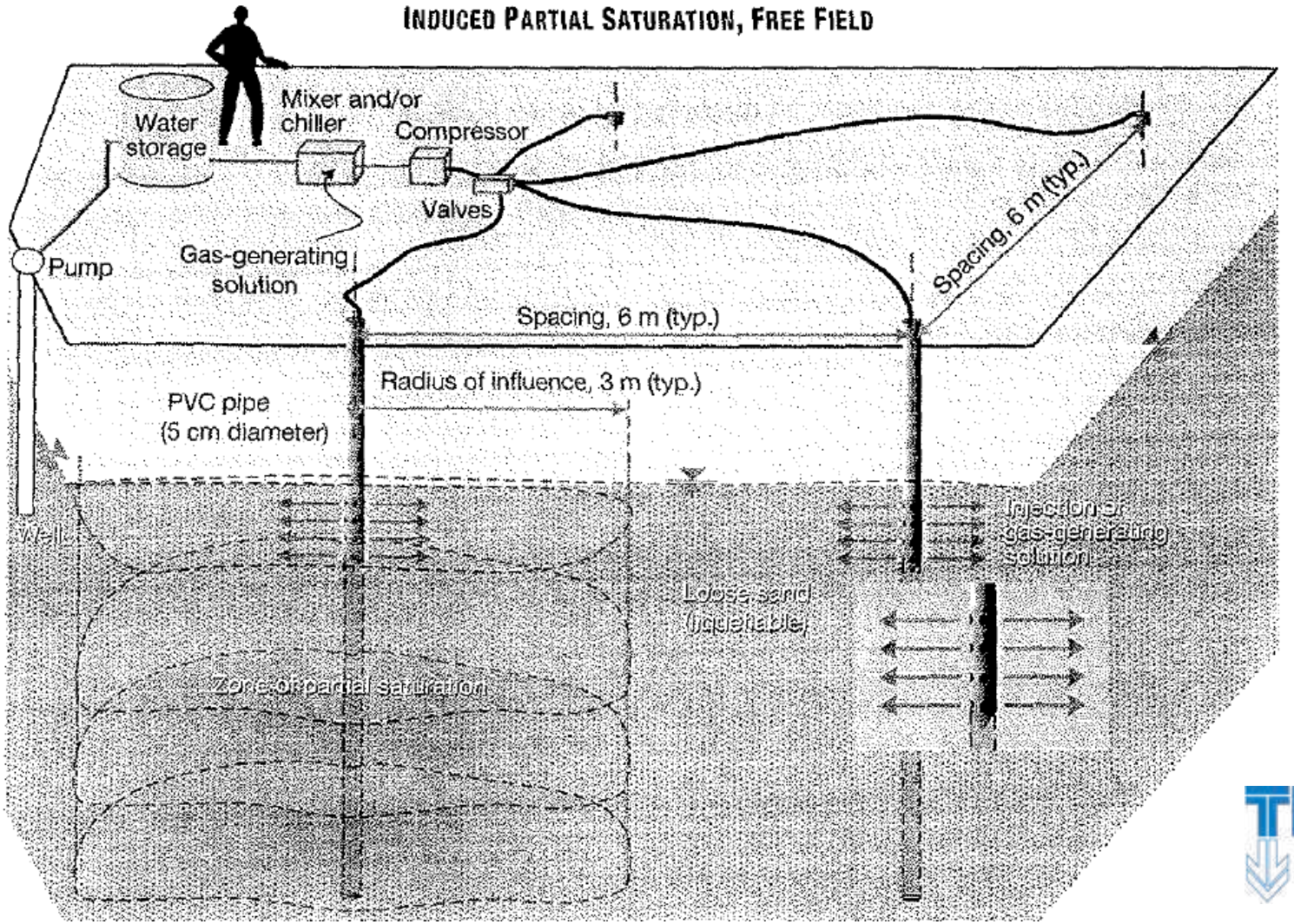

IPS (Indução de Saturação Parcial) por químicos

Uma baixa concentração de solução química compatível com o meio ambiente (ex: percarbonato de sódio) é dissolvida em água e injetada no solo a ser tratada.
A mistura espalha-se para o solo, libertando pequenas bolhas de oxigênio que ficam presas nos poros entre as partículas de areia, sem perturbar o solo.

Investigações recentes em laboratório mostram que as bolhas de gás geradas entre os grãos permanecem presas mesmo na presença de gradientes verticais ou horizontais

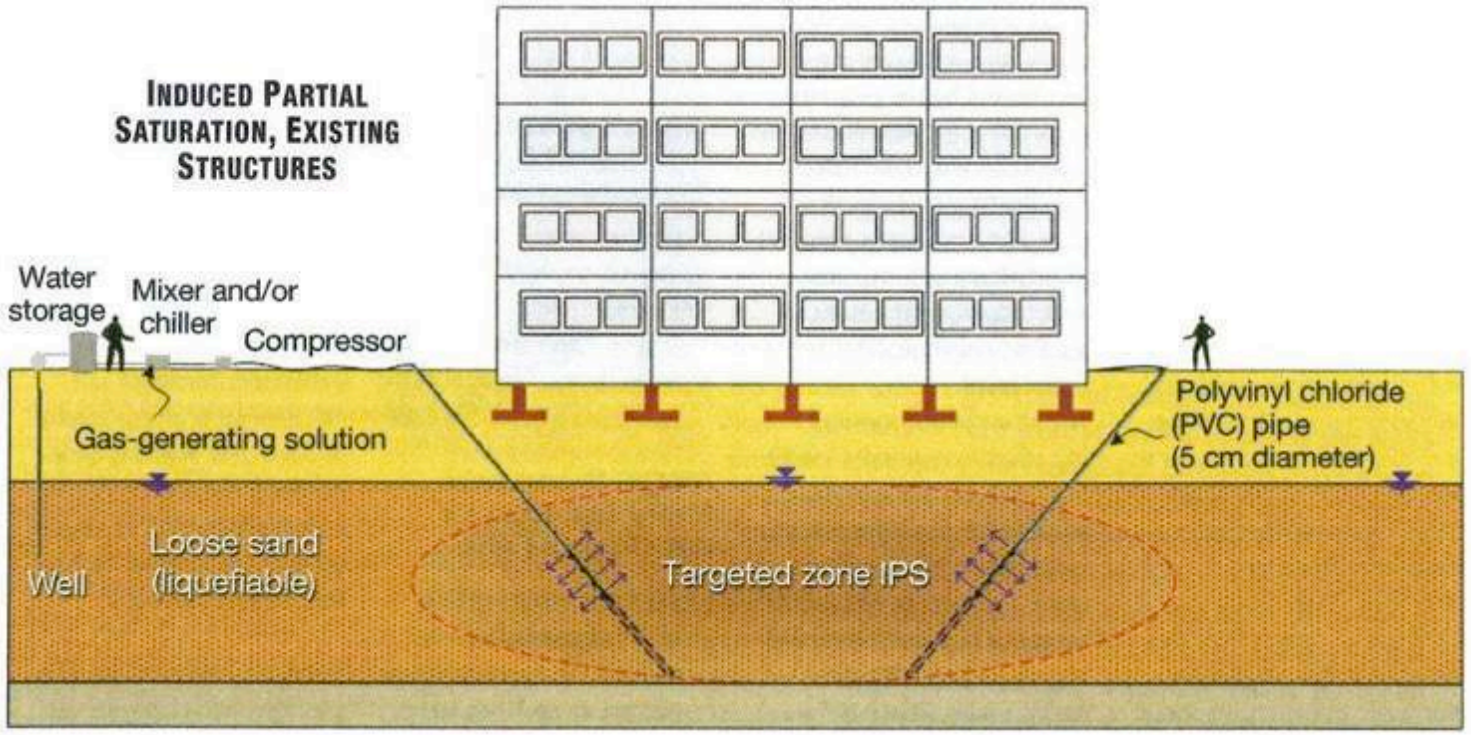

LOW PRESSURE GROUTING OF NANOSILICATE

Why colloidal silica?

- It is a mineral suspension
- Insoluble S_iO_2 particles (4 - 16nm)

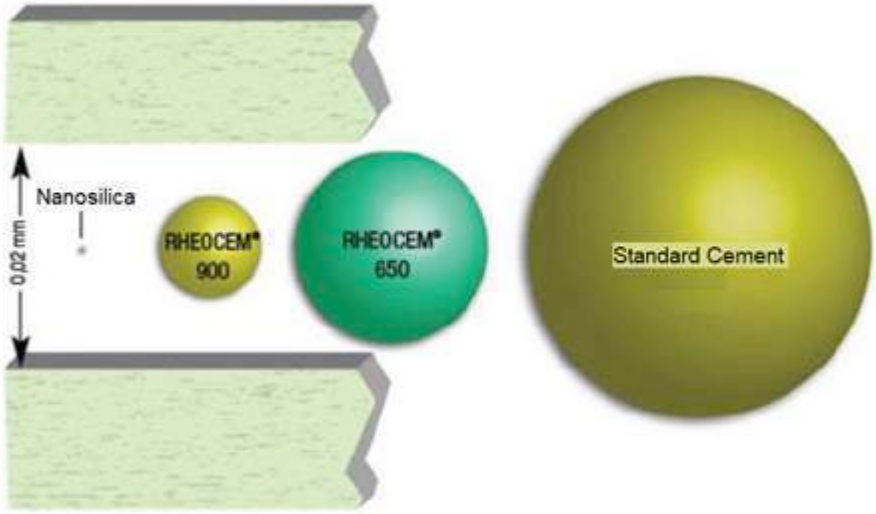

- Common grouting materials

LOW PRESSURE GROUTING OF NANOSILICATE

Why colloidal silica?

- It is a mineral suspension
- Insoluble S_iO_2 particles (4 - 16nm)
- **Low viscosity**

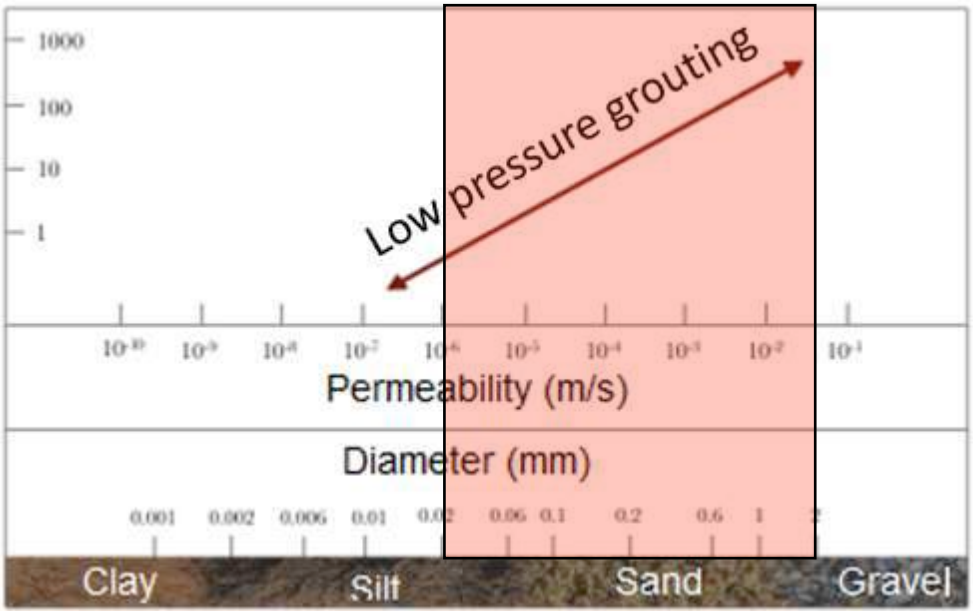

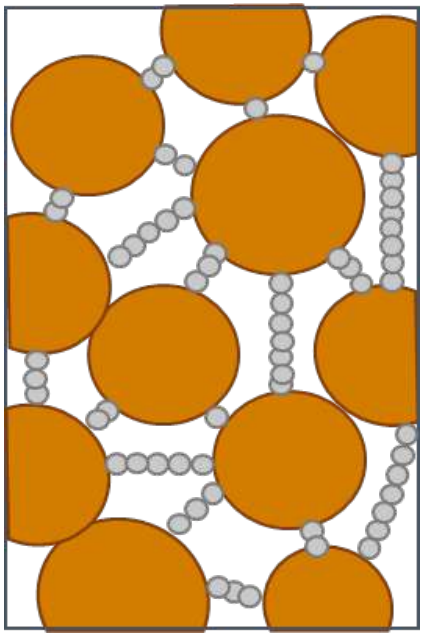

Treated material's structure

LOW PRESSURE GROUTING OF NANOSILICATE

Materials

Fossanova sand:

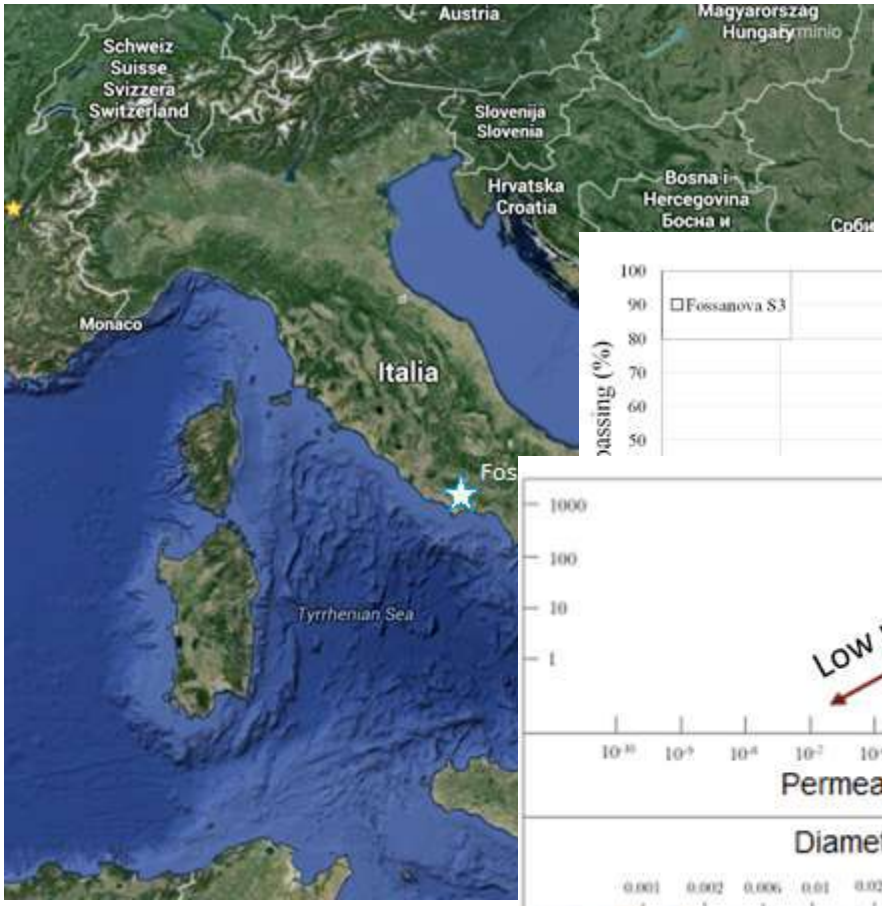

- Google Earth image

LOW PRESSURE GROUTING OF NANOSILICATE

Colloidal silica + sand

Case	Fractions of the different components (%)		
	Nanosilica product	Activator	Water
a	83.3	16.7	-
b	16.6	16.7	66.7
c	8.3	16.7	75.0

a)

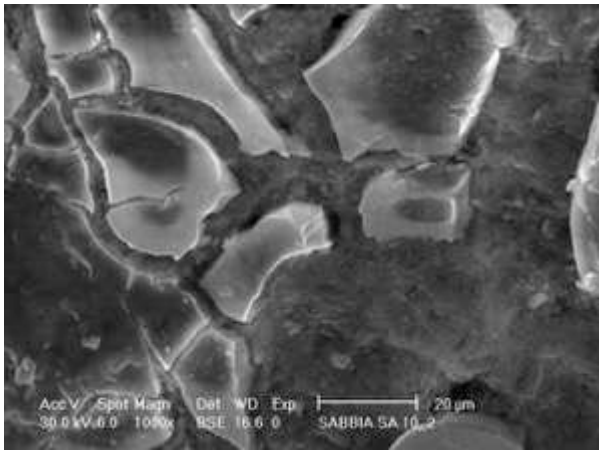

b)

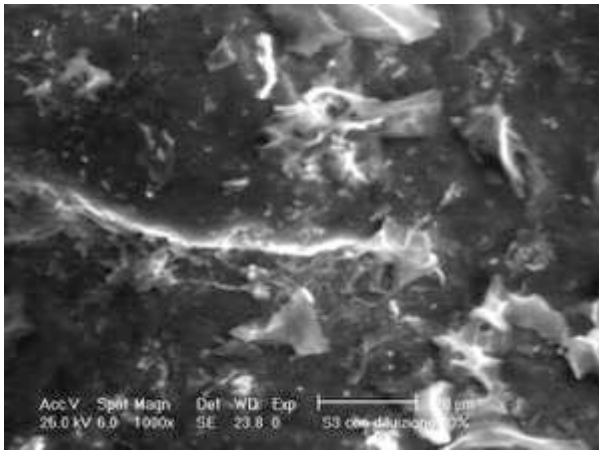

c)

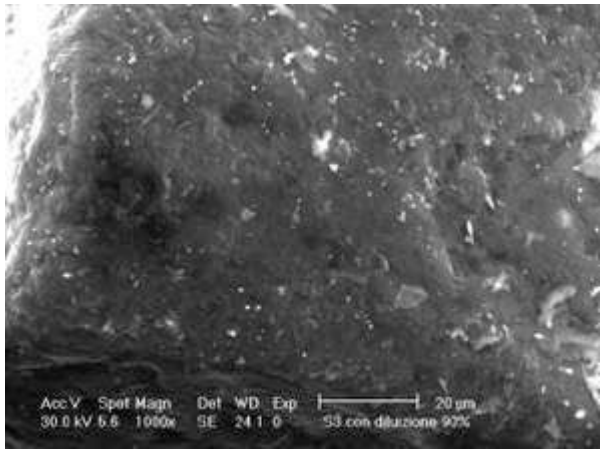

- SEM images of the material treated with decreasing concentration of silica

LOW PRESSURE GROUTING OF NANOSILICATE

Ex. of results: Colloidal silica + sand

- Experimental program on relatively dense specimens

ID	e_0	D_{r0} (%)	σ_c (kPa)	Δq (kPa)	CSR	w_s (%)	DF (%)	n_{liq}
6	0.61	61.16	100	50	0.25	5	56	58
7	0.62	58.26	100	60	0.30	5	56	12
8	0.63	55.36	100	70	0.35	5	56	6

- Experimental program on relatively dense

ID	e_0	D_{r0} (%)	σ_c (kPa)	Δq (kPa)	CSR	w_s (%)	DF (%)	n_{liq}
13	0.72	29.28	200	50	0.13			17
14	0.73	26.38	200	80	0.20	5	56	4
15	0.71	32.17	200	60	0.15	5	56	17
16	0.74	23.48	200	50	0.13	5	56	25
17	0.70	35.07	200	40	0.10	5	56	110

The preformed study prove the effectiveness of low pressure grouting of nanosilica in reducing the liquefaction susceptibility of sand.

What it is still to be done ?

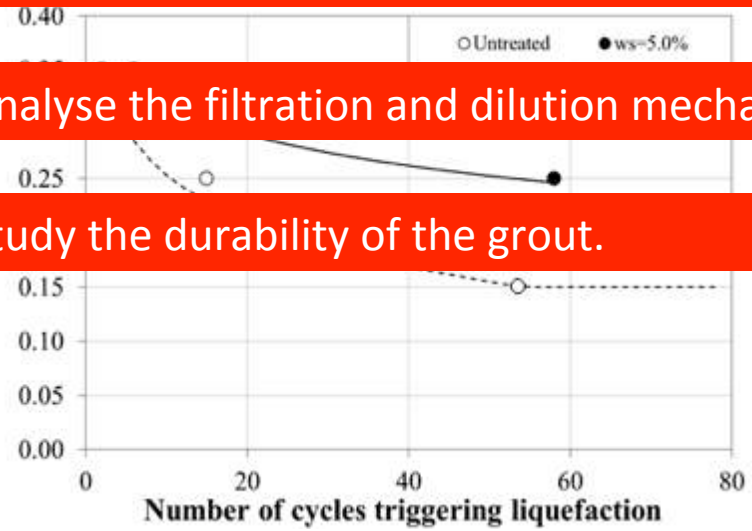

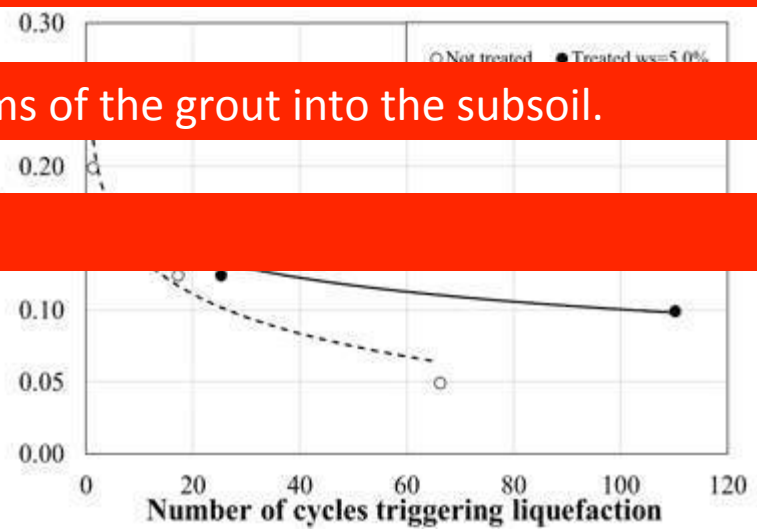

Analyse the filtration and dilution mechanisms of the grout into the subsoil.

Study the durability of the grout.

ADDITION OF FINES - Laponite

University of Napoli Federico II
UNINA

Laponite: *synthetic silicate nanoparticles* ⟶ RD (Na+0.7[(Si8Mg5.5Li0.3)O20(OH)4]-0.7)

- extremely fine
- when added to water, it forms a low-viscosity supension (μ_0<5 cP).
- after a period of time (gel time) it transforms into a high-viscosity gel.
- additives modify gel time (in our case: SPP = sodium pyrophosphate).

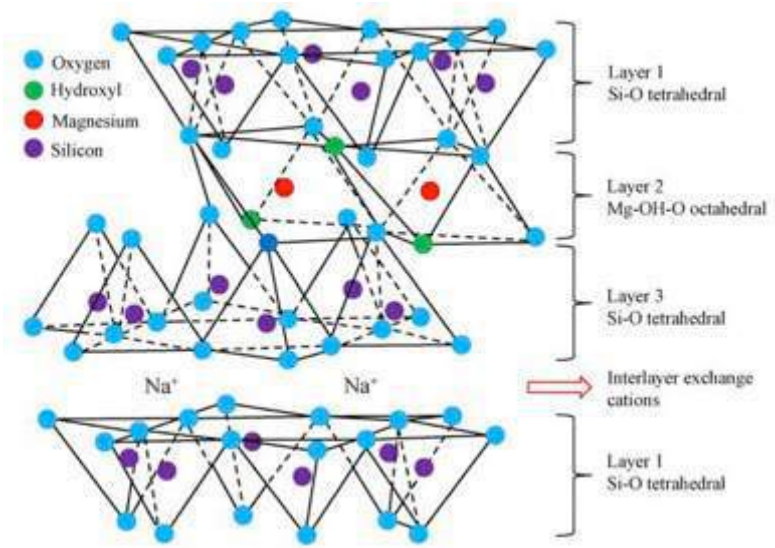

$t > t_{gel,time}$

ADDITION OF FINES - Laponite

University of Napoli Federico II
UNINA

Test	Fluid	Concentration lap (%)	Concentration SPP (%)
PV1	water+lap	1.5	-
PV2	water+lap	3	-
PV3	water+lap+SPP	3	0.06
PV4	water+lap+SPP	3	0.03

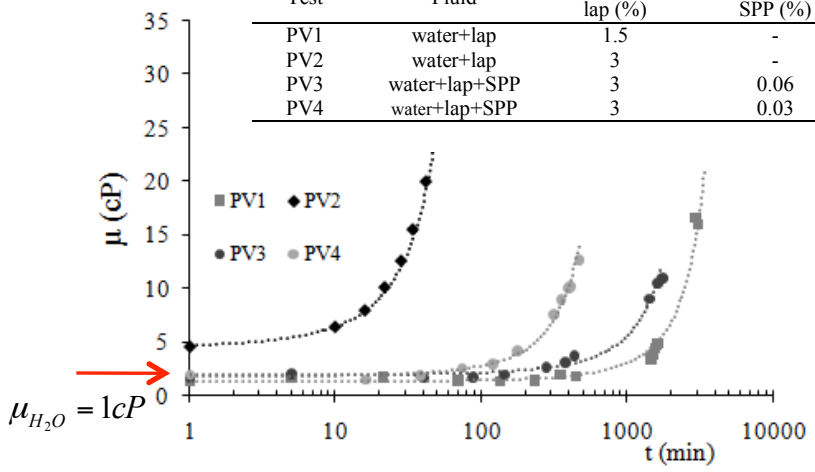

Permeability (cm/sec)	Groutability
$\leq 10^{-6}$	Ungroutable
10^{-5} to 10^{-6}	Groutable with difficulty by grouts with viscosity < 5 cP Ungroutable with grouts having viscosity > 5 cP
10^{-3} to 10^{-6}	Groutable with low viscosity grouts, but difficult with grouts with a viscosity > 10 cP
10^{-1} to 10^{-3}	Groutable with all commonly used chemical grouts
$\geq 10^{-1}$	Requires suspension grouts or chemical grouts containing a filler material

coefficient of permeability

$$k_g = \frac{\gamma_g \cdot \mu_w}{\gamma_w \cdot \mu_g} k_w \approx \frac{1}{\mu_g} k_w$$

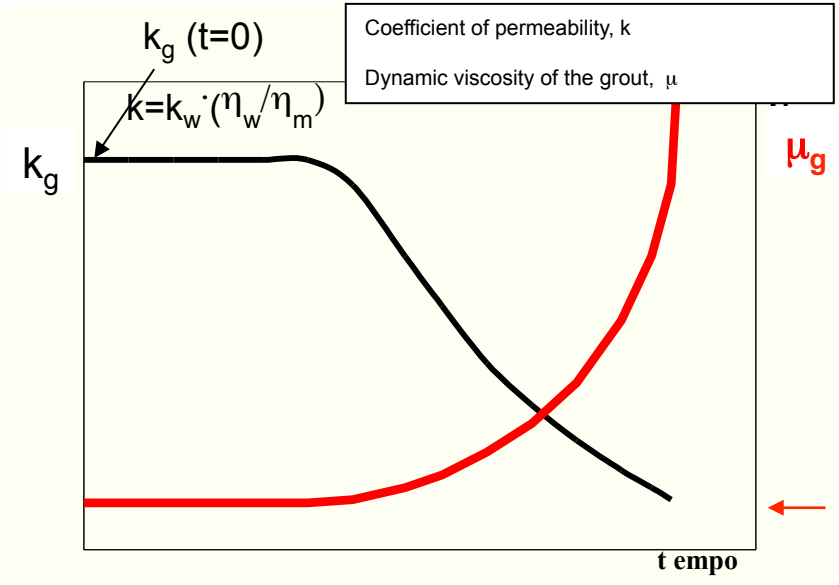

$t_{injection}$

ADDITION OF FINES - Laponite

University of Napoli Federico II
UNINA

Newtonian fluid – permeation process

Constant injection pressure

$$t = \frac{\gamma_g \cdot n}{4 \cdot p \cdot k_g}\left(2 \cdot \ln\left(\frac{R}{R_0}\right) \cdot R^2 + R_0^{\,2} - R^2\right)$$

Constant flow rate

$$t = \frac{\pi \cdot n}{q}\left(R^2 - R_0^{\,2}\right)$$

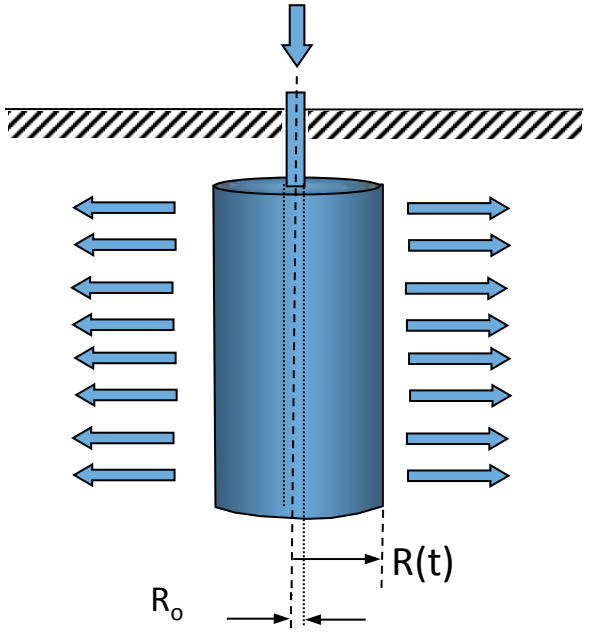

Once μ(t) is given, t_{max} is known and so is $R(t_{max})$. Spacing to be decided on treatment goal (massive treatment, lattice walls, single columns)

TREATED SOIL CHARACTERIZATION

Leigthon Buzzard sand: **addition of laponite**

University of Napoli Federico II
UNINA

Sand (Dr=40%, σ'_c=50 kPa): **CSR=0.128, N_{liq}=12**
Sand/Laponite (Dr=40%, σ'_c=50 kPa): **CSR= 0.135, N_{liq}=38**

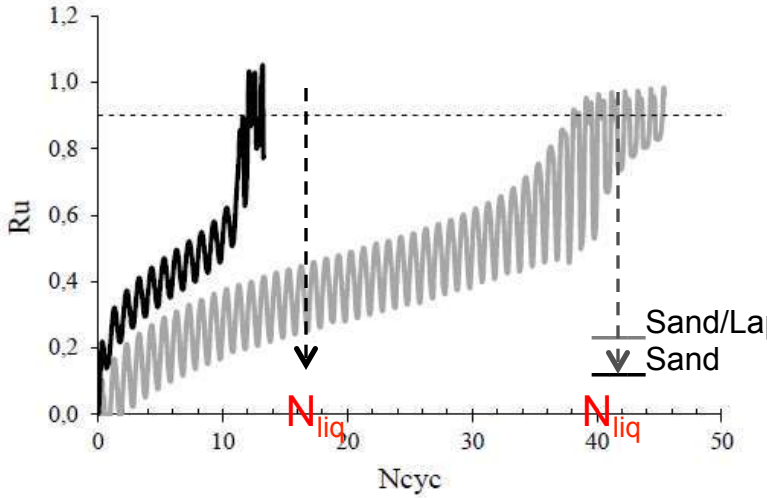

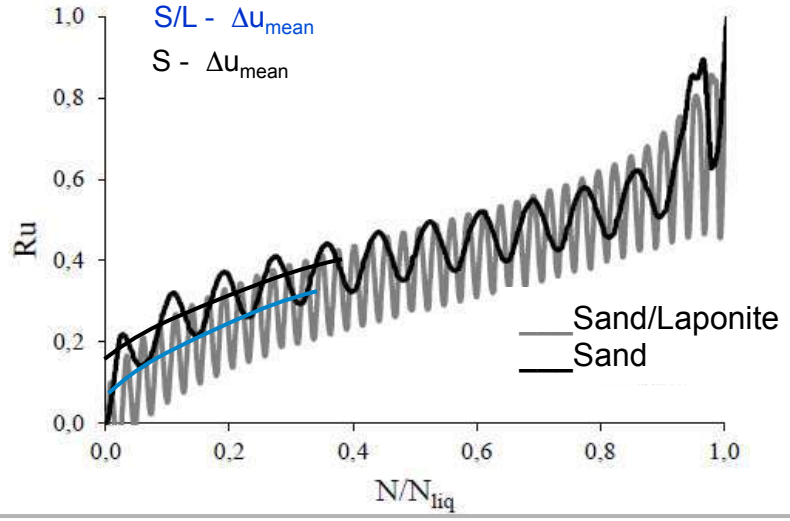

- **The treated specimen liquefies at a large N_{cyc}**
- **The gel-like structure** of the laponite gel **reduces the pore pressure build up**.
- In laponite/sand specimen, the **mean value of the pore pressure increments** in each cycle (Δu_{mean}) **is lower** than in untreated specimen.

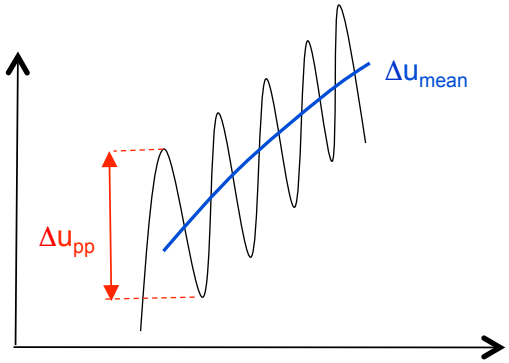

TREATED SOIL CHARACTERIZATION

Leigthon Buzzard sand: **addition of laponite**

University of Napoli Federico II
UNINA

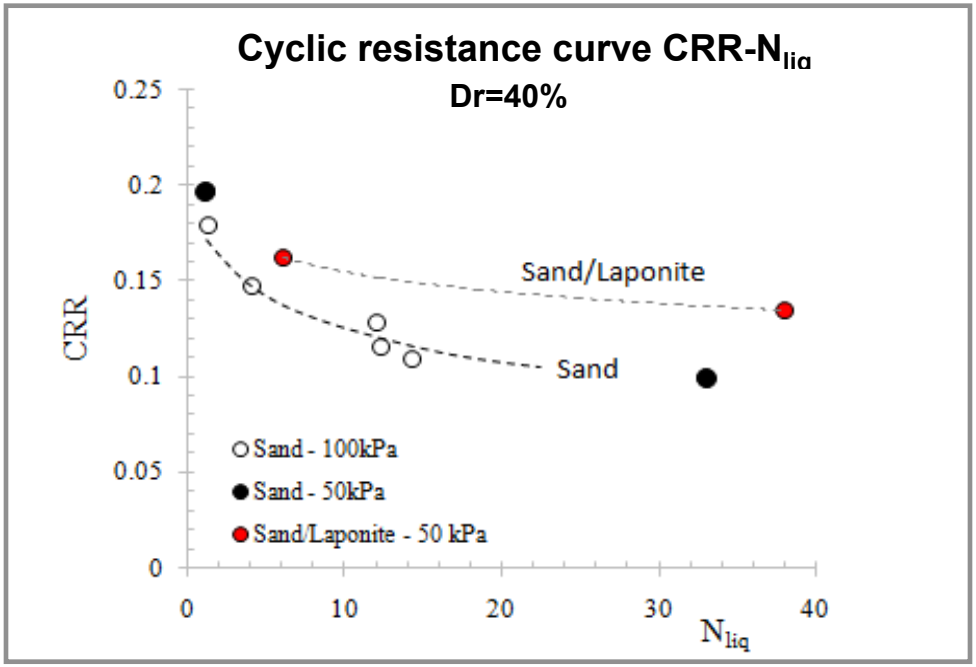

A very low content of laponite (W_{lap}/ W_{sand}=1%) improves the liquefaction resistance of the sand

- **The gel-like structure** of the laponite reduces the volumetric straining during cyclic loading and therefore **reduces the pore pressure build up**
- SEM analysis have **allowed to understand the interaction mechanism** between sand grains and laponite gel.
- **Cyclic Triaxial Tests and Resonant Column Shear** Tests on treated specimens gave **consistent values of CRR increase**

PARTIAL DESATURATION

High desaturation

Limited desaturation

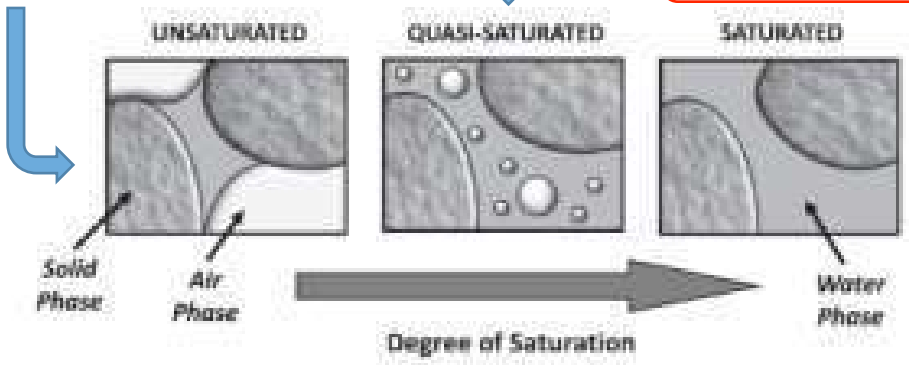

Possible techniques:

- electrolysis;
- chemical method;
- microbial method;
- applying a suction (only in the lab);
- carbon dioxide procedure (only in the lab).

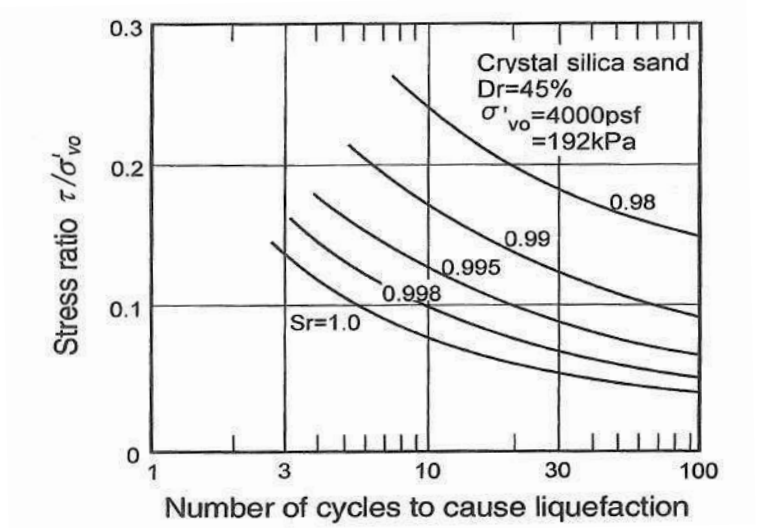

Martin et al. (1978)

PARTIAL DESATURATION

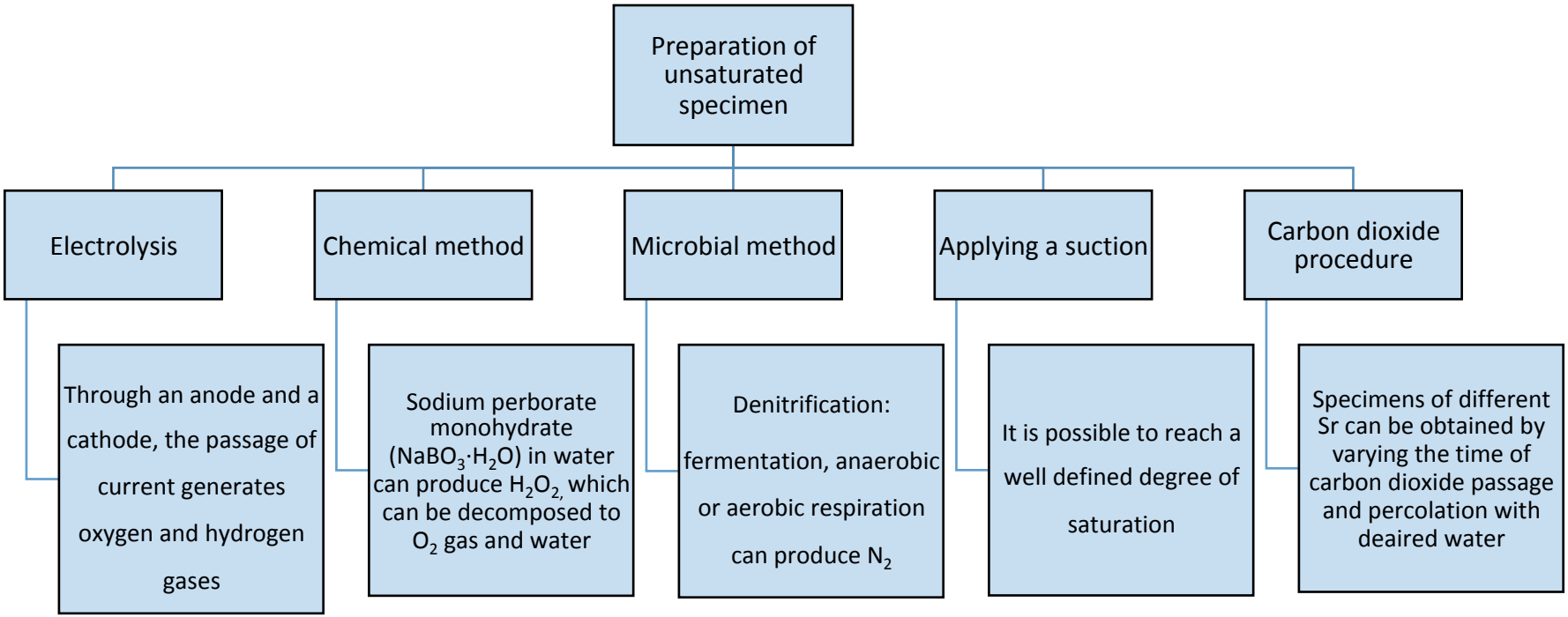

- It is difficult to control lab conditions at very high degrees of saturation
- There is very little (if any) experience worldwide on site

DESATURATION

The presence of little gas bubbles increases the volumetric compressibility of the pore fluid and thus reduces pore pressure build-up.

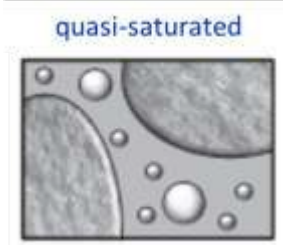

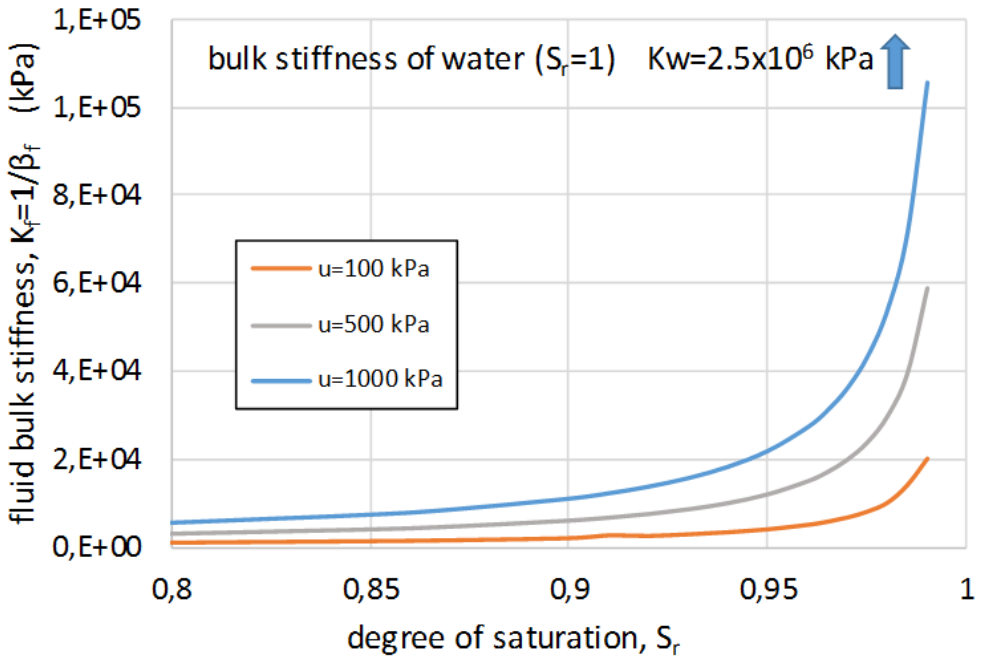

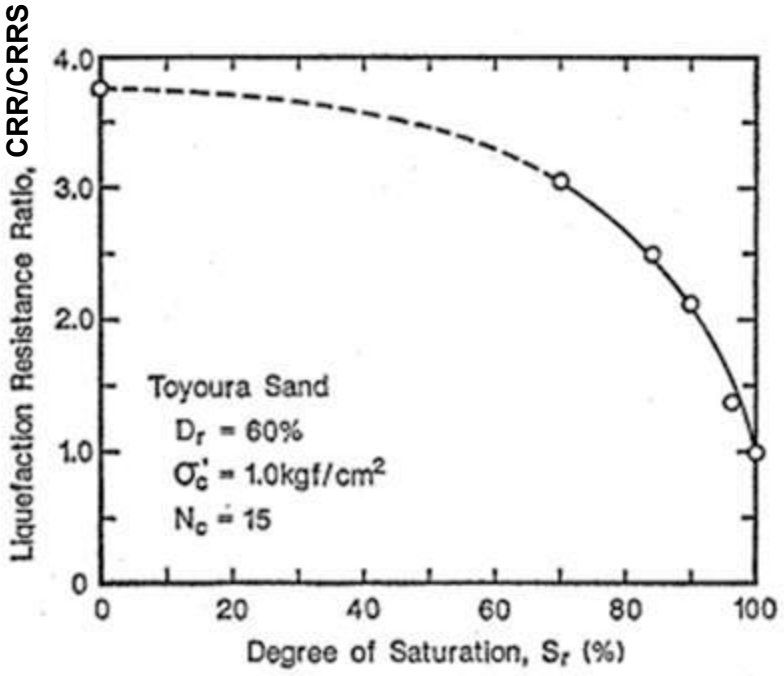

EQUIPMENT

Triaxial cell (Bishop&Wesley and Tokio U.)

Cyclic simple shear purchased with Liquefact funds

Untreated and treated soil

Sand	σ'_c (kPa)	D_R (%)	S_R (%)	N° tests	Apparatus
SA	50	45	100	4	TX-Bishop&Wesley
SA	50	60	100	3	TX-Bishop&Wesley
SA	50	45	55	3	TX-Japanese
SA	50	65	87	6	TX-Japanese
PdC	50*	43	100	2	Cyclic simple shear
PdC	100*	43	100	2	Cyclic simple shear
PdC	50*	43	97	1	Cyclic simple shear
PdC	50*	43	90	2	Cyclic simple shear

Desaturation

Desaturation

*K_0 consolidation

CRR increases as Sr decreases

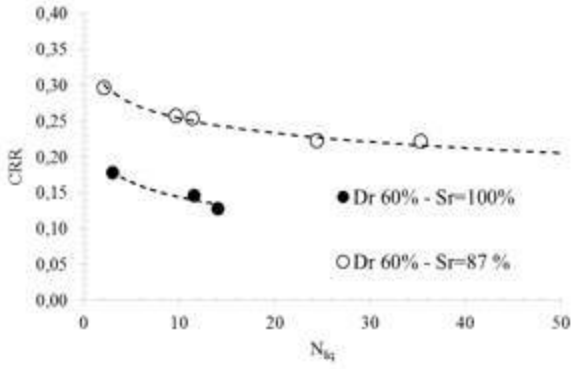

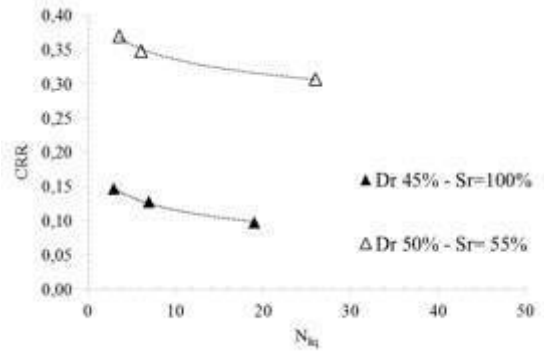

EXPERIMENTAL RESULTS: CYCLIC TESTS

Cyclic simple shear tests:
Pieve di Cento sand

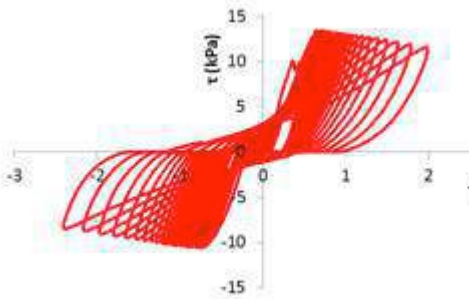

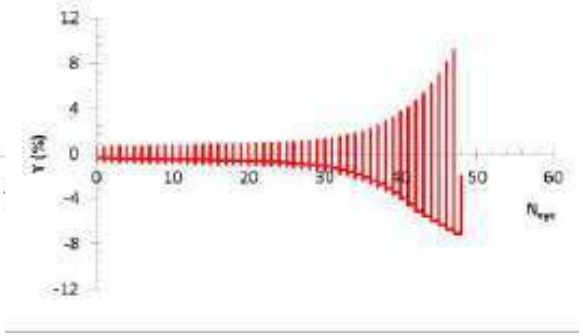

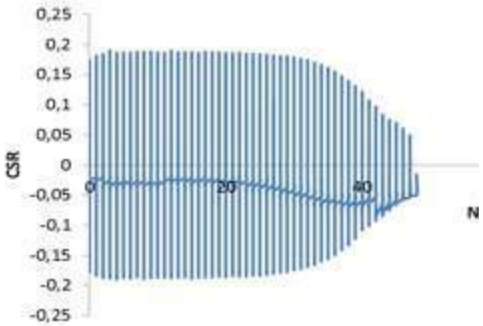

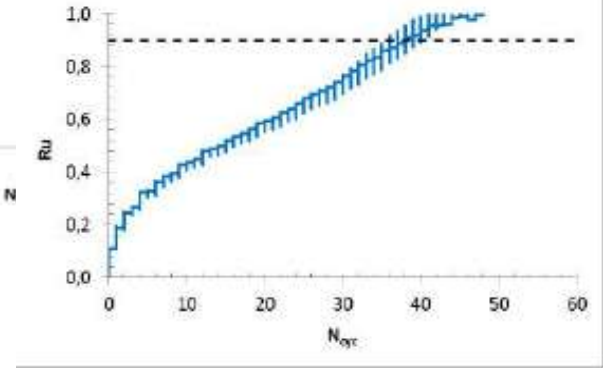

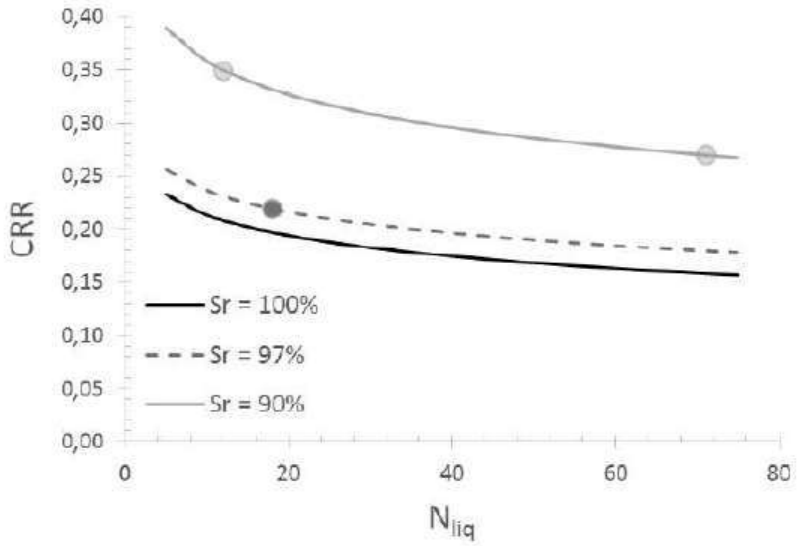

CRR increases as Sr decreases

Field trial

selected case study pilot testing site

GEOLOGICAL SETTING

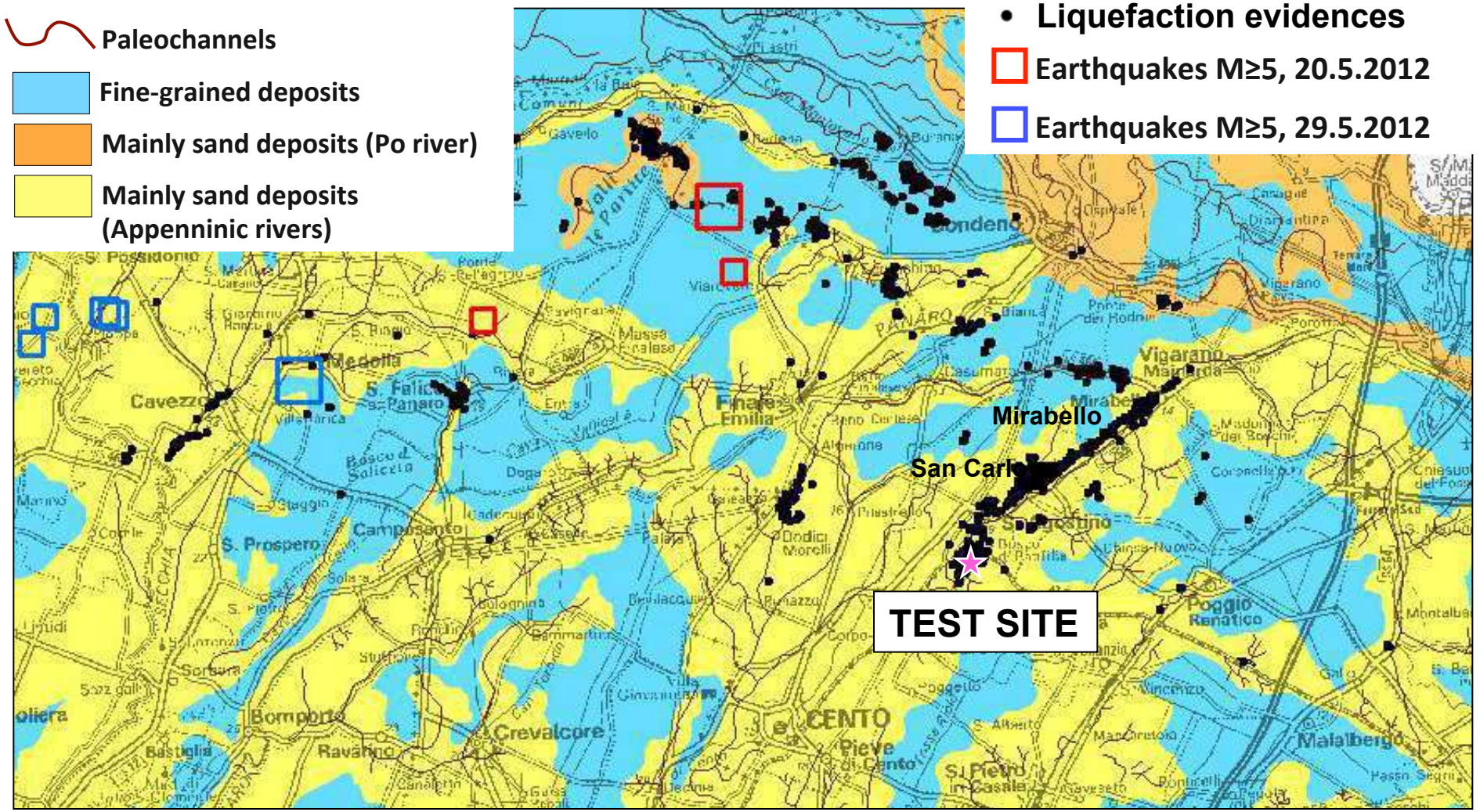

(mod. after Fioravante, 2017)

GEOLOGICAL SETTING

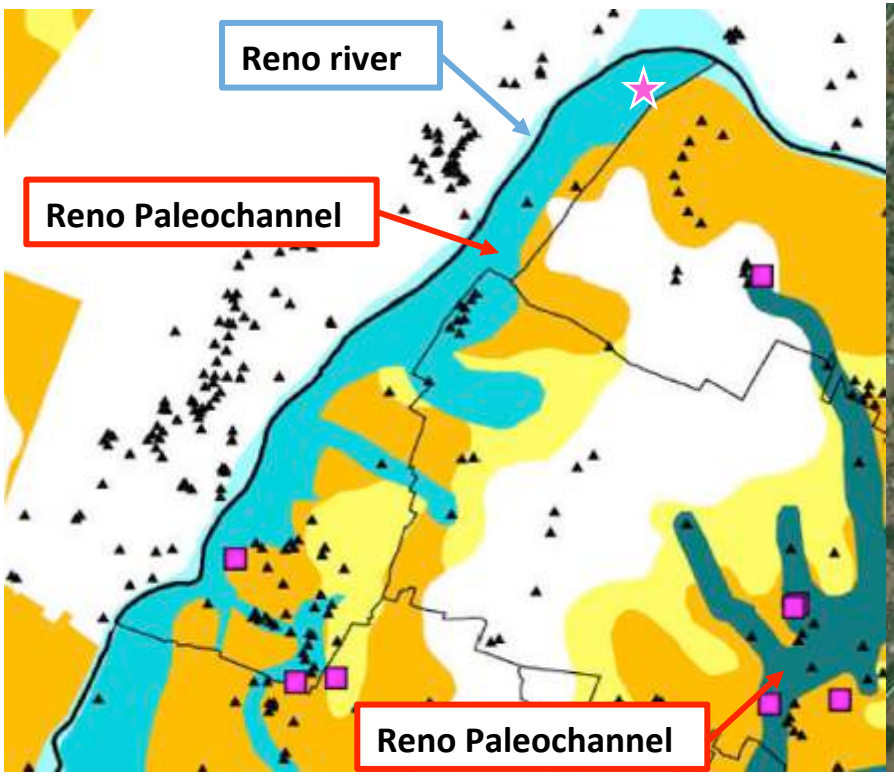

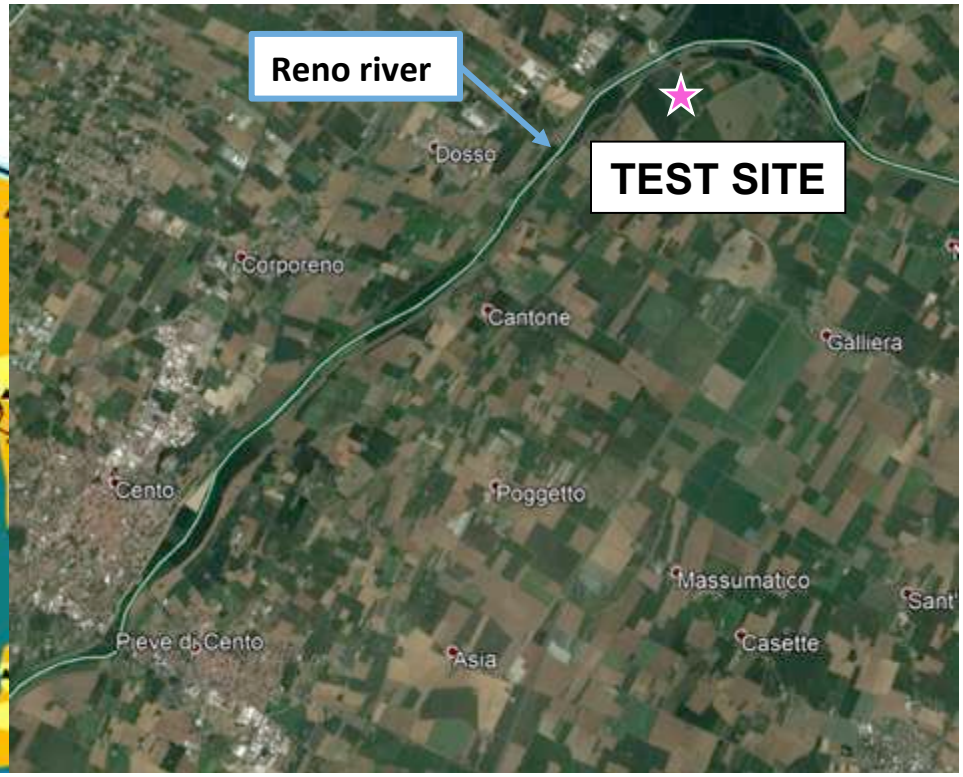

CPTU
Geognostic tests
Coarse sand
Silty sand
Municipal borders

(mod. after Pieve di Cento Municipality)

The test site is located on a paleochannel of Reno river

High variability of the statigrafic sequence

TREVI

FIELD TRIALS AT THE SELECTED CASE STUDY PILOT TESTING

"…Horizontal and Vertical Drains and Induced Partial Saturation will be tested in centrifuge. Among these three, horizontal drains and IPS seem to be the most interesting in terms of innovation and they will be considered as a first choice for the in-situ tests."

Geophysical surveys

Electric tomography was carried out with an array of 96 nails, spaced 0.75 m, capable of investigating up to a depth of about 12 m.

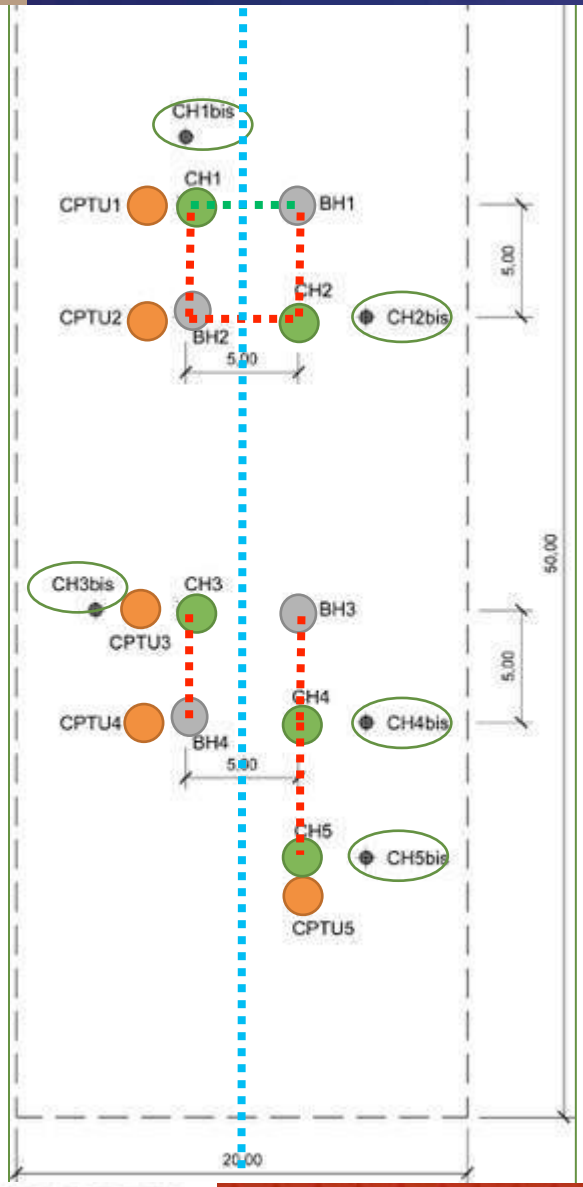

WHAT WAS DONE

The first step taken was the GEOTECHNICAL AND GEOPHYSICAL CHARACTERIZATION of a volume equal to 10.000 m³ (20·50·10)

- #5 CPTU
- #5 drilling with continuous coring (10m deep)
- #4 wash boring (10m deep)
- #6 Seismic Tomography Section(P and S waves)
- #1 Point-to-Point Cross Hole (sensors' spacing 50 cm)
- #1 Electric Tomography (Wenner-Schlumbeger & Dipole-Dipole array) with induced polarization

GEOPHYSICAL SURVEY: SHEAR WAVE VELOCITY

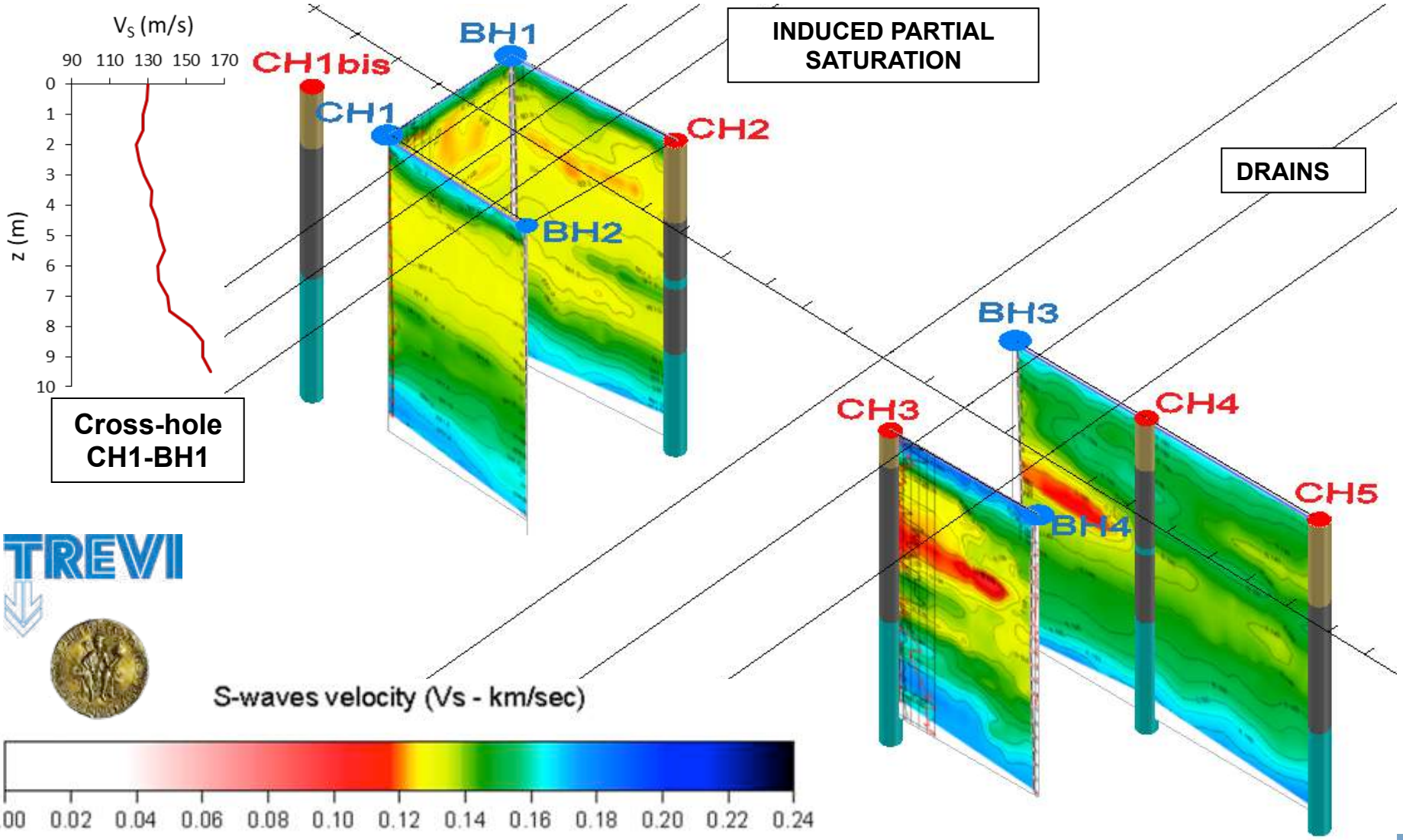

N° Prova **CPTU 4** Data prova **26/07/2017** Operatore G.A.

NOTE

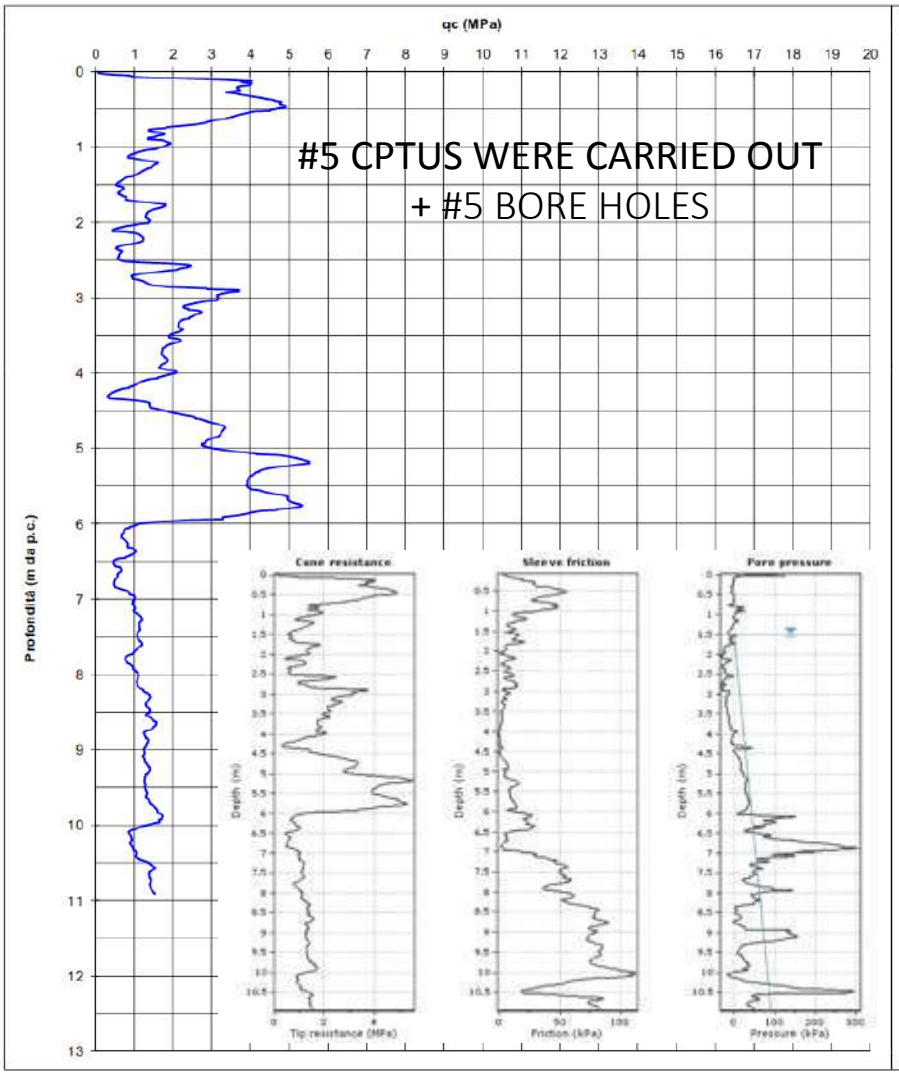

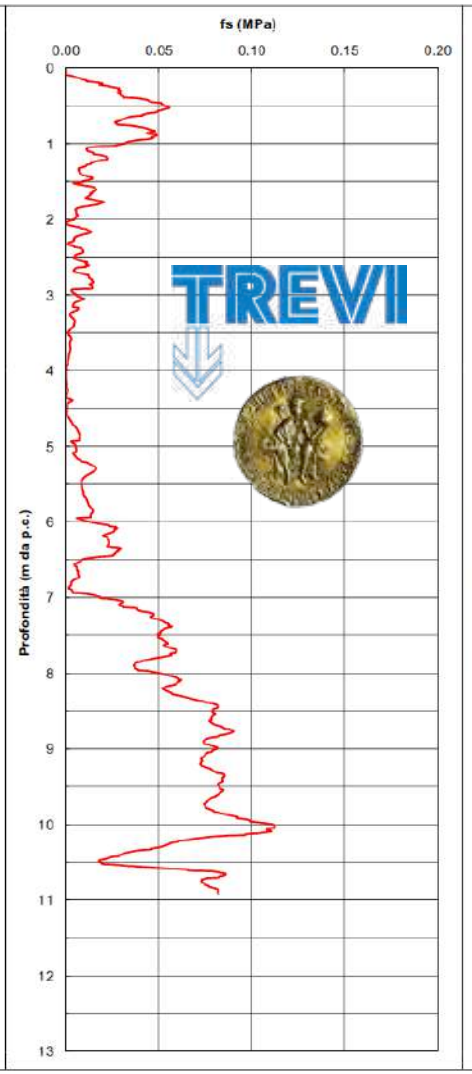

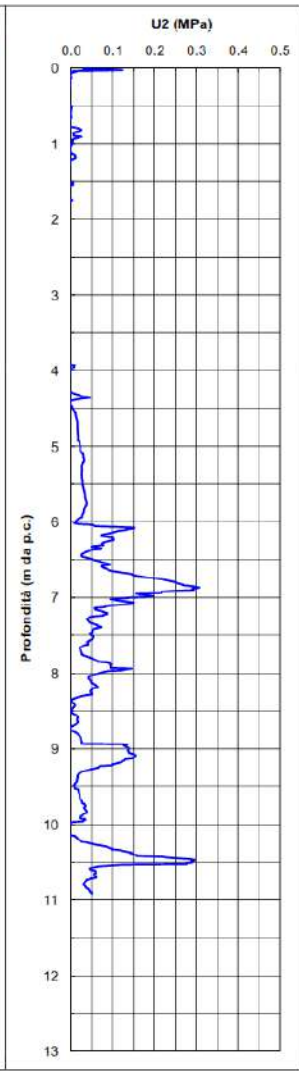

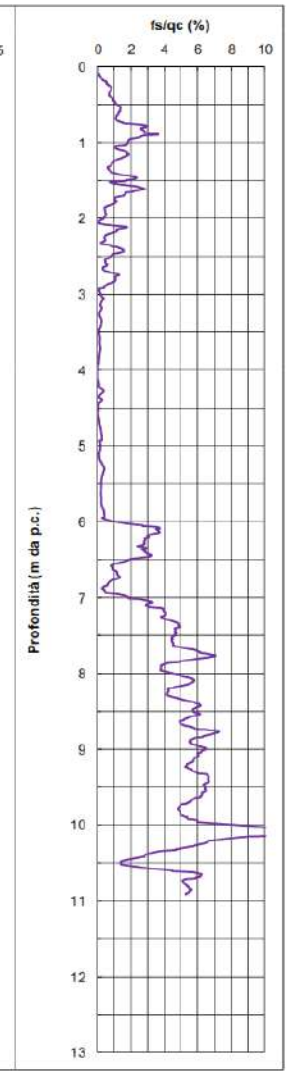

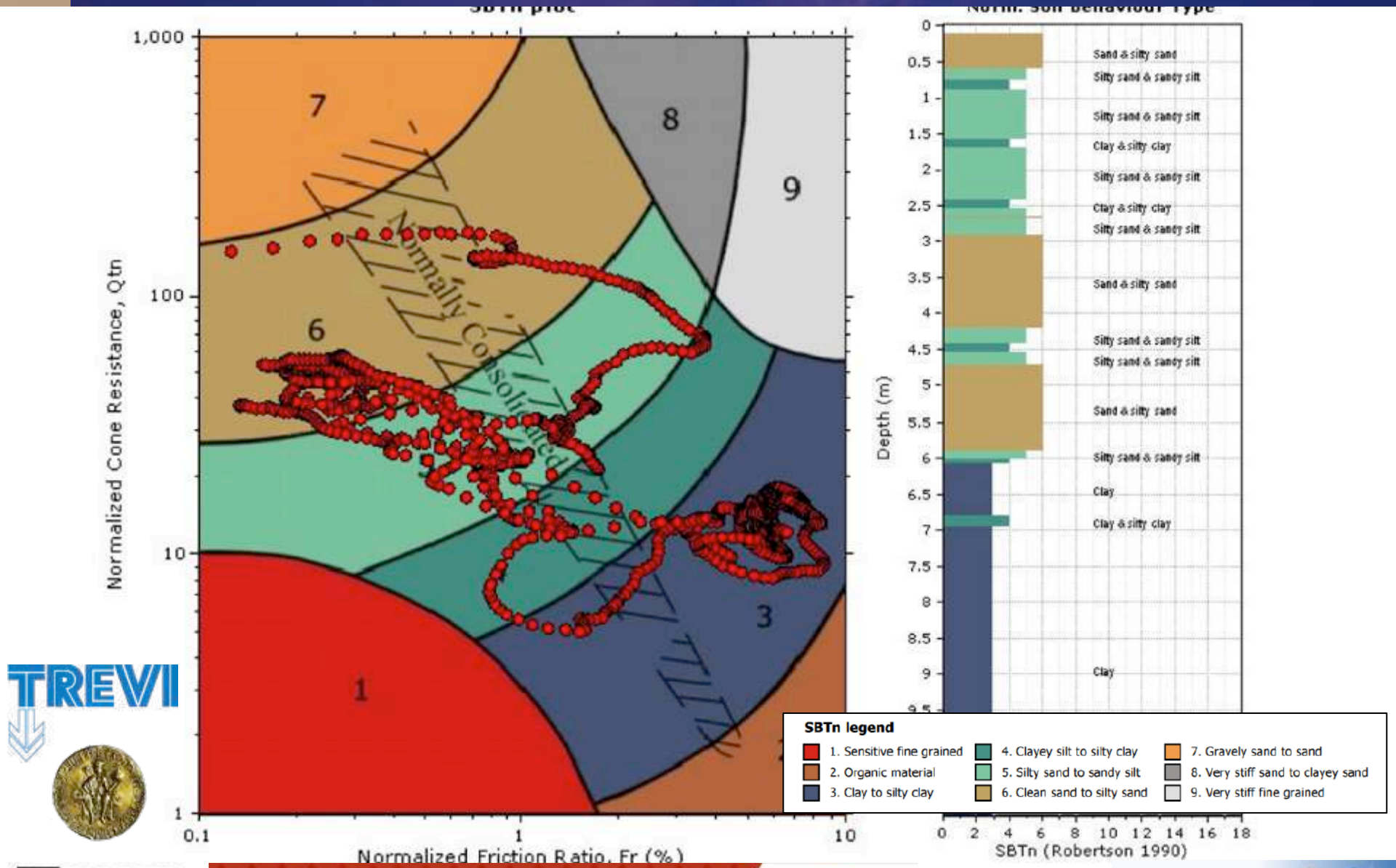
Normalized Cone Resistance, Qtn
1,000
100
10
1
0.1
1
10
Normalized Friction Ratio, Fr (%)
1
2
3
4
5
6
7
8
9
Normally Consolidated
Depth (m)
Sand & silty sand
Silty sand & sandy silt
Clay & silty clay
Clay
SBTn (Robertson 1990)
SBTn legend
1. Sensitive fine grained
2. Organic material
3. Clay to silty clay
4. Clayey silt to silty clay
5. Silty sand to sandy silt
6. Clean sand to silty sand
7. Gravely sand to sand
8. Very stiff sand to clayey sand
9. Very stiff fine grained

CORE HOLE NAME	SPT		Osterberg		GP-S	
	Depth (m)	Blows	Depth (m)	#	Depth (m)	#
CH1	-	-	-	-	-	-
CH1 Bis	4.0-4.5	0 - 0 - 0	2.0-2.5	1	2.5-3.5	1
	5.5-6.0	2 3 2	3.5-4.0	1		
CH2	2.0-2.5	0 - 0 - 0	3.0-3.5	1	4.5-5.5	1
	4.0-4.5	0 - 0 - 0				
	5.5-6.0	3 5 3				
CH2 Bis	-	-	2.5-3.5	1	-	-
CH3	2.0-2.5	0 - 0 - 0	-	-	3.5-4.5	1
	4.5-5.0	2 4 5	-	-		
CH3 Bis	-	-	2.5-3.0	1	-	-
			4.5-5.0	1		
CH4	2.0-2.5	0 - 0 - 0	-	-	5.0-6.0	1
CH4 Bis	-	-	2.0-2.5	1	-	-
			4.5-5.0	1		
CH5	4.0-4.5	0 - 0 - 0	2.0-2.5	1	-	-
	5.5-6.0	1 3 1	3.5-4.0	1		
CH5 Bis	-	-	-	-	2.0-3.0	1
	10		10		5	

Sampling

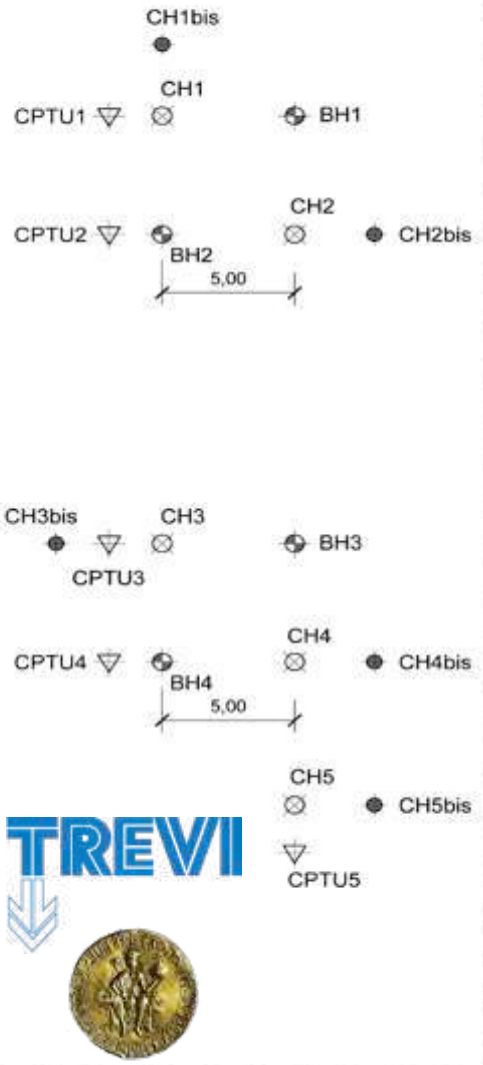

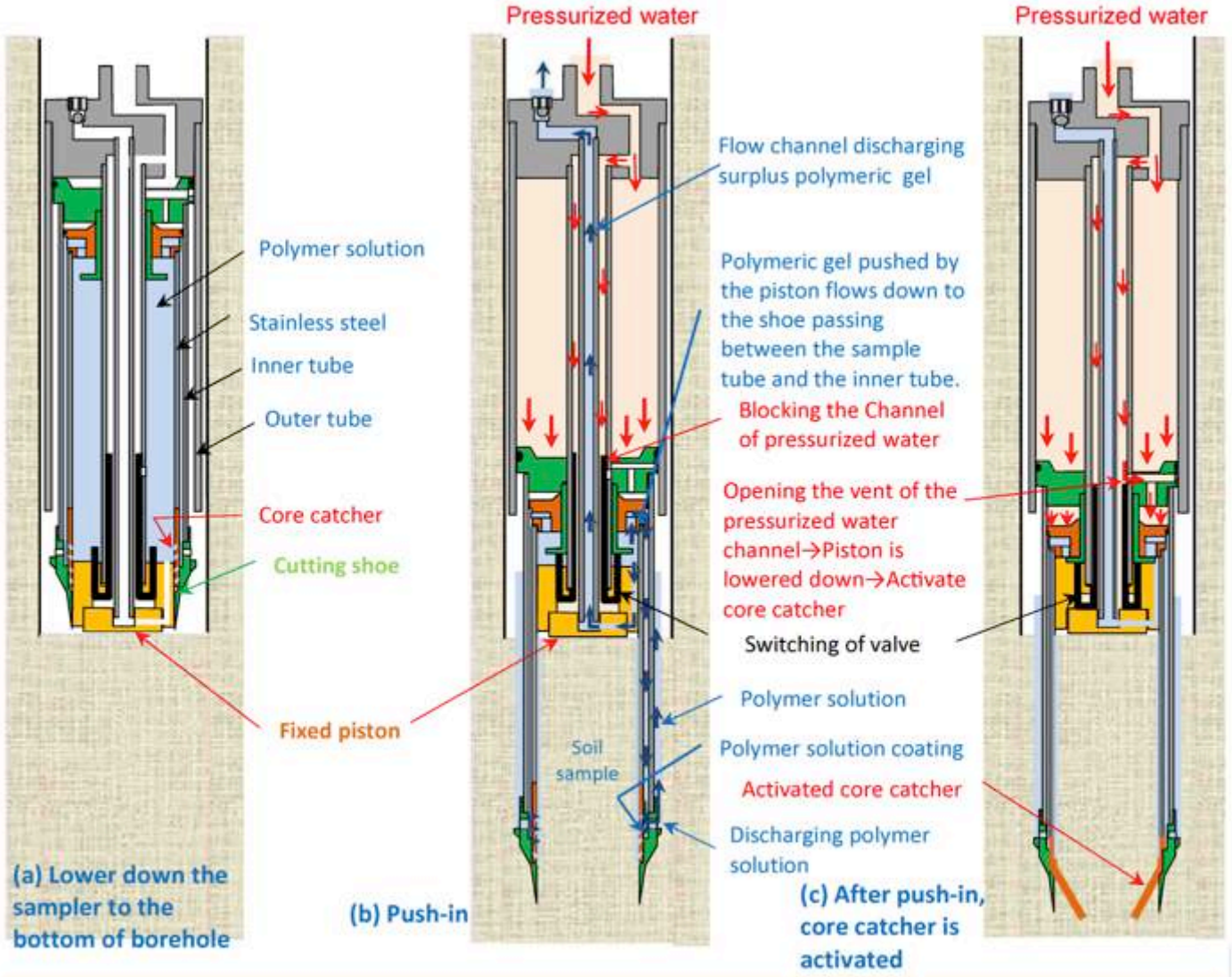

Gel-Push Sampler GP-S

- Amount of inflow water ~5 l/min
- Max water pressure 5 MPa
- Polymer Solution 1÷3%

GEL PREPARATION AND PROBE LOADING; FILL RODS WITH WATER / OPEN THE PUMP / WAIT A FEW MINUTES; EXTRACT THE SAMPLER / CHECK CORE CATCHER /….

Gel Push Sampler GP-S

EXTRACT THE SAMPLER / CHECK CORE CATCHER / SEAL THE SAMPLE

TEST SITE

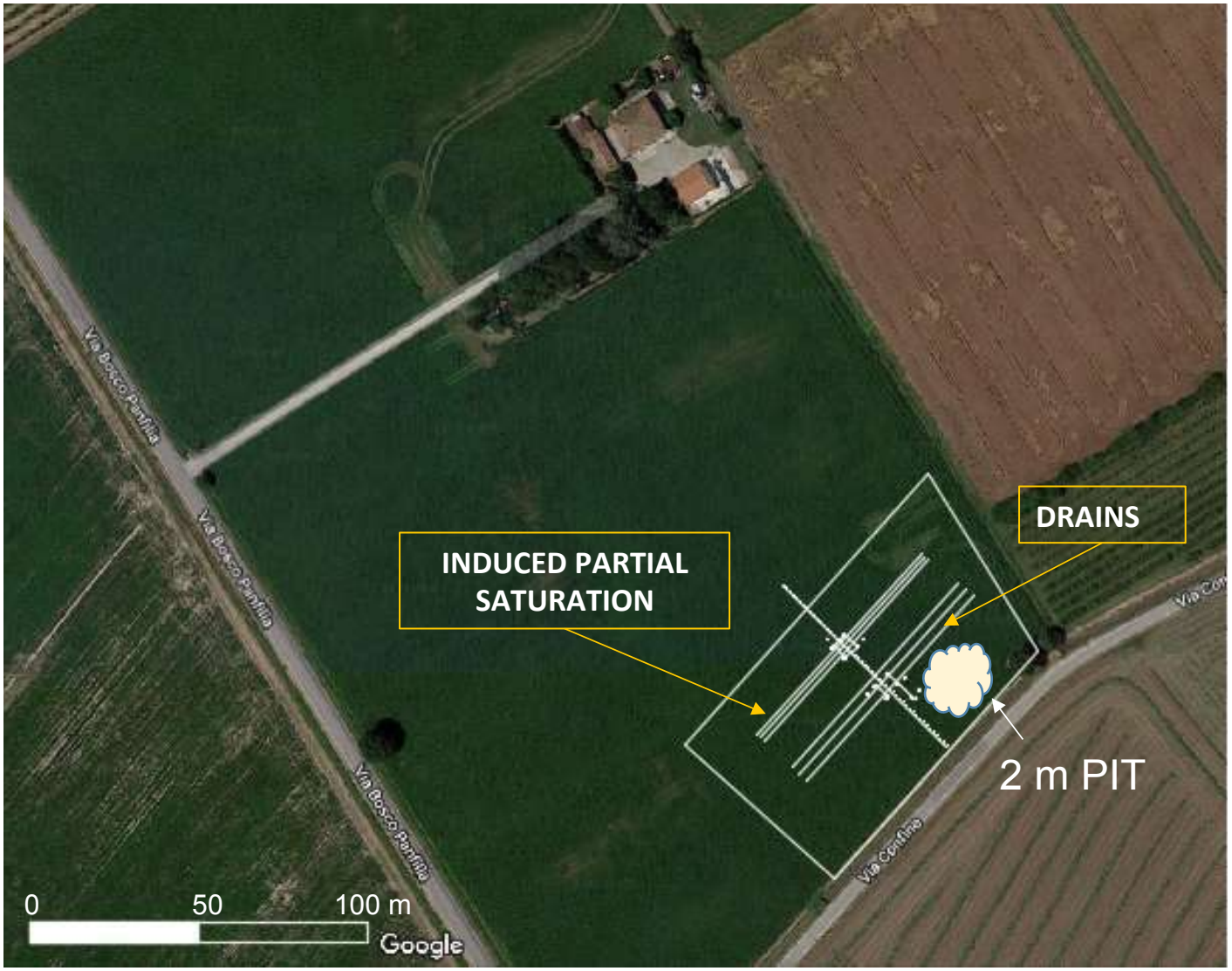
DRAINS
INDUCED PARTIAL SATURATION
2 m PIT
Via Bosco Pamfilia
Via Confinale
0
50
100 m
Google

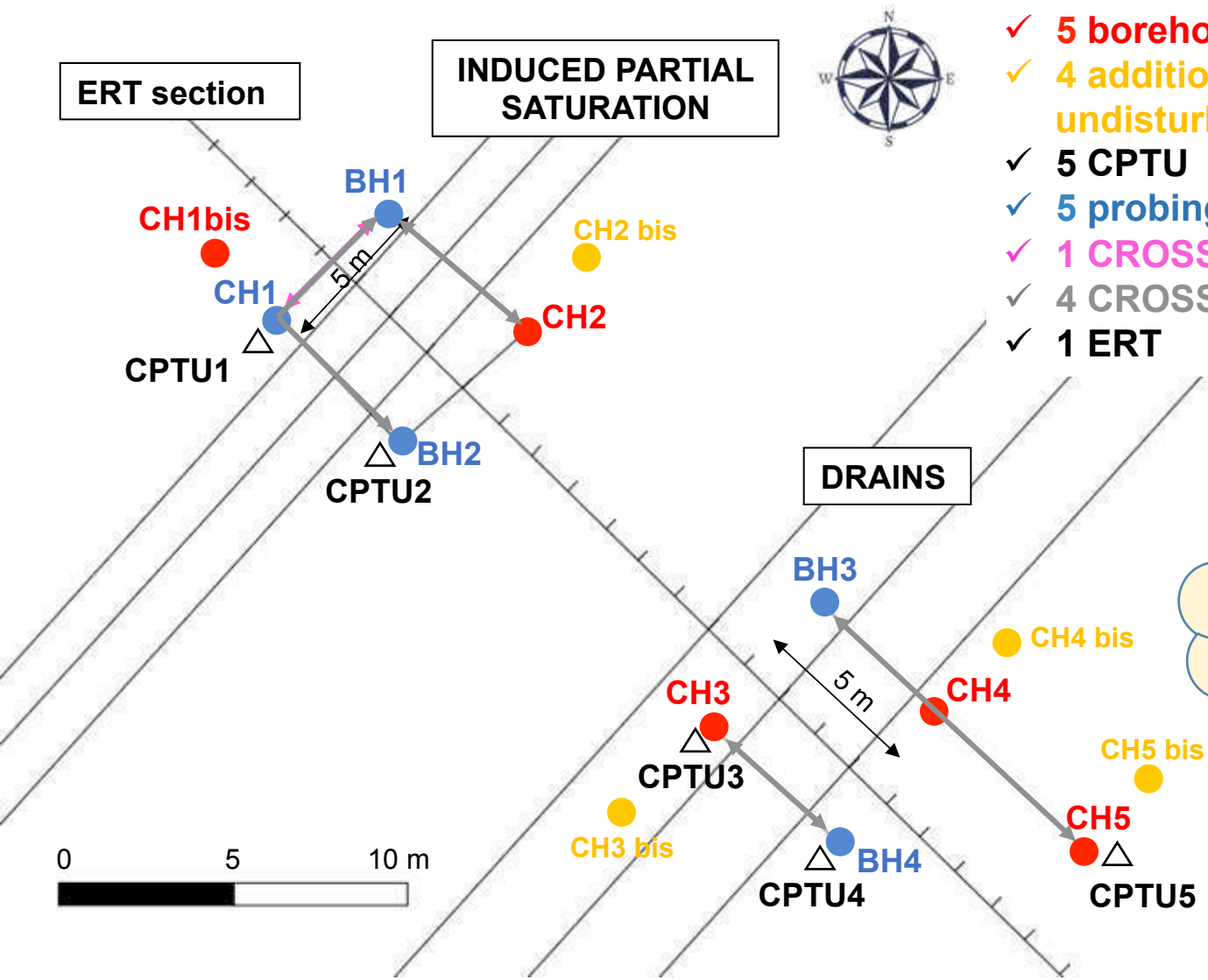

- ✓ 5 boreholes (max depth 10 m)
- ✓ 4 additional boreholes for undisturbed sampling only
- ✓ 5 CPTU
- ✓ 5 probing boreholes
- ✓ 1 CROSS-HOLE CH1-BH1
- ✓ 4 CROSS-HOLE TOMOGRAPHIES
- ✓ 1 ERT

2 m PIT

TRIAL FIELD TEST ON IPS

Partial saturation (IPS)

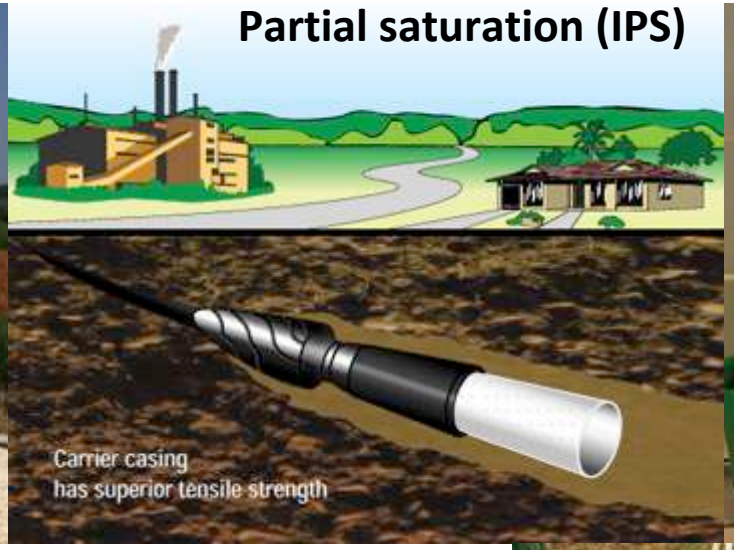

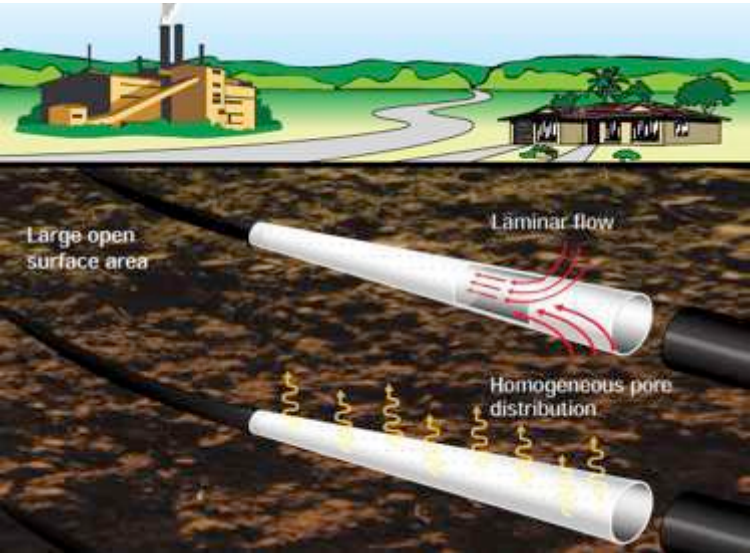

Horizontal Directional Drilling with 3” steel rods, pulled-back with porous HDPE well screen designed to minimize flow resistance; great porosity compared to conventional Well screens !...

Horizontal Drains were alternatively tested

TREVI

TREVI

INSTRUMENTATION ON SITE

2 – 8

4 – 4

4 – 7

6

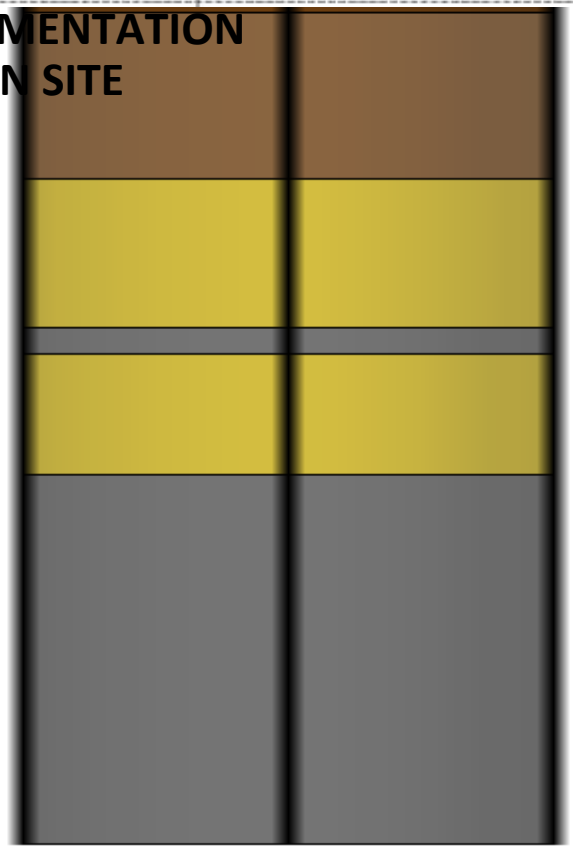

Shaking tests with MEGA-SHAKER performed in three (3) main areas: one on the virgin ground, one in the area treated with HD, the last one in the area treated with IPS.

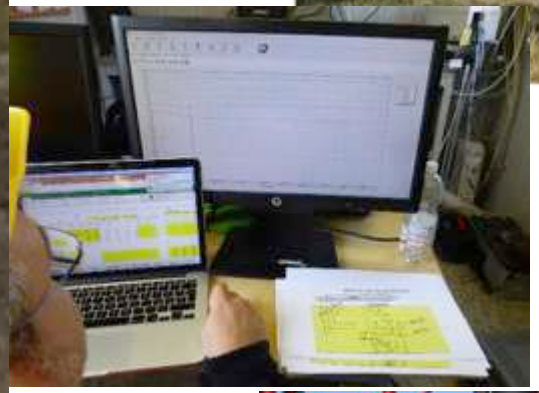

BASE PLATE size

N = 178 kN Hold-weight

M_{plate} = 3629 kg → W_{plate} = 35.6 kN

A_{plate} = 1.92 mq

Q= 213 kN → q = 111 kPa

V = 138 kN → τ = 72 kPa

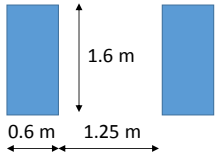

Shaking direction

TREVI

In each test, the static vertical loading of the machine was firstly applied and, after verifying that the consolidation process was completed, a dynamic loading at 10 Hz was applied for a duration of 100 s or 200 s, in the first and in the second phase of shaking, respectively.

The results obtained are very positive and are being processed but confirm the previous results obtained by numerical analyses (www.liquefact.eu)

RESILIENCE

ACKNOWLEDGEMENT

LIQUEFACT project ("Assessment and mitigation of liquefaction potential across Europe: a holistic approach to protect structures / infrastructures for improved resilience to earthquake-induced liquefaction disasters") has received funding from the European Union's Horizon 2020 research and innovation programme under grant agreement No GAP-700748.

Foundation Strengthening of Stilling Basin 7E of Crestuma-lever Dam

Laura Caldeira
LNEC

Contents

- Crestuma-Lever main features
- Identification of boiling causes
- Corrective measures
- Stress-strain analysis
- Verification of the micro piles design
- Conclusions

Crestuma-Lever main features

- The most downstream dam of Douro River
- Constructed between 1977 and 1985
- Design flood 26,000 m^3/s
- Three Kaplan groups 3x39 MW
- Provides water supply and river navigation

Douro – Portuguese hydropower schemes


Crestuma-
Lever


7D
5D
3D
1D
1E
3E
5E
7E
Rio Douro

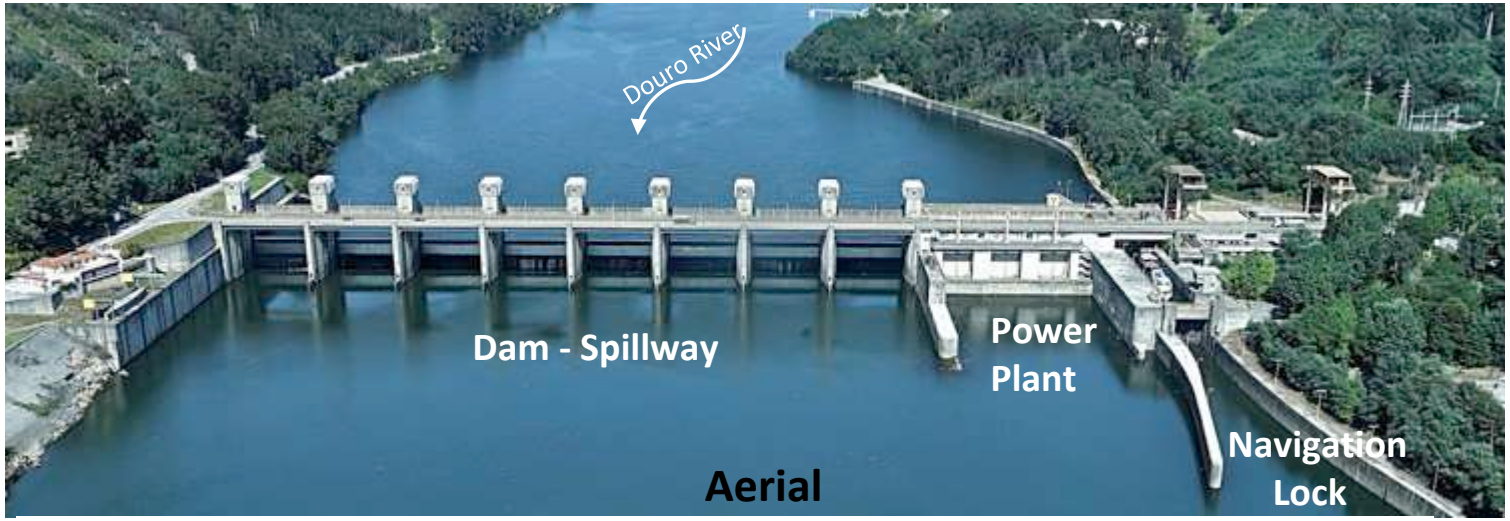

Aerial view

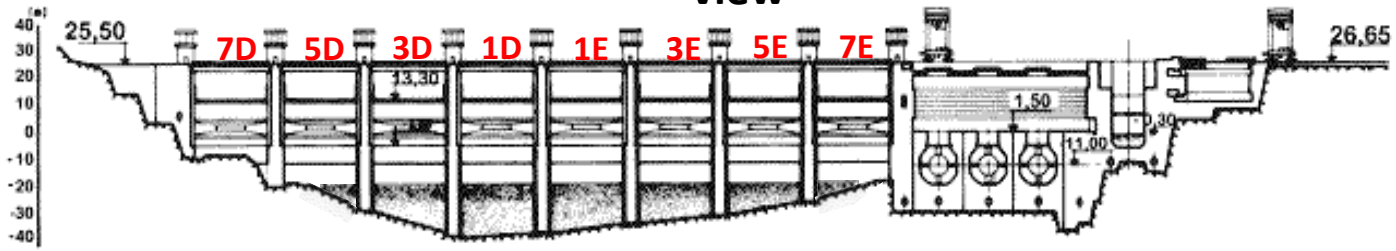

Longitudinal section

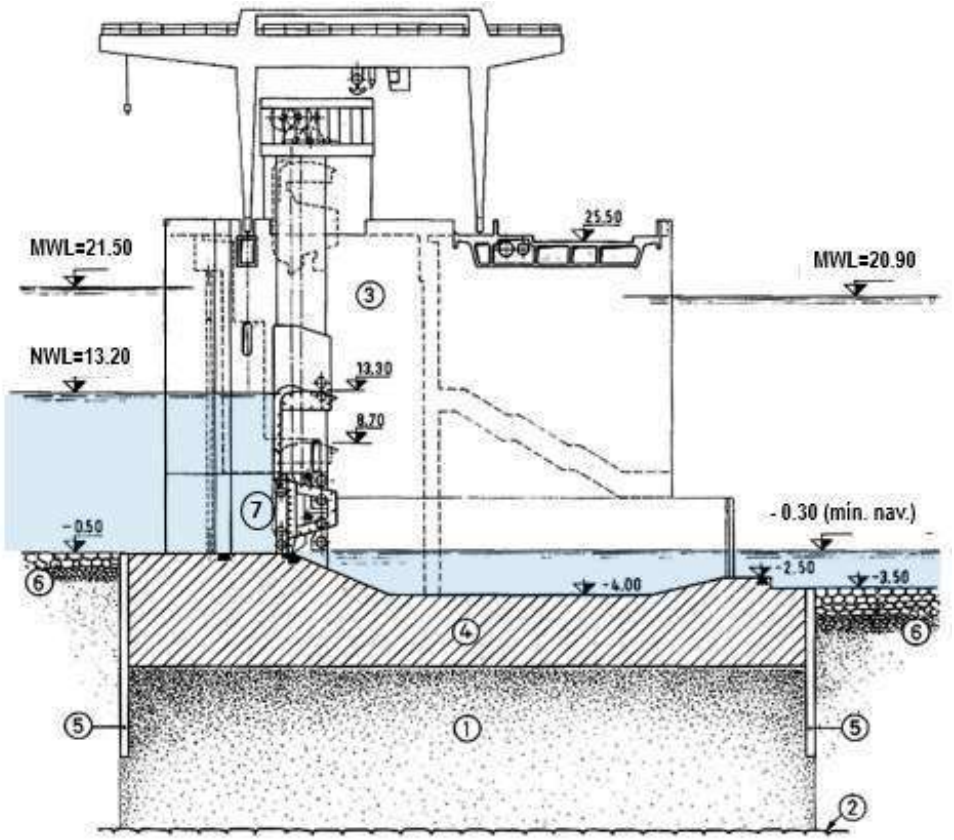

- Gate structure dam – General cross section

1 – Alluvium
2 – Bedrock
3 – Dam pier
4 – Stilling basin
5 – Cut-off wall
6 – Rockfill blanket
7 – Double leaf gate

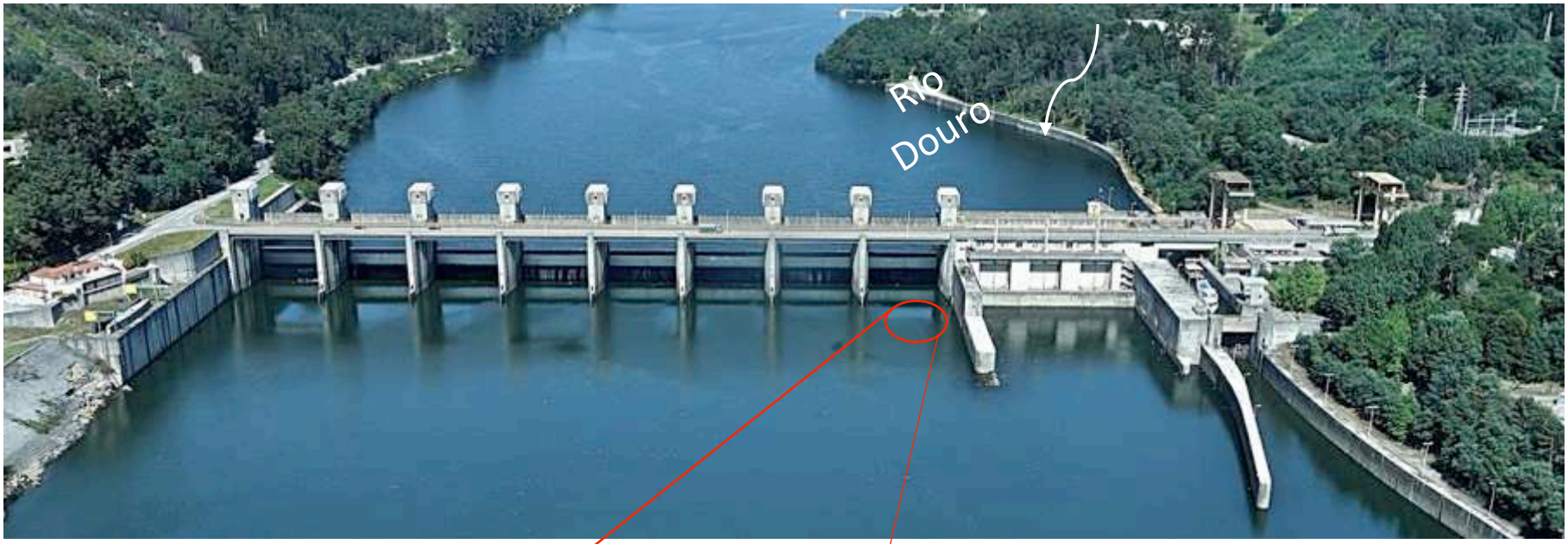
Rio
Douro

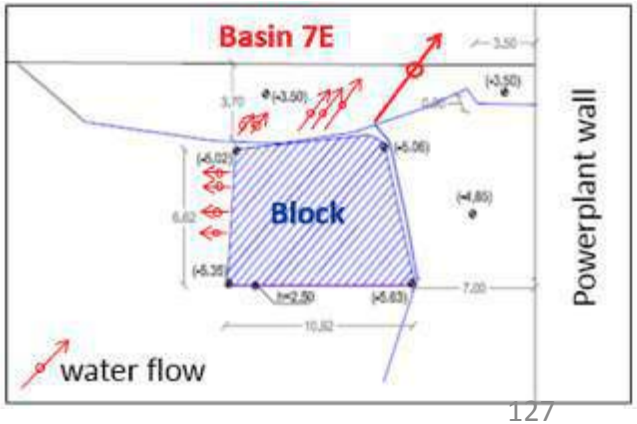
Basin 7E
Block
Powerplant wall
water flow

Identification of boiling causes

Construction phase information

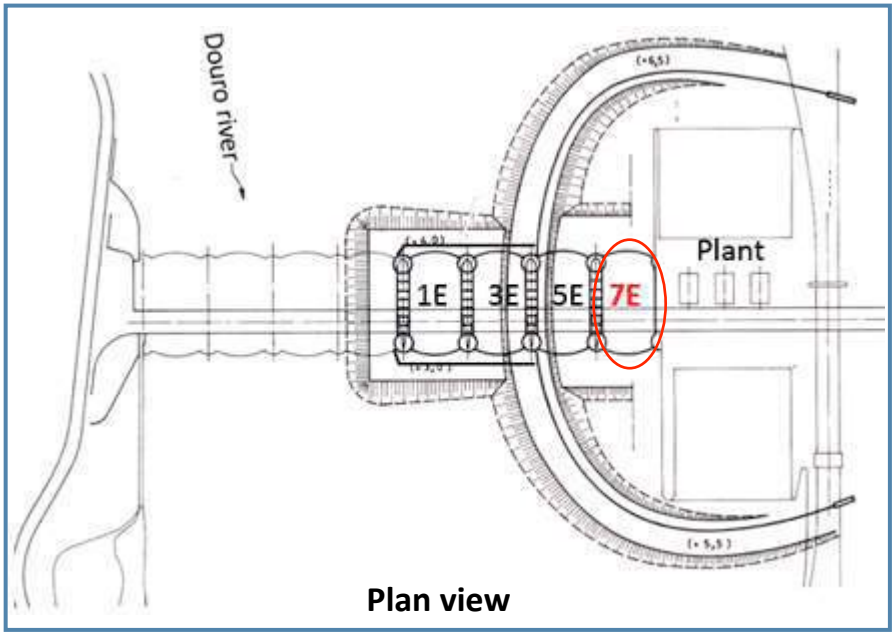

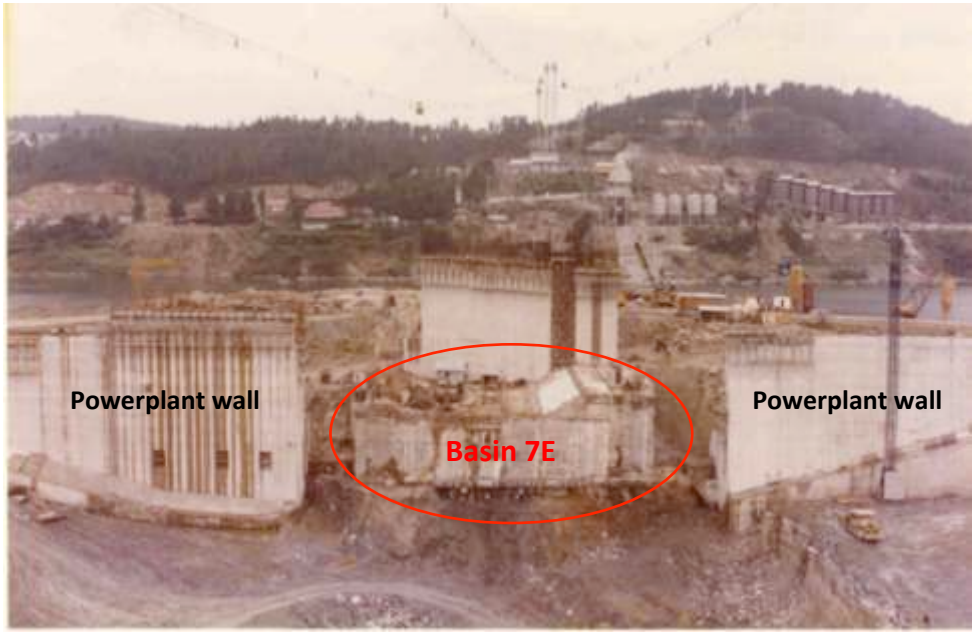

Defects in a panel of the upstream cut-off wall of basin 7E were detected

Geotechnical investigation

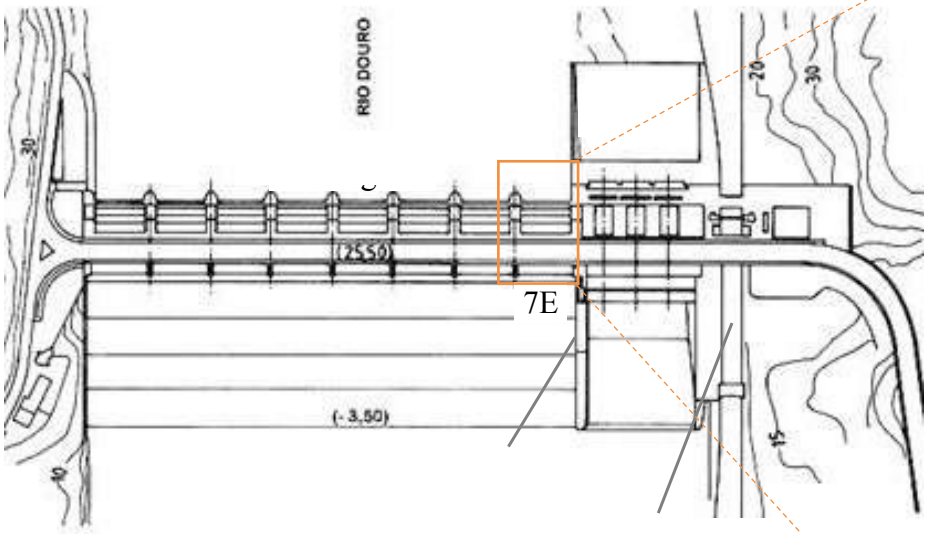

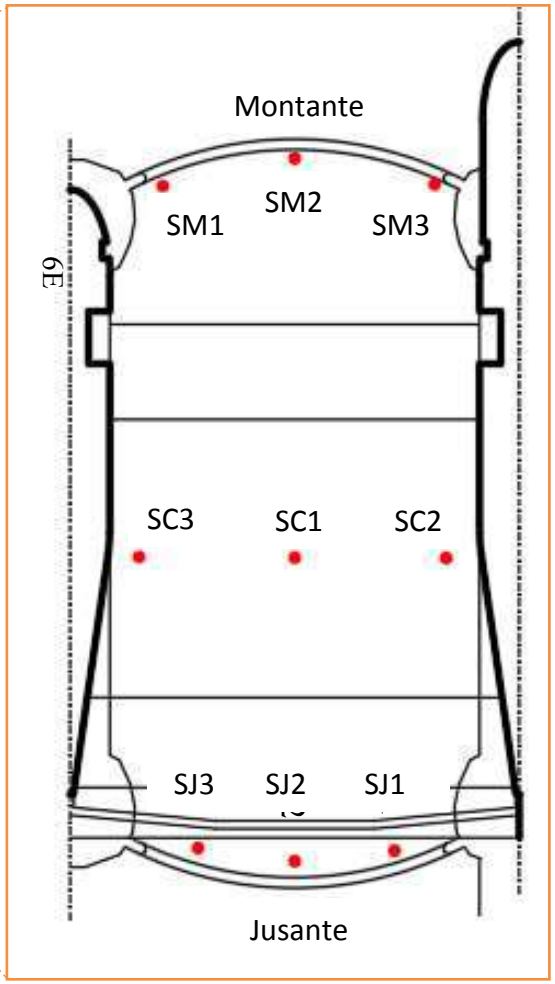

Geotechnical investigation

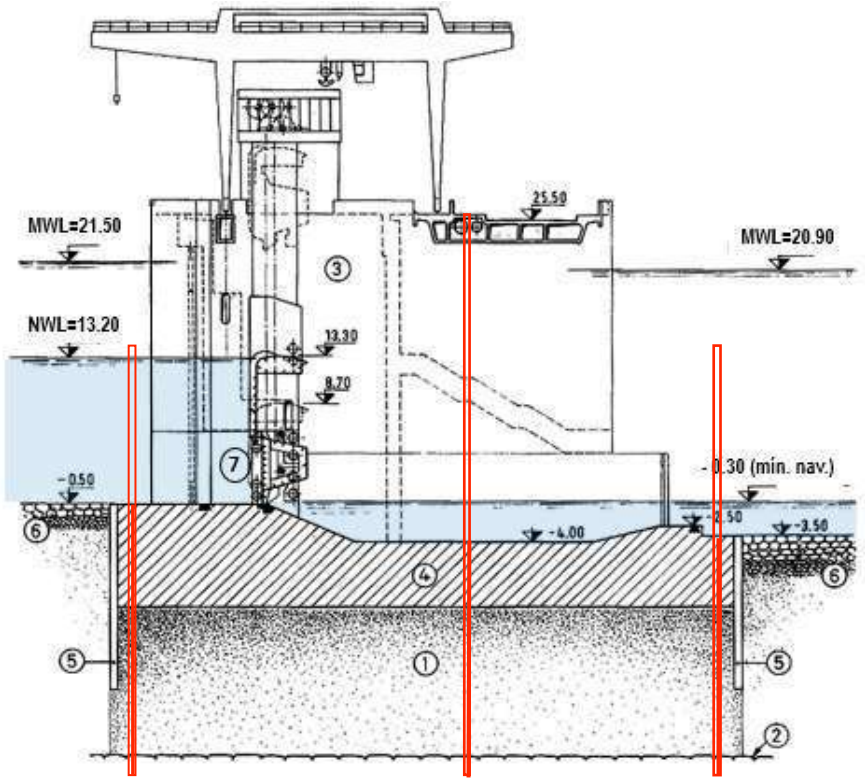

- **Alluvial foundation**
  - Composition and thickness
  - Relative density/ consistency
  - Pore pressures
- **Bedrock**
  - Characteristics and depth

Geotechnical investigation

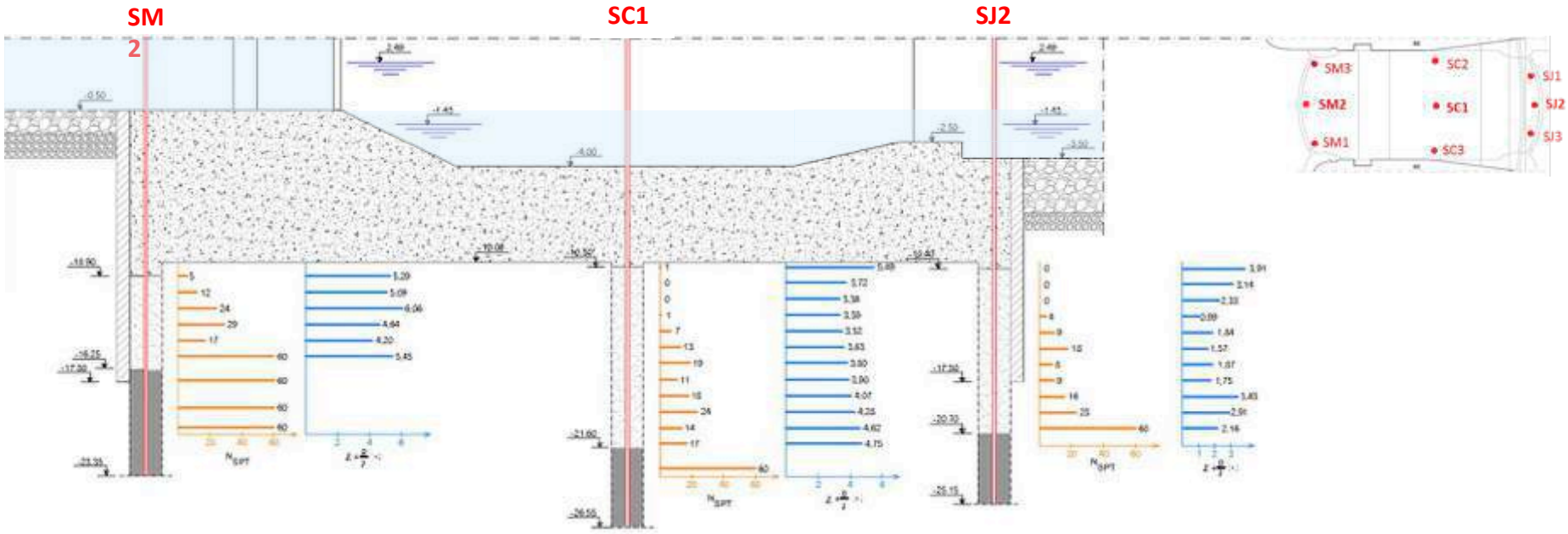

Main result: muddy soils with very low SPTs were identified for the 3 downstream boreholes and for 2 of the central ones (SC1 and SC3), especially on the topmost 3 m.

Numerical modelling

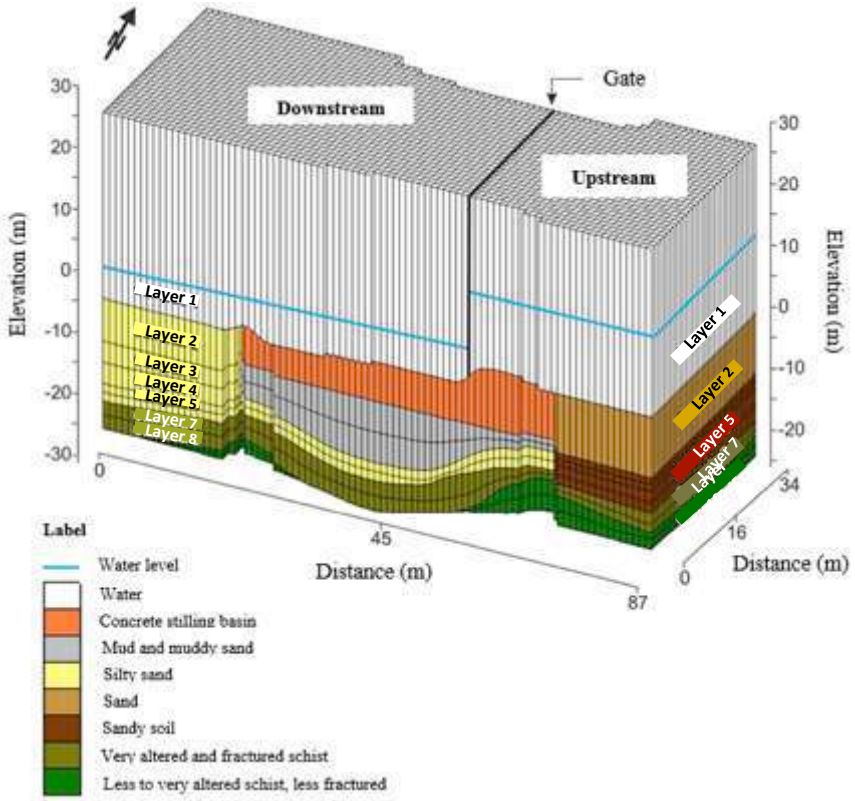

Numerical 3D modelling of the seepage under stilling basin 7E

- Calibration based on seepage conditions identified by geotechnical investigation
- Prediction of their possible evolution after an upstream intervention

Corrective measures

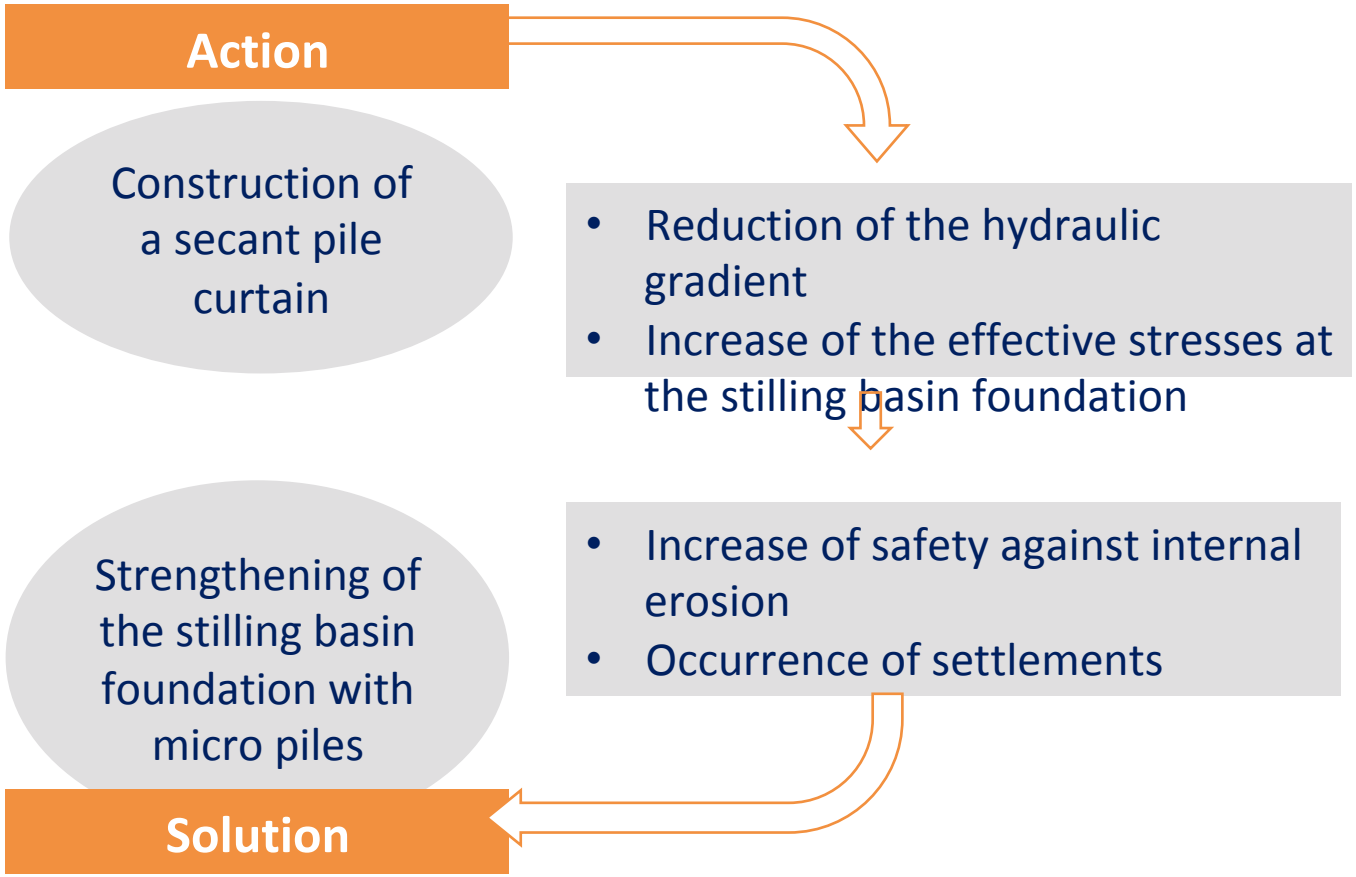
Action
Construction of a secant pile curtain
• Reduction of the hydraulic gradient
• Increase of the effective stresses at the stilling basin foundation
Strengthening of the stilling basin foundation with micro piles
• Increase of safety against internal erosion
• Occurrence of settlements
Solution

General solution

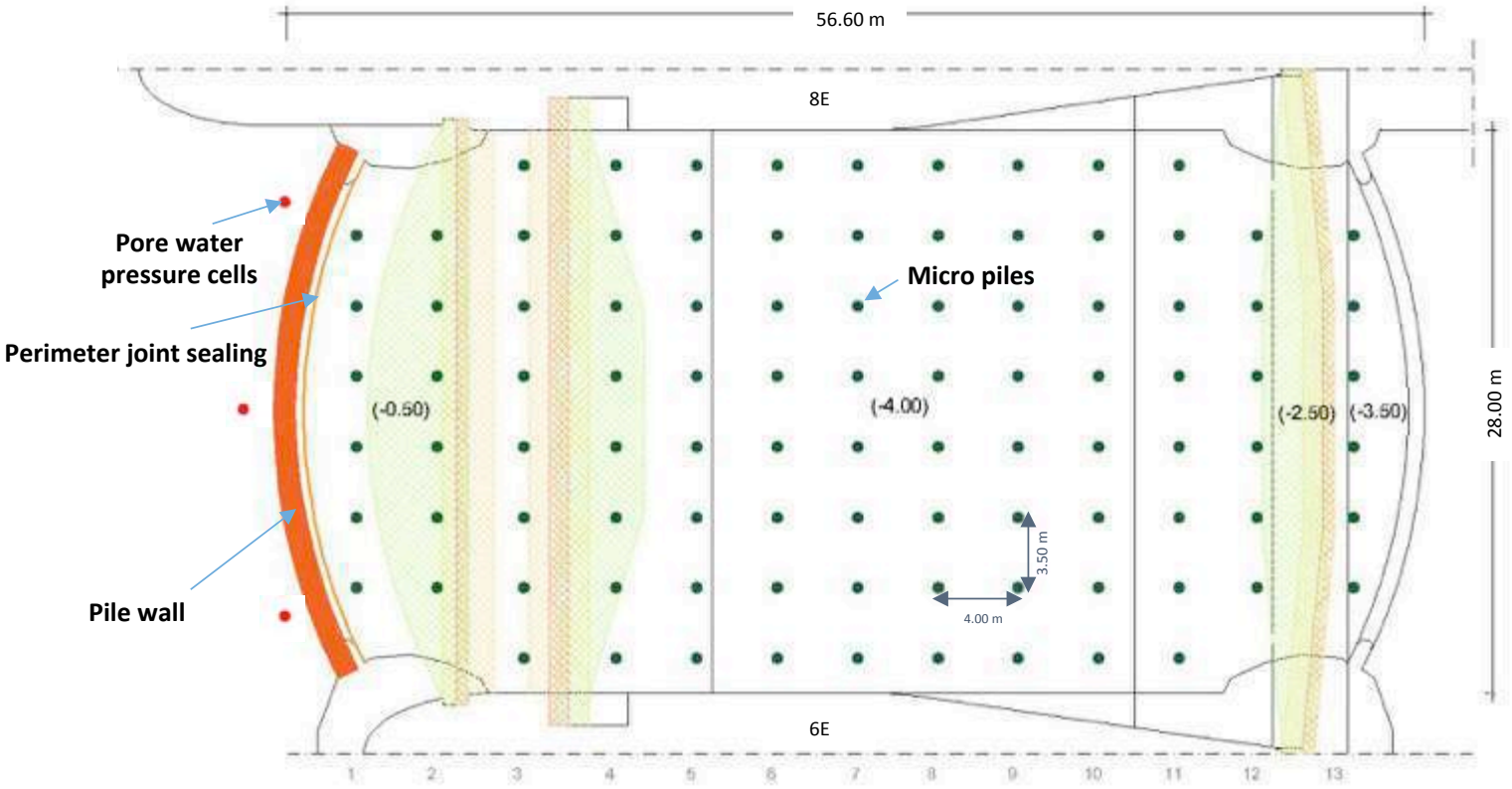

Stilling basin plan

Upstream watertight solution

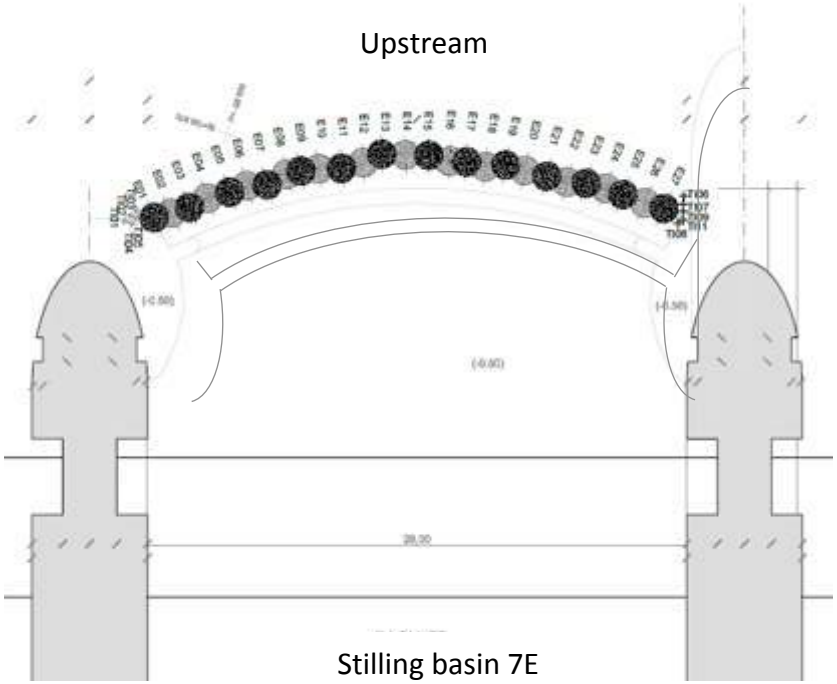

Upstream watertight solution

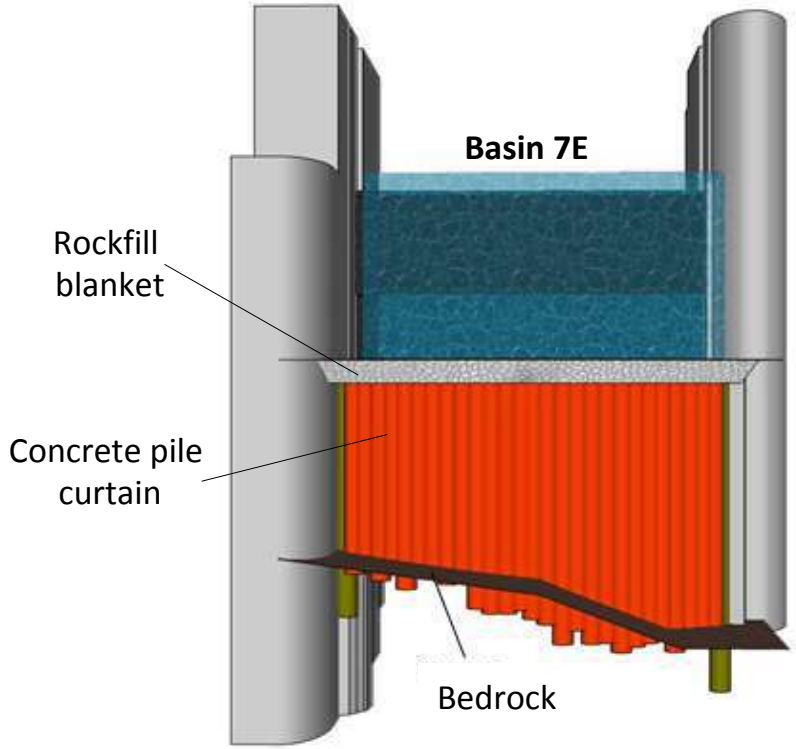

Upstream view

Pile concreting

Lateral sealing

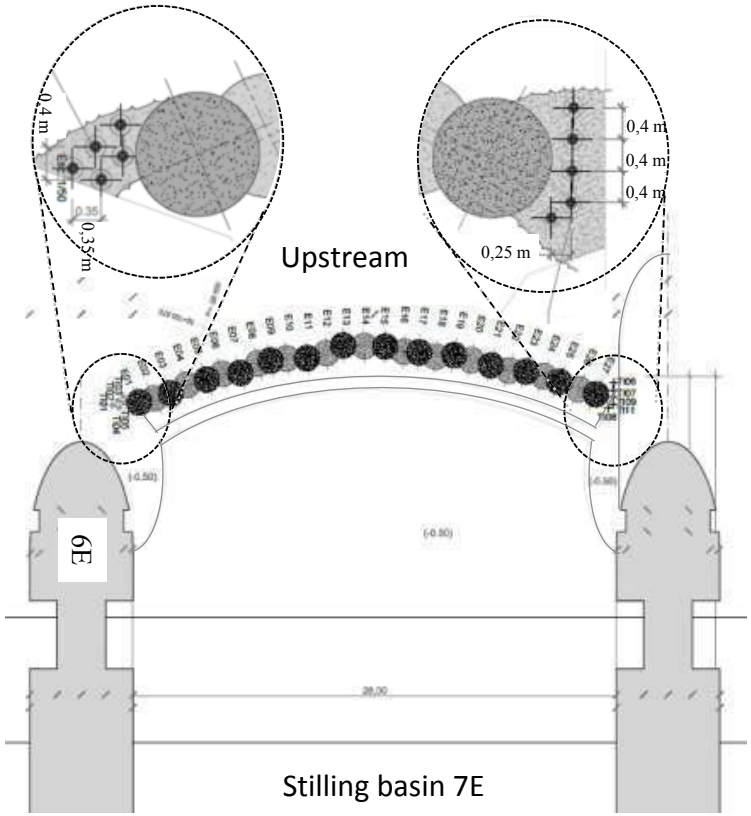

Top sealing

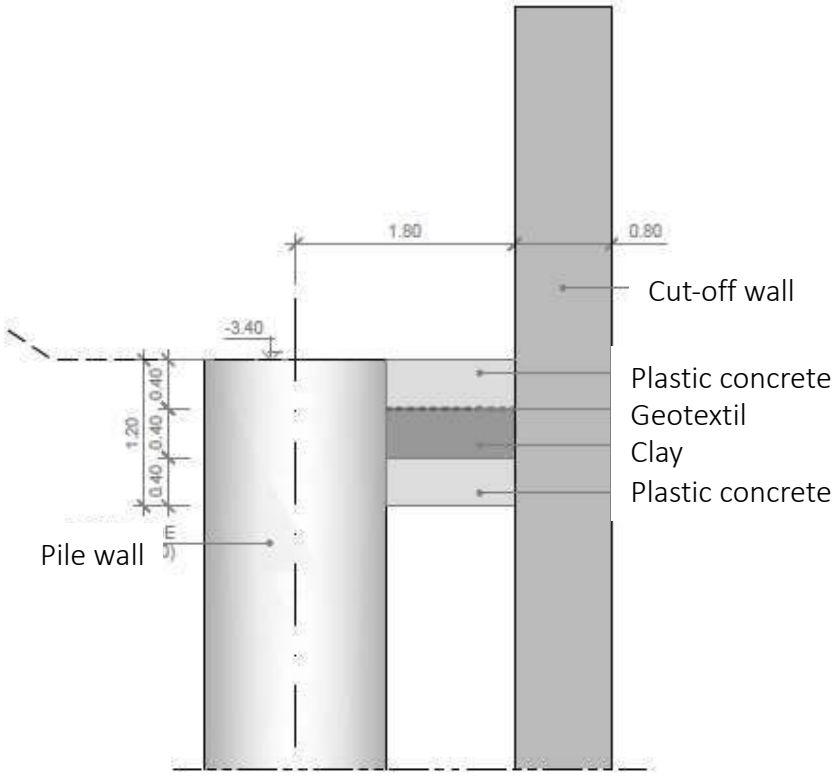
1.80
0.80
Cut-off wall
-3.40
Plastic concrete
Geotextil
Clay
Plastic concrete
1.20
0.40
0.40
0.40
E
Pile wall

Foundation strengthening

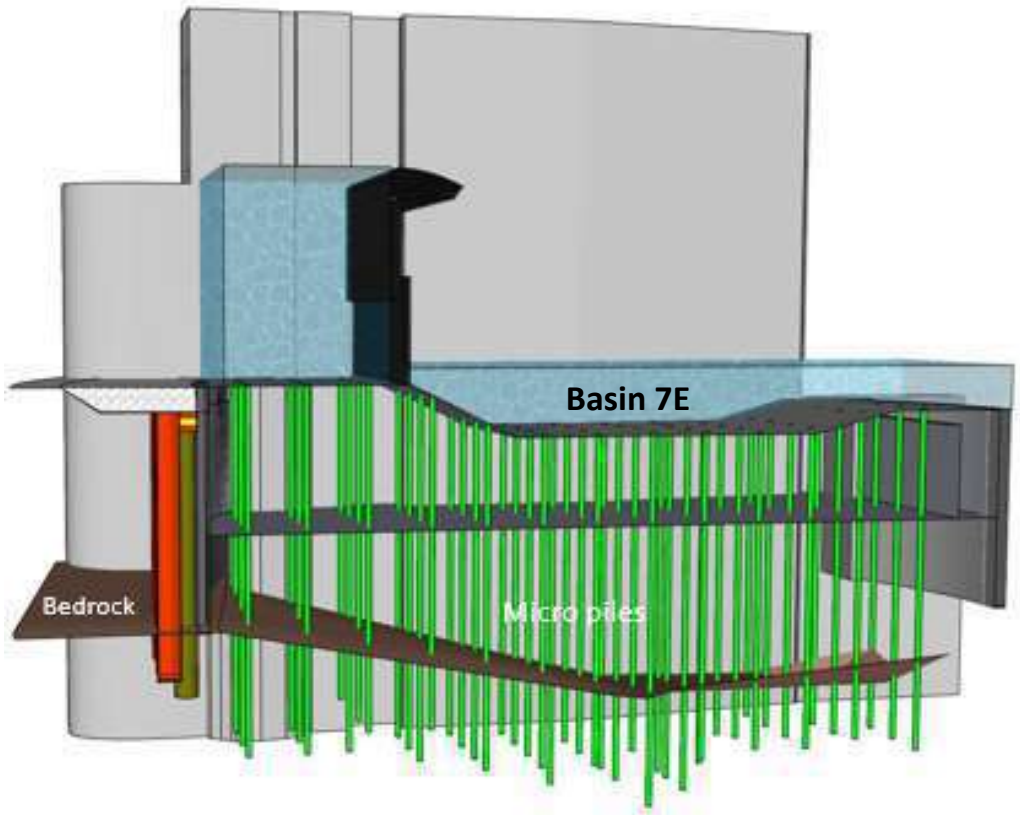

Micro piles cross section

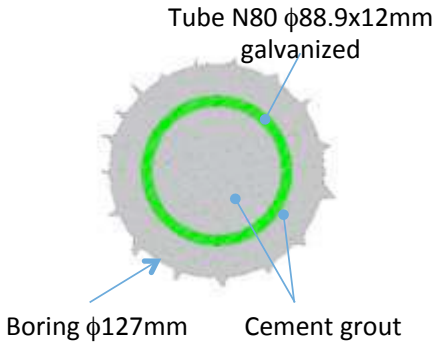

Foundation strengthening

Stress-strain analysis

3D Numerical modelling

Objectives

- Evaluation of the displacements of the stilling basin after the construction of the secant pile curtain.
- Determination of the axial forces to which micro-piles are subject and displacements
- Verification of micro-piles design

Geological-geotechnical scenario

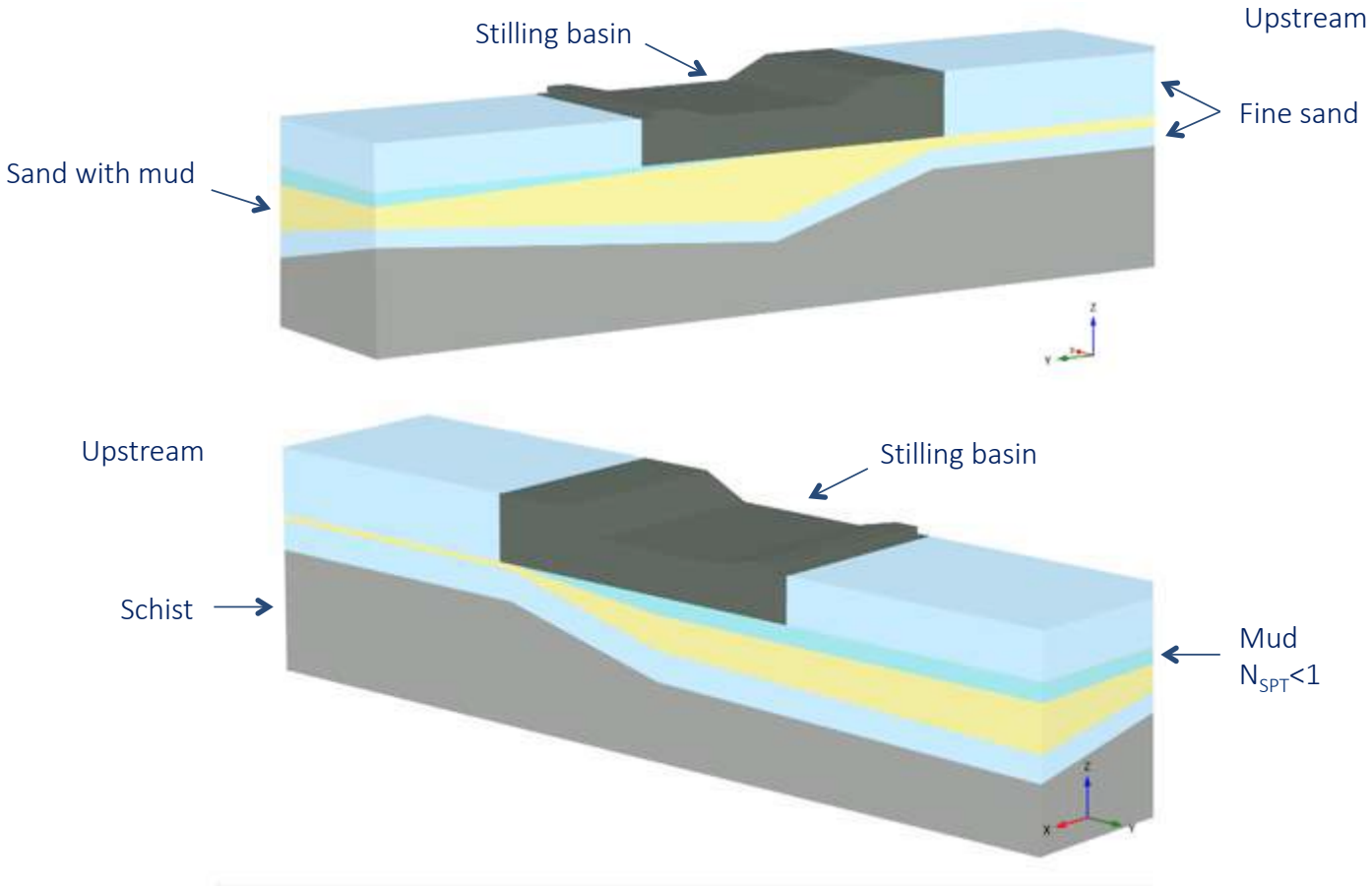

Geological-geotechnical scenario

Upstream

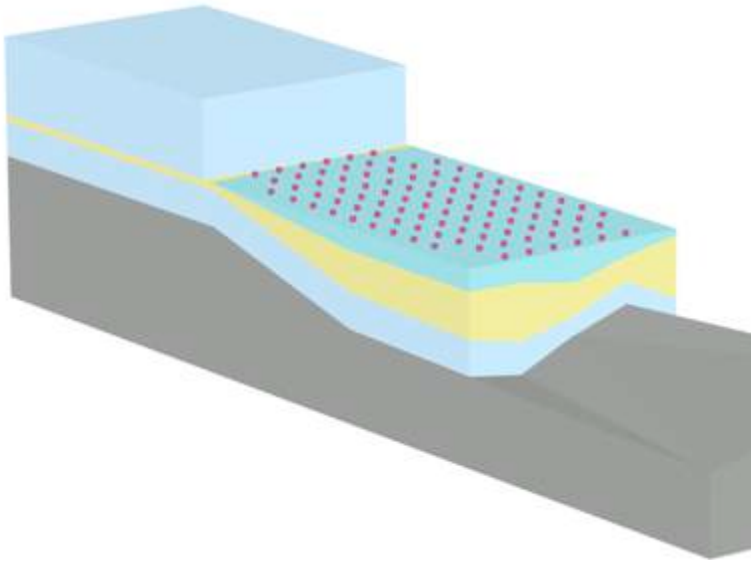

Upstream

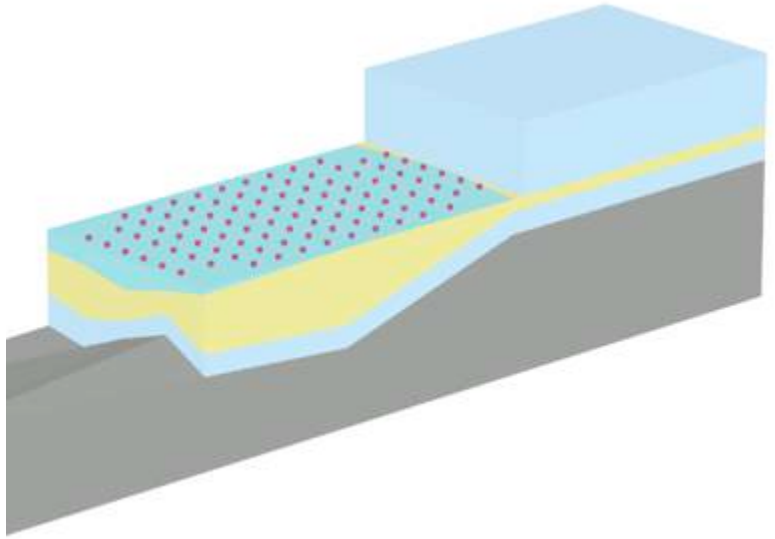

Designation	E (MPa)	υ	c' (kPa)	ϕ' (º)
Muddy soils (N_{SPT} < 1)	5	0.40	-	18
Very fine muddy sand	12.5	0.35	-	27
Fine to very fine sand	25	0.35	-	31
Schist	200	0.25	300	45

Geological-geotechnical scenario

Upstream

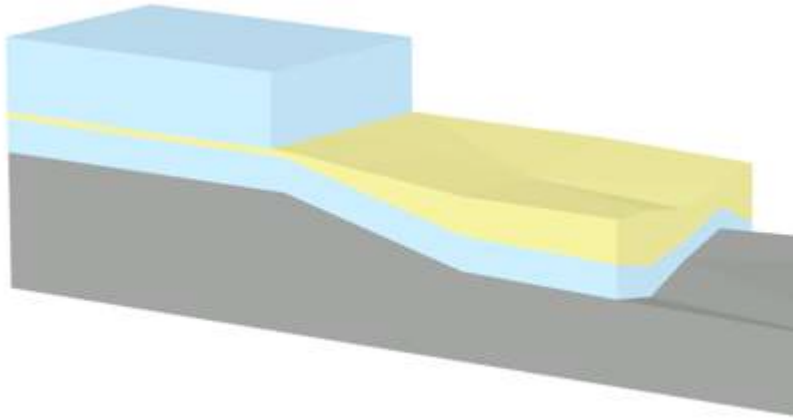

Upstream

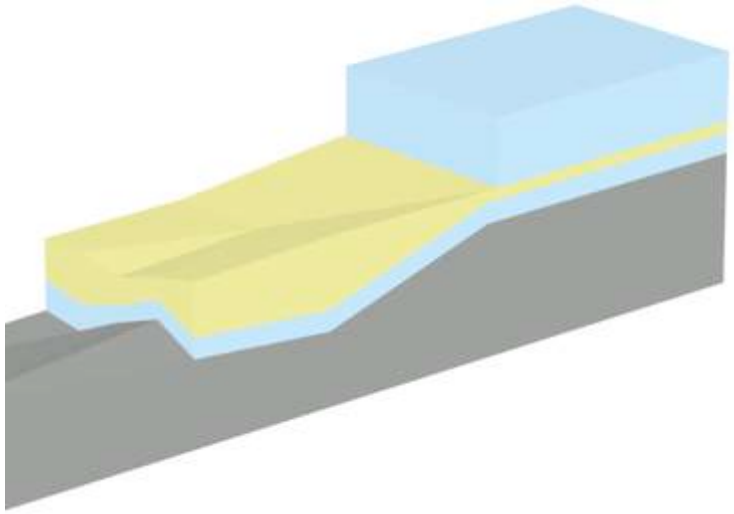

Designation	E (MPa)	υ	c' (kPa)	ϕ' (º)
Muddy soils (N_{SPT} < 1)	5	0.40	-	18
Very fine muddy sand	12.5	0.35	-	27
Fine to very fine sand	25	0.35	-	31
Schist	200	0.25	300	45

Geological-geotechnical scenario

Upstream

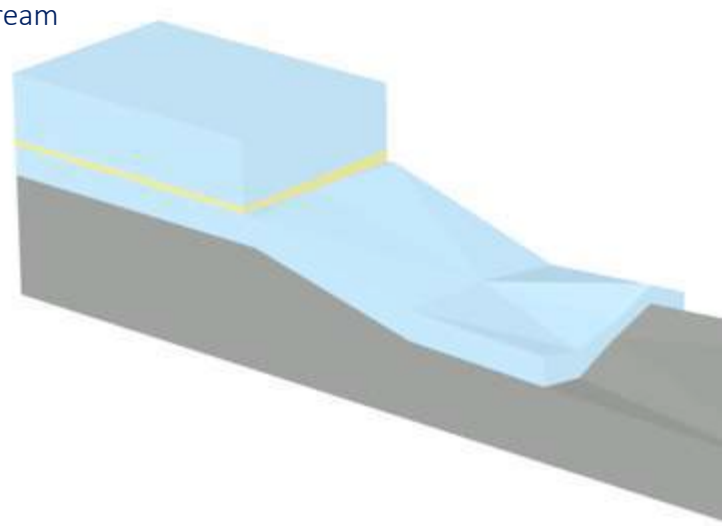

Upstream

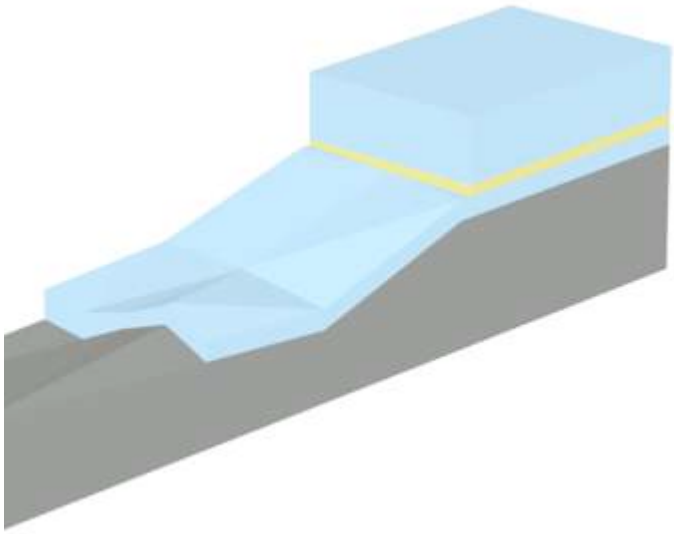

Designation	E (MPa)	υ	c' (kPa)	ϕ' (º)
Muddy soils (N_{SPT} < 1)	5	0.40	-	18
Very fine muddy sand	12.5	0.35	-	27
Fine to very fine sand	25	0.35	-	31
Schist	200	0.25	300	45

Geological-geotechnical scenario

Upstream

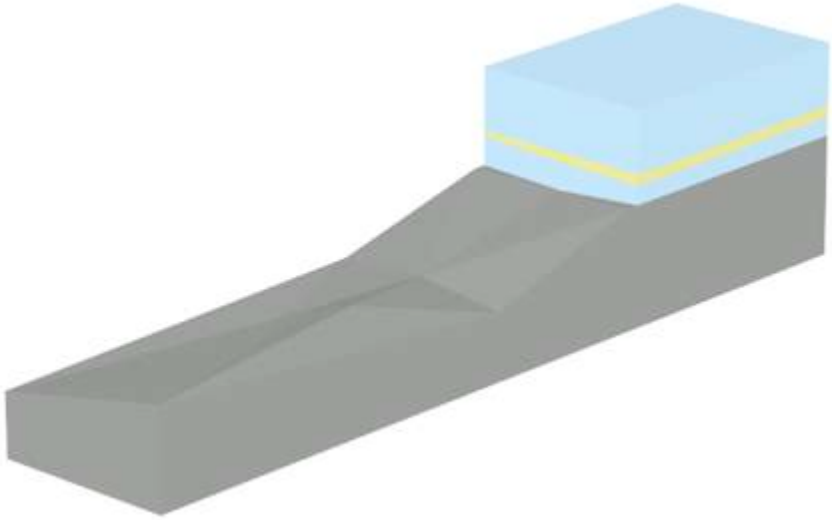

Designation	E (MPa)	υ	c' (kPa)	ϕ' (º)
Muddy soils (N_{SPT} < 1)	5	0.40	-	18
Very fine muddy sand	12.5	0.35	-	27
Fine to very fine sand	25	0.35	-	31
Schist	200	0.25	300	45

Structures

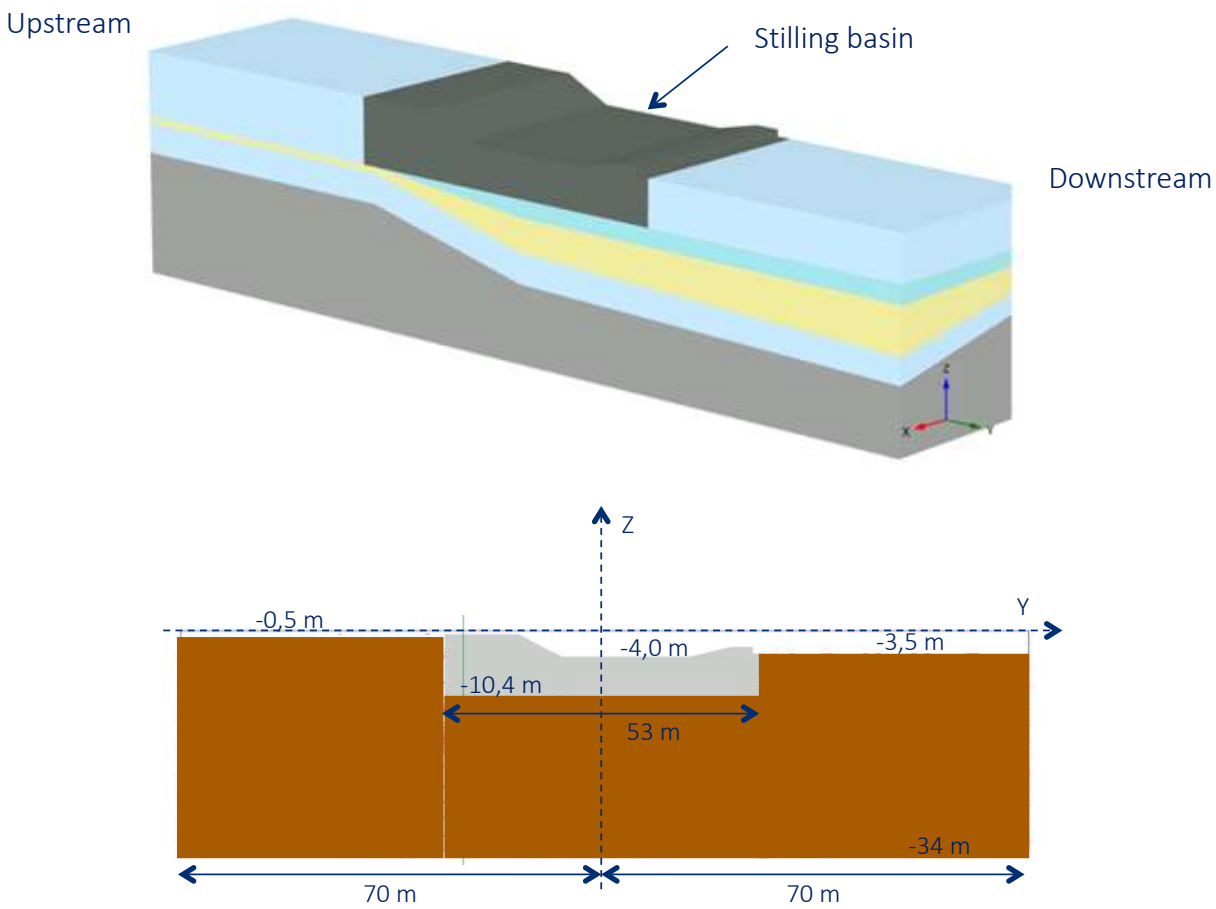
Upstream
Stilling basin
Downstream
Z
Y
-0,5 m
-4,0 m
-3,5 m
-10,4 m
53 m
-34 m
70 m
70 m

Structures

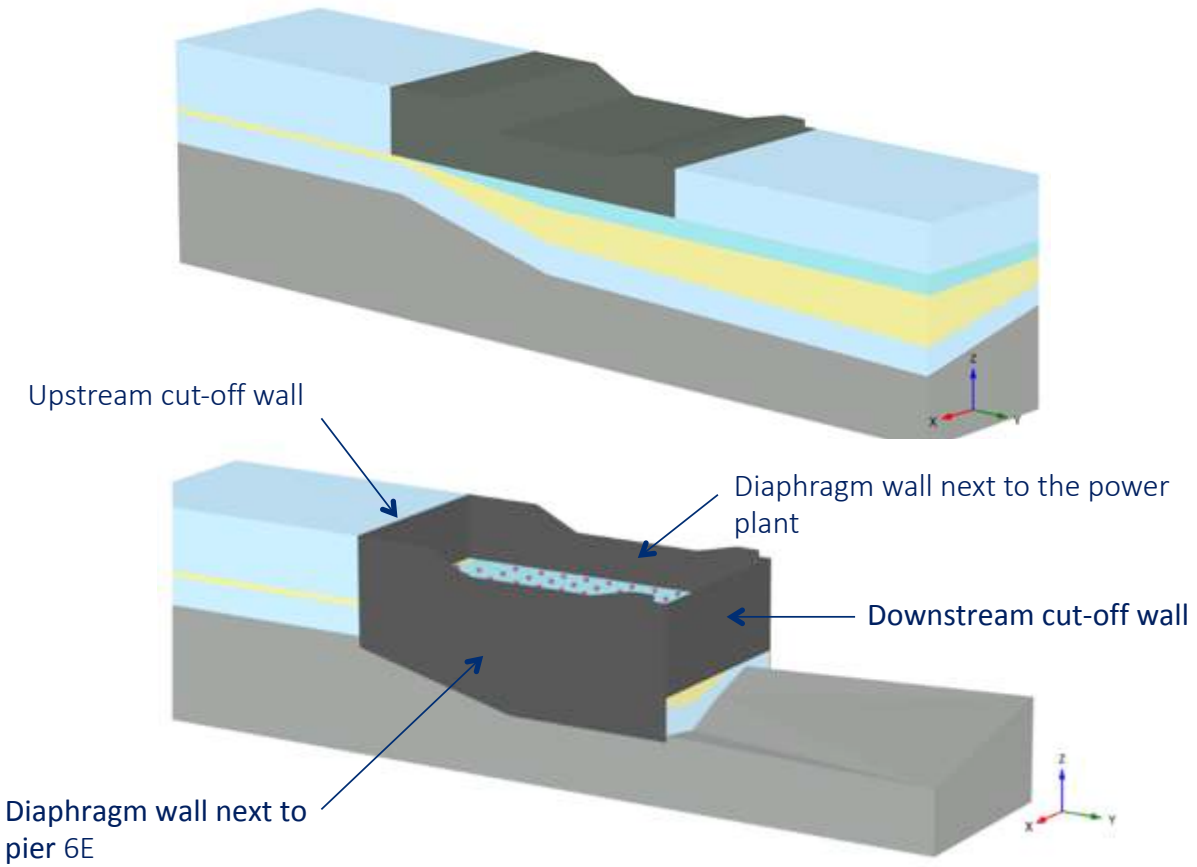
Upstream cut-off wall
Diaphragm wall next to the power plant
Downstream cut-off wall
Diaphragm wall next to pier 6E

Structures

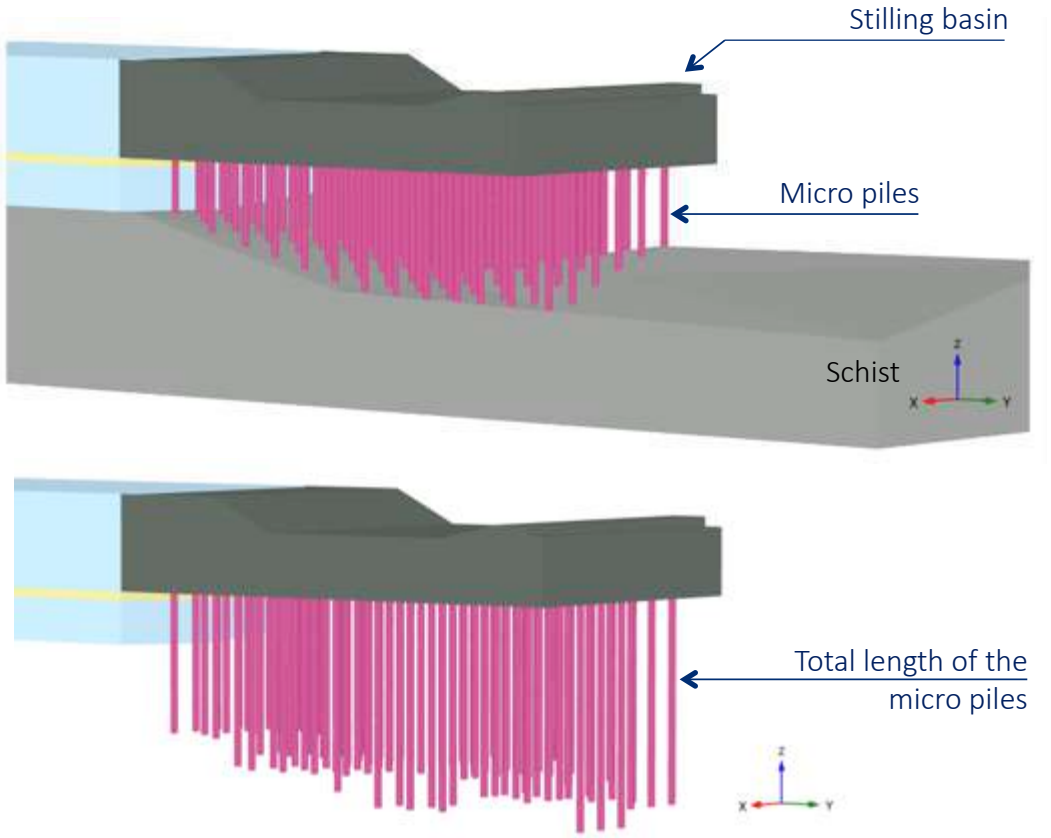
Stilling basin
Micro piles
Schist
Total length of the
micro piles

Structures

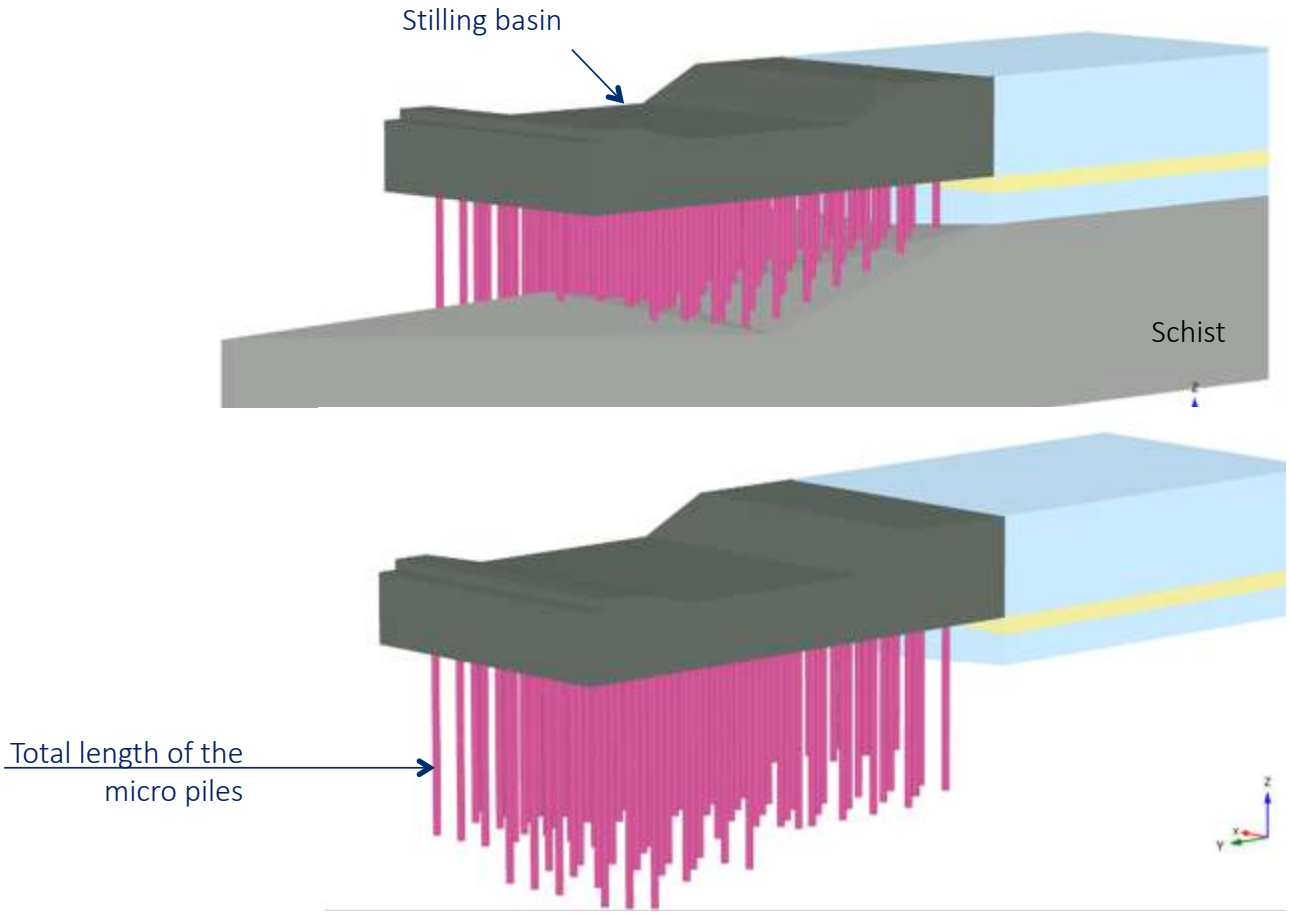

Upstream and downstream water levels

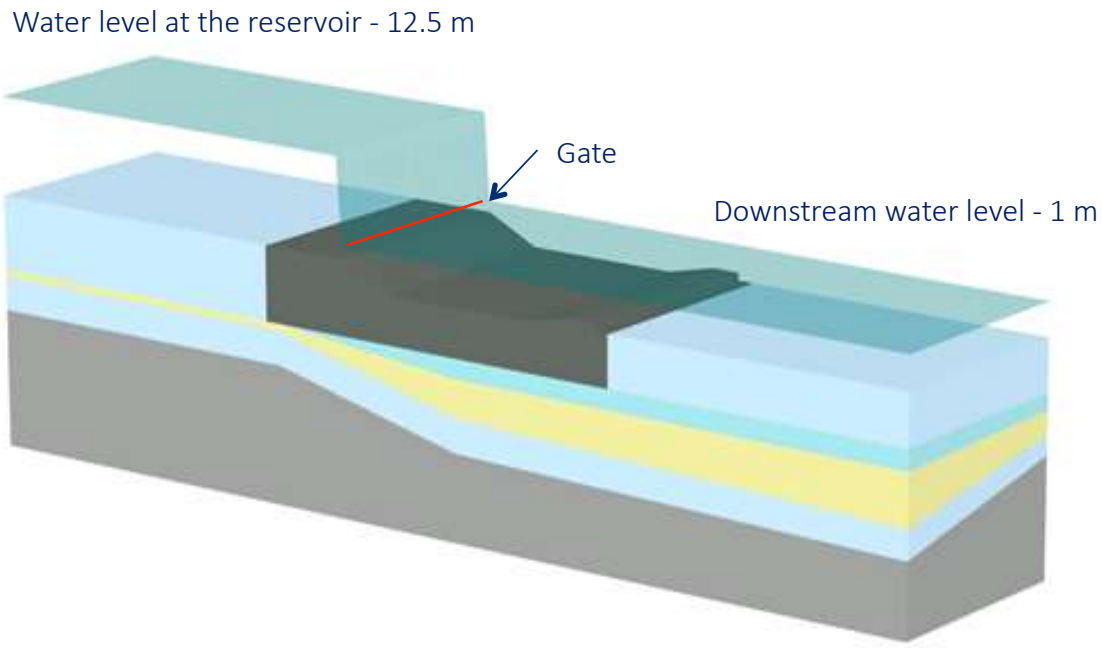

Piezometer levels measured before the construction of the pile curtain

Water level at the reservoir – 12.5 m

Downstream water level - 1 m

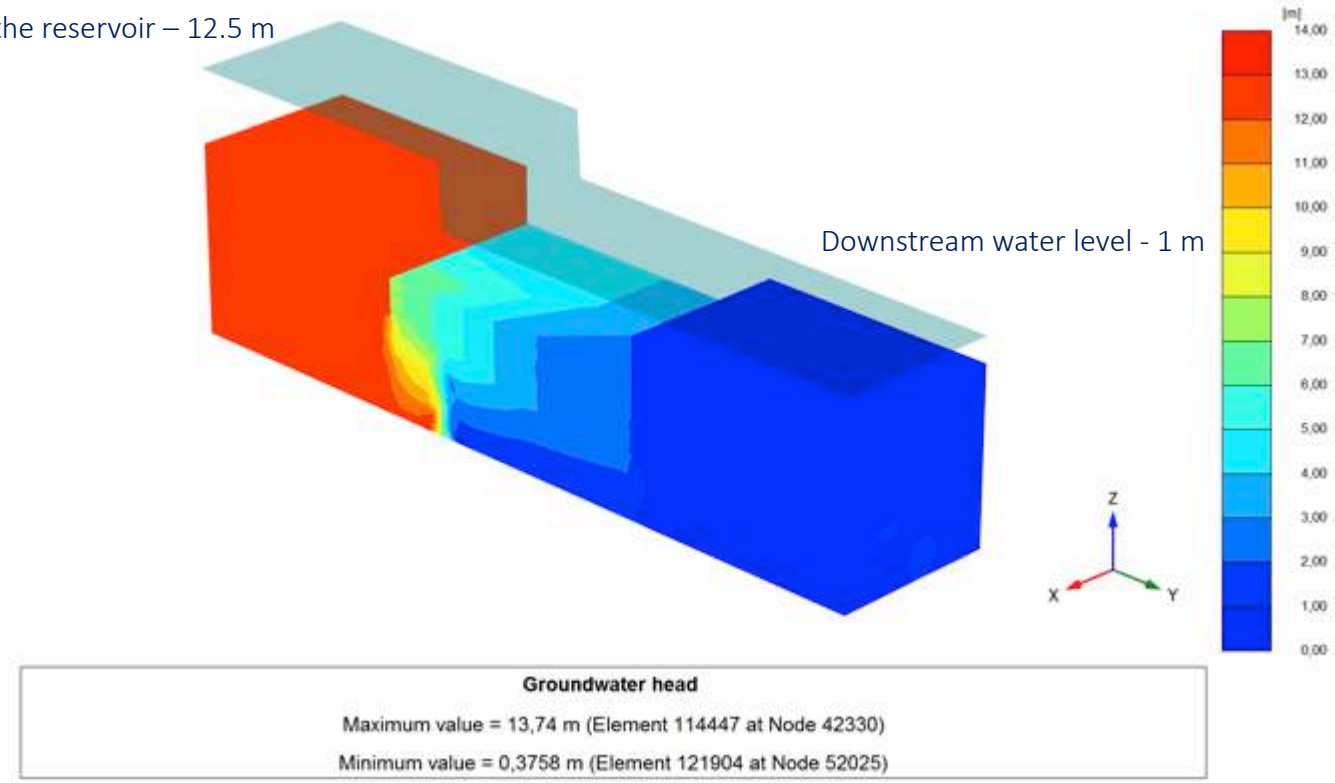

Piezometer levels after the construction of the pile curtain

Water level at the reservoir – 12.5 m

Downstream water level - 1 m

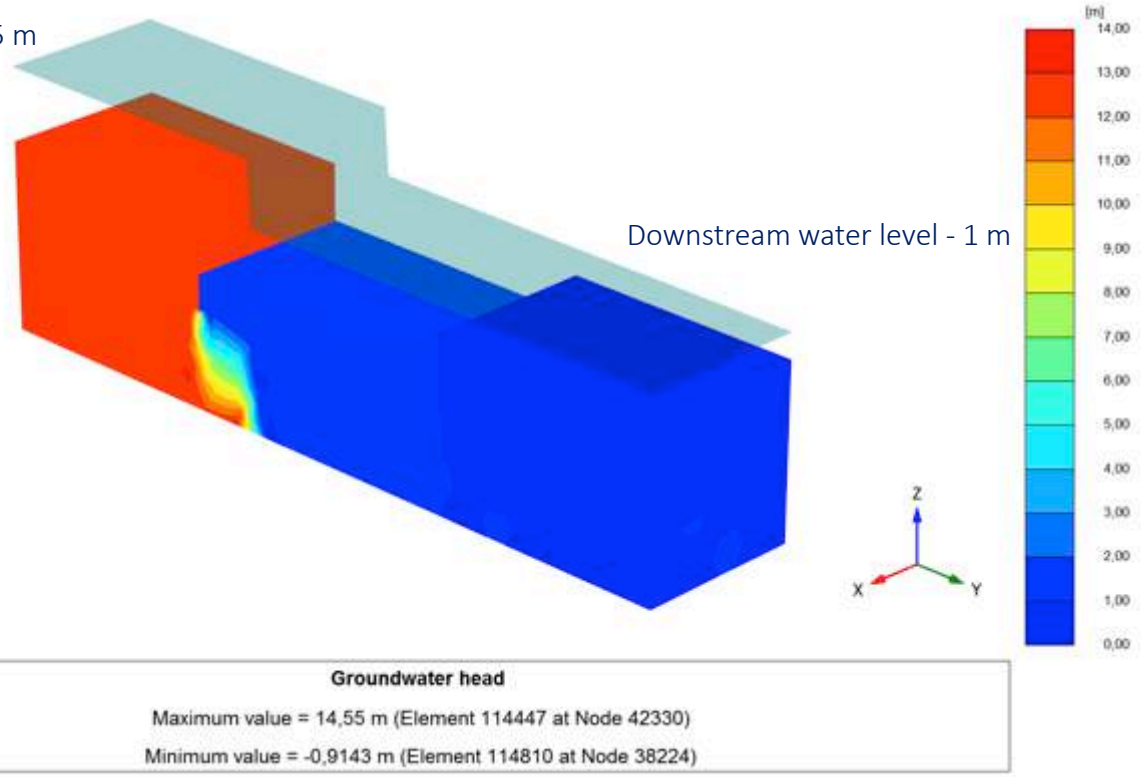

Vertical total stresses after the construction of the pile curtain

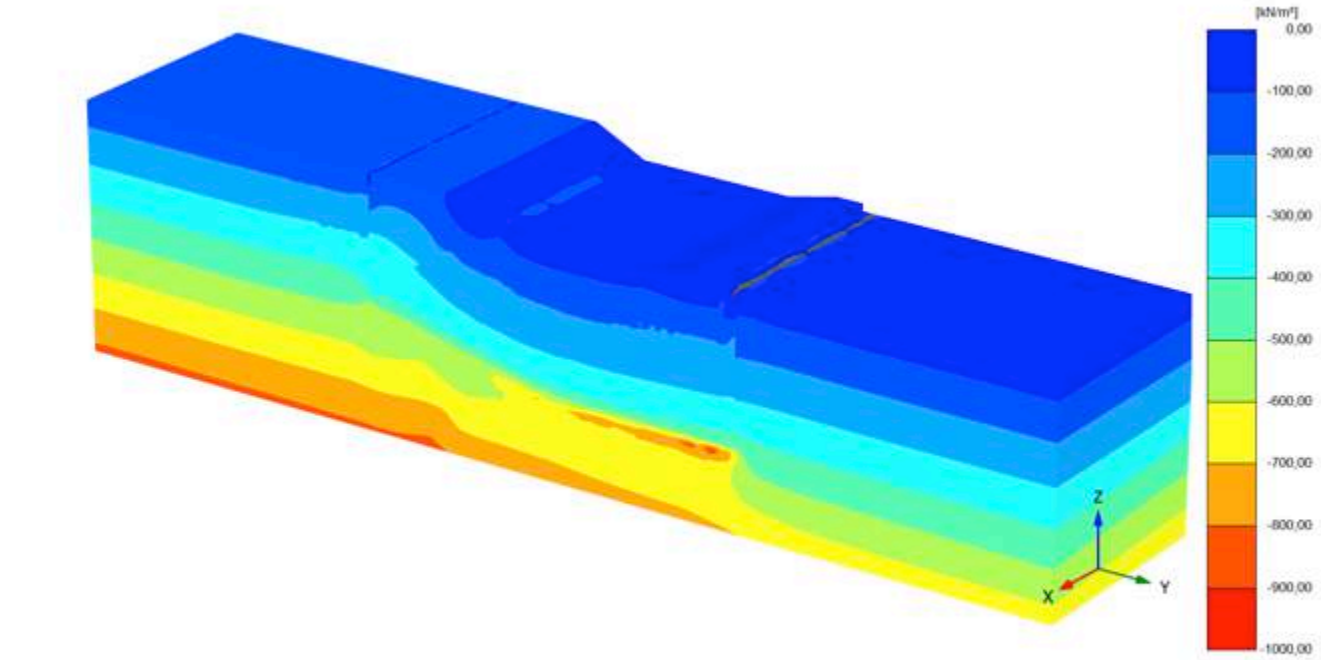

Cartesian total stress σ_{zz}

Maximum value = 379,3 kN/m² (Element 21243 at Node 37376)

Minimum value = -2816 kN/m² (Element 22008 at Node 41092)

Vertical effective stresses before the construction of the pile curtain

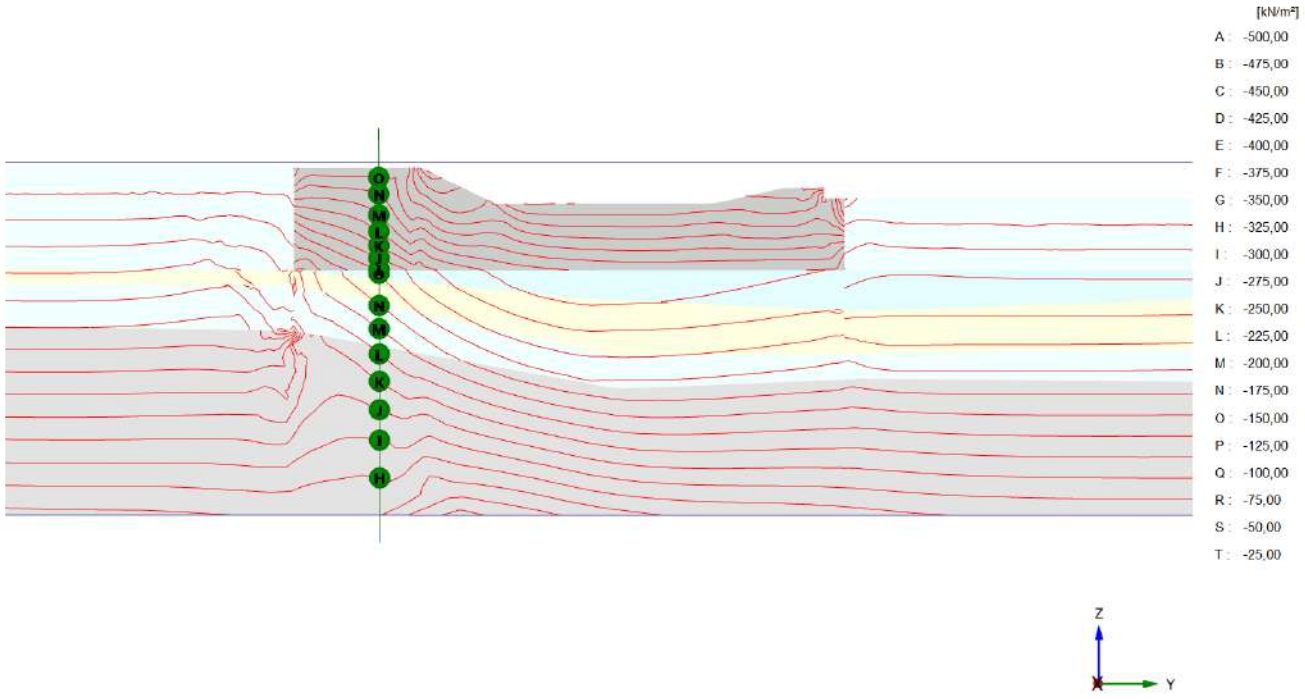

Vertical effective stresses after the construction of the pile curtain

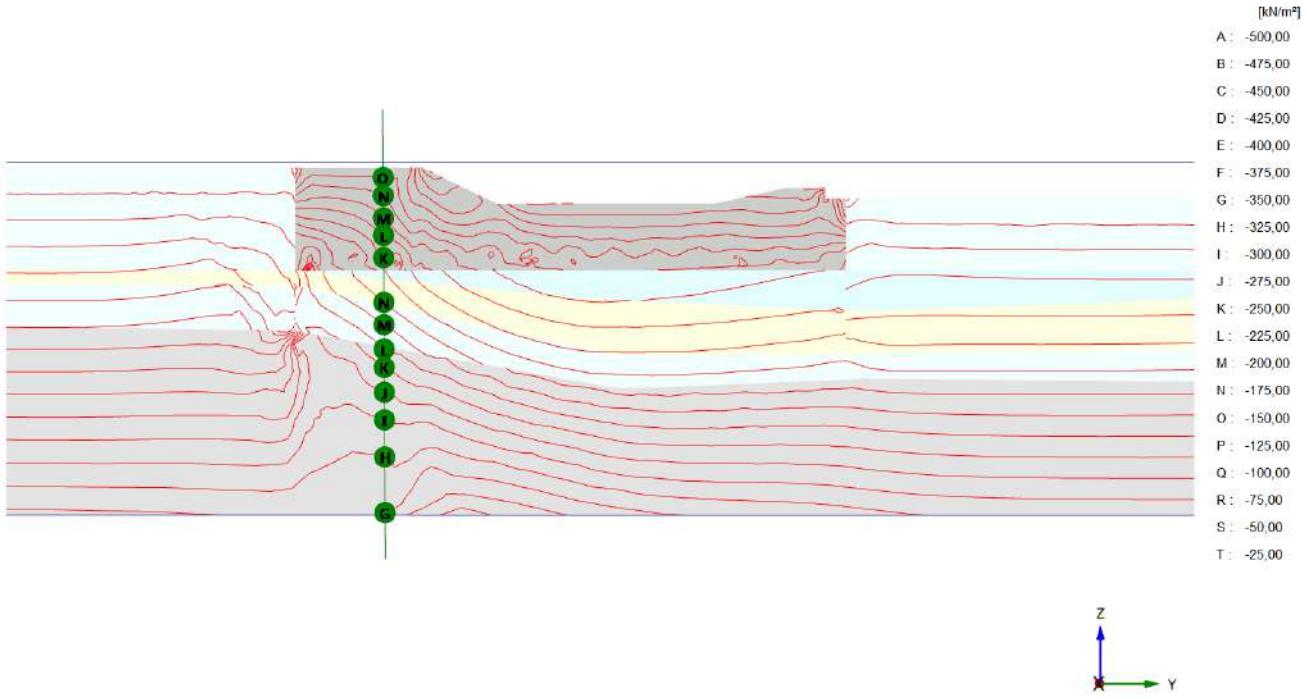

Total displacements after the construction of the pile curtain

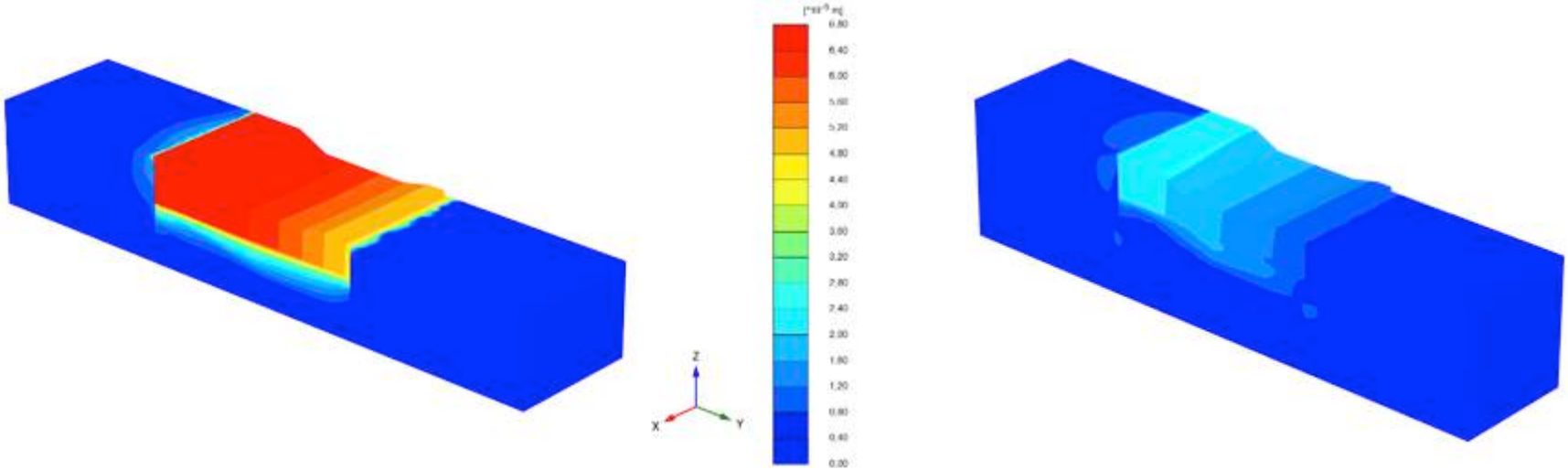

(a) Without micro piles

(b) with micro piles

Total displacements after the construction of the pile curtain

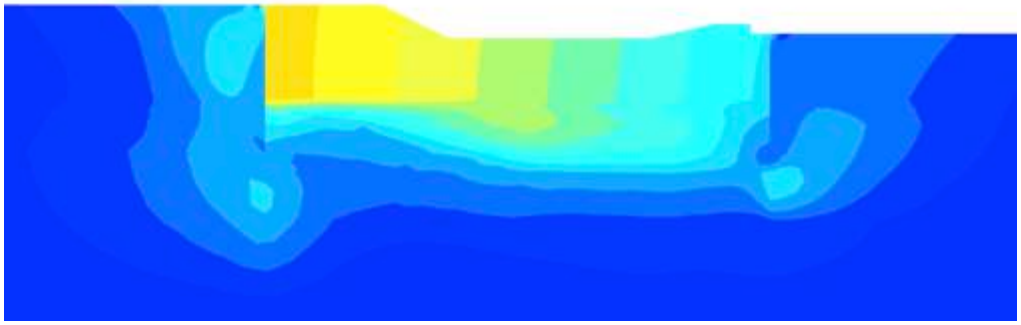

(a) Next to pier 6E

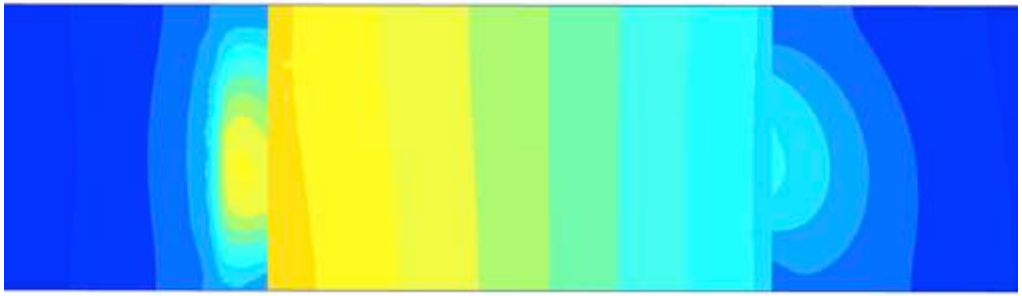

(b) At the stilling basin base

Total displacements after the construction of the pile curtain

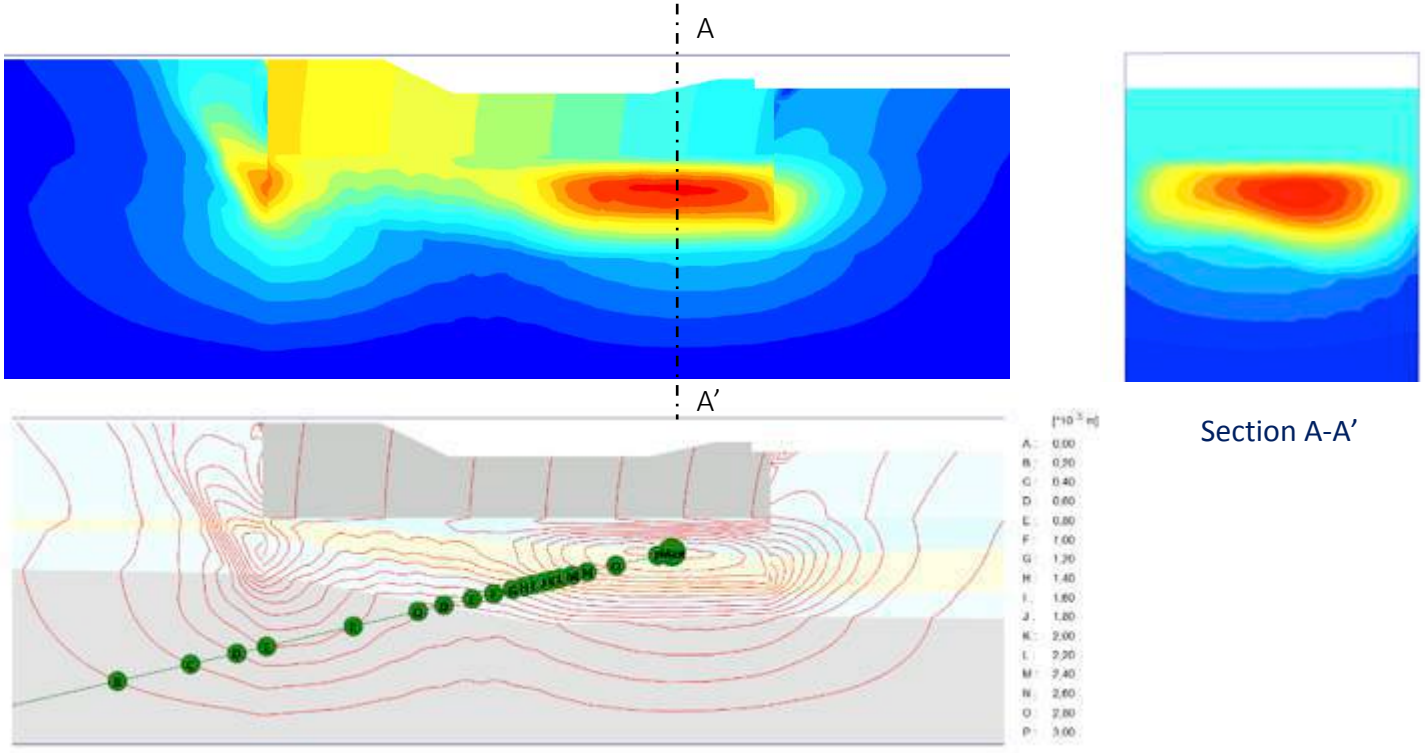

Section A-A'

(c) Central cross section

Displacements vectors after the construction of the pile curtain

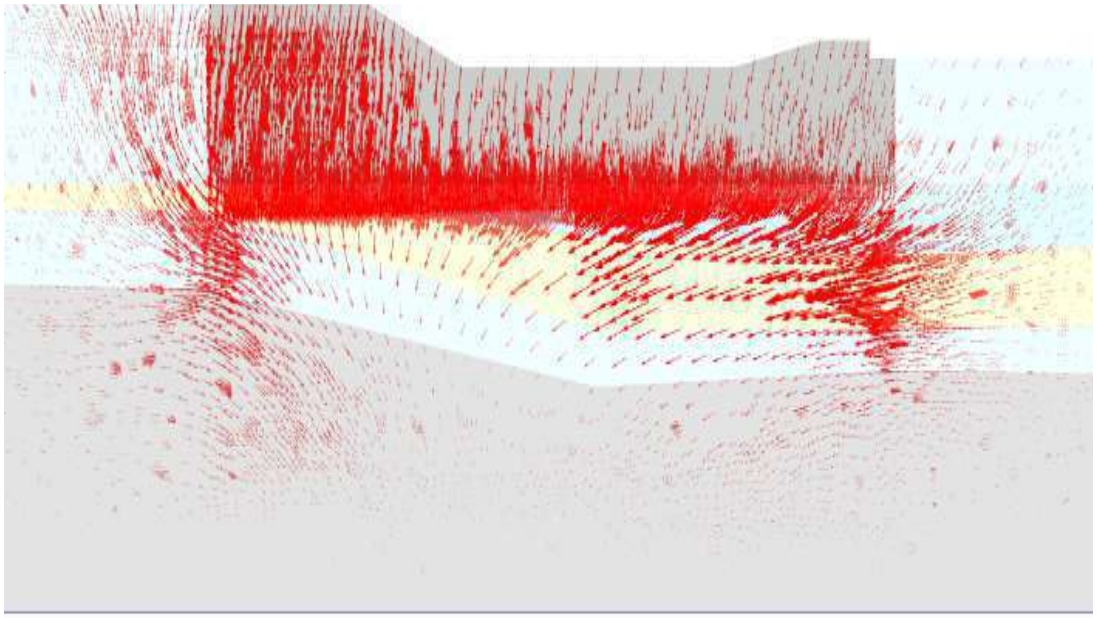

Micro pile deformation after the construction of the pile curtain

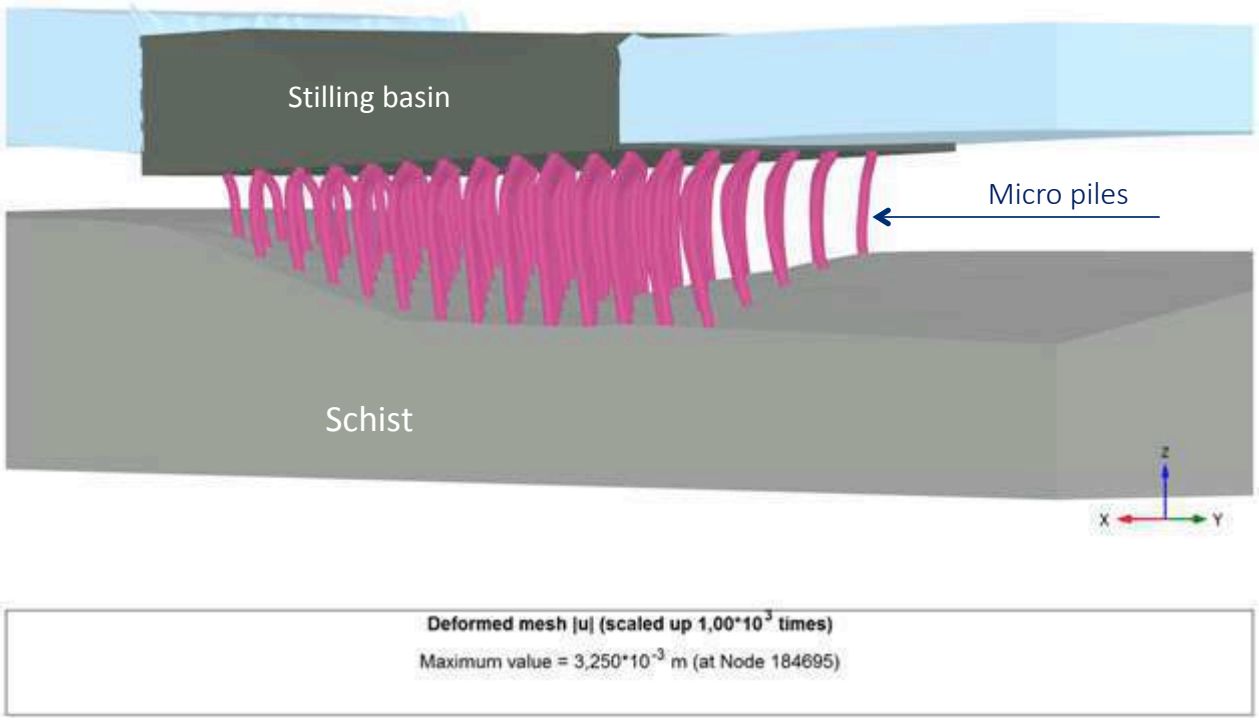

Micro pile deformation and axial forces after the construction of the pile curtain

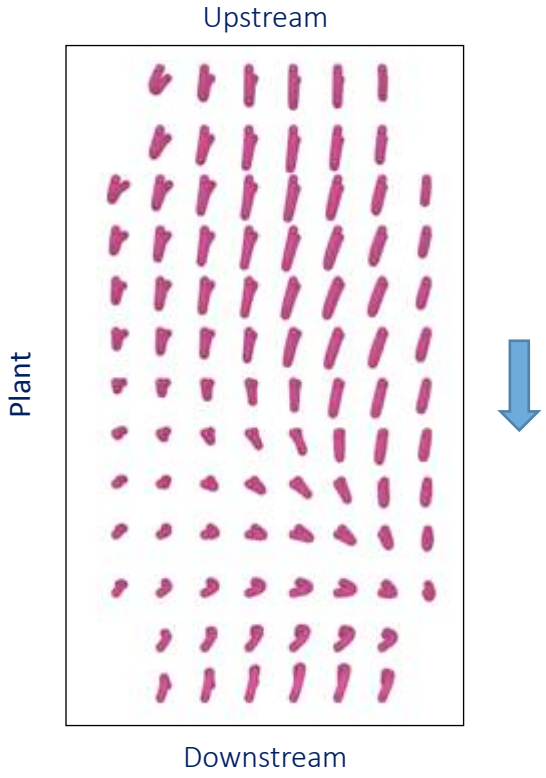

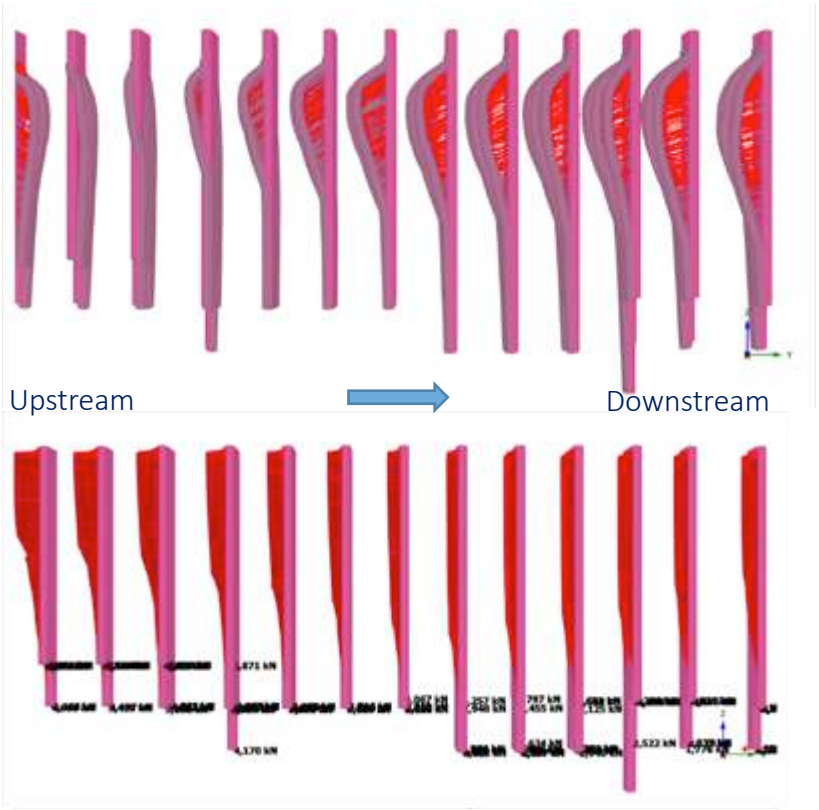

Some micro pile axial forces after the construction of the pile curtain

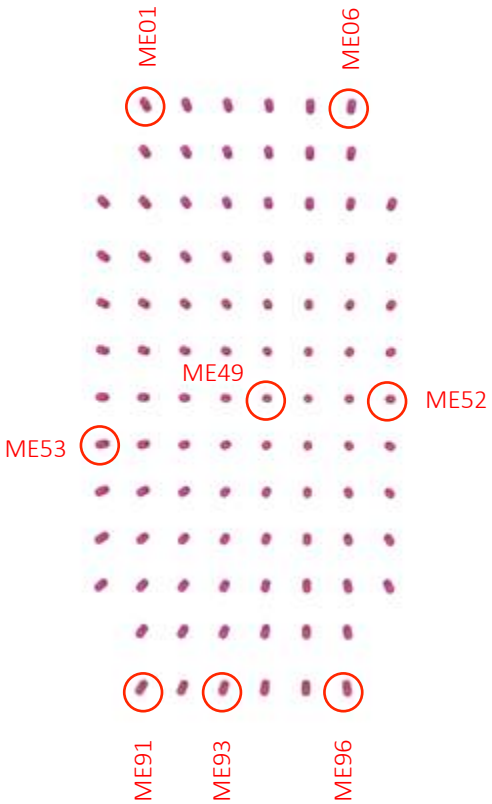

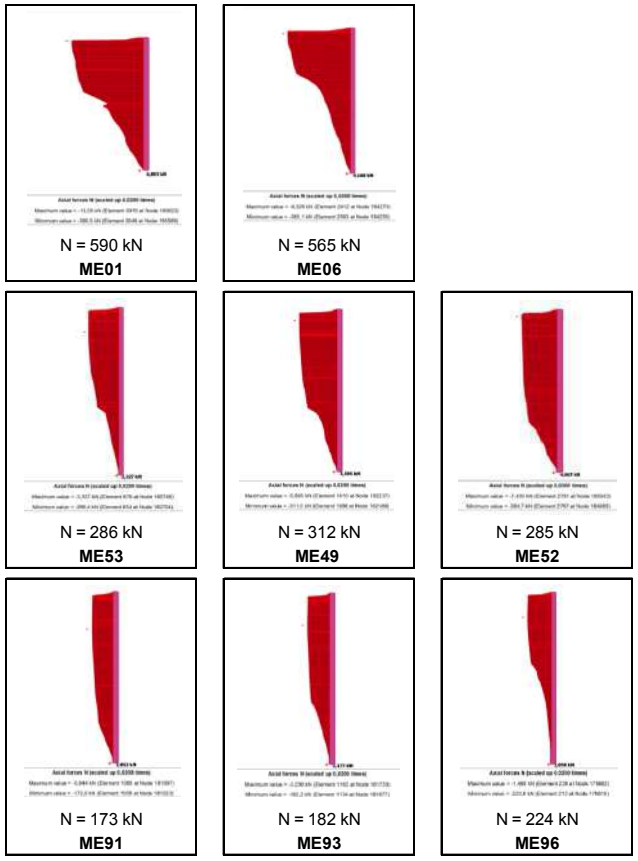

Verification of the micro pile design

Resistant capacity of the micro piles in compression:

- Hypothesis 1: contribution only of the section of the micro piles inserted in the schist mass
- Hypothesis 2: contribution of alluvial soils
- Single-shear unit resistance weighted by the injection method (global or IRS).
- The values of the unit soil-cement paste strength obtained from the FHWA report (2000)

Micro pile	N_{rd} (hip. 1) (kN)	N_{rd} (hip. 2) (kN)
ME01	973	1062
ME06	817	945
ME52	652	874
ME53	781	1074
ME96	832	977
ME93	850	1067
ME91	703	908

Buckling resistance of the micro piles

- Scenario A: without soil improvement above the sealing
- Scenario B: com grout injection using IRS method above the sealing, improvement of the properties of the surrounding soil
- Calculation of the buckling resistance of the micro piles with finite elements program SeismoStruct v7.0 (SEISMOSOFT, 2014).
- Support conditions simulated with springs, with perfectly plastic elastic behaviour
- Non-linear constitutive and geometrical calculations

Micro pile	F_{rd} (kN)	
	Scenario A	Scenario B
ME01	646	-
ME06	678	746
ME52	546	601
ME53	612	674
ME96	479	-
ME93	532	-
ME91	251	-

Compressive and buckling resistance of the micro piles

	ME01	ME06	ME53
	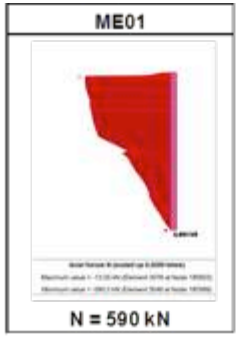	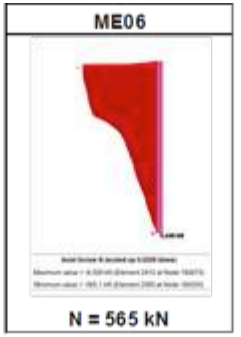	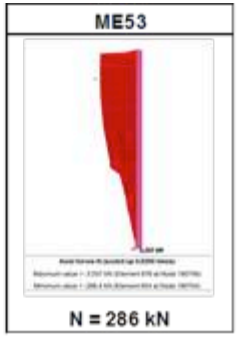
Axial force.....	N = 590 kN	N = 565 kN	N = 286 kN
Compressive resistance.....	1167 kN	981 kN	937 kN
Buckling resistance	646 kN	650 kN	500 kN

	ME52	ME91	ME93	ME96
	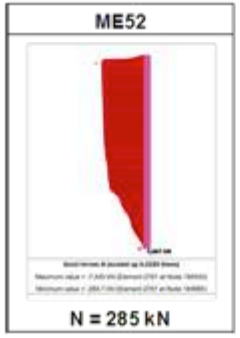	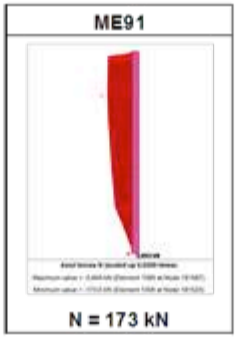	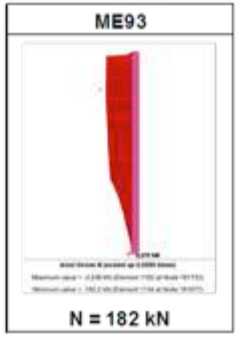	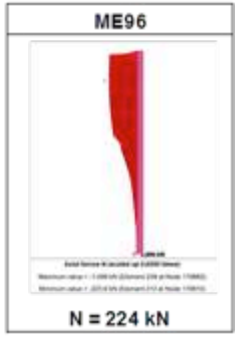
Axial force.....	N = 285 kN	N = 173 kN	N = 182 kN	N = 224 kN
Compressive resistance.....	837 kN	844 kN	1020 kN	998 kN
Buckling resistance	509 kN	251 kN	410 kN	344 kN

Conclusions

- The recent intervention in basin 7E allowed for a significant improvement regarding the Crestuma-Lever dam safety
- Some specific characteristics of this basin (geological composition, defects of the panels of the upstream cut-off wall and the constructive planning) could increase the risk of internal erosion and/or undesired movements when compared to the other basins
- The stilling basin deforms as a rigid body, settling further upstream and downstream, after the construction of the upstream waterproofing curtain
- The decrease of pore water pressures under the stilling basin implies a reduction of the pressure acting on the upstream and downstream cut-off walls, which leads to their inward bending
- The micro-piles reduce stilling basin settlements in a relevant way
- The axial force on the micro piles are larger upstream and lower downstream
- The compressive resistance of the micro piles exceeds the acting forces
- Contrary to what would be expected, the buckling ultimate limit state is the most conditioning in this specific scenario

Acknowledgments

LNEC

- Joana Carreto
- Luís Miranda
- Rute Ramos
- João André

EDP

- Celso Lima
- Magda Queralt
- Irene Fernandes

Thank you for your attention

Stabilization of Highway Embankment Over Soft Soils

Rui Tomásio, Alexandre Pinto

JETsj – Geotecnia

ÍNDICE

1. Introdução
2. Condicionamentos
3. Soluções Adotadas
4. Modelos de Cálculo
5. Construção
6. Instrumentação
7. Considerações Finais

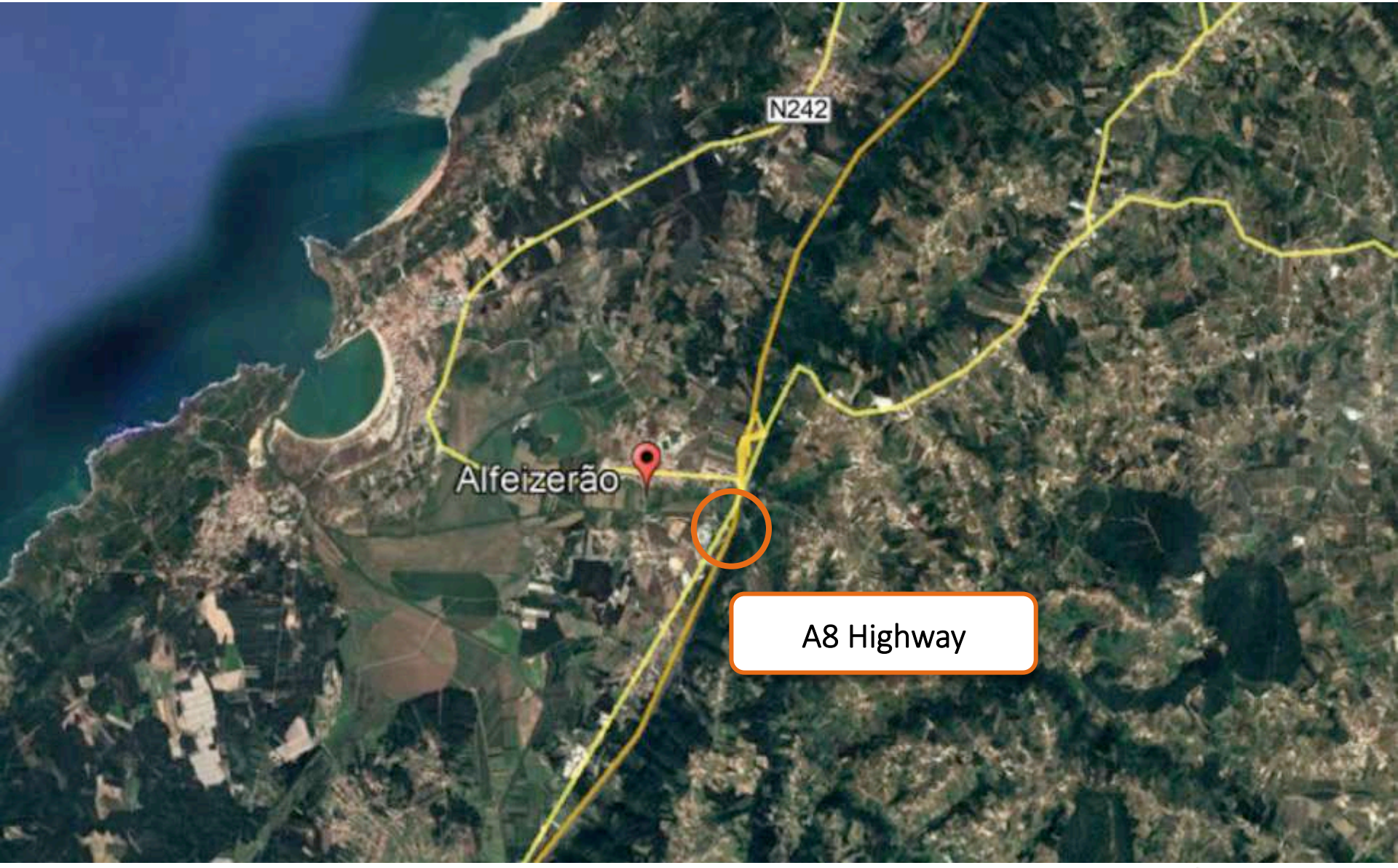
N242
Alfeizerão
A8 Highway

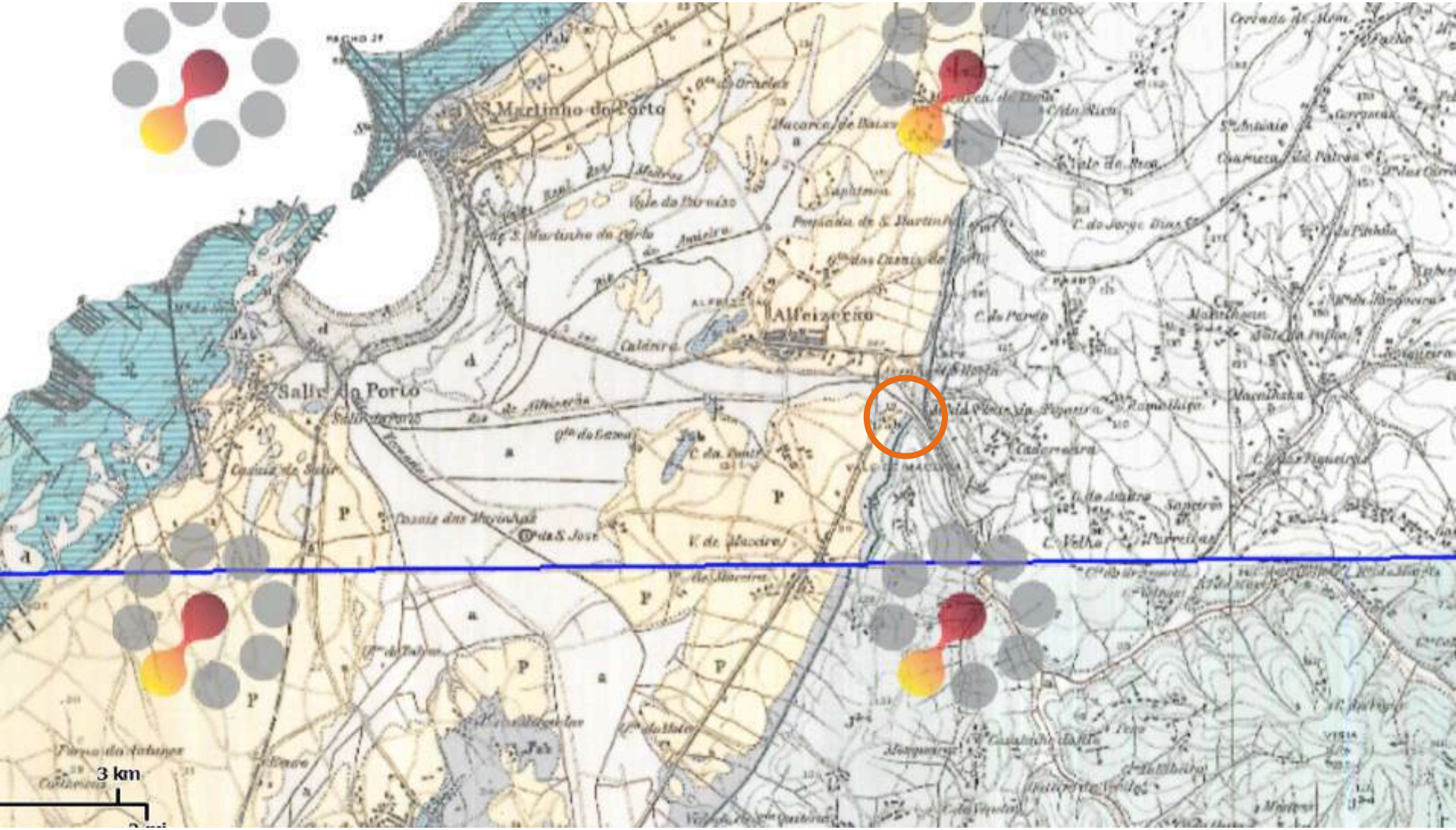
S. Martinho do Porto
Alfeizerão
Salir do Porto
3 km


N8
N
Gabion Wall
A8
Houses
Unstable area

Cross section after the construction of the motorway A8 platform

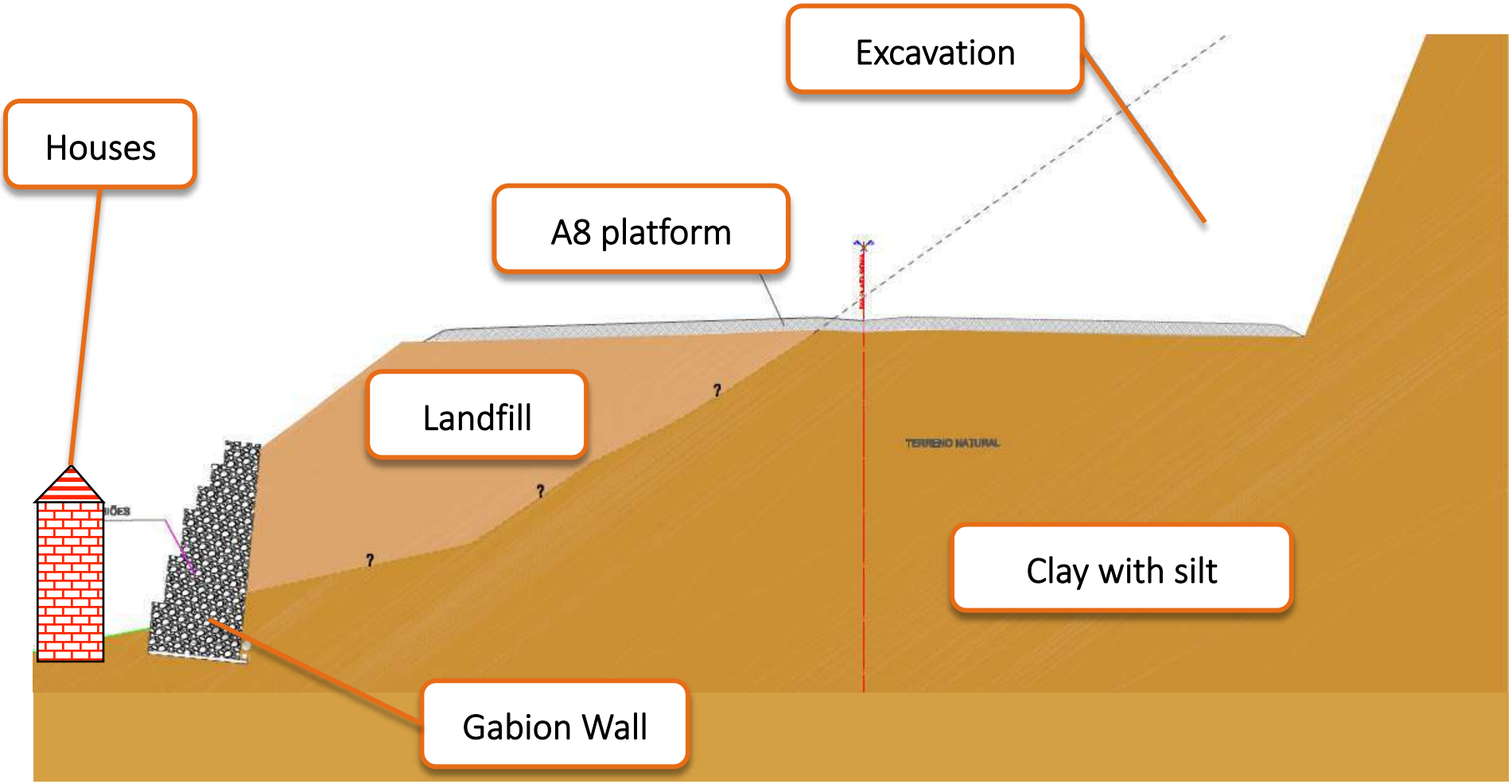


Gabion Wall
Houses

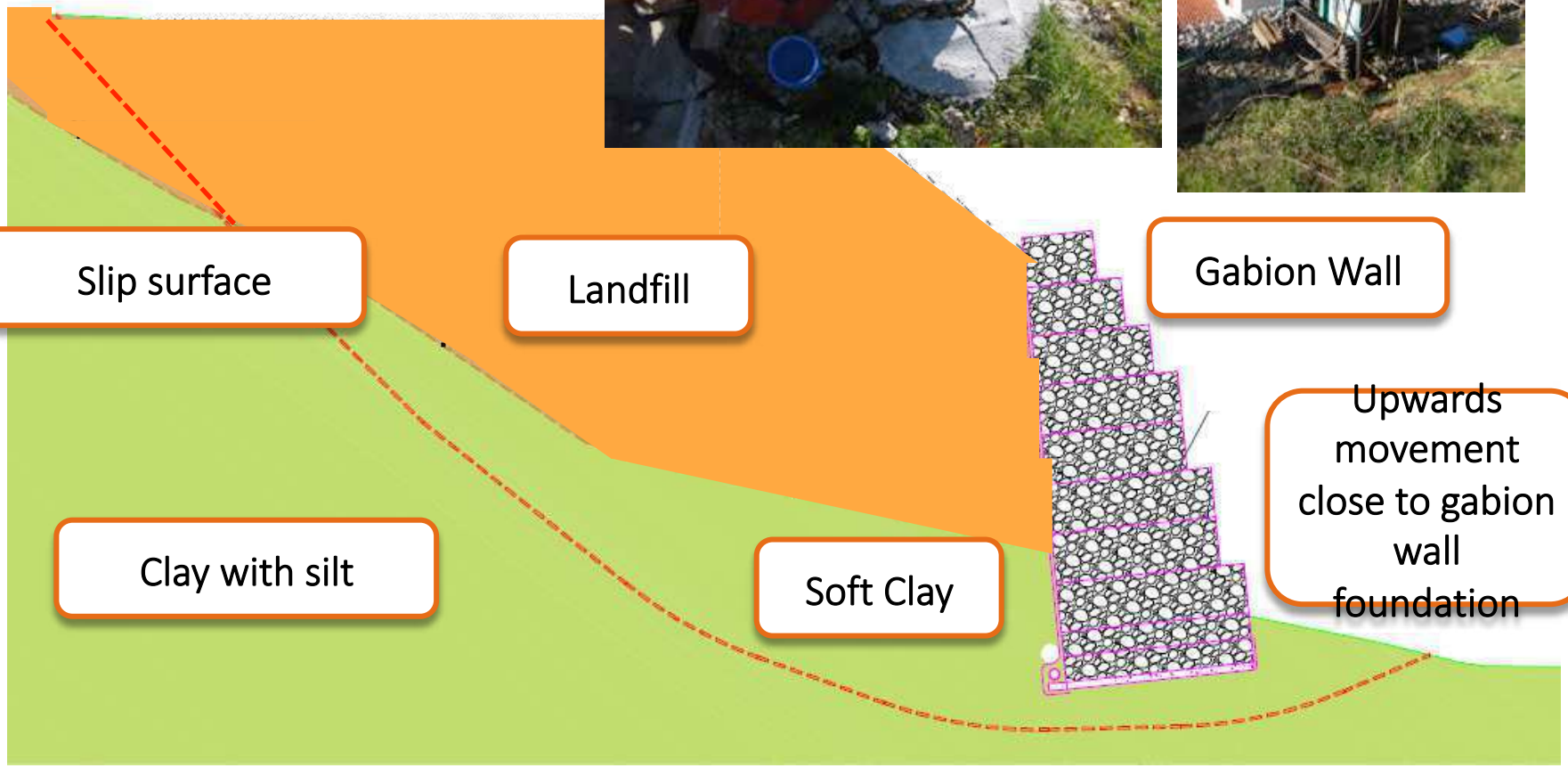
Cracks at platform
Slip surface
Landfill
Gabion Wall
Upwards movement close to gabion wall foundation
Clay with silt
Soft Clay


A 8
Leiria
Nazaré
Alcobaça
(A 29) Porto
Alfeizerão
S. Martinho
Porto
1000 m

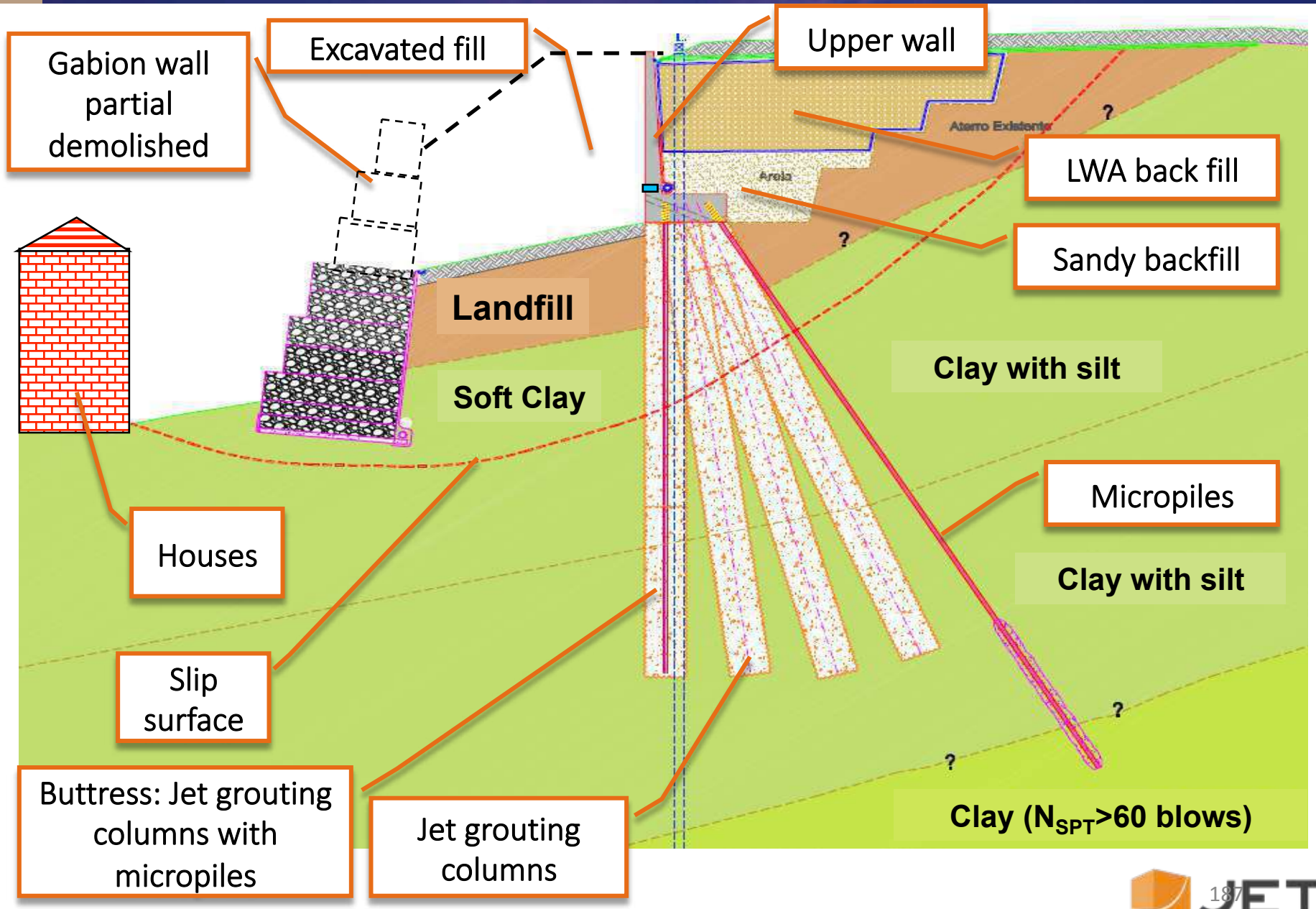
Gabion wall partial demolished
Excavated fill
Upper wall
LWA back fill
Sandy backfill
Landfill
Soft Clay
Clay with silt
Houses
Micropiles
Clay with silt
Slip surface
Buttress: Jet grouting columns with micropiles
Jet grouting columns
Clay (NSPT>60 blows)
Aterro Existente
Areia
?

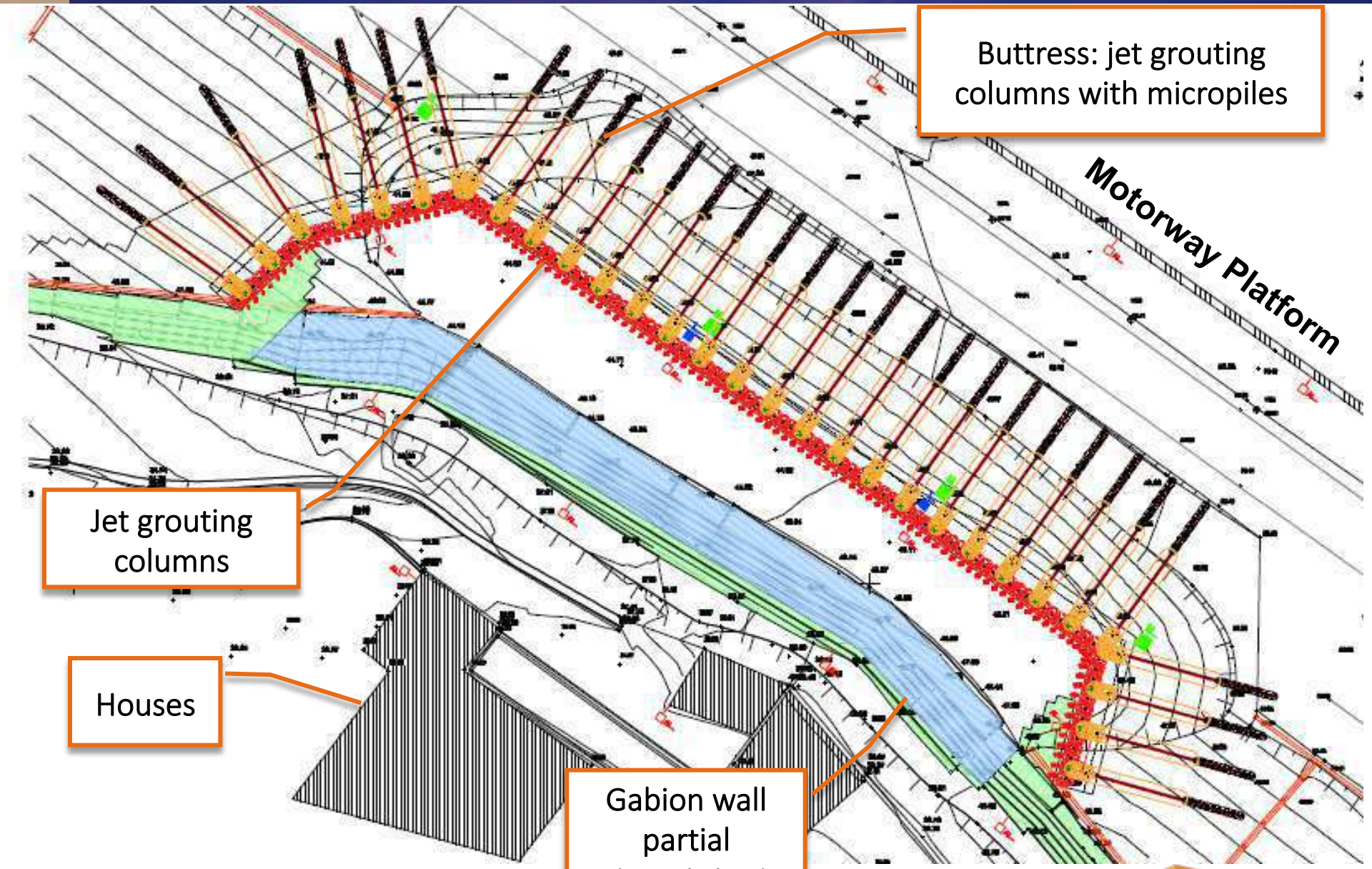
Buttress: jet grouting columns with micropiles
Motorway Platform
Jet grouting columns
Houses
Gabion wall partial demolished

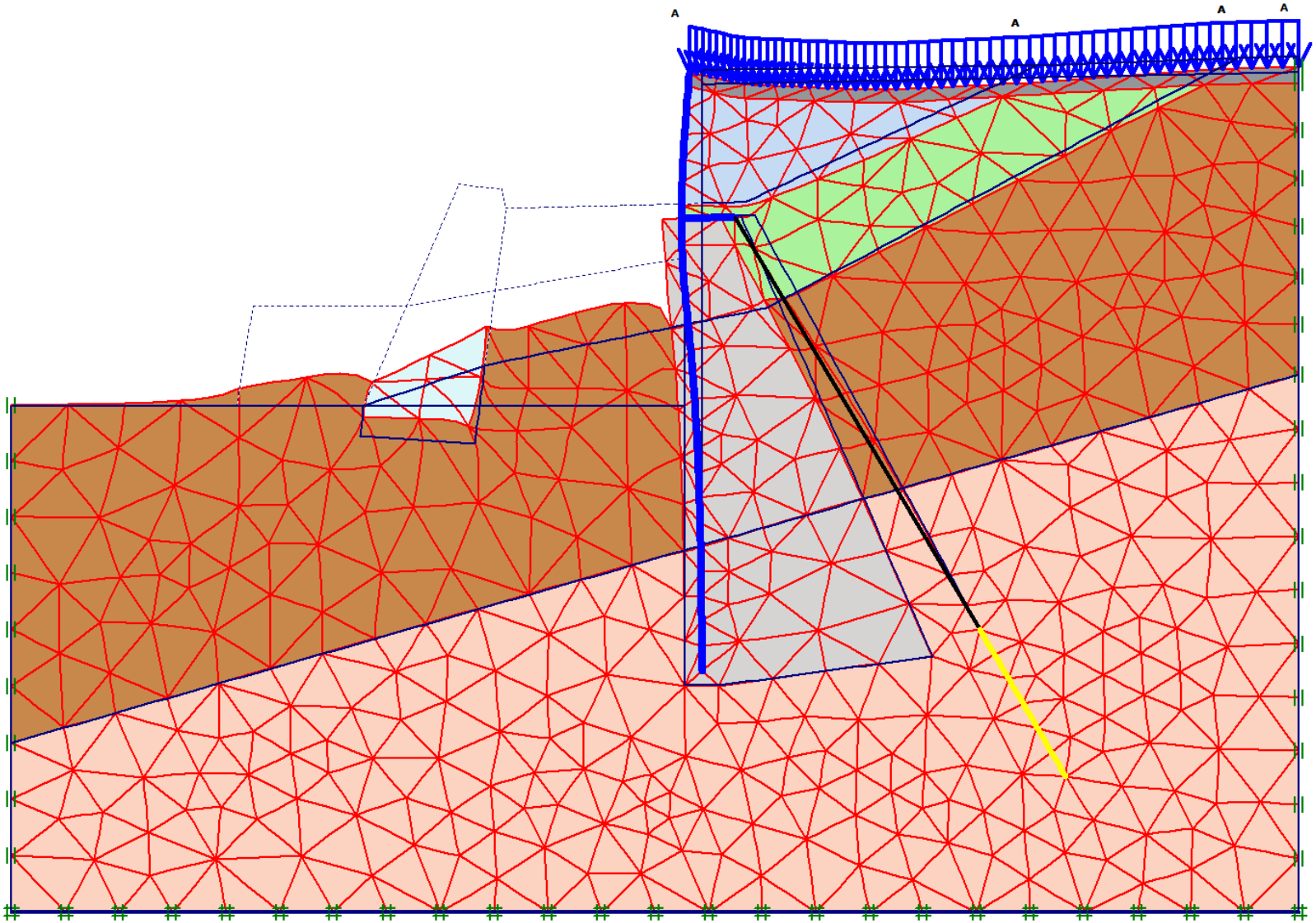
A
A
A
A


Base of the upper wall
Micropiles


Transfer of the sand from the big bags to the upper wall backfill

Jet grouting test columns

Gathering of jet grouting cores for UCS tests

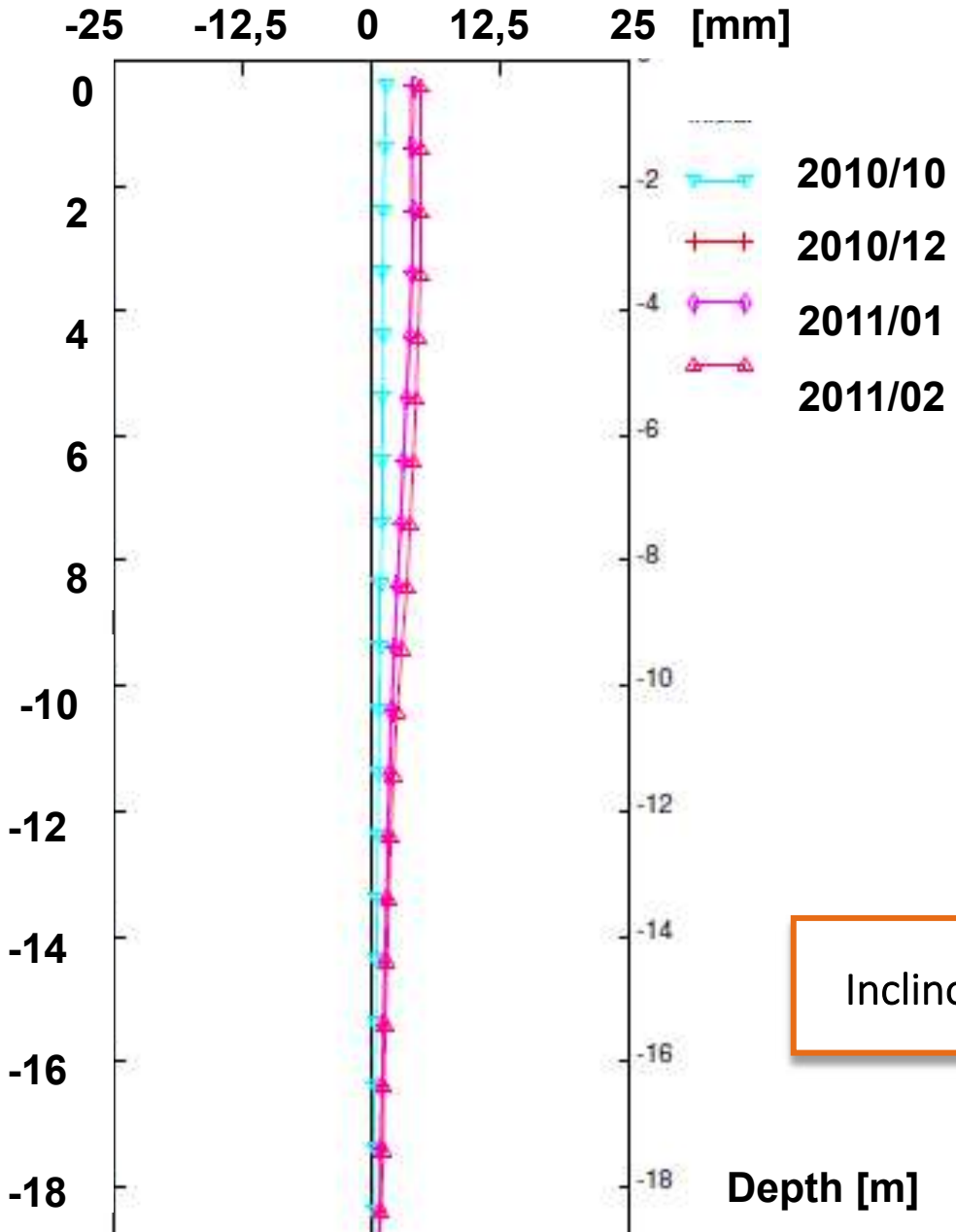
-25
-12,5
0
12,5
25
[mm]
0
2
4
6
8
-10
-12
-14
-16
-18
-2
-4
-6
-8
-10
-12
-14
-16
-18
2010/10
2010/12
2011/01
2011/02
Depth [m]


Inclinometer


OBRIGADO PELA ATENÇÃO

2SGT2019
2nd SEMINAR ON TRANSPORTATION GEOTECHNICS

Soil Improvement Challenges on Alluvial Zones

28-29 January 2019 | Vila Franca de Xira | Portugal

Soil Treatment with Jet-Grouting Associated to Retaining Structures of the Machico-Caniçal Expressway in Madeira Island

Carlos Oliveira Baião; Miguel Menezes Conceição; Vitória Conceição Rodrigues; José Mateus de Brito

CONSULTORES DE ENGENHARIA E ARQUITETURA, S.A.

Organização

Sociedade Portuguesa de Geotecnia

Comissão Portuguesa de Geotecnia nos Transportes

Comissão Portuguesa de Geossintéticos

Apoios

LABORATÓRIO NACIONAL DE ENGENHARIA CIVIL

ORDEM DOS ENGENHEIROS

SUMMARY

1. General description of the Machico-Caniçal expressway section
2. Some references to the most relevant geological and geotechnical aspects of the area
3. Geotechnical characterization of the slope deposits
4. Main aspects related with the design and the construction of the special foundations with jet-grouting
5. Conclusions

GENERAL DESCRIPTION

- The Machico-Caniçal expressway section, 8km in length, is located in the south-eastern side of Madeira Island, along the coastline, connecting the Airport to Caniçal, where an important commercial port exists

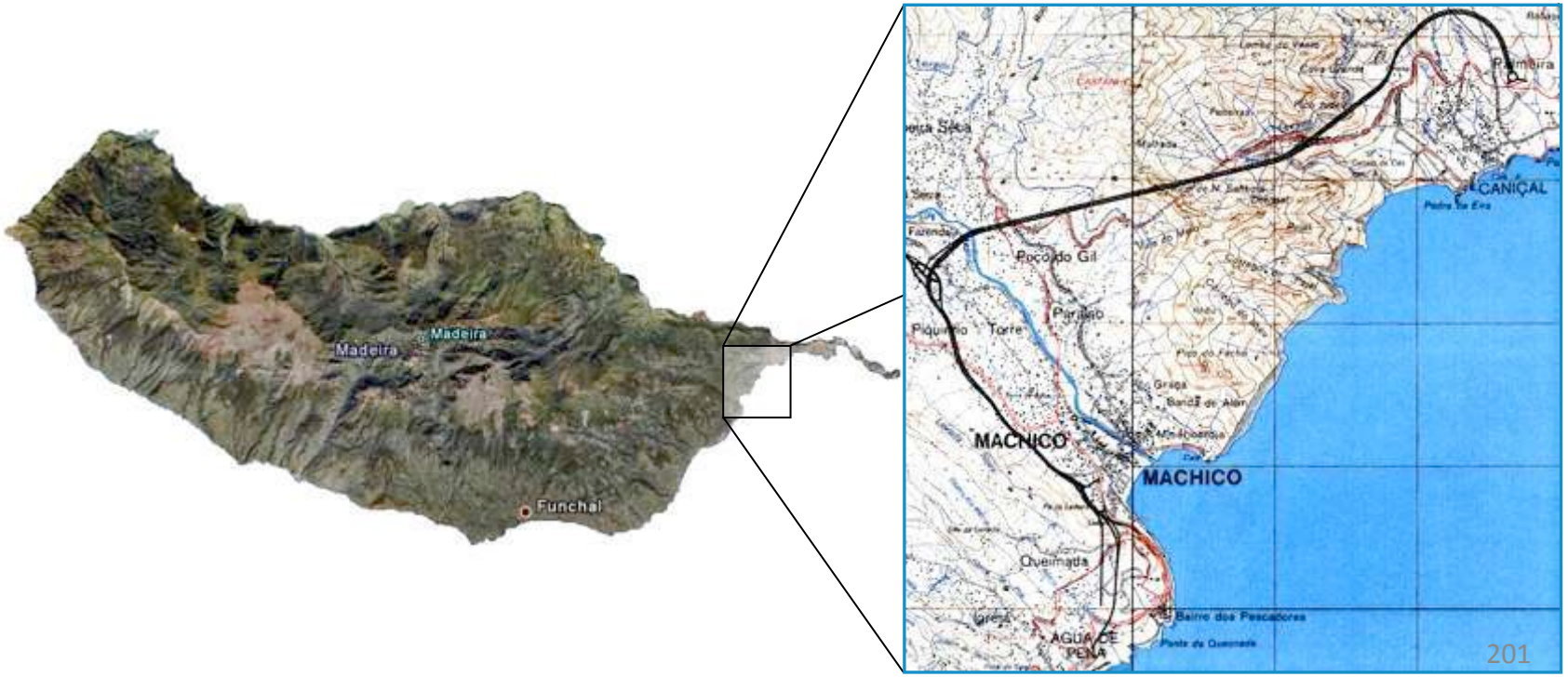

GENERAL DESCRIPTION

- It is part of Madeira Island VR1 expressway that connects Ribeira Brava to Caniçal, through Funchal city
- The expressway included the construction of 8 tunnels, 5 of them double, and 4 double bridges and viaducts
- The tunnels had a total length of 9.750 m
- The bridges and viaducts had a total length of 1.144 m
- An important set of retaining structures were also designed, with a total length of 2.750 m, 1.900 m corresponding to retaining structures with heights equal to or higher than 8 m

GENERAL AND GEOLOGICAL PLANT

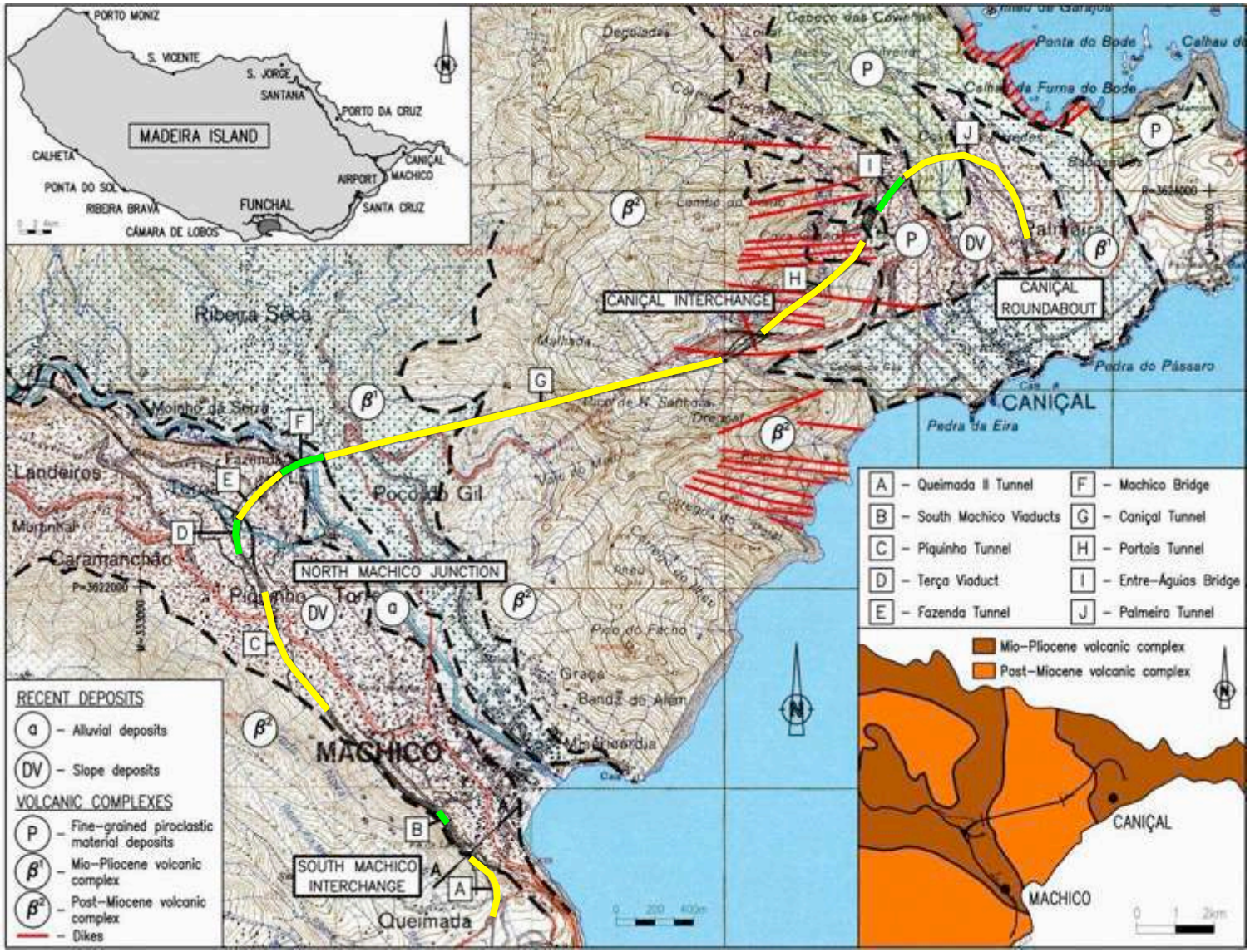

GEOLOGICAL AND GEOTECHNICAL ASPECTS

- The expressway was constructed on Post-Miocene (β^2) and Mio-Pliocene (β^1) volcanic complexes formations
- The β^2 complex, of a substantially heterogeneous constitution, is formed by alternate layers of basaltic lava flows and pyroclastic materials (breccia), usually interstratified, also intercalated with generally less important layers of tuffs
- The β^1 complex is also very heterogeneous and is formed by a chaotic pile of coarse materials resulting from the projection of angular blocks and volcanic bombs encased, to a more or less significant degree, in fine pyroclastic material

GEOLOGICAL AND GEOTECHNICAL ASPECTS

- These complexes are generally covered by alluvial deposits and/or slope deposits

- The alluvial deposits, accumulated along the Machico river, generally very coarse and heterogeneous, are constituted by rounded blocks or rolled fragments and pebbles of basalt, covered in a sandy-silt or clay-silt disaggregated matrix. This formation resulted from the deposition of transported material under torrential conditions either by the Machico river itself or its tributaries. This formation has been surveyed at depths ranging from around 6 to 18 m

GEOLOGICAL AND GEOTECHNICAL ASPECTS

- The slope deposits result from landslides and rock falls. They cover most of the slopes where the expressway was constructed and gradually increase in thickness towards the base. These deposits have been surveyed with depths ranging from 0,3 to 21 m

GEOTECHNICAL CHARACTERIZATION

- Given that one of the major obstacles to the works was the thickness of the slope deposits that covered a substantial part of the expressway, which made it impossible its complete removal, a geotechnical characterization of these deposits was carried out in order to better understand their behavior
- The water level occurred mainly at the base of this formation, along the contact with the volcanic bedrock
- These deposits were generally in limit equilibrium conditions due to their depth, geotechnical characteristics, underlying substrate inclination and, above all, water level variations

GEOTECHNICAL CHARACTERIZATION

- They easily became unstable, provoking landslide areas of great significance
- Analysis carried out on the matrix using the x-ray diffraction method showed that the clay fraction was essentially montmorillonite (around 95%) consisting the rest on kaolinite and chlorite (around 5%) and ilite (traces) minerals
- In the fine grained fraction, 66% passed through the #200 mesh and the lower limits below 2mm and 2μ mesh ranged between 42% to 22% and 72% to 38%, respectively

SPECIAL FOUNDATIONS WITH JET-GROUTING

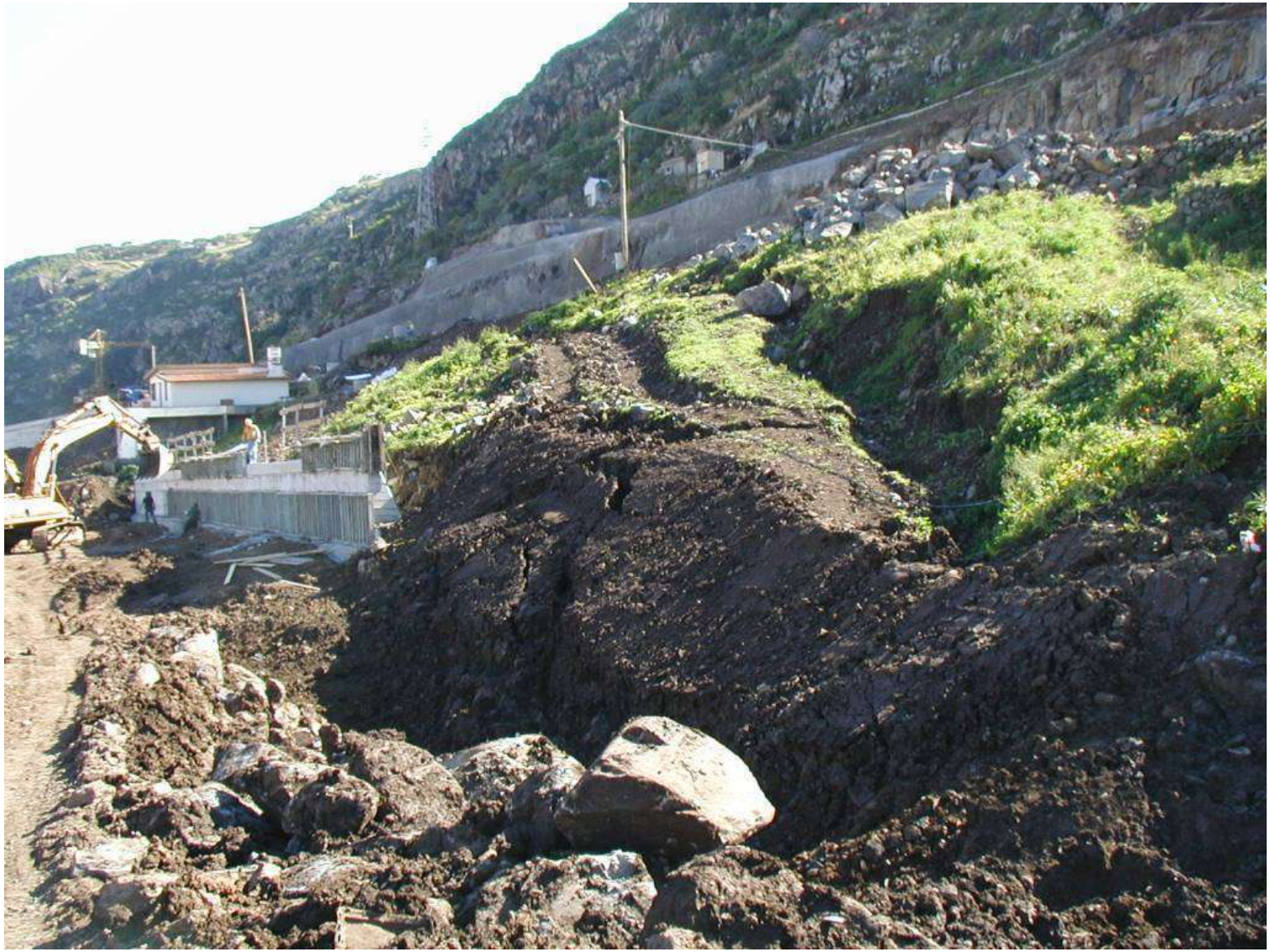

GEOTECHNICAL CHARACTERIZATION

- Liquid Limit (LL) over 56%
- Plasticity Index (PI) between 21 and 80%
- Water content (w) of 28%
- Volume weight (g) of 18,4 kN/m^3
- Specific gravity (G) between 2,53 and 2,90
- Sand equivalent (SE) between 14 and 16%
- The maximum and residual resistance parameters, in terms of effective stresses, were determined using alternating direct shear tests performed according to the testing technique indicated in Blondeau (1976)

GEOTECHNICAL CHARACTERIZATION

- The tests results provided the following residual resistance parameters: c'_{res} = 12 kPa and $ø'_{res}$ = 14°
- In terms of residual resistance, the cohesion value had no meaning since the soil was already in a state in which its electro-chemical bonds had been practically destroyed. Hence, the residual resistance was expressed only in terms of the residual friction angle. This parameter is closely associated with the percentage of clay size particles (<2μ) and the plasticity index

GEOTECHNICAL CHARACTERIZATION

- Using the Skempton equation, considering the clay percentage obtained in the identification tests, residual friction angles ranged between 18º and 10º

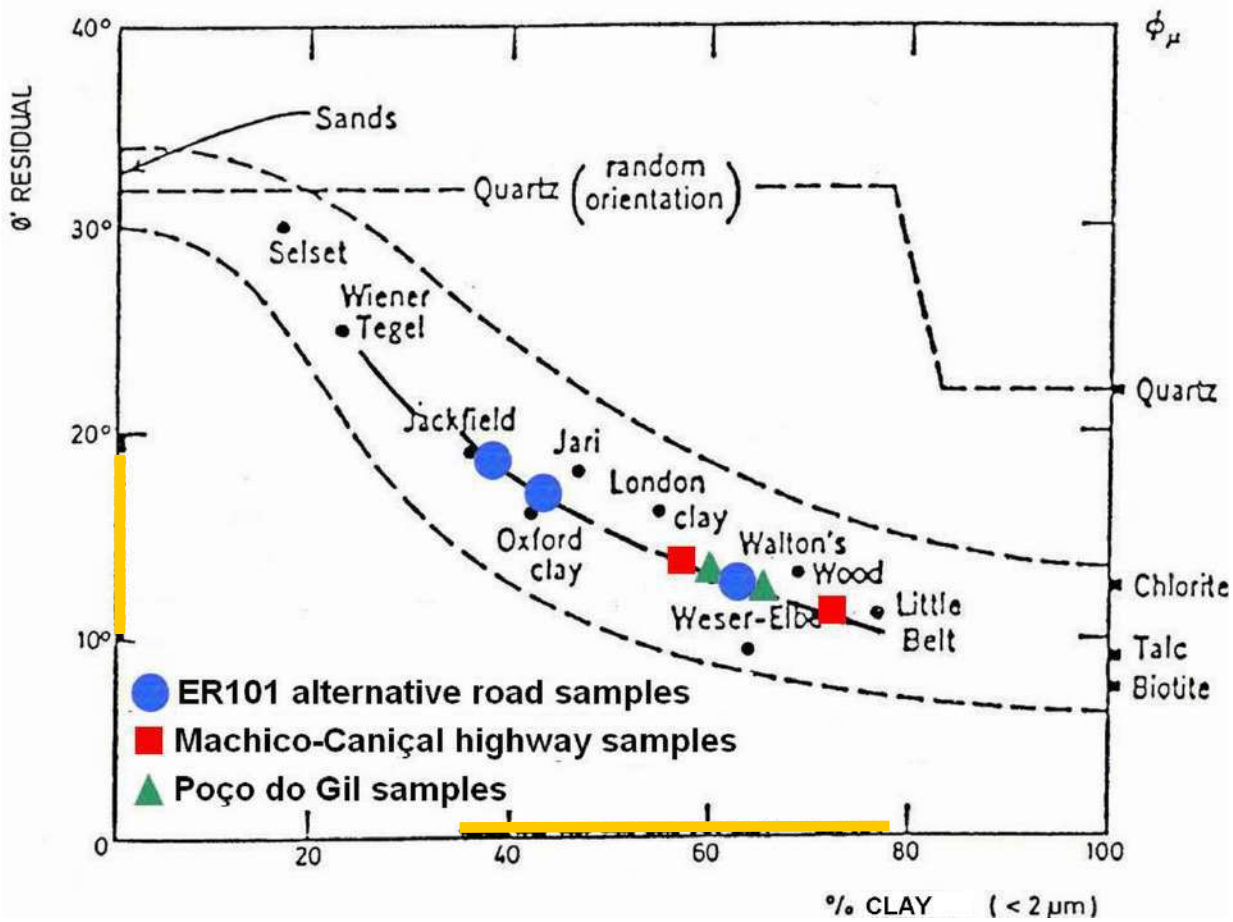

GEOTECHNICAL CHARACTERIZATION

- Resorting to the Kanji equation, attending to the plasticity index values obtained, $ø'_{res}$ ranged between 14º and 10º

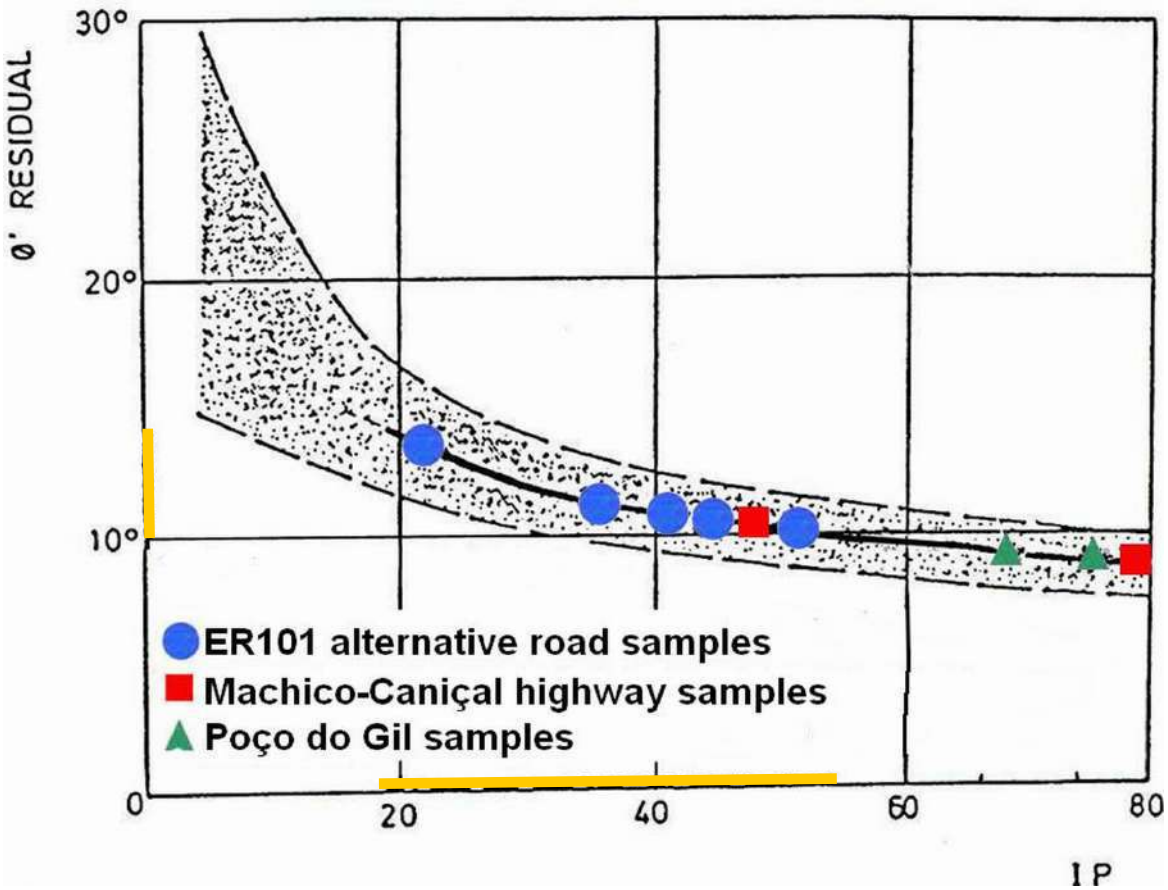

GEOTECHNICAL CHARACTERIZATION

- The value of the undrained residual strength cu_{res} = 14 kPa was estimated from the residual strength parameters in terms of the normal stress, according to the Mohr-Coulomb failure criterion
- An evaluation of the resistance parameters was also performed analysing the conditions under which various landslides occurred, not just in the area of the expressway itself, but also along the entire western slope of the Machico river, and taking into account different variable values of slope inclination, friction angle, submersion degree and slope height

GEOTECHNICAL CHARACTERIZATION

- As a result of all studies performed, the following parameters were obtained: cu_{res} = 14 kPa, c'_{res} = 0 kPa and $ø'_{res}$ = 14º
- However, to take into account the favourable contribution of gravel and blocks and the irregularity of the bedrock to the shear strength, it was considered that more favourable parameters could be adopted in the design:
  - **cu_{res} = 20 kPa**
  - **c'_{res} = 0 kPa**
  - **$ø'_{res}$ = 16º**

SPECIAL FOUNDATIONS WITH JET-GROUTING
MACHICO SOUTH INTERCHANGE

- Where the expressway or the various branch roads were located over quite thick deposits it was necessary to assure suitable foundation conditions for different retaining structures. Thus, it was necessary to use soil improvement technics
- The selected solution was the use of soil improvement guaranteed by Ø1000 mm diameter jet-grouting columns, generally crossing the deposits all the way to the bedrock
- Some columns were reinforced with "Schedule" Ø73mm tubes, in order to promote a better connection and resistance at the interface with the bedrock

SPECIAL FOUNDATIONS WITH JET-GROUTING
MACHICO SOUTH INTERCHANGE

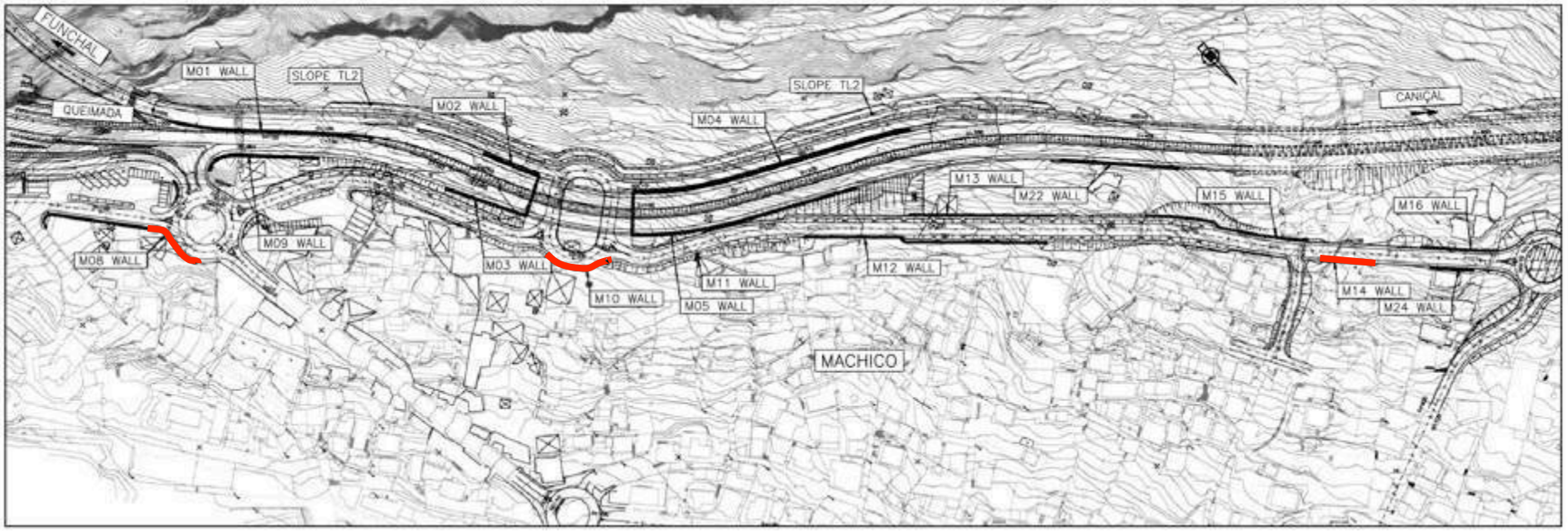

SPECIAL FOUNDATIONS WITH JET-GROUTING
MACHICO SOUTH INTERCHANGE

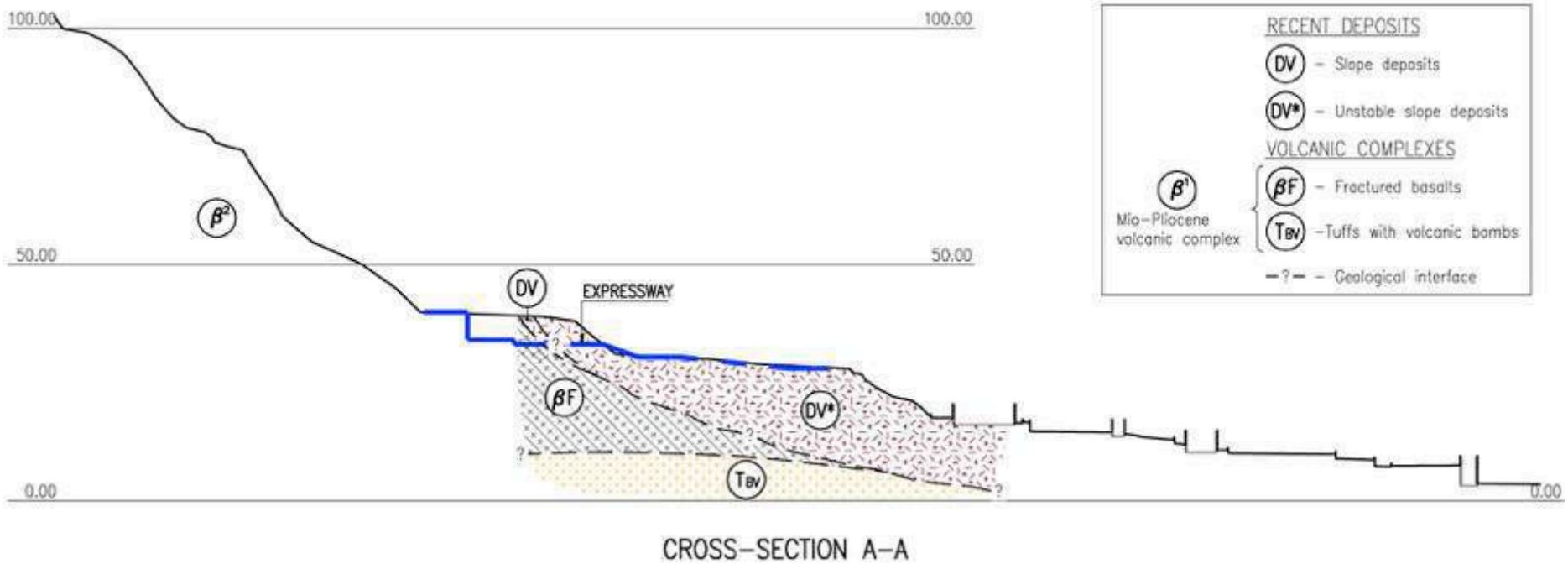

CROSS-SECTION A-A

SPECIAL FOUNDATIONS WITH JET-GROUTING
MACHICO SOUTH INTERCHANGE

SPECIAL FOUNDATIONS WITH JET-GROUTING
MACHICO SOUTH INTERCHANGE

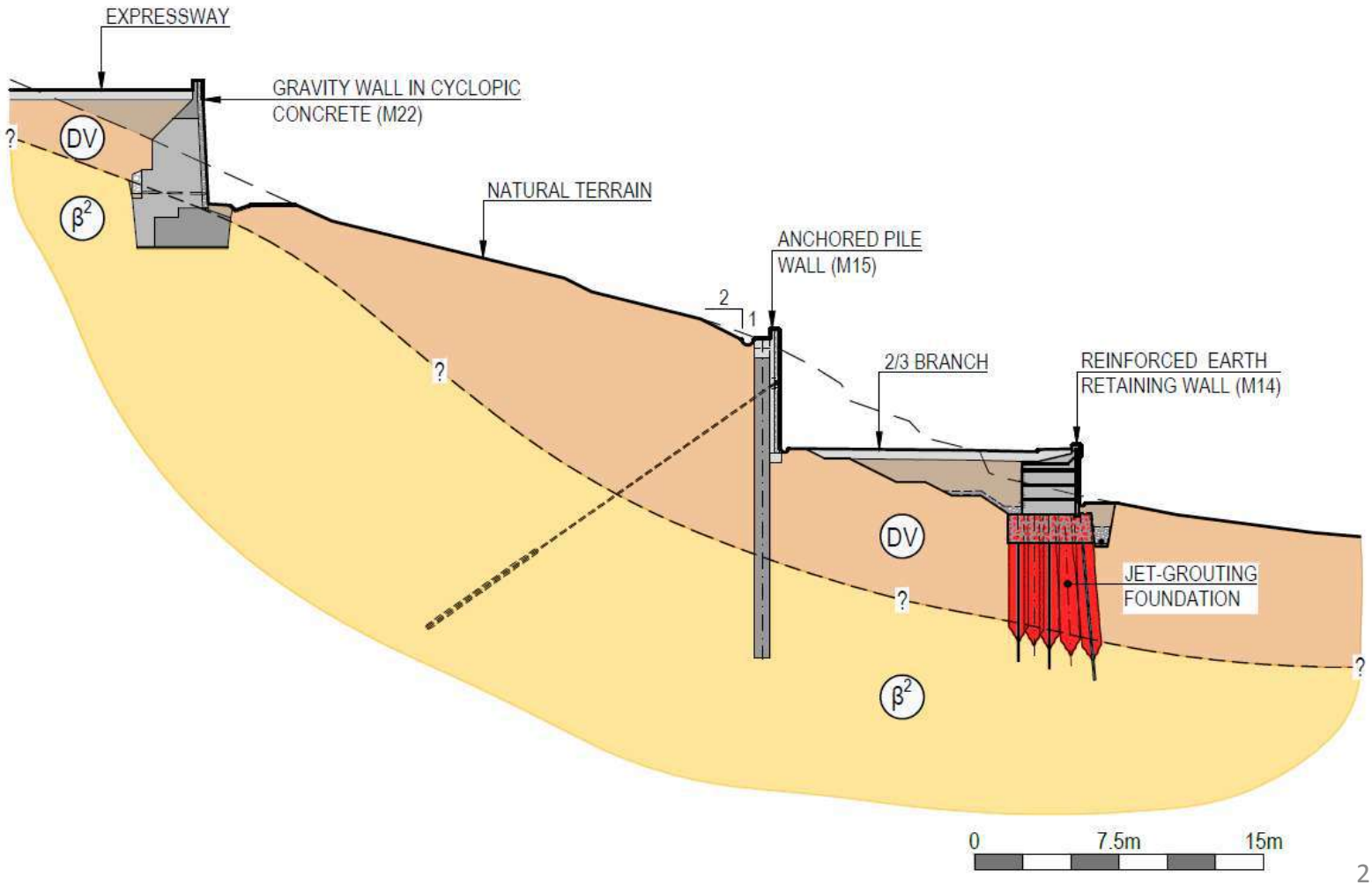

SPECIAL FOUNDATIONS WITH JET-GROUTING
MACHICO SOUTH INTERCHANGE

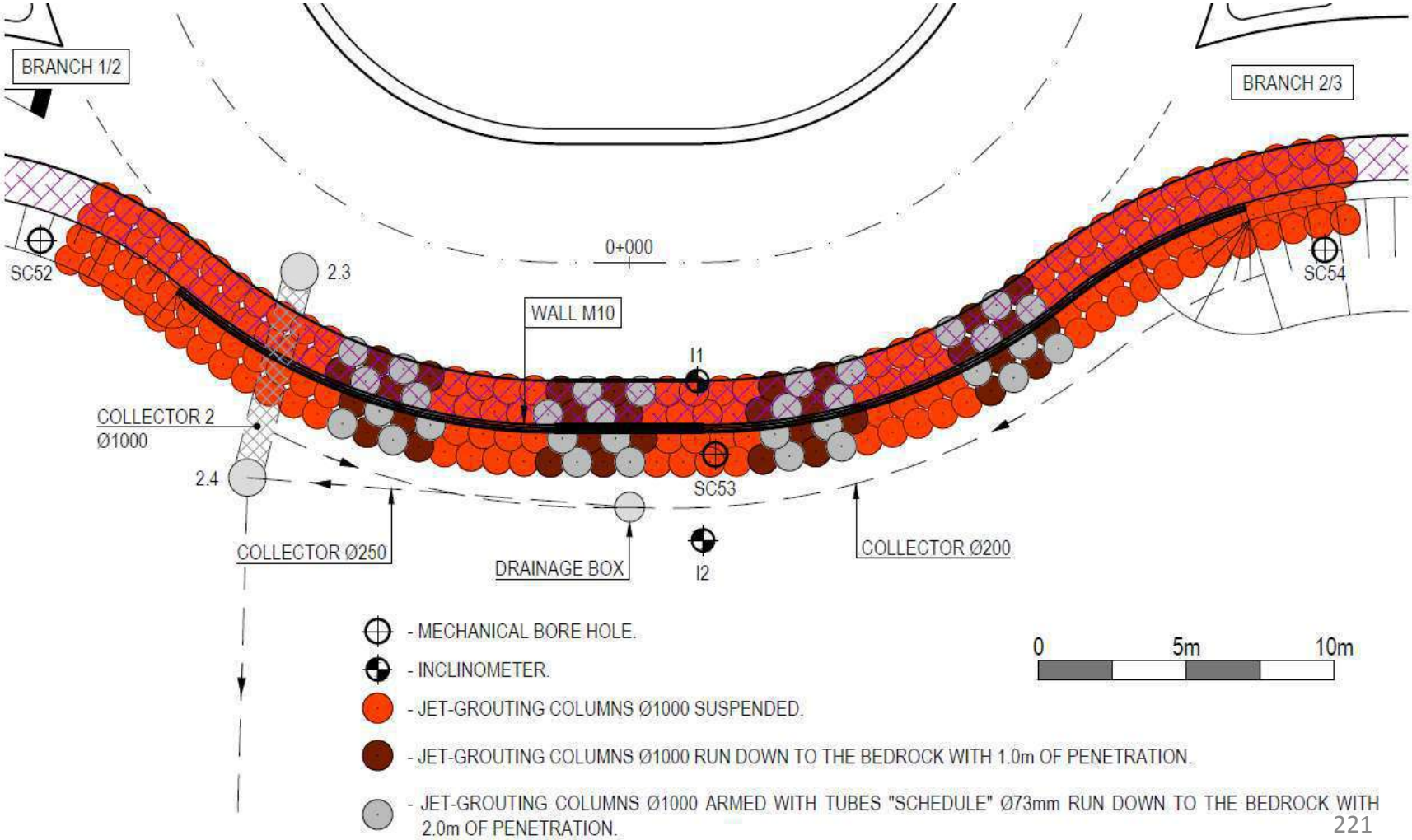

SPECIAL FOUNDATIONS WITH JET-GROUTING
MACHICO SOUTH INTERCHANGE

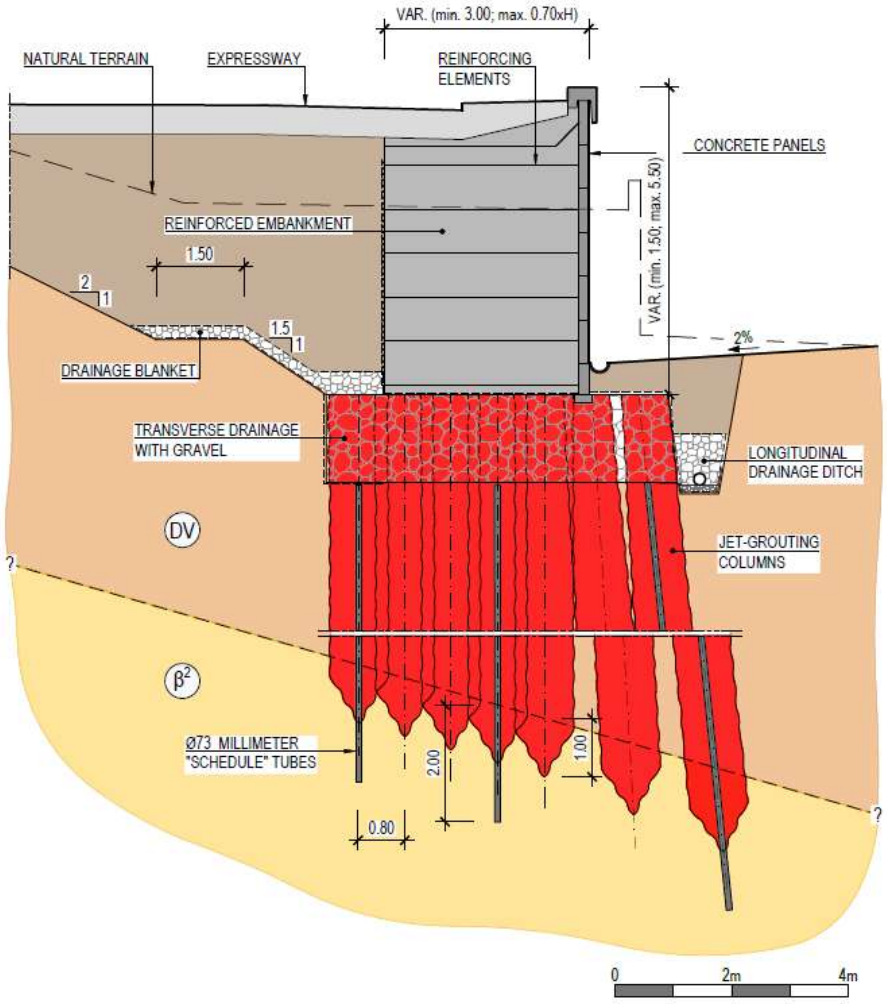

SPECIAL FOUNDATIONS WITH JET-GROUTING
MACHICO SOUTH INTERCHANGE

- Jet-grouting characteristics obtained in uniaxial compression test:
  - Failure resistance (σ'): ≥ 4 MPa
  - Elastic modulus (E): ≥ 500 MPa

SPECIAL FOUNDATIONS WITH JET-GROUTING
MACHICO SOUTH INTERCHANGE

SPECIAL FOUNDATIONS WITH JET-GROUTING
MACHICO SOUTH INTERCHANGE

SPECIAL FOUNDATIONS WITH JET-GROUTING
MACHICO SOUTH INTERCHANGE

SPECIAL FOUNDATIONS WITH JET-GROUTING
MACHICO SOUTH INTERCHANGE

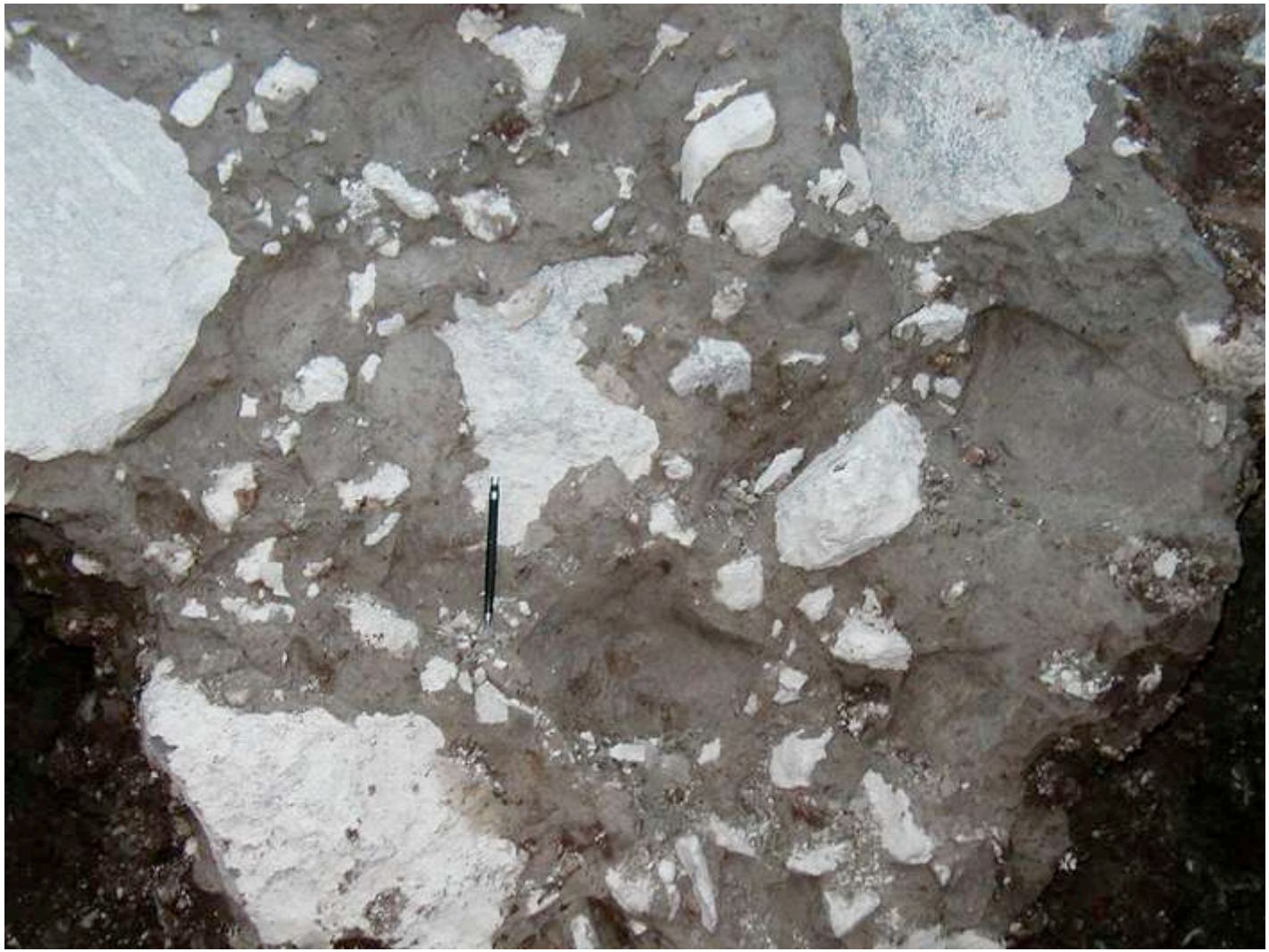

SPECIAL FOUNDATIONS WITH JET-GROUTING
MACHICO SOUTH INTERCHANGE

SPECIAL FOUNDATIONS WITH JET-GROUTING
MACHICO SOUTH INTERCHANGE

SPECIAL FOUNDATIONS WITH JET-GROUTING
MACHICO SOUTH INTERCHANGE

SPECIAL FOUNDATIONS WITH JET-GROUTING
MACHICO SOUTH INTERCHANGE

SPECIAL FOUNDATIONS WITH JET-GROUTING
MACHICO SOUTH INTERCHANGE

SPECIAL FOUNDATIONS WITH JET-GROUTING
MACHICO SOUTH INTERCHANGE

SPECIAL FOUNDATIONS WITH JET-GROUTING
EAST PORTAL OF PORTAIS TUNNEL

- At this location the expressway ran along an area in which slope deposits occurred with significant thickness, sometimes up to 10 m
- There was evidence that these deposits reached the buildings at Barro village, close to the construction site, which showed significant damages
- For this reason, in addition to ensuring the stability of the retaining structures necessary to the expressway, an attempt was made to substantially improve the overall stability of the slope deposits mass

SPECIAL FOUNDATIONS WITH JET-GROUTING
EAST PORTAL OF PORTAIS TUNNEL

SPECIAL FOUNDATIONS WITH JET-GROUTING
EAST PORTAL OF PORTAIS TUNNEL

SPECIAL FOUNDATIONS WITH JET-GROUTING
EAST PORTAL OF PORTAIS TUNNEL

SPECIAL FOUNDATIONS WITH JET-GROUTING
EAST PORTAL OF PORTAIS TUNNEL

SPECIAL FOUNDATIONS WITH JET-GROUTING
EAST PORTAL OF PORTAIS TUNNEL

SPECIAL FOUNDATIONS WITH JET-GROUTING
EAST PORTAL OF PORTAIS TUNNEL

SPECIAL FOUNDATIONS WITH JET-GROUTING
EAST PORTAL OF PORTAIS TUNNEL

SPECIAL FOUNDATIONS WITH JET-GROUTING
EAST PORTAL OF PORTAIS TUNNEL

- The solution was to build one retaining structure away from the expressway, a little further up on the slope, where the thickness of the deposits was smaller. Thus, the slope deposits potentially instable mass was reduced
- An anchored pile wall was defined, reducing the excavation in the slope deposits up to about 3,0 m
- Where the depth of the bedrock was greater than the bottom of the excavation, it was necessary to improve ground properties to ensure an adequate behaviour of the structure, in particular its ability to mobilize the passive earth pressure

SPECIAL FOUNDATIONS WITH JET-GROUTING
EAST PORTAL OF PORTAIS TUNNEL

- Given that jet-grouting technology was available on site, slope deposits were thus treated using it, along a 30 m long and 4 m wide section
- Jet-grouting ∅1000 mm diameter columns were executed through the deposits into the bedrock
- The columns were set in a 1 m (longitudinal to the wall) x 0,7 m (transverse to the wall) grid
- Two areas of about 2 m long were left untreated at the base, to allow natural percolation of the soil and, thus, prevent groundwater raise behind the wall

SPECIAL FOUNDATIONS WITH JET-GROUTING
EAST PORTAL OF PORTAIS TUNNEL

- At the right side of the expressway, due to the deposits thickness, it was impossible to design shallow foundations for the retaining structures that supported the road embankments, making it necessary the use of deep foundations through soil improvement technics
- The solution was to build reinforced concrete walls founded on Ø1000 mm diameter jet-grouting piles, driven through the deposits into the bedrock to ensure adequate foundation

SPECIAL FOUNDATIONS WITH JET-GROUTING
EAST PORTAL OF PORTAIS TUNNEL

- In both cases, in some columns, it was foreseen a reinforcement with "Schedule" Ø73mm metallic tubes, with the aim of promoting a better connection of the aforementioned jet columns to the rocky substrate, and increase the shear strength at the interface

SPECIAL FOUNDATIONS WITH JET-GROUTING
EAST PORTAL OF PORTAIS TUNNEL

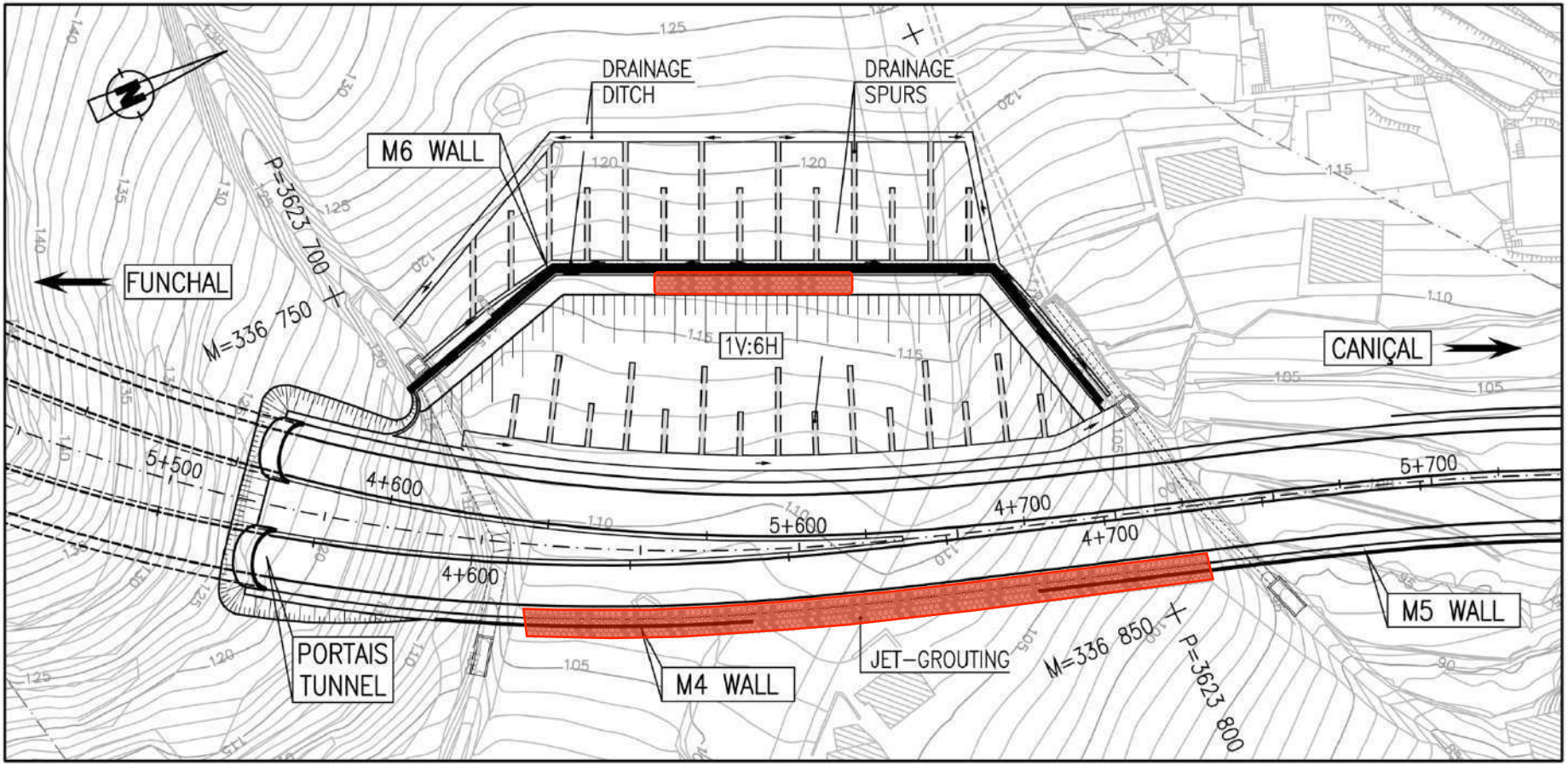

SPECIAL FOUNDATIONS WITH JET-GROUTING
EAST PORTAL OF PORTAIS TUNNEL

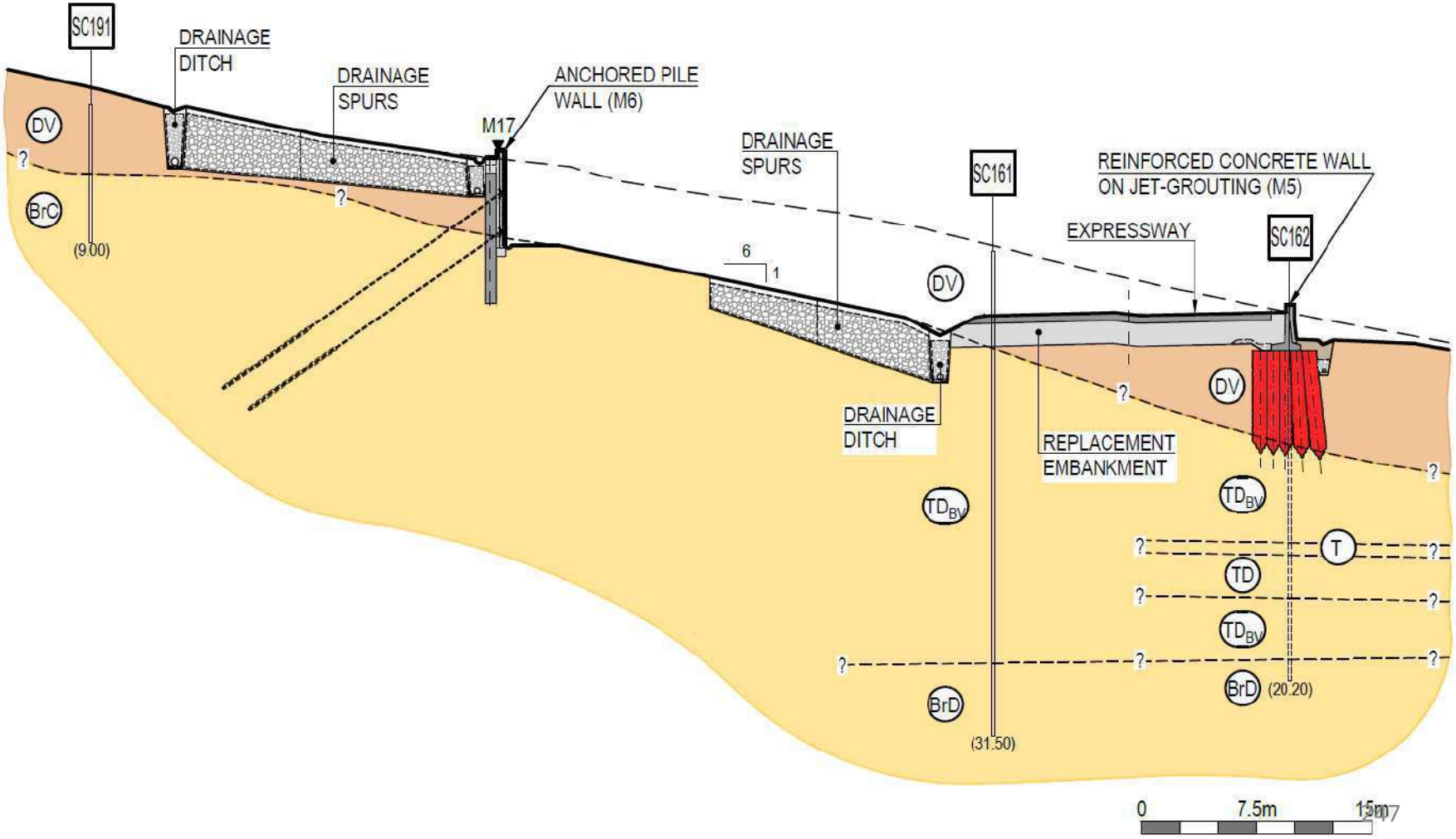

SPECIAL FOUNDATIONS WITH JET-GROUTING
EAST PORTAL OF PORTAIS TUNNEL

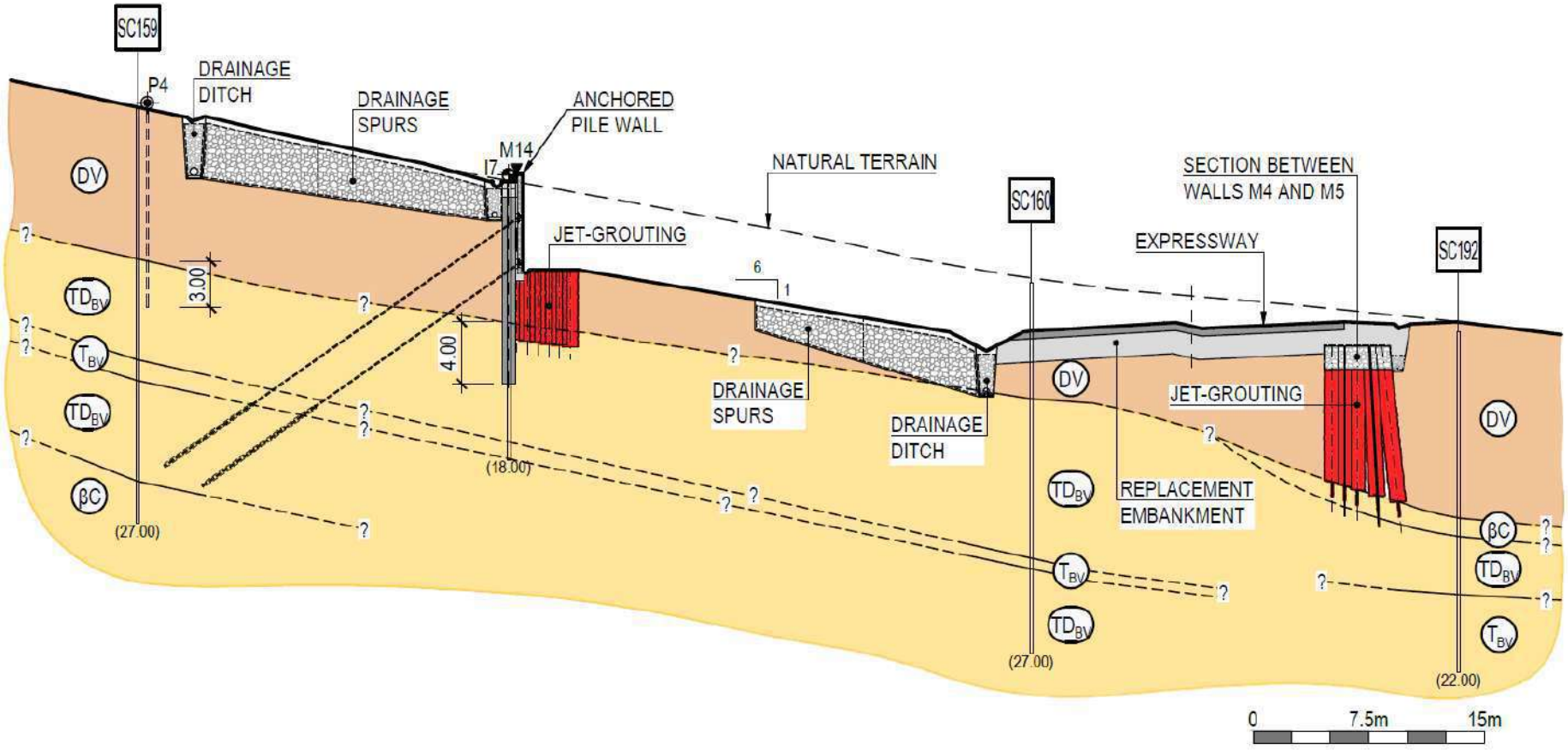

SPECIAL FOUNDATIONS WITH JET-GROUTING
EAST PORTAL OF PORTAIS TUNNEL

- Jet-grouting characteristics obtained in uniaxial compression test:
  - Failure resistance (σ'): ≥ 4 MPa
  - Elastic modulus (E): ≥ 500 MPa

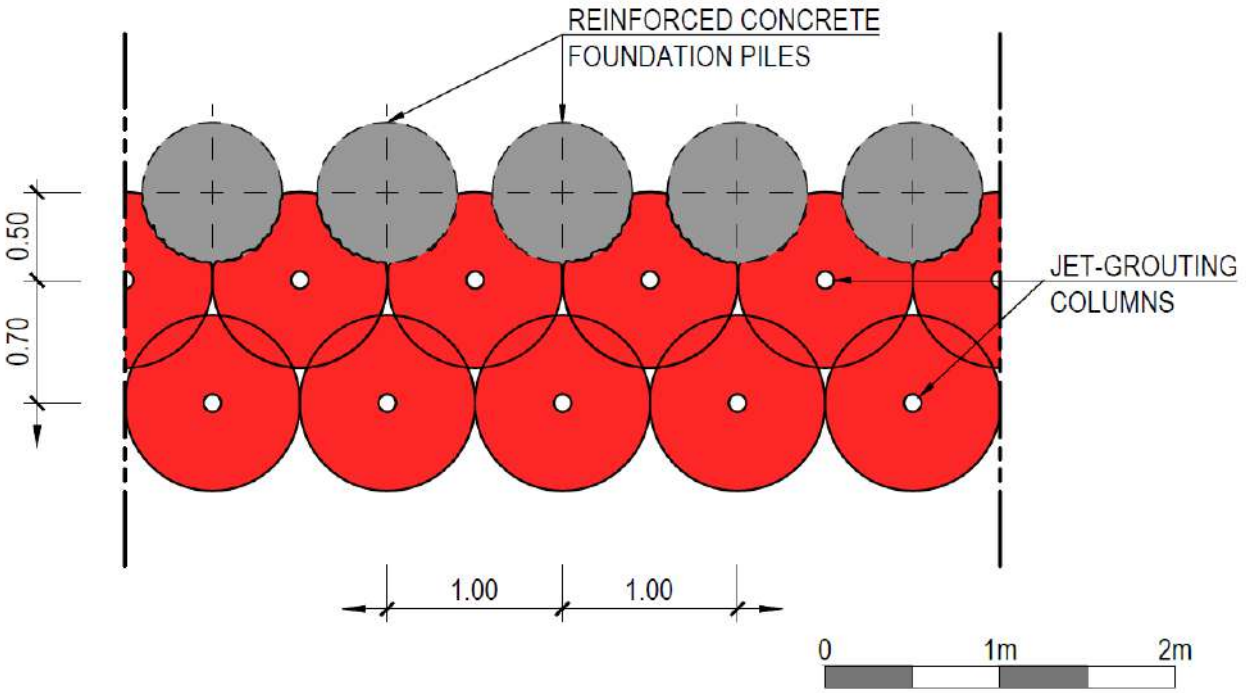

SPECIAL FOUNDATIONS WITH JET-GROUTING
EAST PORTAL OF PORTAIS TUNNEL

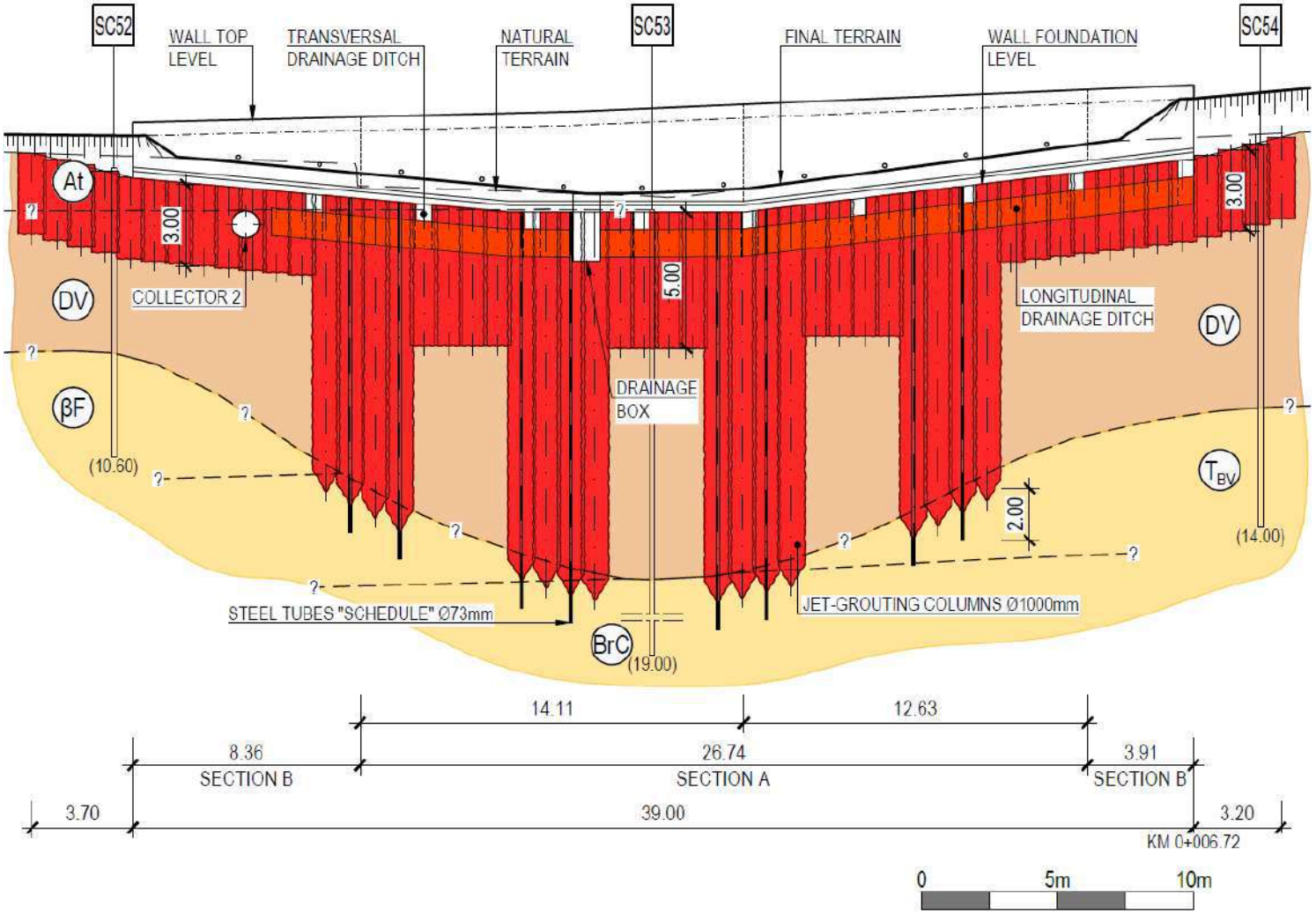

SPECIAL FOUNDATIONS WITH JET-GROUTING
EAST PORTAL OF PORTAIS TUNNEL

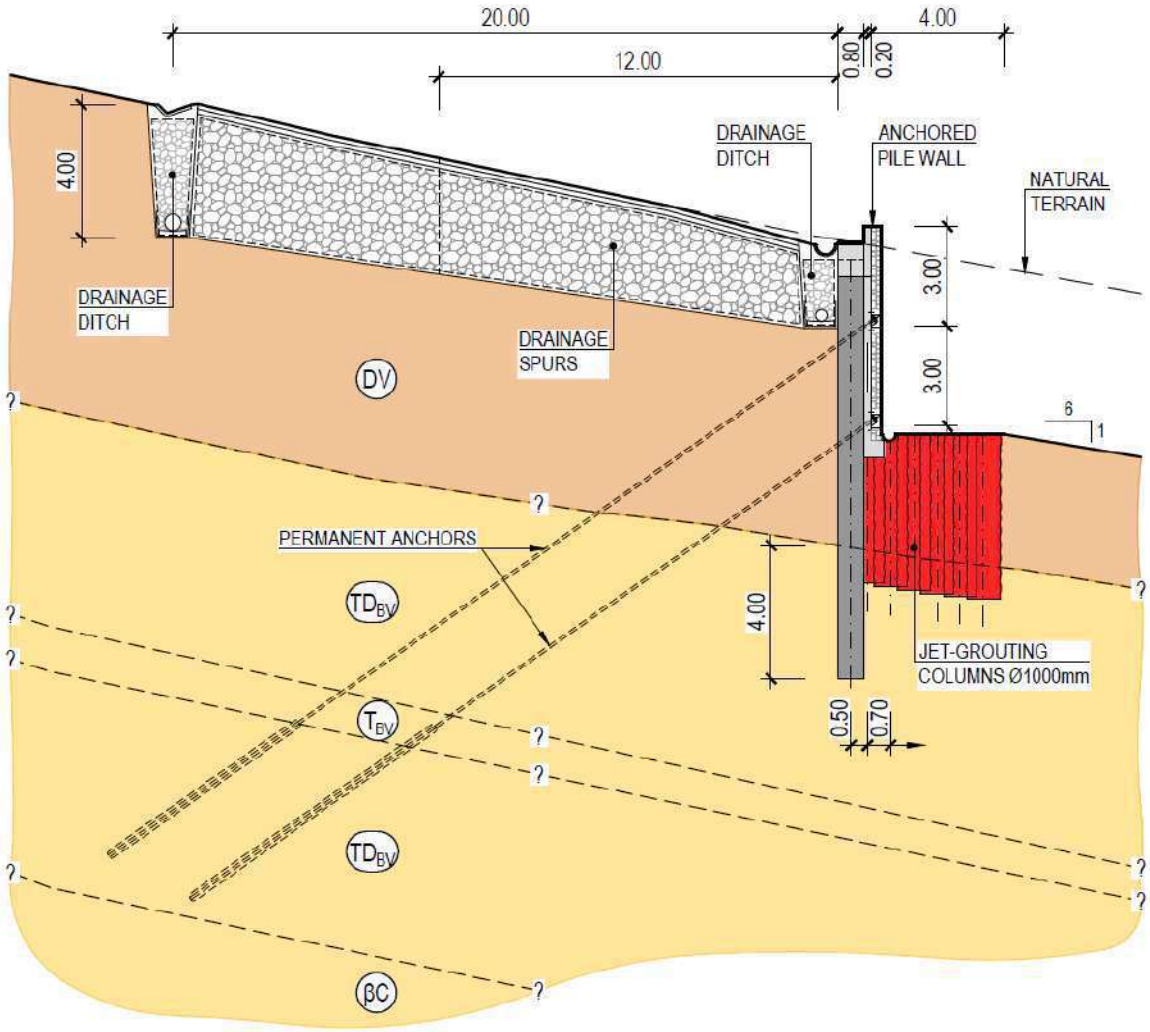

SPECIAL FOUNDATIONS WITH JET-GROUTING
EAST PORTAL OF PORTAIS TUNNEL

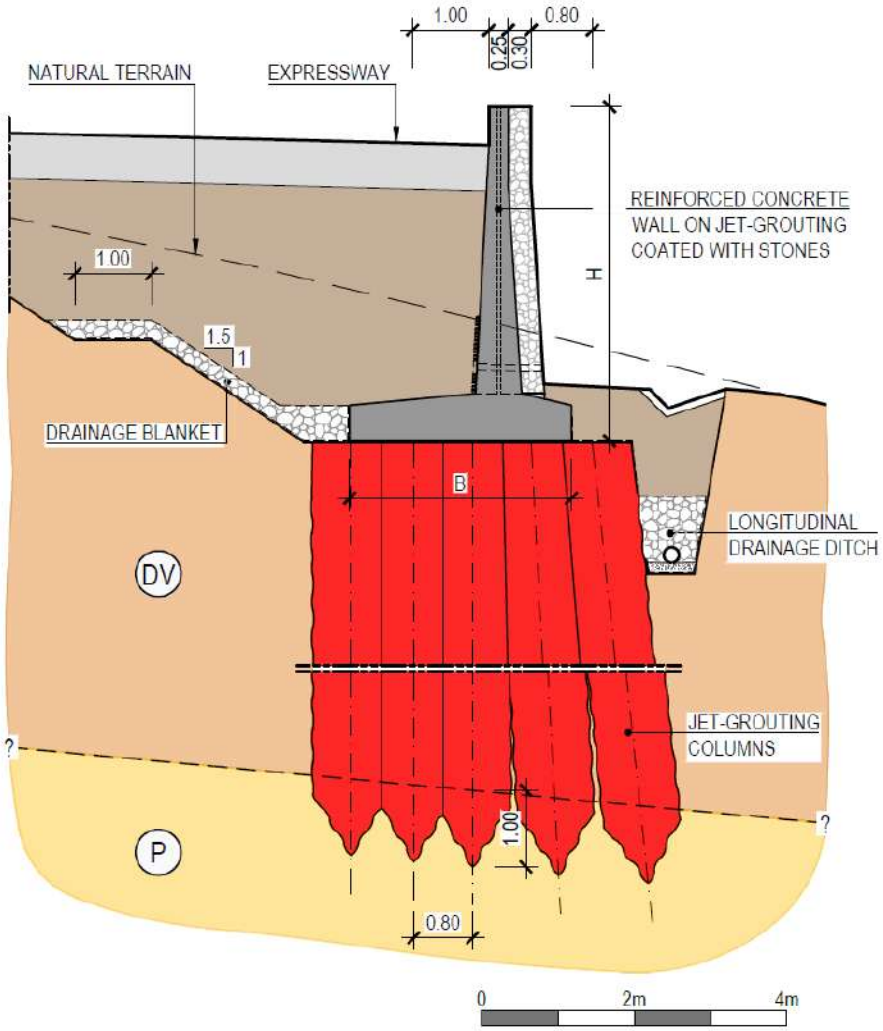

SPECIAL FOUNDATIONS WITH JET-GROUTING
EAST PORTAL OF PORTAIS TUNNEL

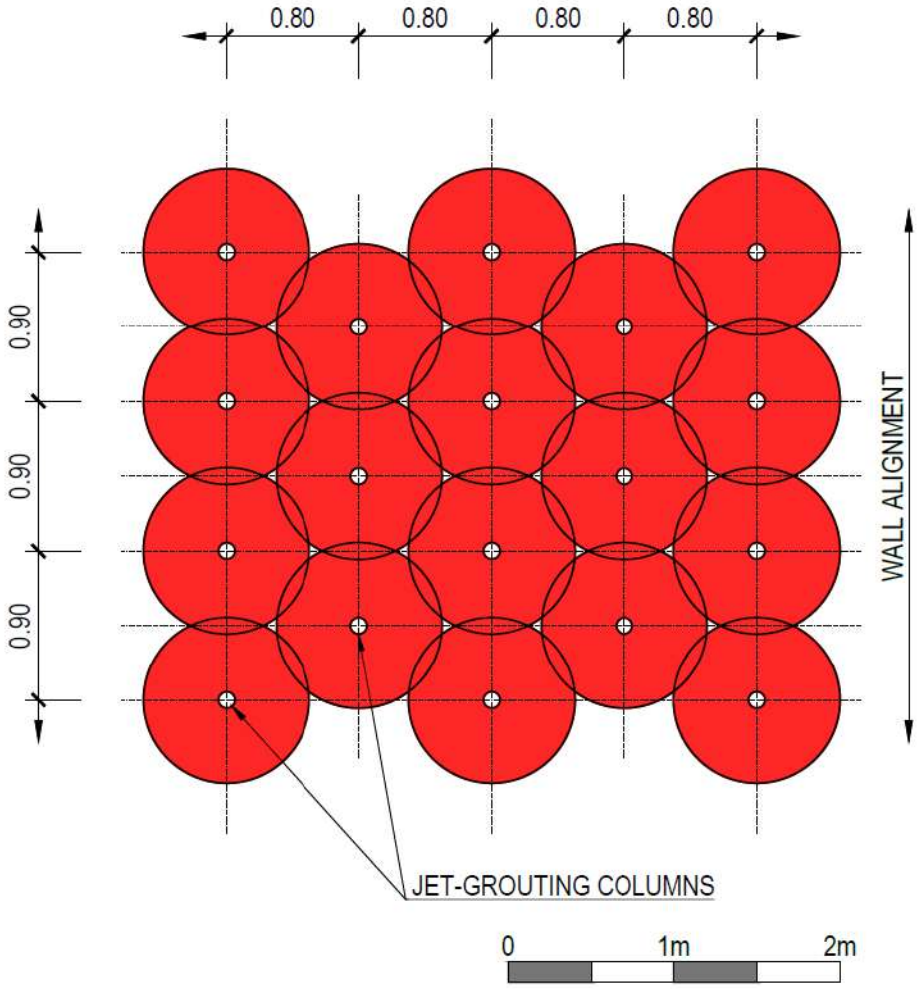

SPECIAL FOUNDATIONS WITH JET-GROUTING
EAST PORTAL OF PORTAIS TUNNEL

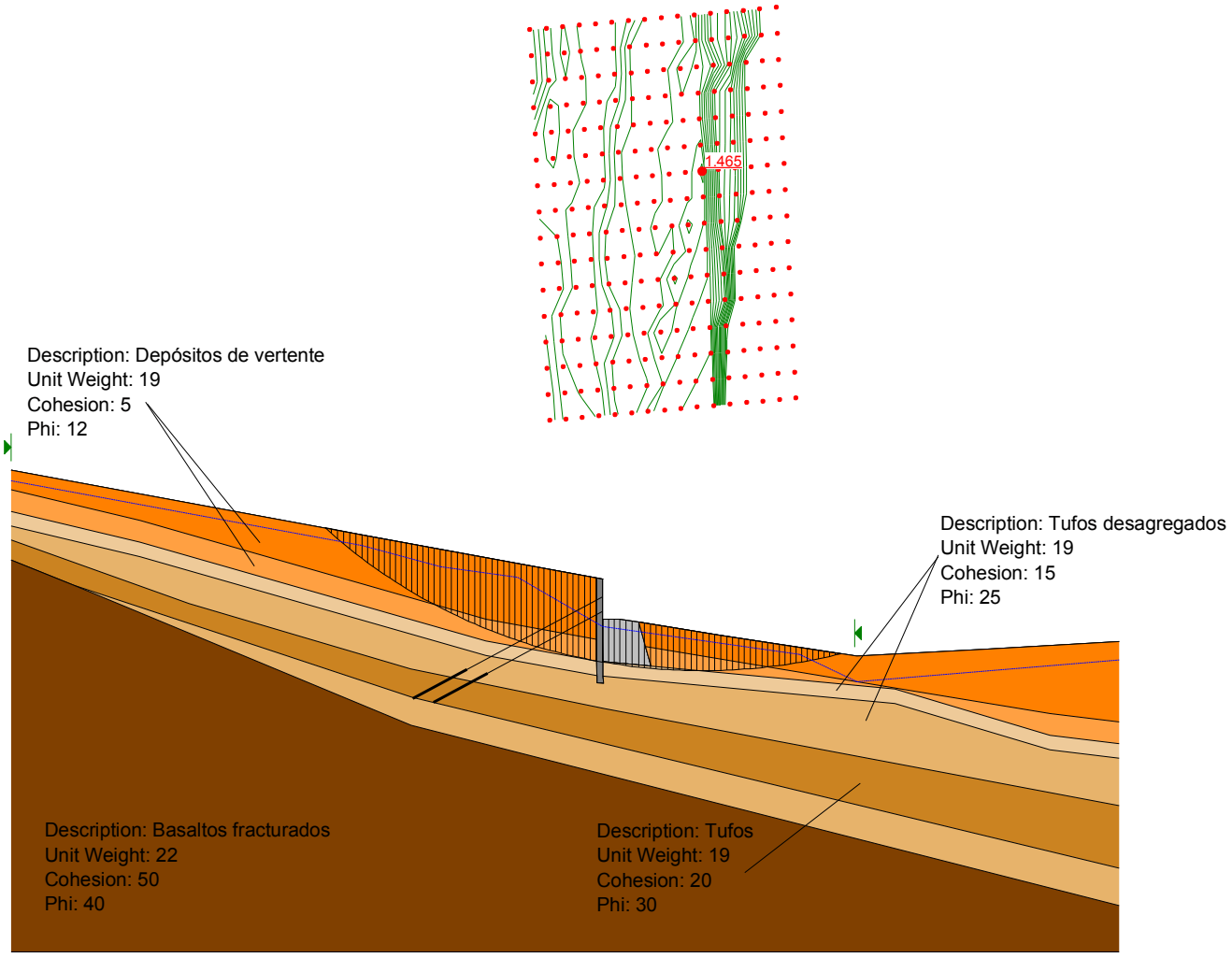

SPECIAL FOUNDATIONS WITH JET-GROUTING
EAST PORTAL OF PORTAIS TUNNEL

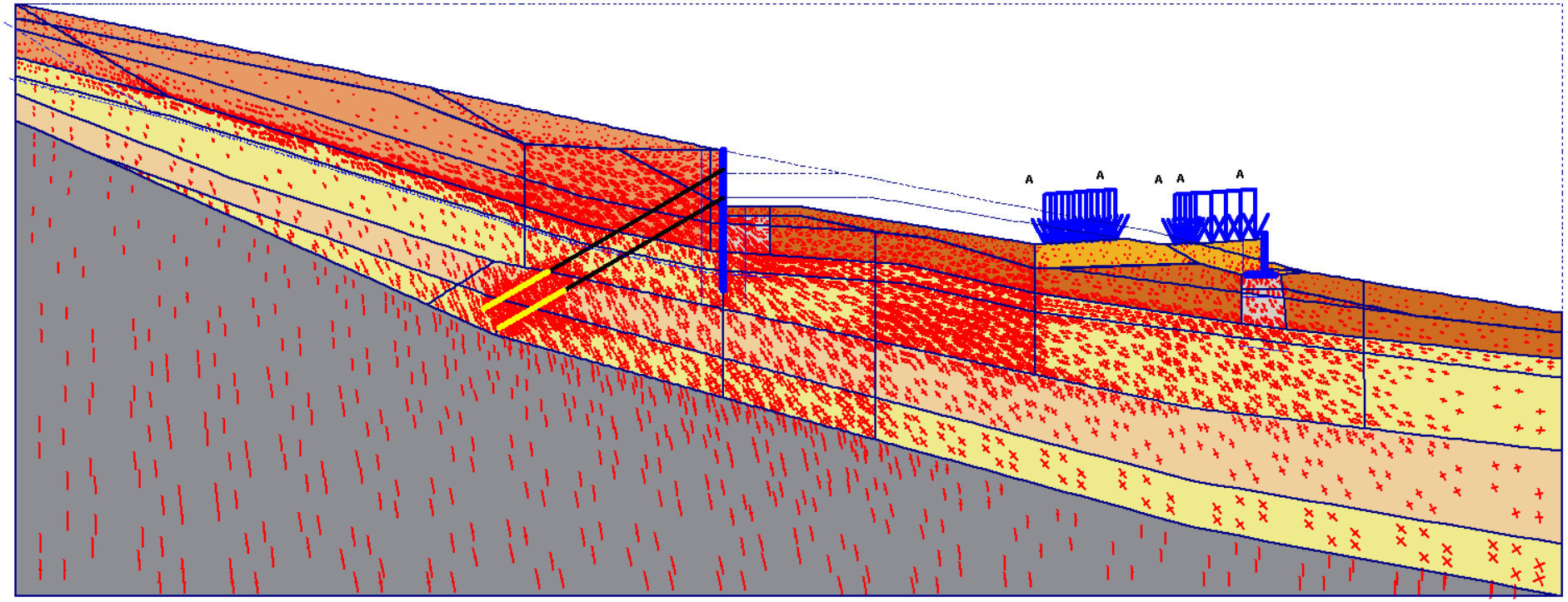

SPECIAL FOUNDATIONS WITH JET-GROUTING
EAST PORTAL OF PORTAIS TUNNEL

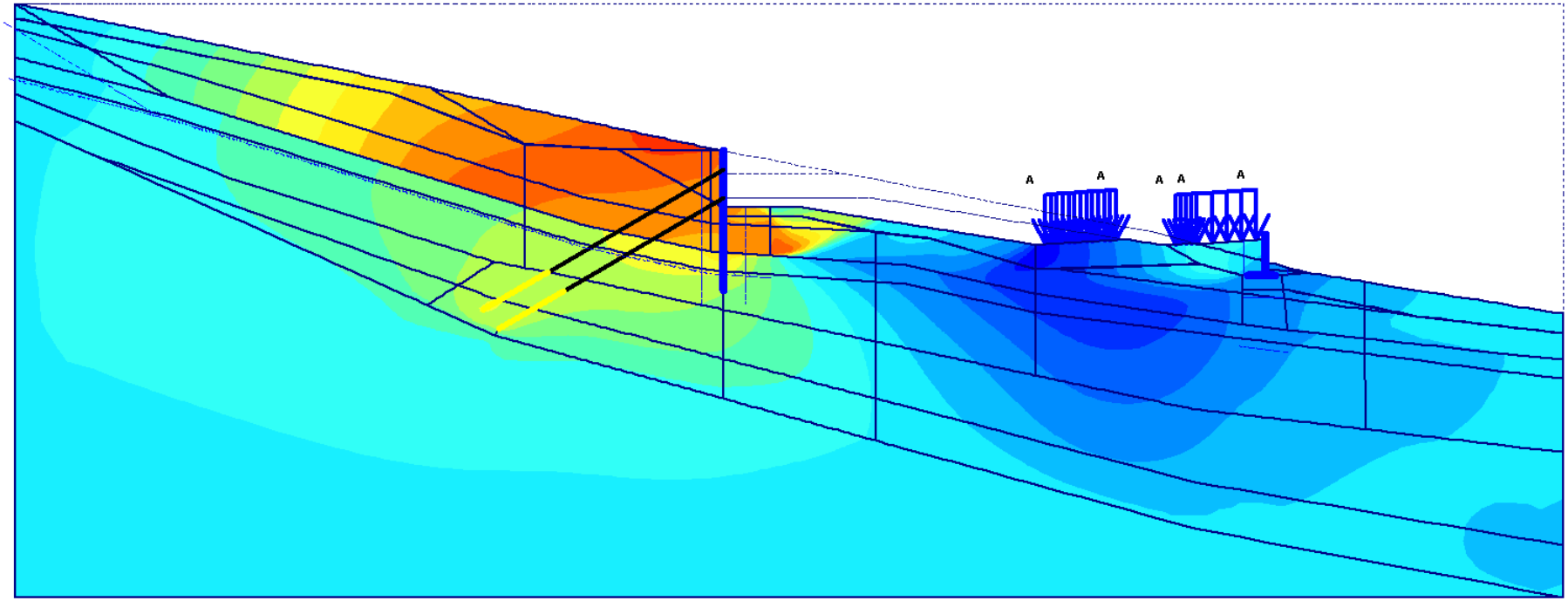

SPECIAL FOUNDATIONS WITH JET-GROUTING
EAST PORTAL OF PORTAIS TUNNEL

SPECIAL FOUNDATIONS WITH JET-GROUTING
EAST PORTAL OF PORTAIS TUNNEL

SPECIAL FOUNDATIONS WITH JET-GROUTING
EAST PORTAL OF PORTAIS TUNNEL

CONCLUSIONS

- The design of soil improvement solutions associated with the retaining structures of the Machico-Caniçal expressway section was subject to constraints of several nature, mainly due to the existence of areas with thick slope deposits with very poor strength characteristics and densely occupied areas
- It should be stressed out how essential it was to fully understand the geological occurring conditions during design, allowing an appropriate geomechanical characterization of the slope deposits and, thus, ensuring the optimization of the planned solutions

CONCLUSIONS

- To each case, it was given special attention, in order to adapt the design and the construction methods so as to obtain economically and technically adequate solutions
- The use of the jet-grouting improvement technique proved to be perfectly adequate for the type of soils under analysis, and was applied with total success

Soil Treatment with Jet-Grouting Associated to Retaining Structures of The Machico-Caniçal Expressway in Madeira Island

THANK YOU FOR YOUR ATENTION

Ground Improvement Solutions at Myriad Sana Hotel

João Falcão

Organização

Sociedade Portuguesa de Geotecnia

Comissão Portuguesa de Geotecnia nos Transportes

Comissão Portuguesa de Geossintéticos

Apoios

LABORATÓRIO NACIONAL DE ENGENHARIA CIVIL

ORDEM DOS ENGENHEIROS

MAIN RESTRAINTS

MAIN SOLUTIONS

DESIGN

MONITORING AND SURVEY

MAIN CONCLUSIONS


Site

The ground is composed by alluvium soils with an average thickness of about 17 m, resting over the Miocene heterogeneous materials, composed by sands and limestones.

The alluvium soils are essentially formed by silts and clays with NSPT blows not bigger than 9.

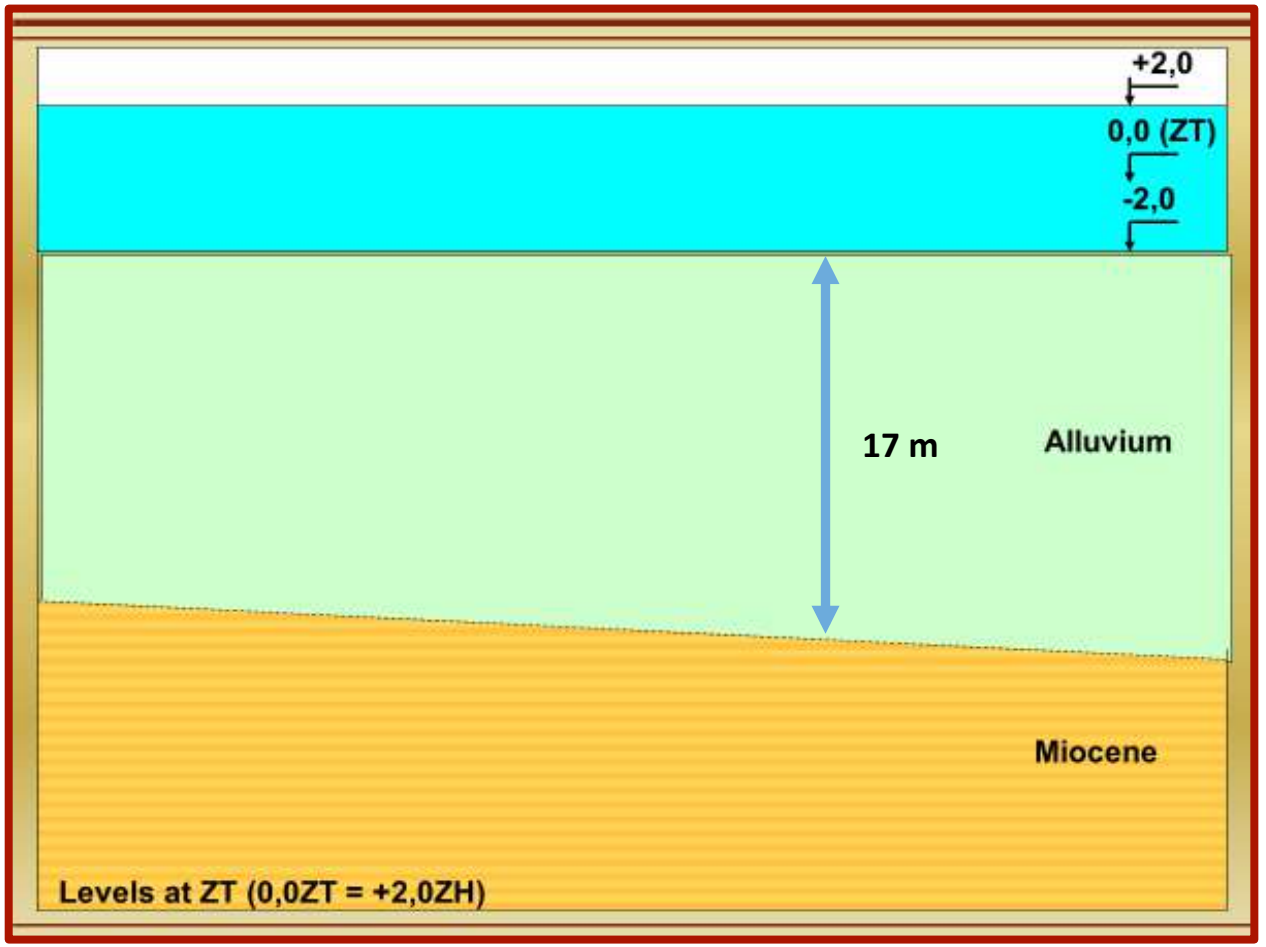

Main Geotechnical Parameters

Material	N_{SPT}	$\phi'(^o)$	c'(kPa)	c_u(kPa)	γ(kN/m^3)	E'(MPa)
Alluvium	<9	18	0	8 - 22	16	4 - 10
Miocene	>60	35	40	200	20	50

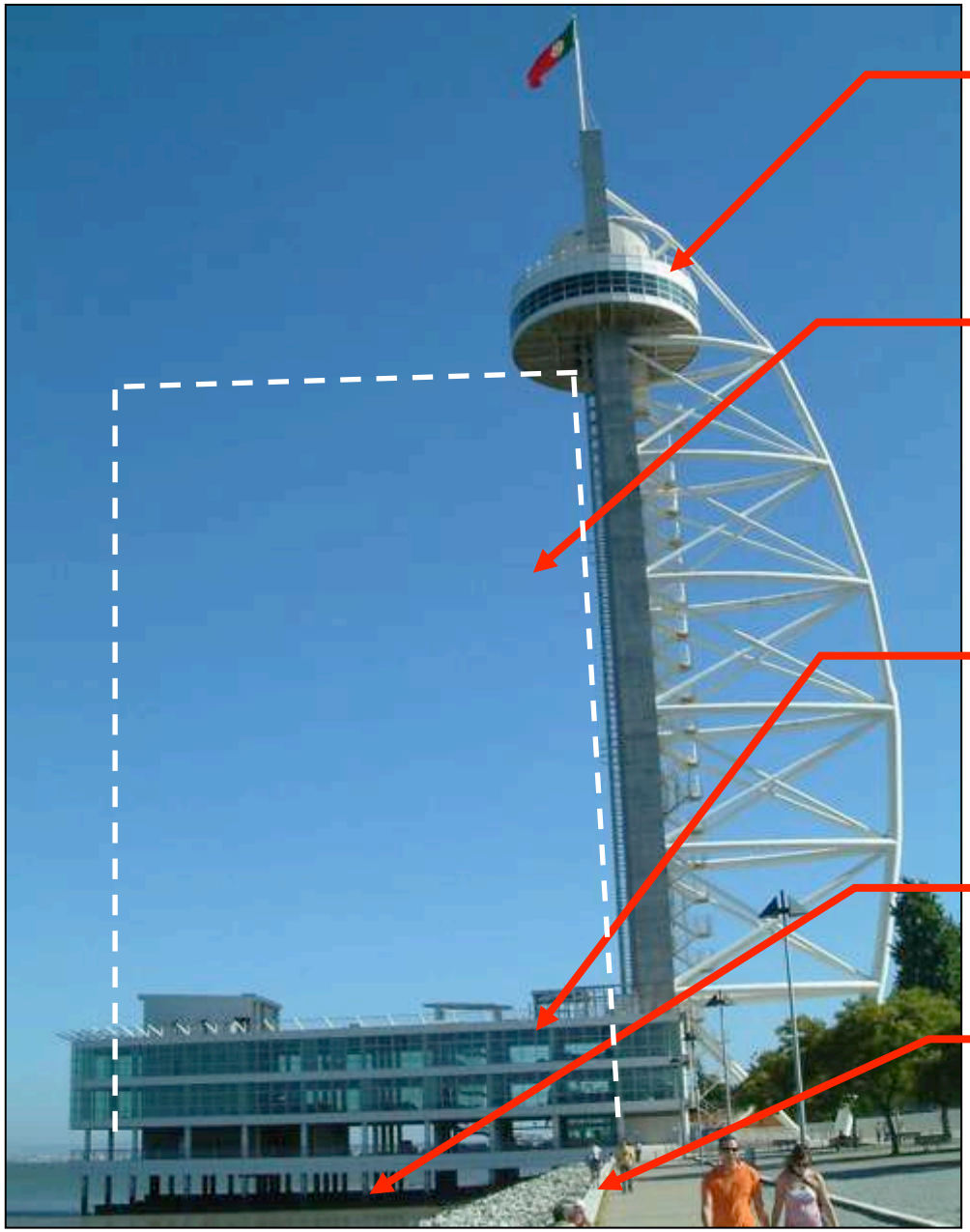
Vasco da Gama Tower
Hotel shape
Existent and demolish building
Tagus River
Riverside wall

The foundation of the previously existent building was composed by 69 circular driven piles with permanent steel casing Ø630 × 8mm

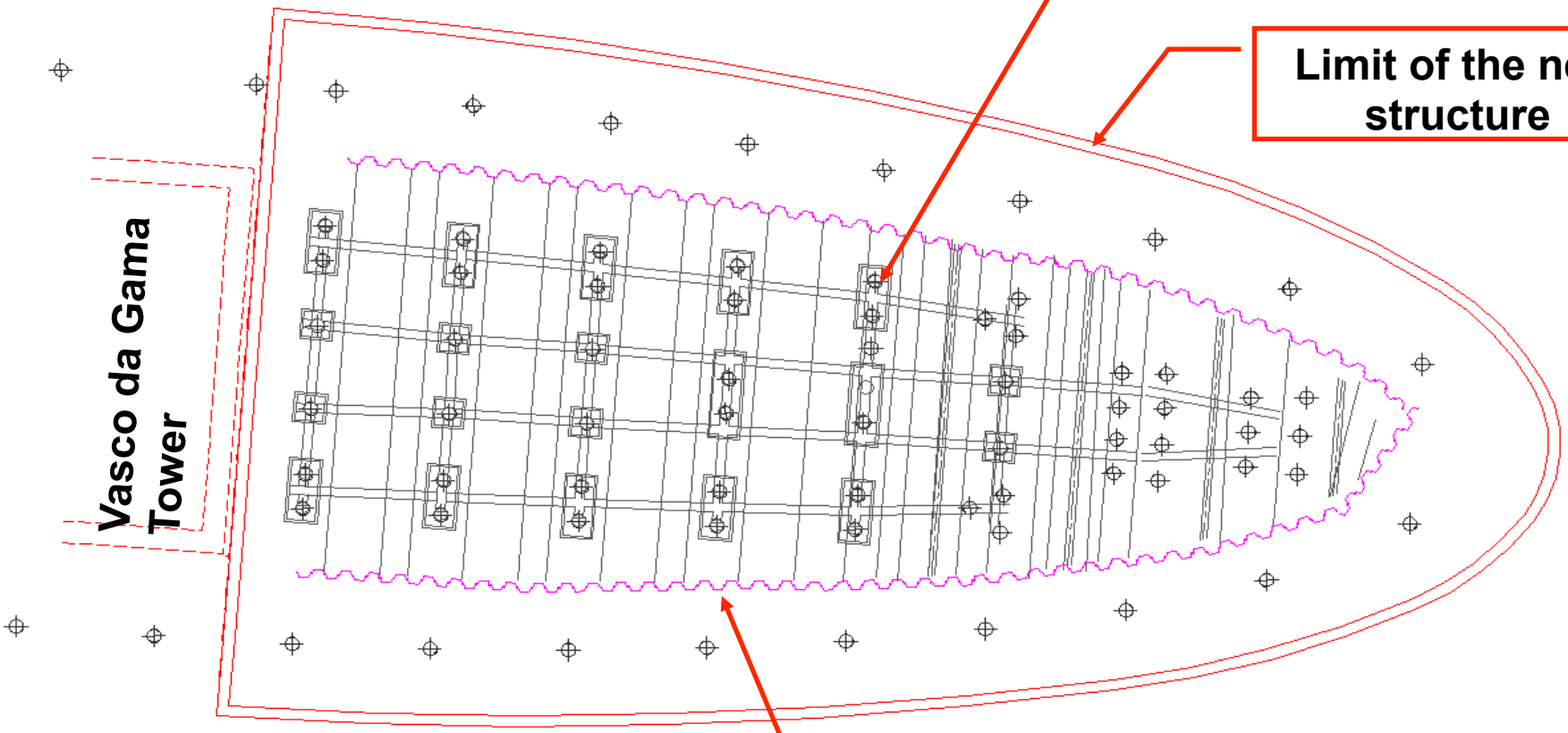

Execução das fundações do edifício demolido


peripheral pillar piles

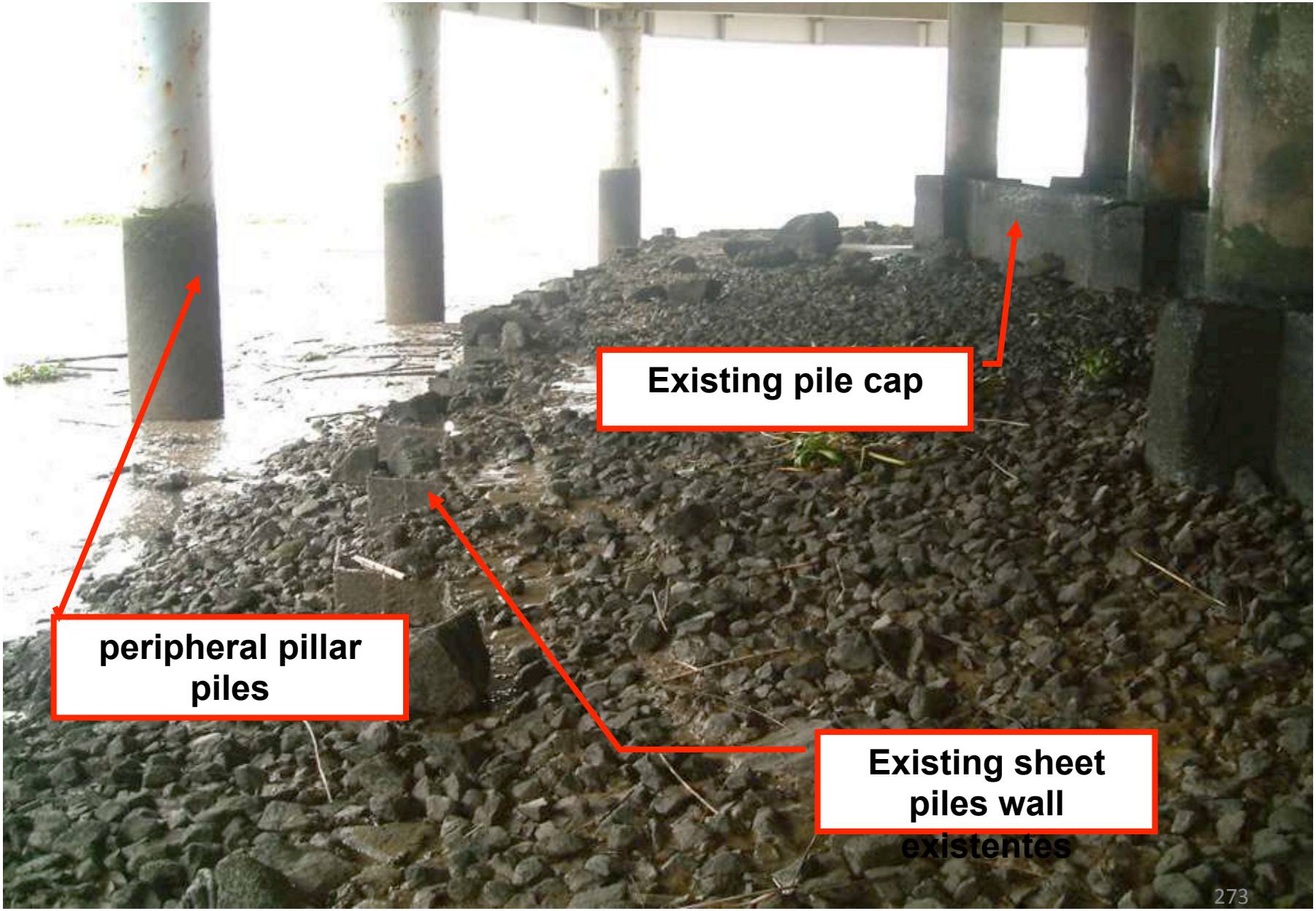
Existing pile cap
peripheral pillar piles
Existing sheet piles wall existentes

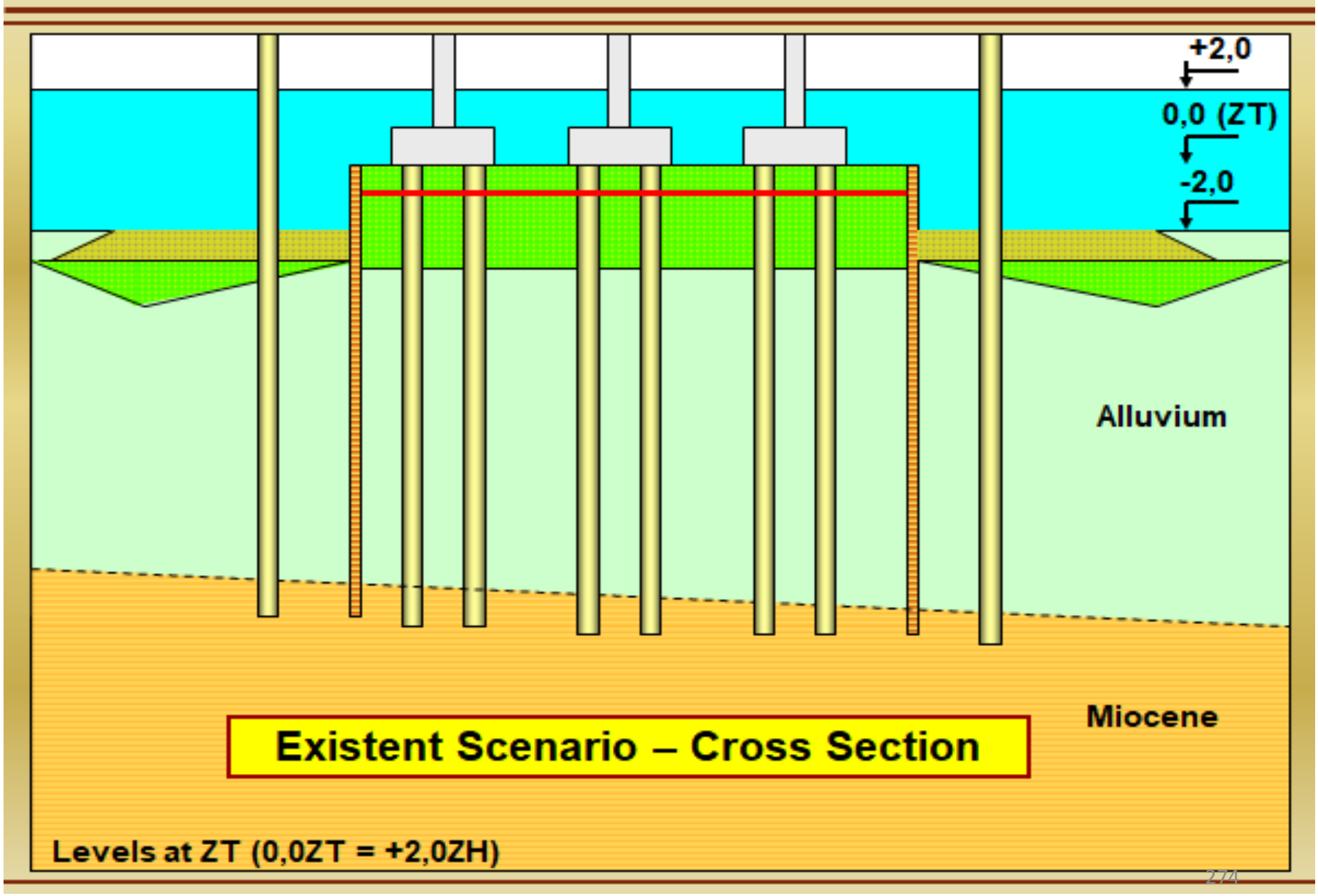
+2,0
0,0 (ZT)
-2,0
Alluvium
Miocene
Existent Scenario – Cross Section
Levels at ZT (0,0ZT = +2,0ZH)

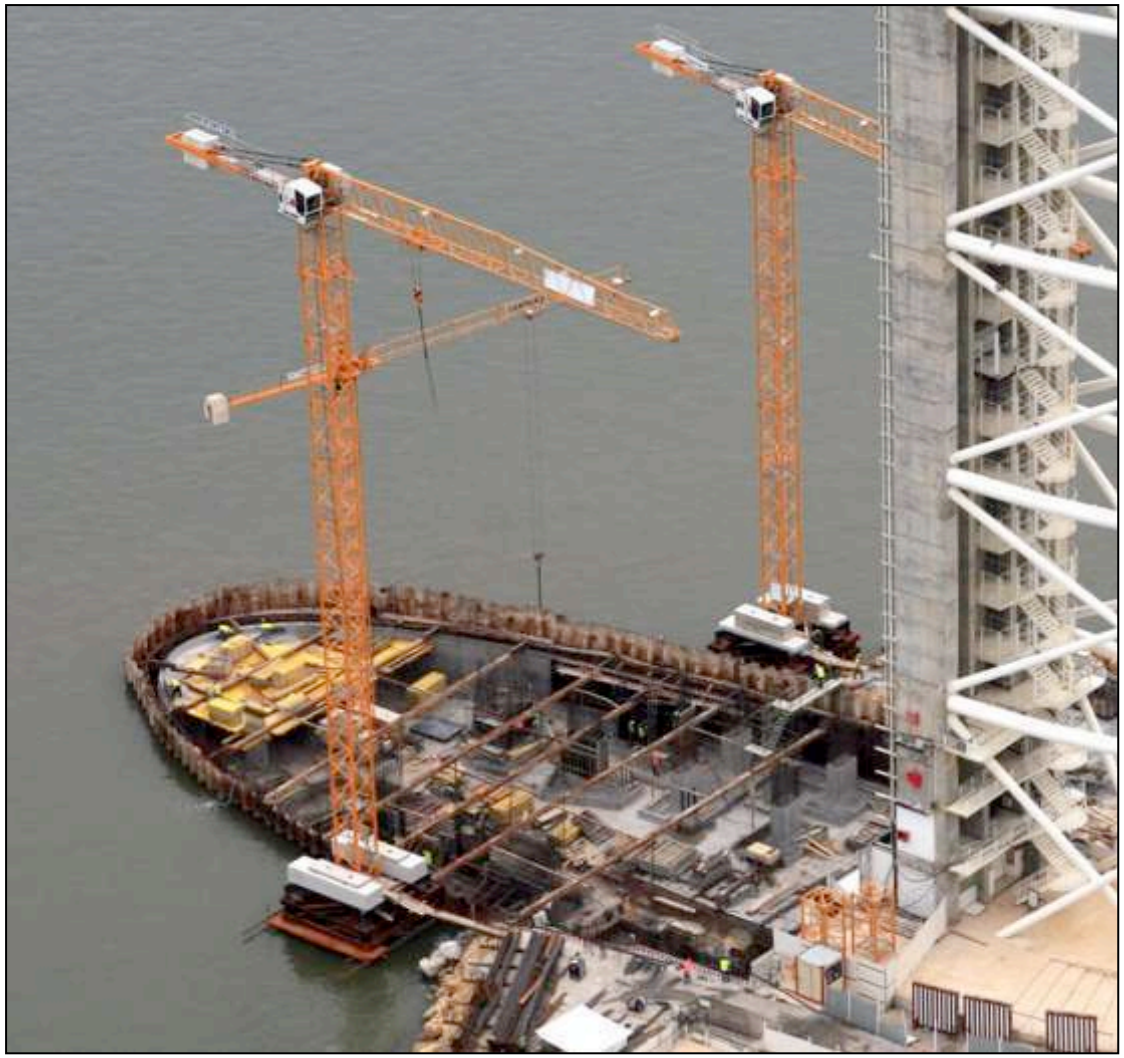

MAIN RESTRAINTS

MAIN SOLUTIONS

DESIGN

MONITORING AND SURVEY

MAIN CONCLUSIONS

MAIN SOLUTIONS

- A temporary "hybrid" cofferdam, composed, at the riverside main perimeter, by a tied / propped sheet piles wall and, at the land side, by an anchored jet grouting columns wall;

- A bottom jet grouting sealing slab, to stiff horizontally the cofferdam and to prevent the water in flow from the excavation base;

- Large diameter reinforced concrete bored piles as foundation of the main structural vertical elements.

- Steel micropiles to nail the jet grouting sealing slab and as foundation of the lightest structural elements, in this case sealed inside jet grouting columns.

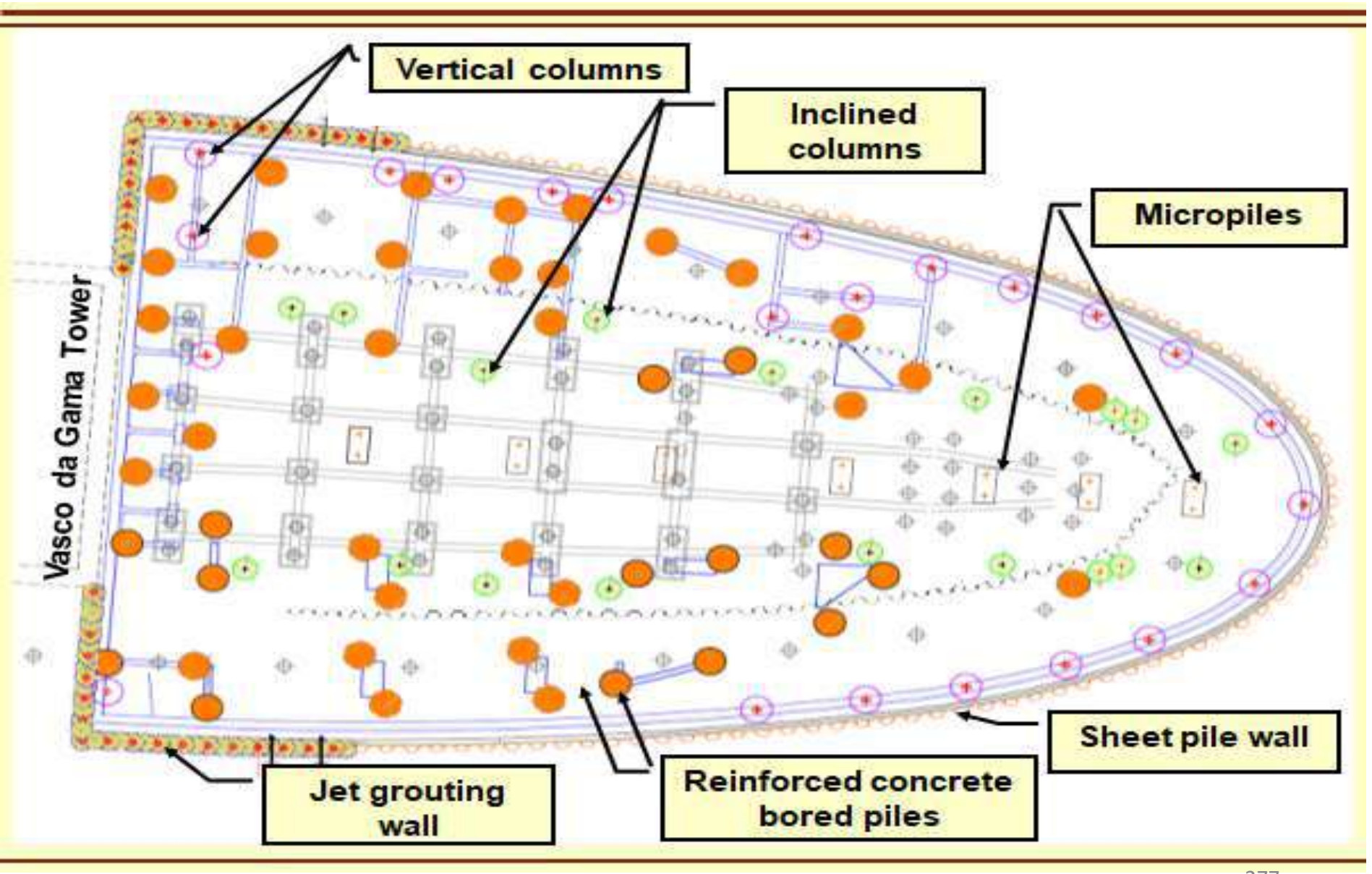
Vertical columns
Inclined columns
Micropiles
Vasco da Gama Tower
Sheet pile wall
Jet grouting wall
Reinforced concrete bored piles

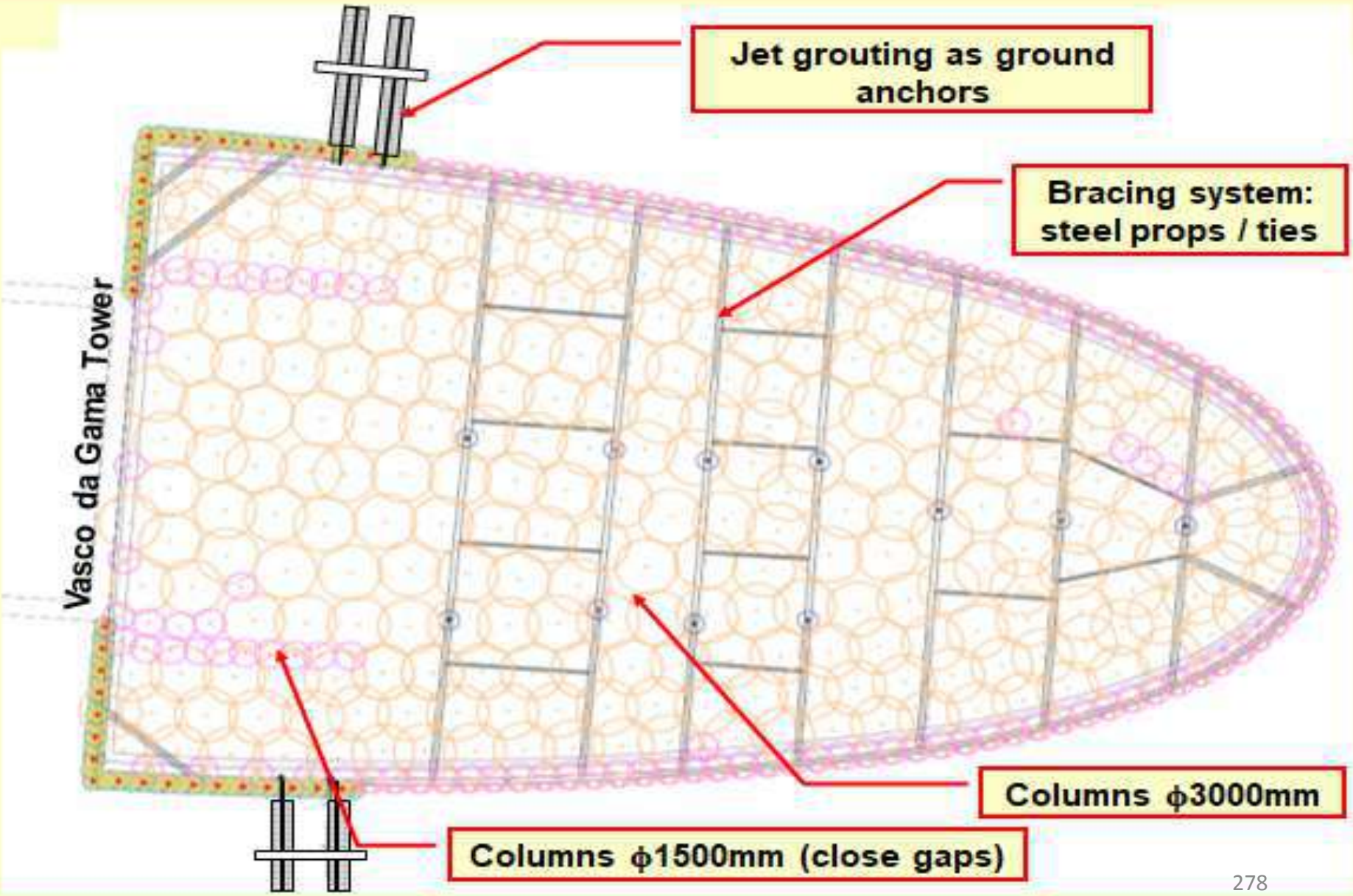
Jet grouting as ground anchors
Bracing system: steel props / ties
Vasco da Gama Tower
Columns ϕ3000mm
Columns ϕ1500mm (close gaps)

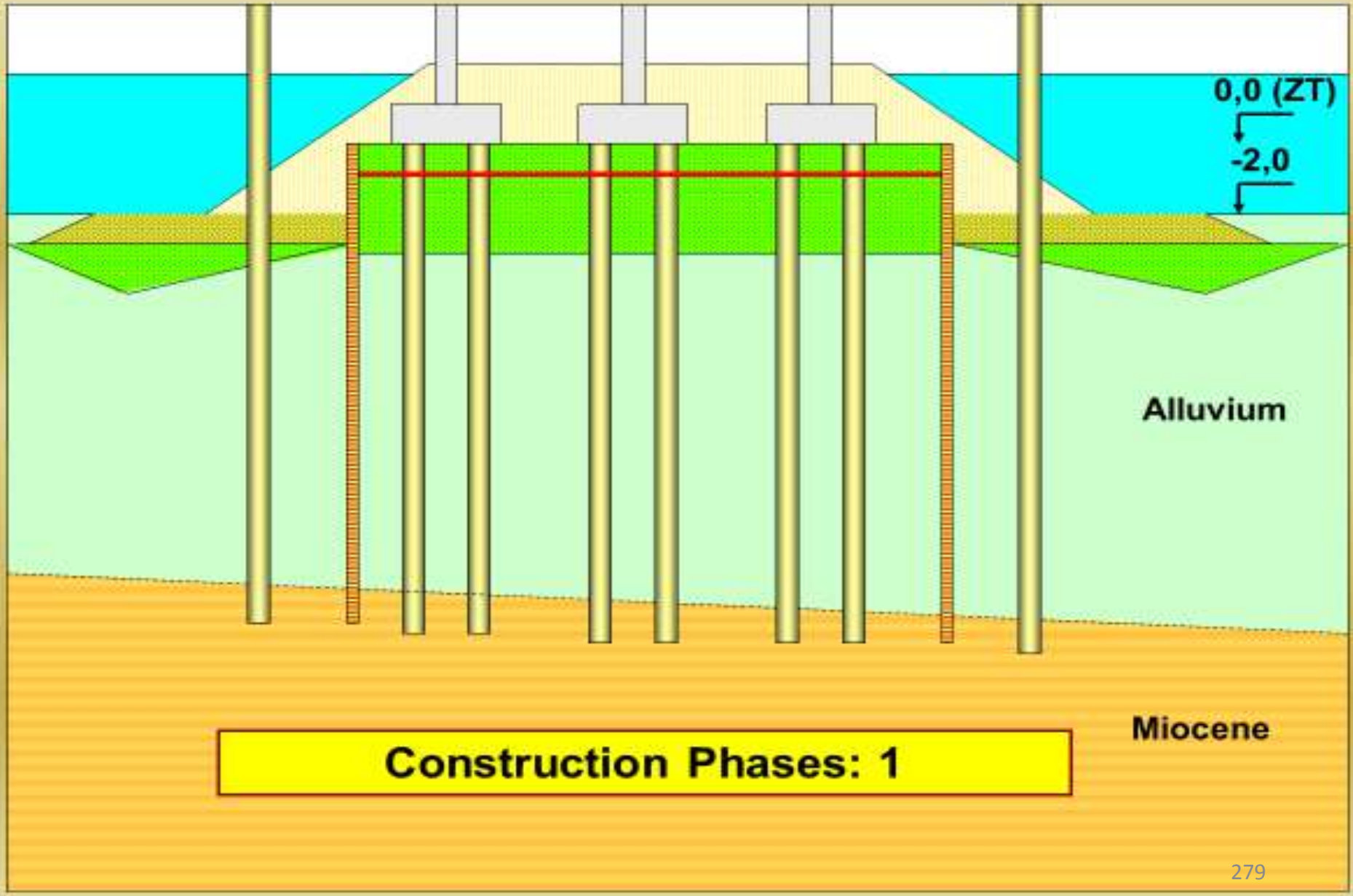
0,0 (ZT)
-2,0
Alluvium
Miocene
Construction Phases: 1

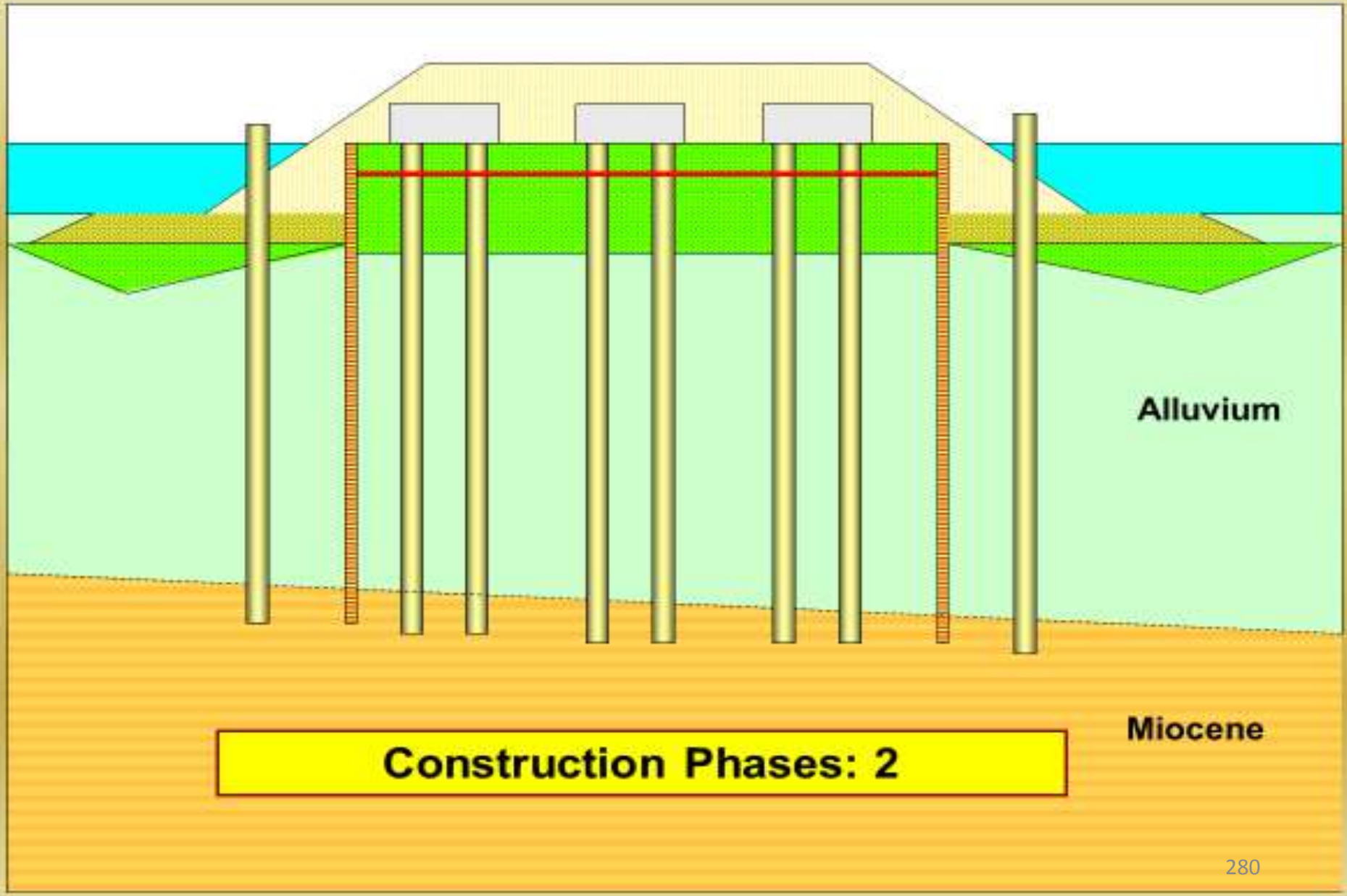
Alluvium
Miocene
Construction Phases: 2

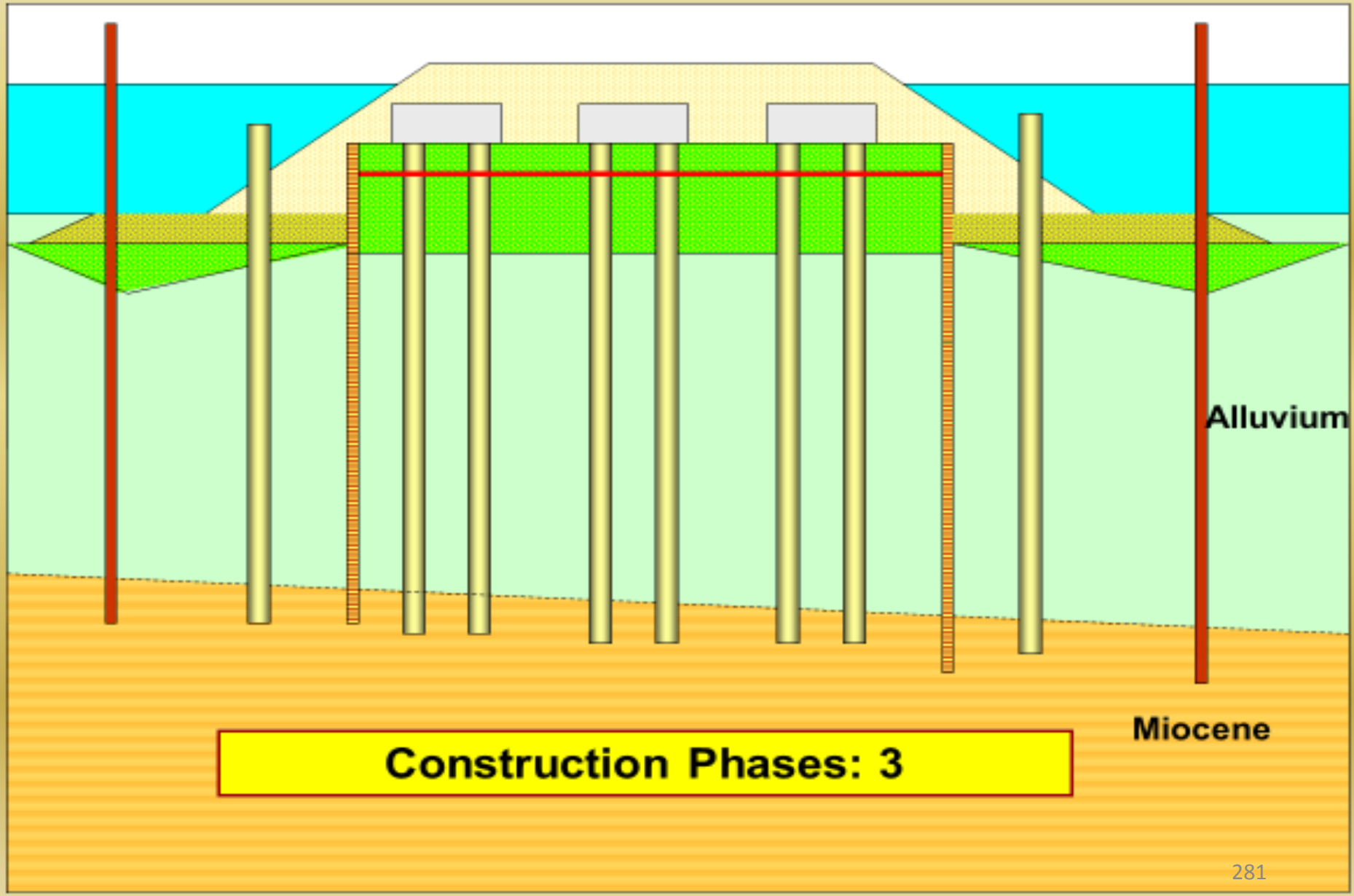
Alluvium
Miocene
Construction Phases: 3

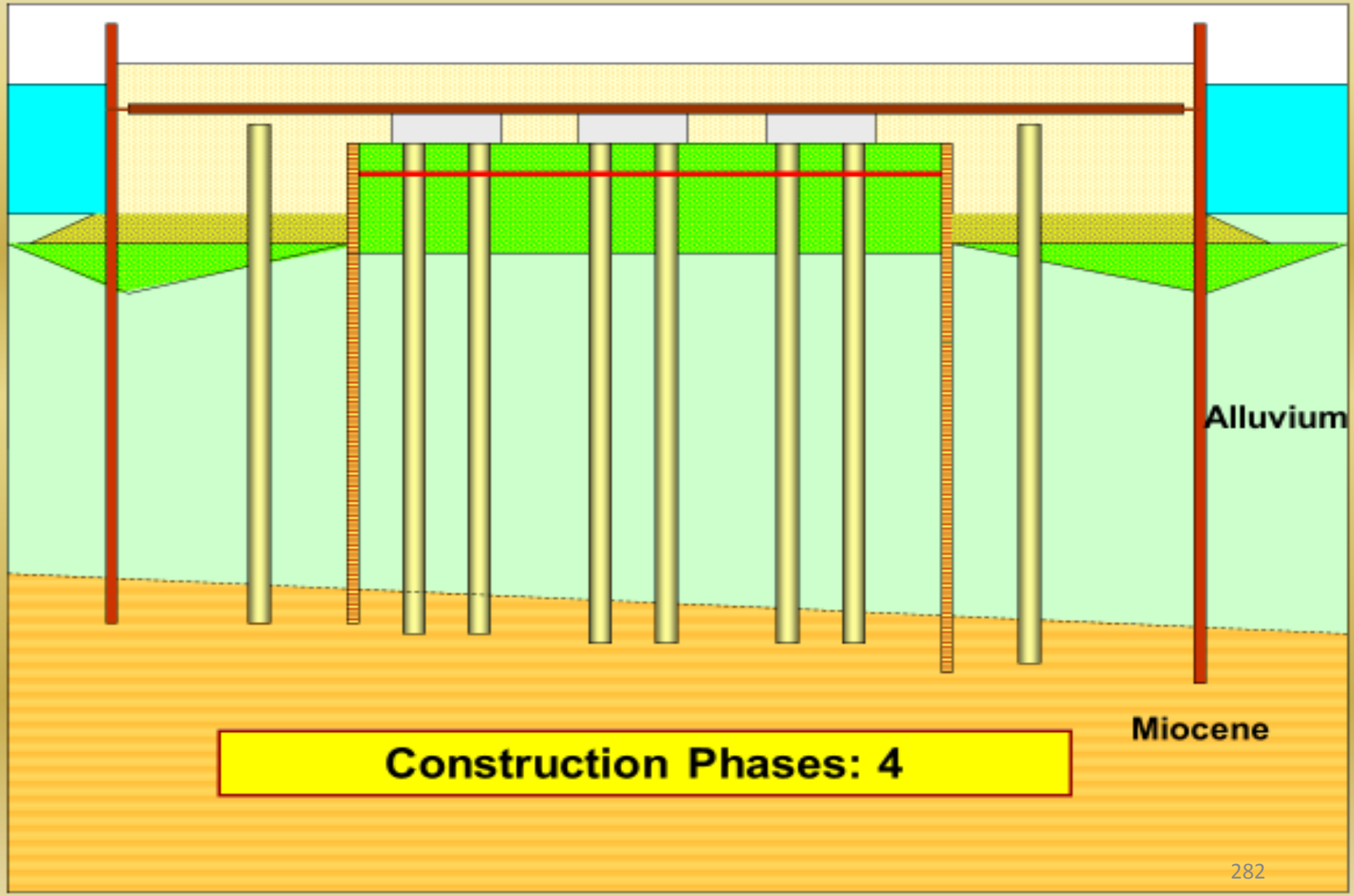
Alluvium
Miocene
Construction Phases: 4

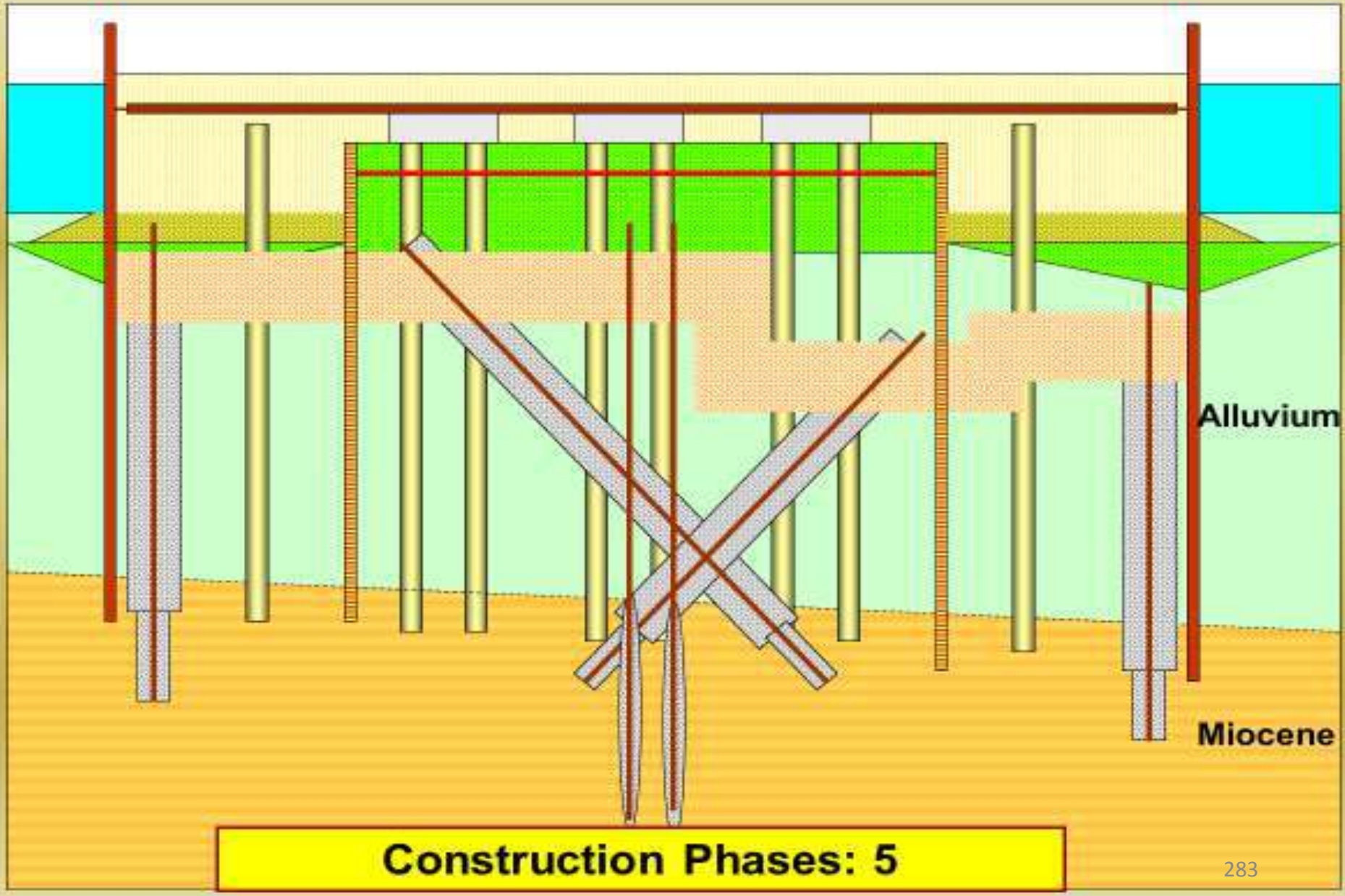
Alluvium
Miocene
Construction Phases: 5

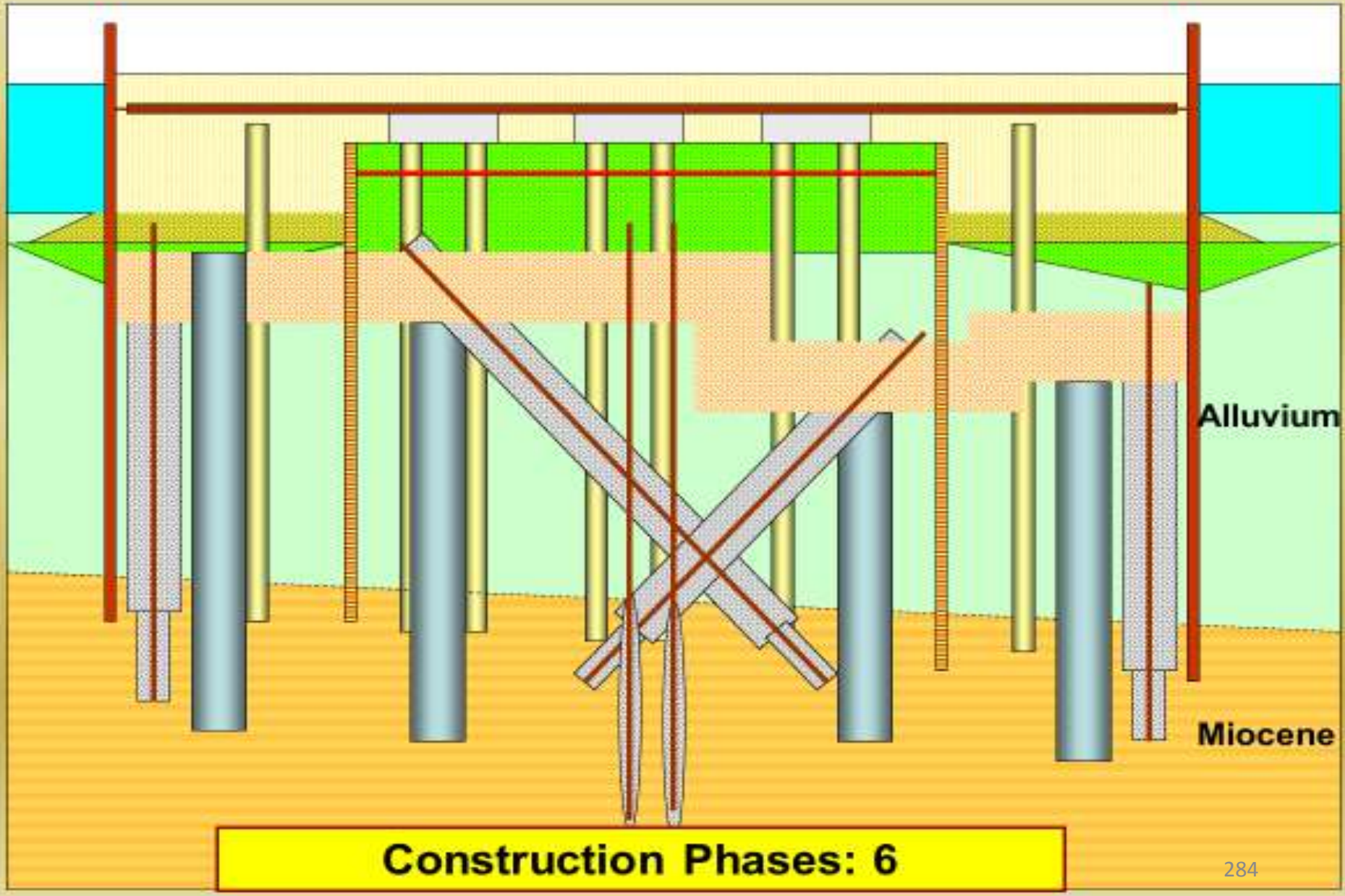
Alluvium
Miocene
Construction Phases: 6

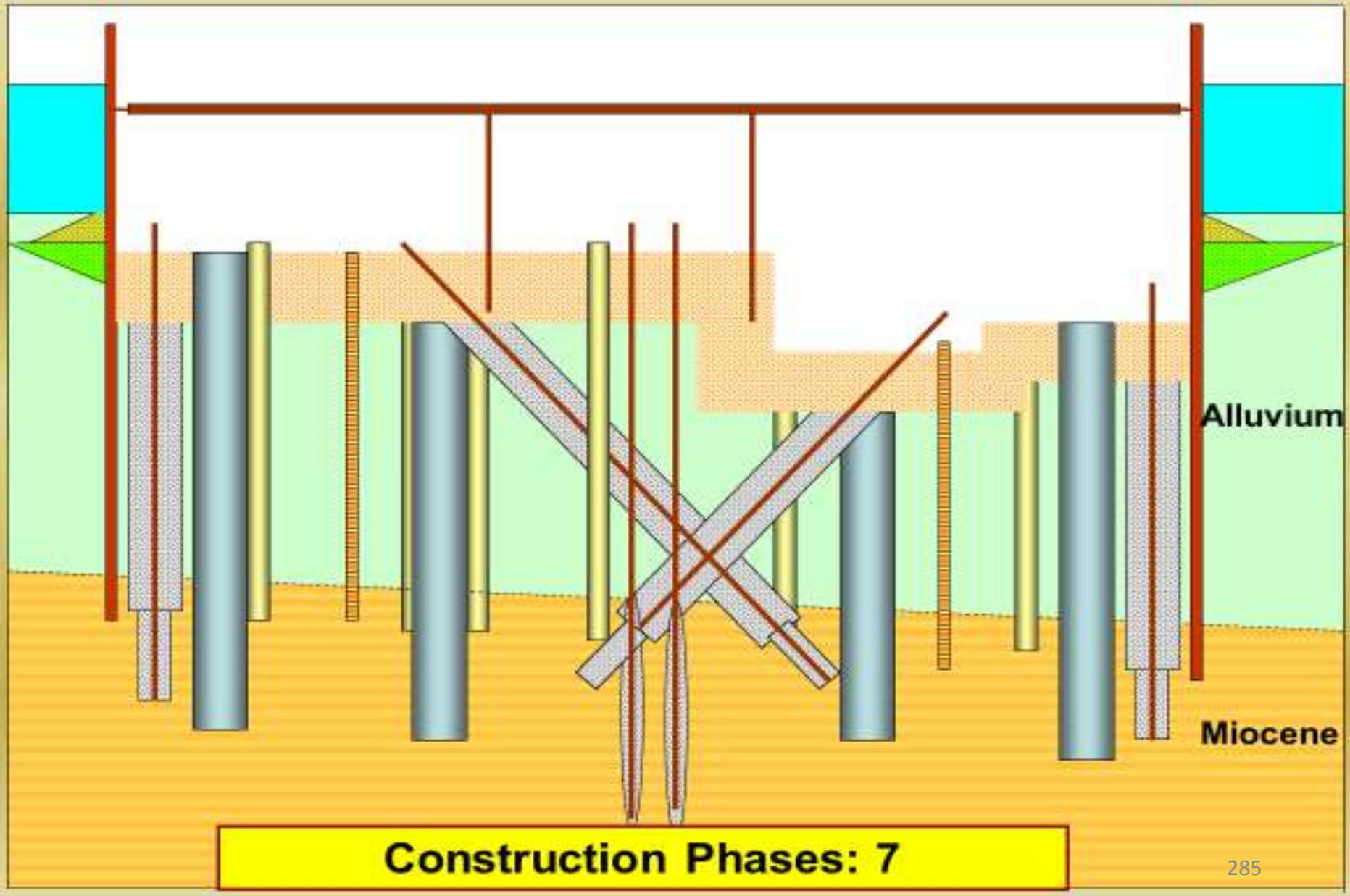
Alluvium
Miocene
Construction Phases: 7

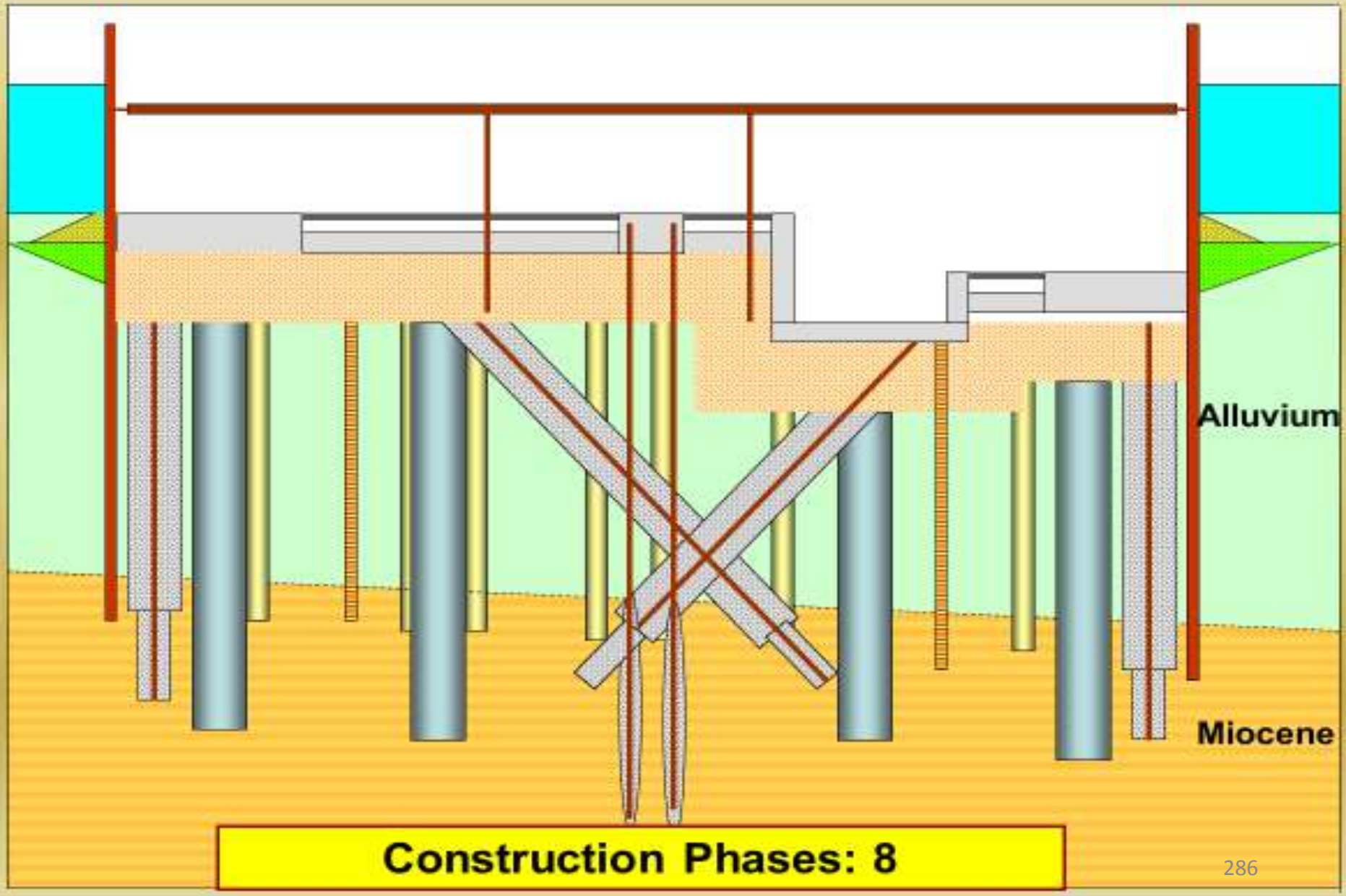
Alluvium
Miocene
Construction Phases: 8

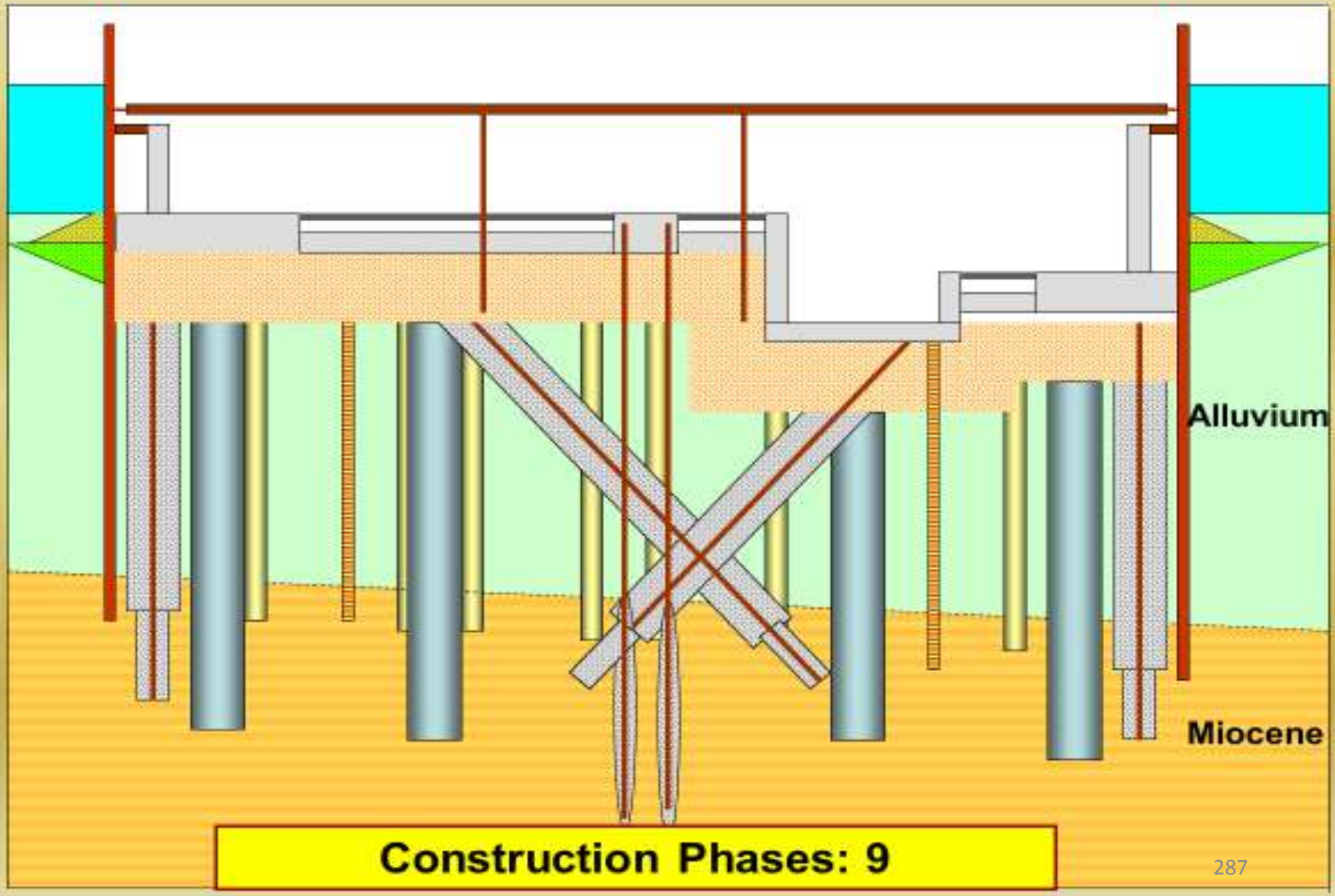
Alluvium
Miocene
Construction Phases: 9

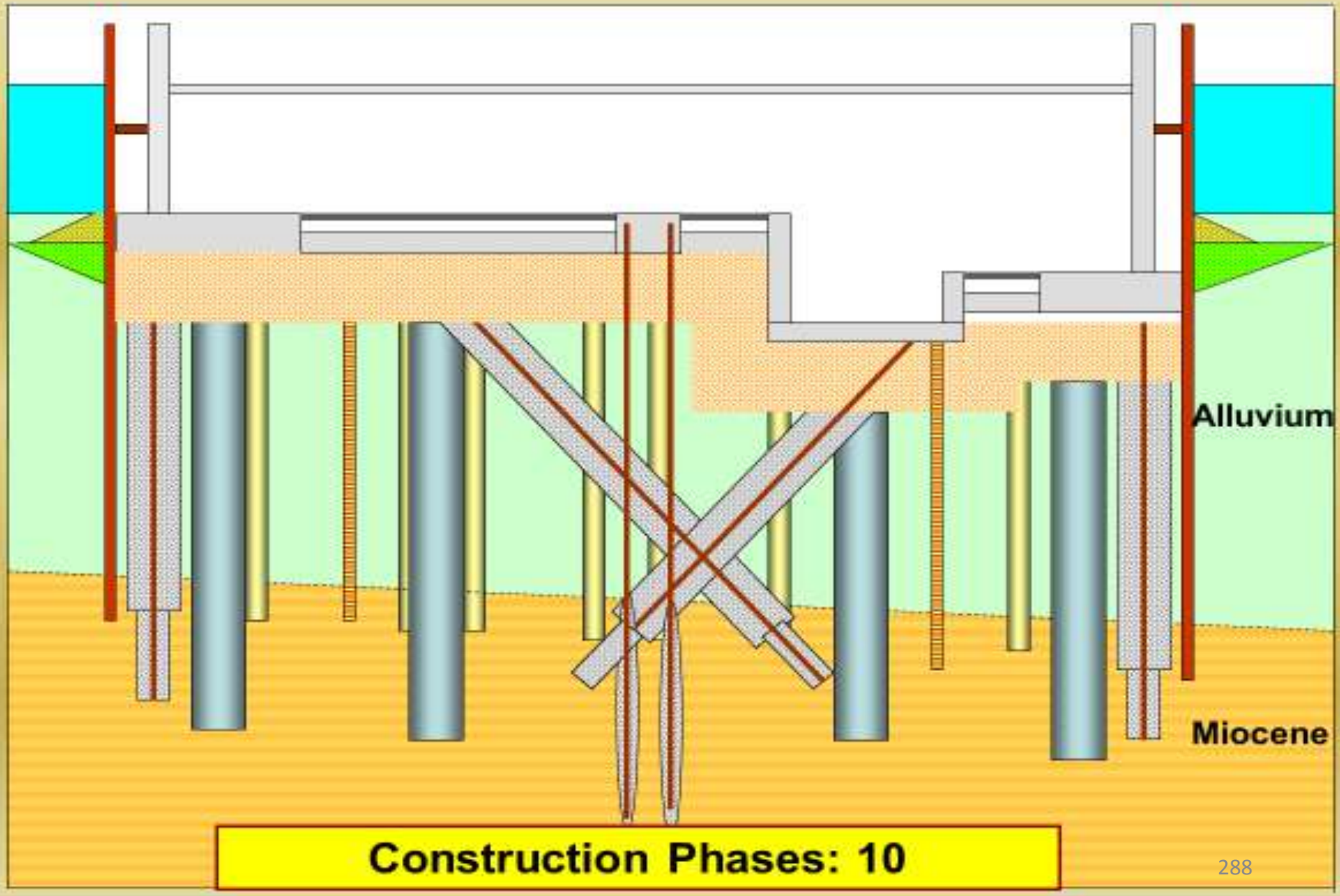
Alluvium
Miocene
Construction Phases: 10

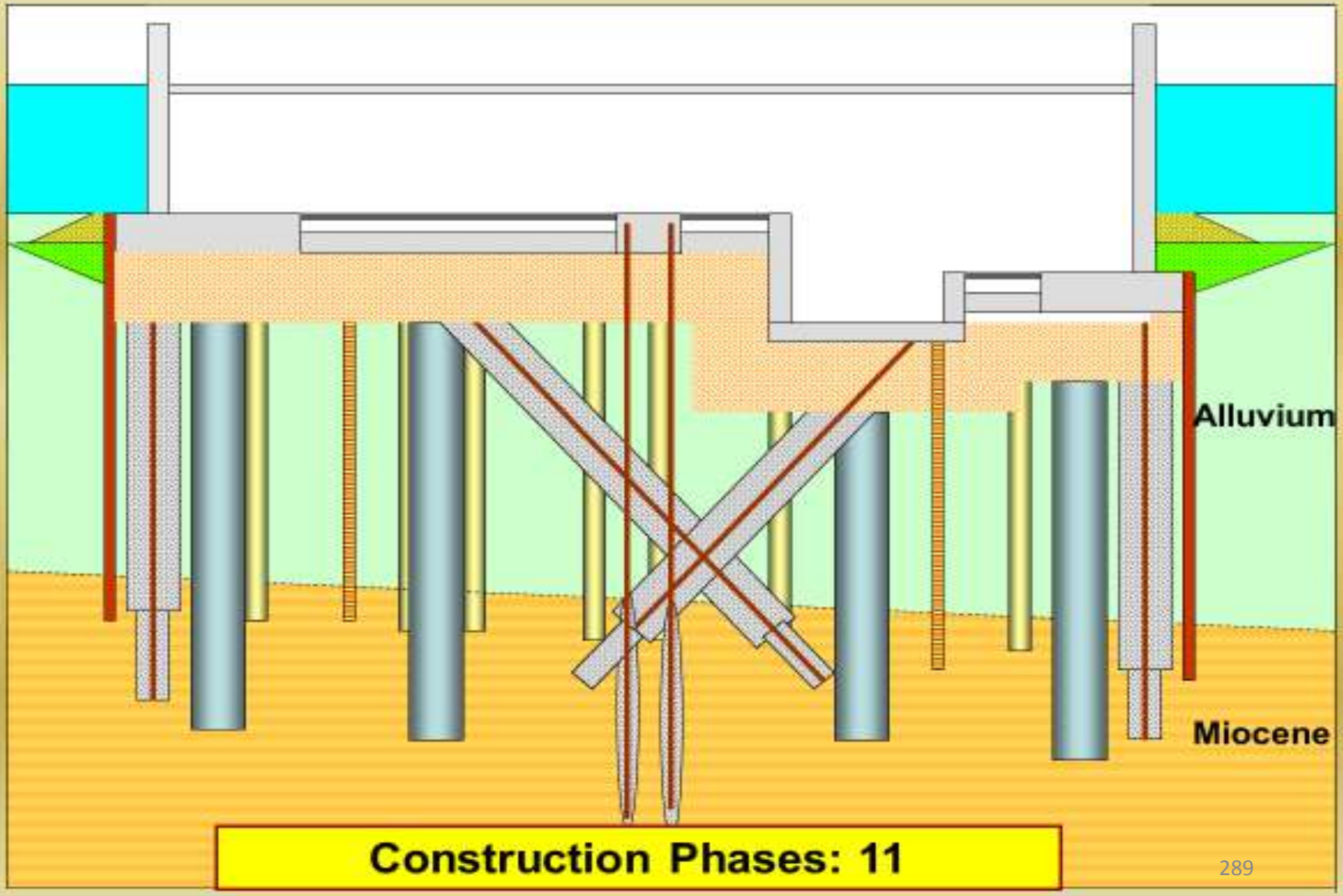
Alluvium
Miocene
Construction Phases: 11

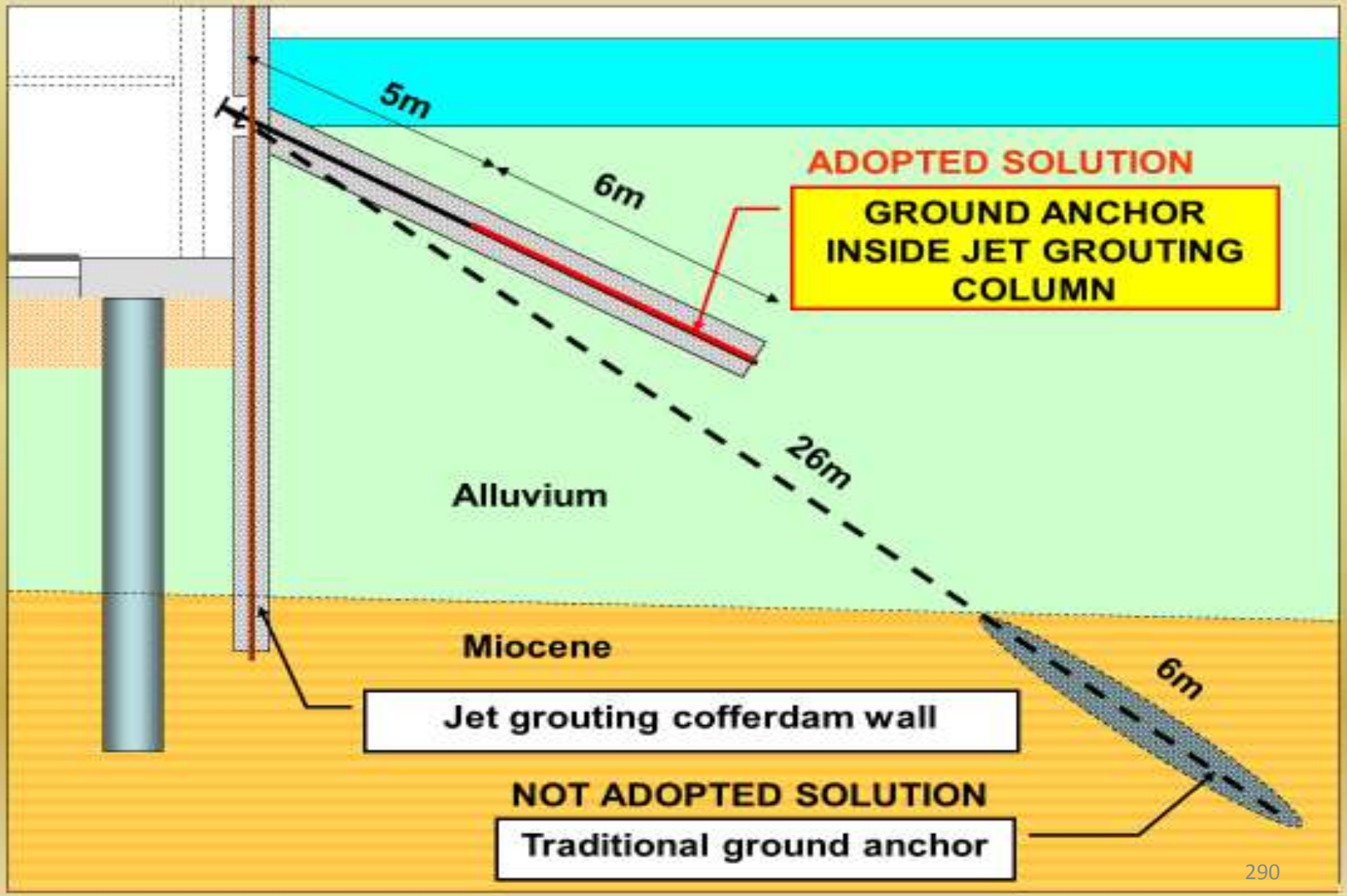
5m
6m
ADOPTED SOLUTION
GROUND ANCHOR INSIDE JET GROUTING COLUMN
26m
Alluvium
Miocene
6m
Jet grouting cofferdam wall
NOT ADOPTED SOLUTION
Traditional ground anchor

In order to obtain safe and permanent working conditions, above water level, the works started with the execution of a temporary working platform, formed by a granular fill, resting over a biaxial geogrid, made from polypropylene (tension resistance of 20kN/m

Jet grouting columns wall, ϕ1.000m spaced 0,60m, and reinforced with hollow steel tubes N80 ϕ177,8 × 9 mm (API 5A), resting over the limestone substratum.


Tecnasol

The bracing system was vertically supported on steel micropiles

Below the excavation level, the cofferdam wall was previously braced by one horizontal sealing slab, composed by jet grouting columns ϕ3.000 mm and ϕ1.500mm with thickness of 2 m,

- **Bored piles ϕ1.500mm embedment 4,5m at the Miocene**
- **Cross hole tests.**
- **steel micropiles to nail the jet grouting sealing slab.**
- **Steel micropiles as foundation of the lightest structural elements,**
- **Seismic loads are accommodated through the bending of large diameter bored piles, as well as through some inclined steel micropiles, sealed inside jet grouting columns.**
- **All the foundation elements, bored piles and micropiles, were capped by a reinforced concrete mat slab, cast against the horizontal jet grouting sealing slab**

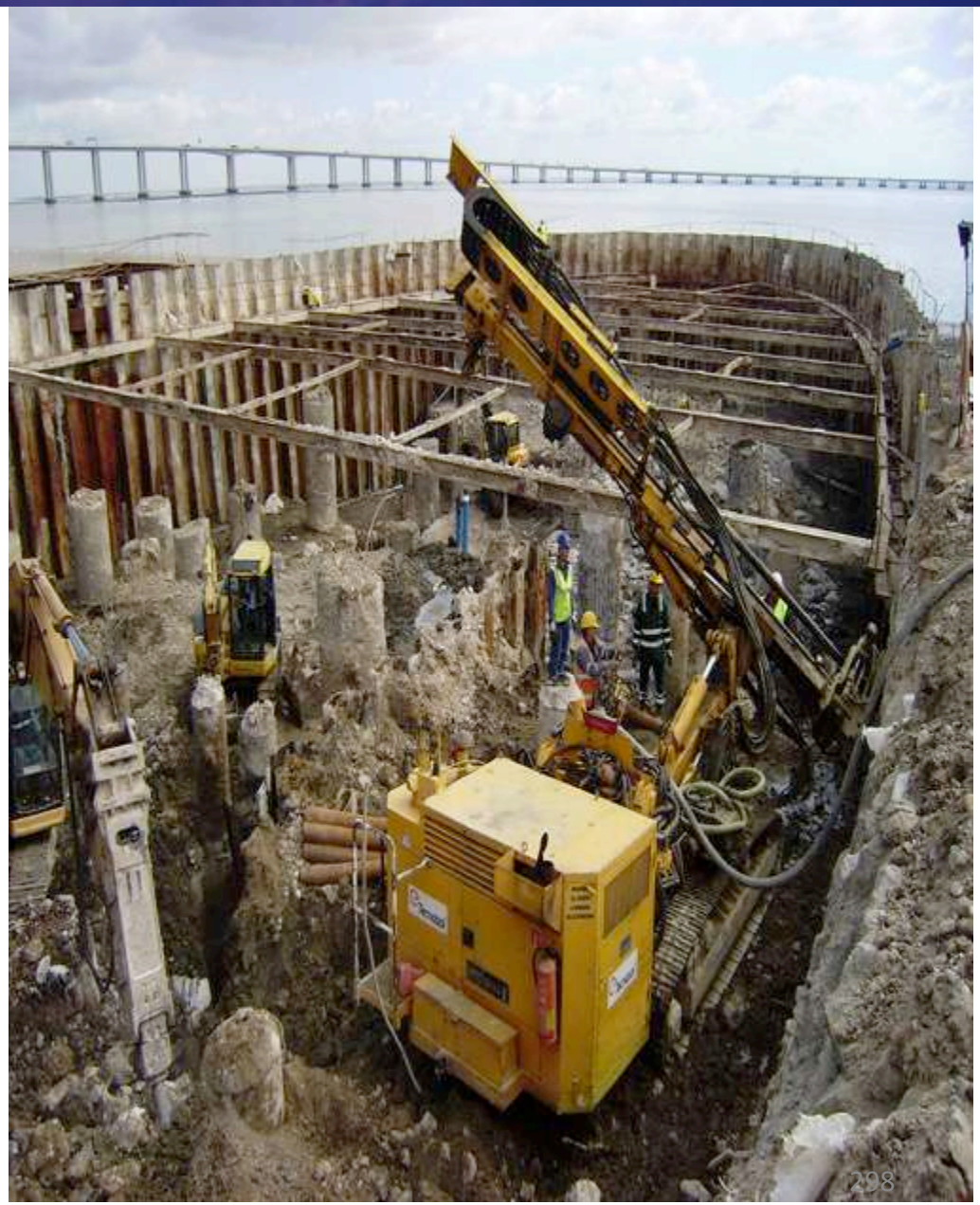

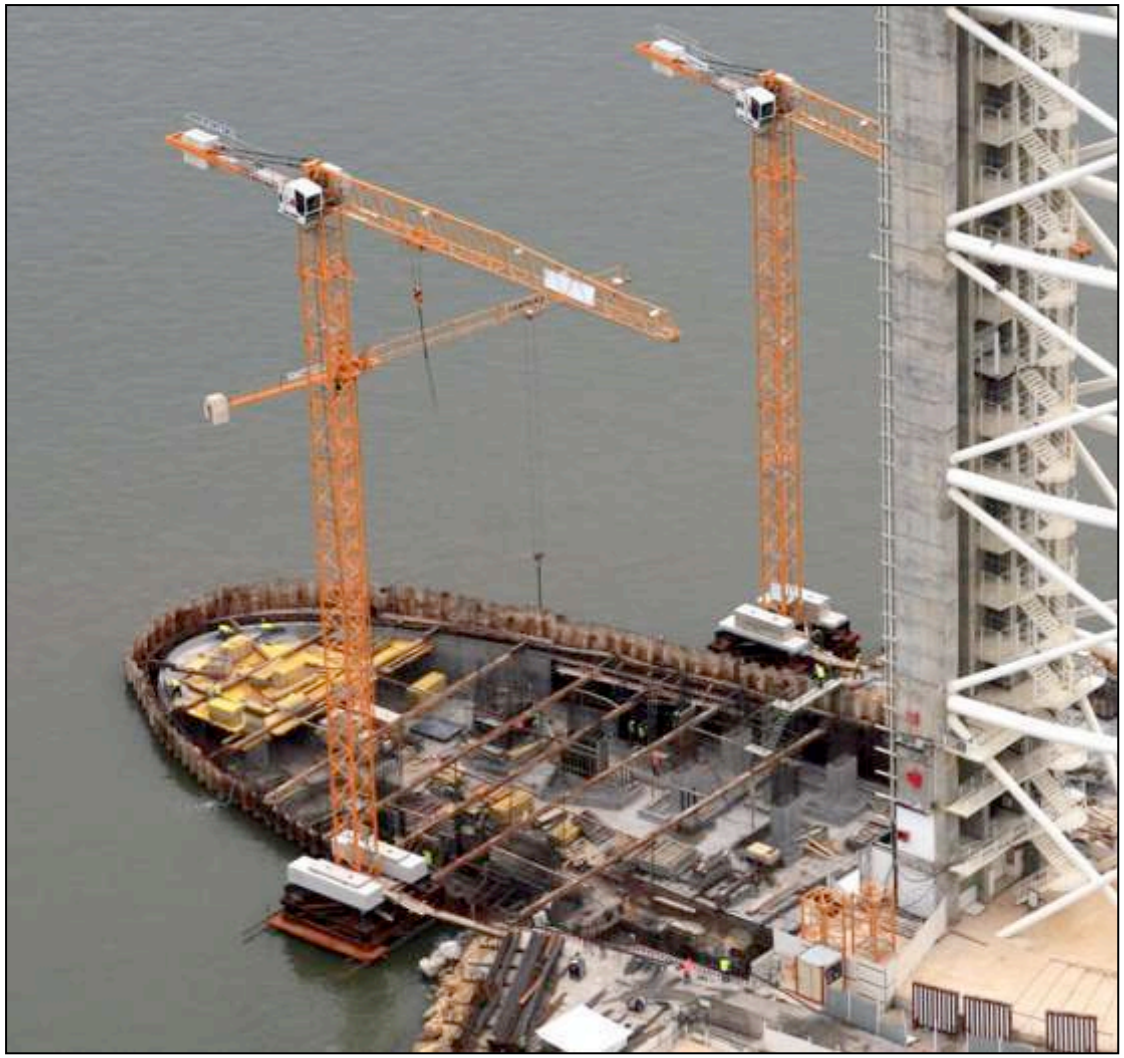

MAIN RESTRAINTS

MAIN SOLUTIONS

DESIGN

MONITORING AND SURVEY

MAIN CONCLUSIONS

The design of the cofferdam walls, including its bracing systems, was performed using a 2D finite element numerical model (Plaxis Professional V.8)

Internal forces and displacements at the cofferdam walls, as well as on the supported soil, were analyzed and predicted for all the main construction stages.

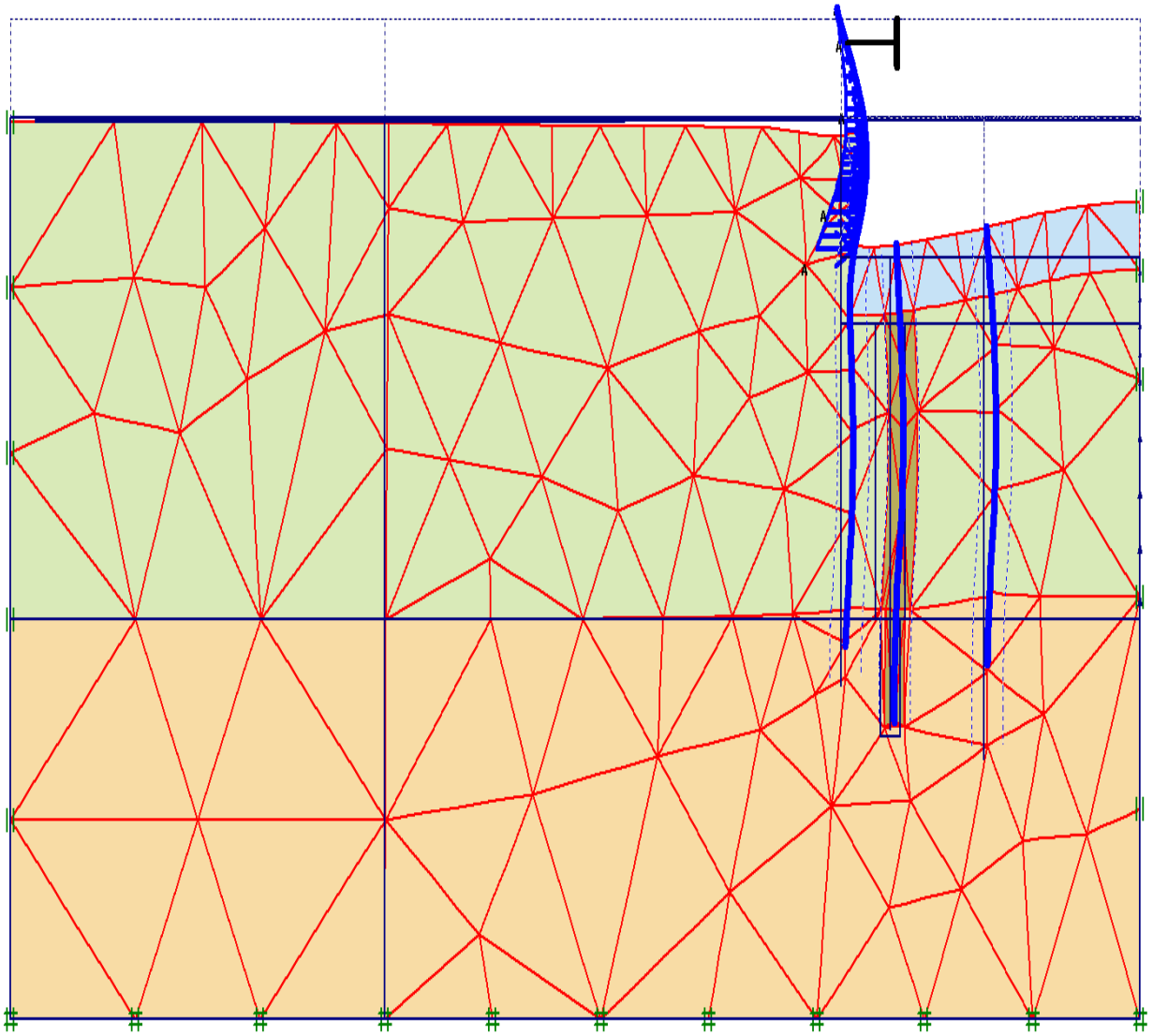

All the main geotechnical parameters were established taking into account the results of previous laboratorial tests

Main Geotechnical Parameters

Material	N_{SPT}	$\phi'(^o)$	c'(kPa)	c_u(kPa)	γ(kN/m^3)	E'(MPa)
Alluvium	<9	18	0	8 - 22	16	4 - 10
Miocene	>60	35	40	200	20	50
Jet Grouting	-	-	200-400	500	18	1.000

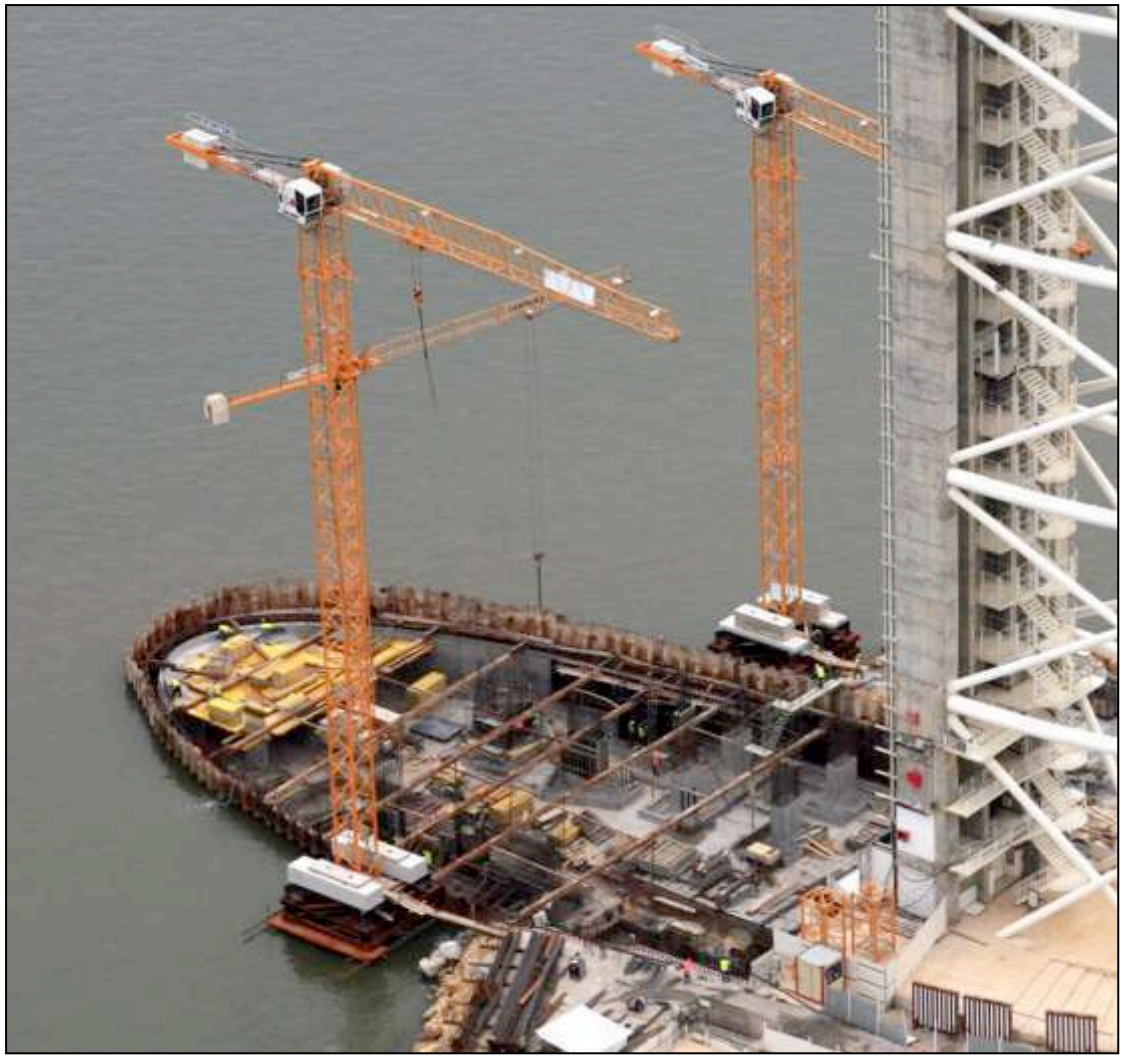

MAIN RESTRAINTS

MAIN SOLUTIONS

DESIGN

MONITORING AND SURVEY

MAIN CONCLUSIONS

Considering the context and the complexity of the described solutions, a monitoring and survey plan was applied

The following equipments/ devices were installed:

- **inclinometers (7un.),**
- **topographic targets (21 un.)**
- **topographic marks (5un.)**

Measurements were commonly performed, at least, twice a week until the cast of the ground level structural slab.

The obtained displacements were in general lesser than the predicted ones

The results of inclinometer I1, point out the importance of the jet grouting botoom slab for the cofferdam horizontal stiffness.

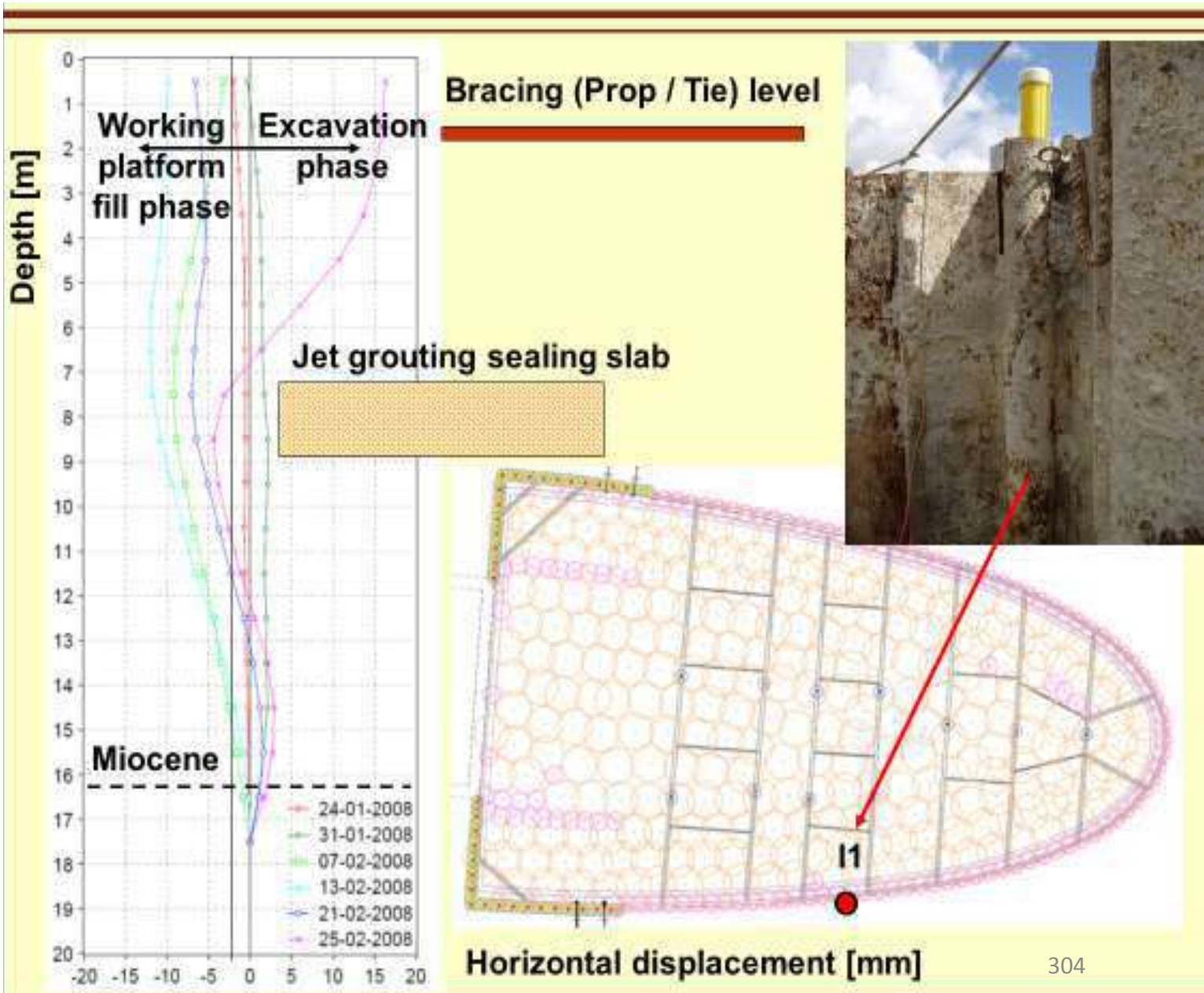

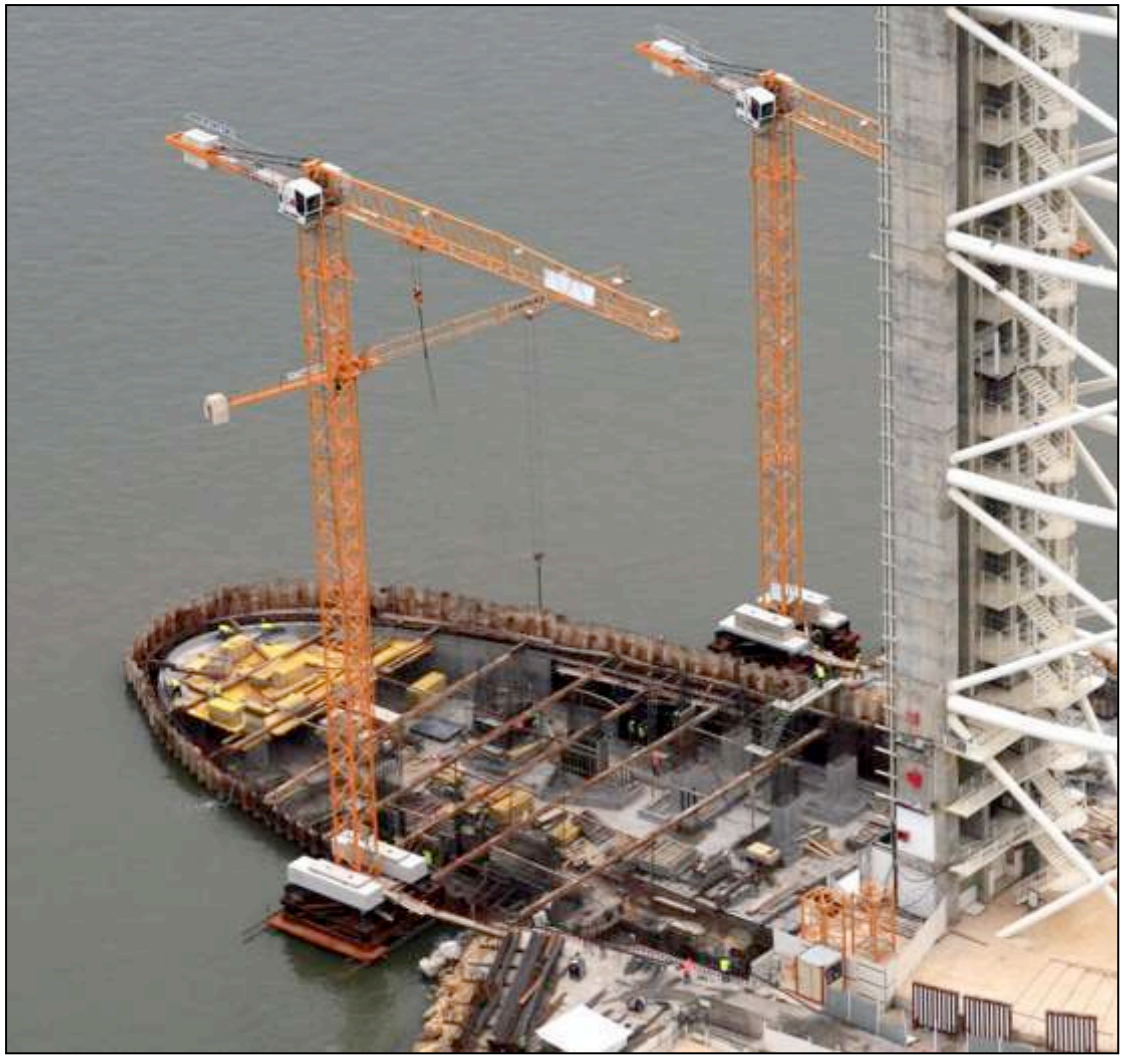

MAIN RESTRAINTS

MAIN SOLUTIONS

DESIGN

MONITORING AND SURVEY

MAIN CONCLUSIONS

- **Maximum profit from the existent foundations**
- **The majority of the geotechnical works were performed before the excavation phase**
- **Maximum integration between temporary and final solutions**
- **Versatility of ground improvement solutions using jet grouting elements (foundation +retaining walls + water control)**

Thank you for your kind attention!

DONO DE OBRA: AZITEJO

ARQUITECTURA: NUNO LEÓNIDAS ARQUITECTOS

EMPREITEIROS: EDIFER / TECNASOL

PROJECTO GEOTECNIA: JETSJ GEOTECNIA

PROJECTO ESTRUTURAS: GAPRES

2SGT2019
2nd SEMINAR ON TRANSPORTATION GEOTECHNICS

Soil Improvement Challenges on Alluvial Zones

28-29 January 2019 | Vila Franca de Xira | Portugal

Soil improvement by precast driven pile rigid inclusions for embankments on very soft soils

Rafael Gil Lablanca

Rodio

Organização

Sociedade Portuguesa de Geotecnia

Comissão Portuguesa de Geotecnia nos Transportes

Comissão Portuguesa de Geossintéticos

Apoios

LABORATÓRIO NACIONAL DE ENGENHARIA CIVIL

ORDEM DOS ENGENHEIROS

PROJECTOS

1. PONTE SOBRE O RIO TRANCÃO – Sacavém, Lisboa

Imagens ©2019 Google,Dados do mapa ©2019 Google

- Corresponde a uma das intervenções da obra de substituição do tabuleiro da ponte sobre o rio Trancão em Sacavém
- A RODIO realizou os trabalhos de fundação da plataforma de encontro da nova ponte com a estrada de ligação

2. "SUD EUROPE ATLANTIQUE" (LGV SEA)

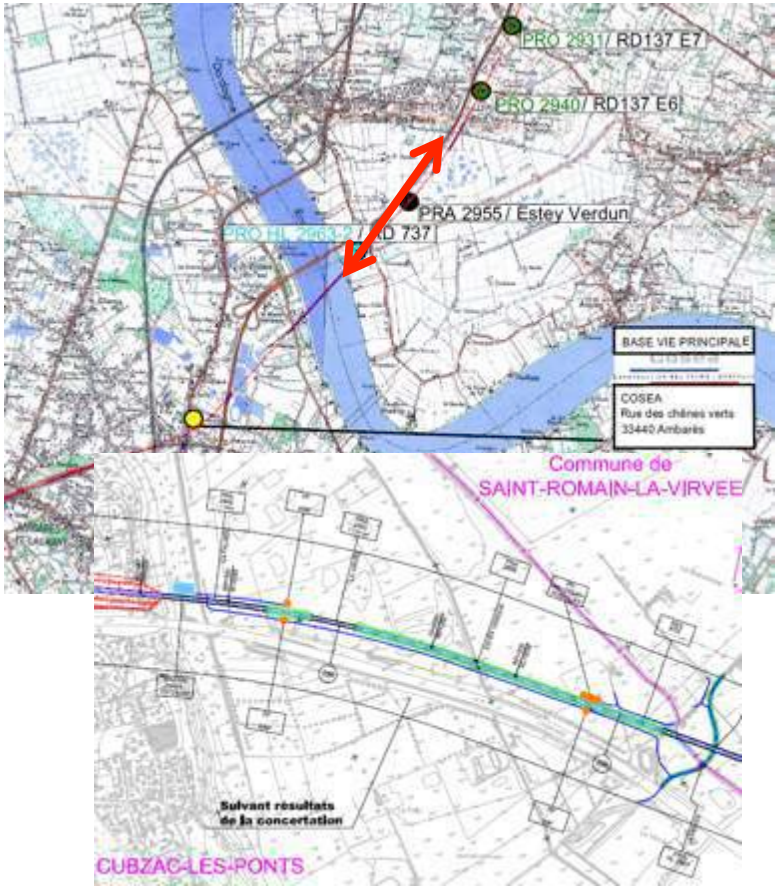

- O lote 15 (secção G) apresenta uma extensão de 18 km, onde se encontram 23 trabalhos de movimentações de terras, 21 infraestruturas fabris, 2 viadutos e um canal
- Para atravessar a Várzea do Rio Dordonha foram executados um viaduto e três aterros de 2 a 6 metros de altura.

PONTE SOBRE O RIO TRANCÃO. DESCRIÇÃO GEOLÓGICA-GEOTÉCNICA

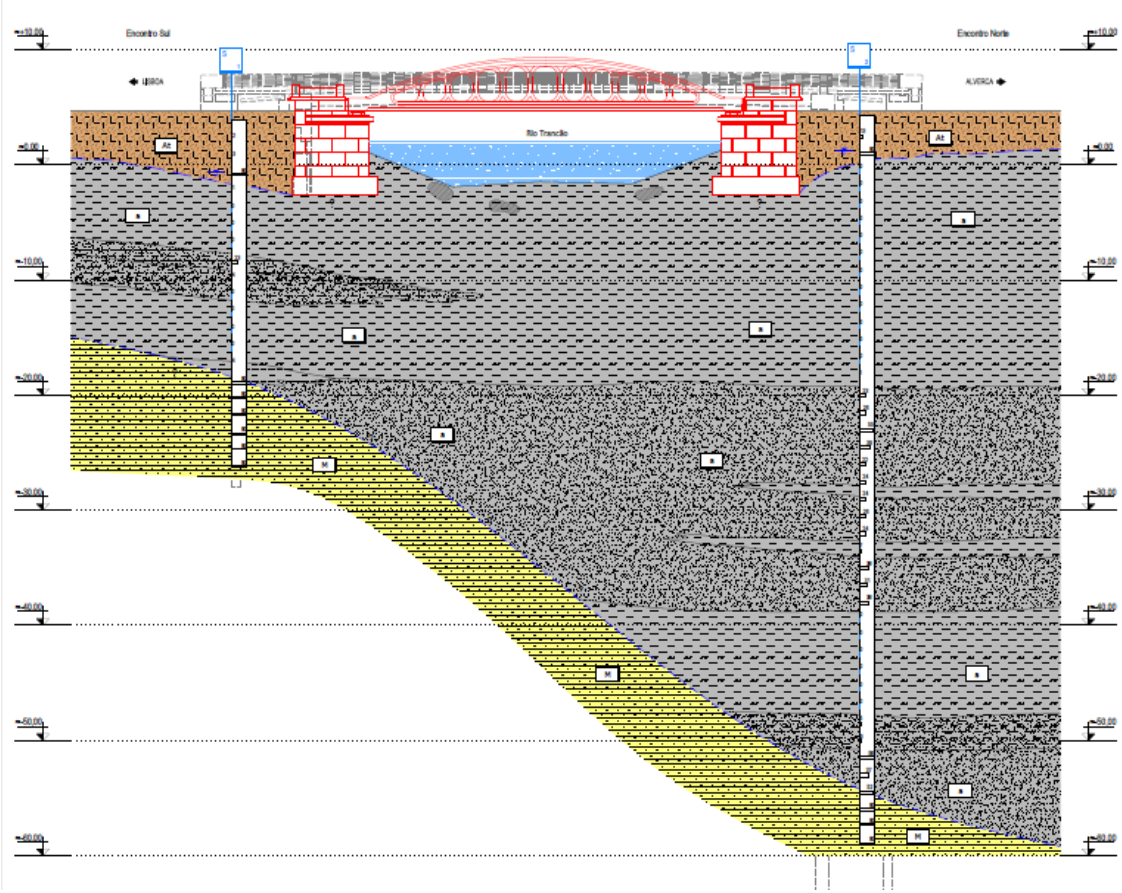

- Perfil geotécnico:
  - Aterros com cerca de 2 metros de altura
  - Depósitos aluvionares de espessura variável;
  - Terrenos Miocénicos

PONTE SOBRE O RIO TRANCÃO. SOLUCÃO DE FUNDACÃO

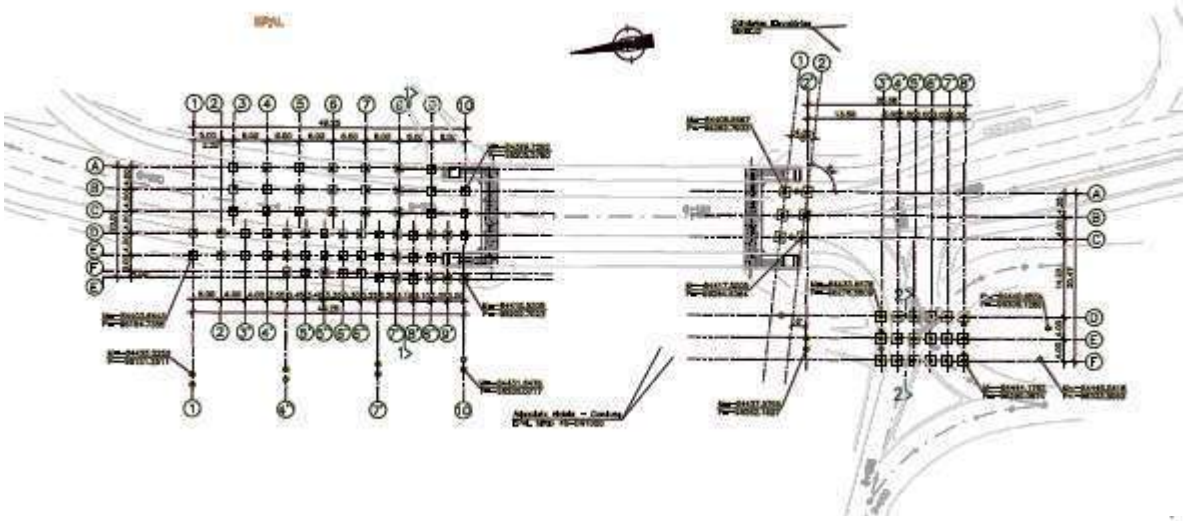

TRIEDE
Consultoria e Projecto de Engenharia Civil, S.A.

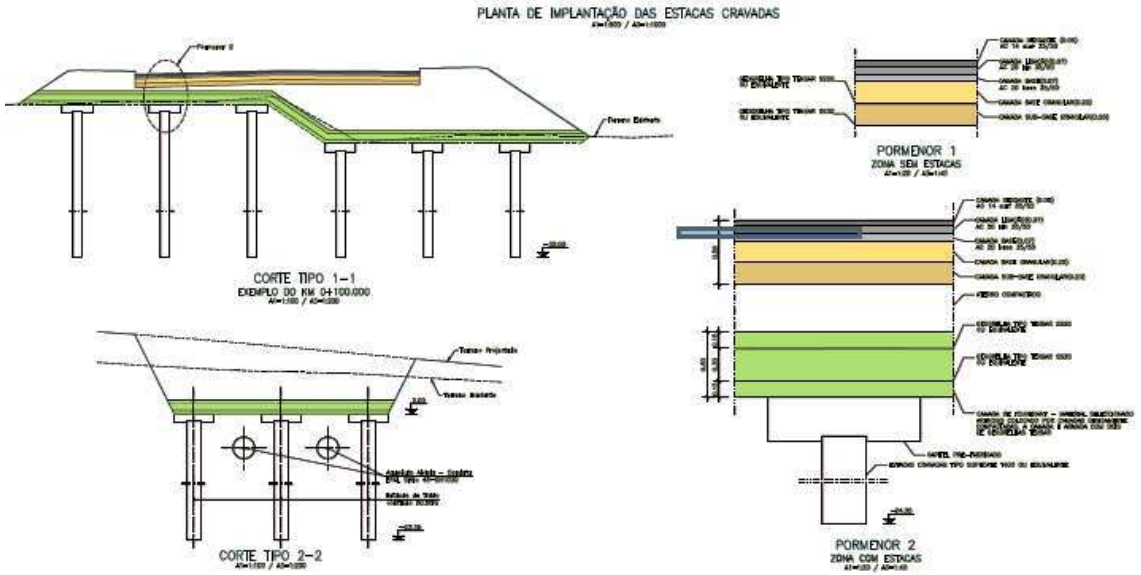

PONTE SOBRE O RIO TRANCÃO. CARACTERÍSTICAS DAS ESTACAS

- Estaca CK-400 Classe I (EN 12794) com 31 metros de comprimento total
- Detalhes:
  - Classe de Resistência C50/60
  - Betão vibrado em moldes de cofragem
  - Junta tipo ABB de classe A (EN 12794)
- Rastreabilidade do processo construtivo

Betonagem nos moldes de cofragem

Transporte e armazenagem das peças

Etiqueta de identificação da estaca

PONTE SOBRE O RIO TRANCÃO. EXECUÇÃO DA OBRA

Transporte e elevação das estacas

- Martelo de cravação
  - JUNTTAN PM 25
  - 9 toneladas

- Quantidades totais:
  - 103 estacas
  - 2008 ml
- Rendimento médio:
  - 180 ml/dia

Cravação das estacas

Descabeçamento das estacas

PANTANO DE LA VIRVÉE. DESCRIÇÃO GEOLÓGICA-GEOTÉCNICA

Formation		Identification							Cisaillement				Compressibilité et fluage									
					Limites d'Atterberg				Triaxial UU		Triaxial CU+u							Consolidation verticale		Consolidation radiale		Fluage
		w_n (%)	γ_d (kN/m^3)	γ_h (kN/m^3)	w_P (%)	I_P (%)	I_C (%)	MO (%)	c_U (kPa)	φ_U (°)	c' (kPa)	φ' (°)	C_c	C_s	σ'_p (kPa)	σ'_{v0} (kPa)	e_0	C_v (m²/s)	k_v estimé (m/s)	C_r (m²/s)	k_h estimé (m/s)	C_α
Argile de tête	Nombre de valeurs	16	5	0	5	5	5	5	0	0	0	0	0	0	0	0	0	0	0	0	0	0
	Min	24,0	6,8		25,0	24,0	0,6	6,0														
	Max	84,0	15,8		74,0	69,0	1,4	11,6														
	Moyenne	**44,2**	**11,8**		**39**	**42**	**1**	**8**														
	Ecart-type	19,4	3,6		20	18	0	2														
Tourbe	Nombre de valeurs	9	6	2	2	2	2	3	0	0	1	1	4	4	4	4	4	4	5	4	6	4
	Min	232,8	1,6	10,3	42	22	-4,8	60,8					4,801	1,012	19	10	9,163	$1{,}00.10^{-5}$	$3{,}00.10^{-11}$	$7{,}19.10^{-8}$	$1{,}10.10^{-6}$	0,0034
	Max	586,8	3,4	11,0	84	93	-3,7	196					8,934	1,327	23	12	14,767	$1{,}02.10^{-7}$	$6{,}70.10^{-9}$	$2{,}65.10^{-6}$	$1{,}70.10^{-7}$	0,0257
	Moyenne	**435,3**	**2,3**	**10,6**	**63**	**58**	**-4**	**111**			**7**	**1**	**6,799**	**1,160**	**21**	**11**	**11,707**	$\mathbf{3{,}42.10^{-8}}$	$\mathbf{2{,}00.10^{-9}}$	$\mathbf{8{,}64.10^{-7}}$	$\mathbf{4{,}85.10^{-8}}$	**0,0142**
	Ecart-type	109,5	0,7	0,5	30	50	1	74					1,770	0,134	2	1	2,950	$4{,}31.10^{-8}$	$2{,}81.10^{-9}$	$9{,}65.10^{-7}$	$6{,}14.10^{-8}$	0,0086
Argile vasarde	Nombre de valeurs	65	41	14	13	13	13	20	3	3	4	4	28	28	28	28	28	28	42	28	41	28
	Min	45,2	3,9	13,4	27	13	-4	6	7	0	7	3	0,499	0,023	13	13	1,22	$1{,}50.10^{-5}$	$1{,}10.10^{-11}$	$5{,}87.10^{-8}$	$3{,}50.10^{-10}$	0,0019
	Max	280,5	13,3	15,6	94	60	1	25	11	0	17	25	2,652	0,539	111	60	5,683	$9{,}51.10^{-8}$	$1{,}40.10^{-9}$	$9{,}72.10^{-7}$	$6{,}80.10^{-9}$	0,1120
	Moyenne	**90,2**	**8,1**	**14,5**	**47**	**41**	**0**	**10**	**10**	**0**	**11**	**15**	**1,139**	**0,151**	**50**	**33**	**2,504**	$\mathbf{1{,}68.10^{-8}}$	$\mathbf{1{,}72.10^{-10}}$	$\mathbf{2{,}00.10^{-7}}$	$\mathbf{1{,}66.10^{-9}}$	**0,0206**
	Ecart-type	30,8	1,7	0,7	19	14	1	5	2	0	5	9	0,479	0,121	26	13	0,981	$1{,}61.10^{-8}$	$2{,}24.10^{-10}$	$1{,}61.10^{-7}$	$1{,}61.10^{-9}$	0,0226

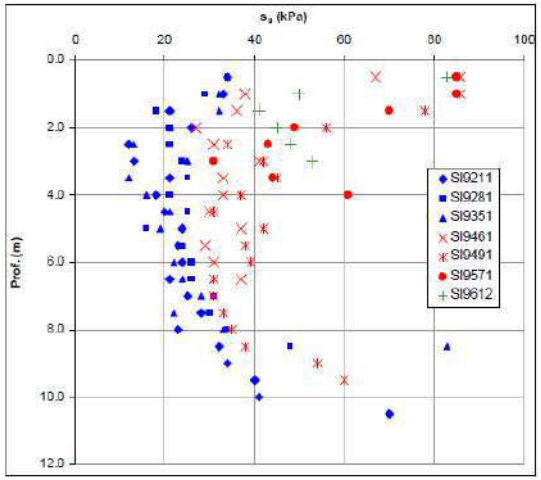

- Formações sob os aterros:
  - Solo residual de argilas e siltes;
  - Turfas até 3,7 metros de espessura (não de identifica na zona sul);
  - Argila lodosa ou lodos com 4,2 a 10,3 metros de espessura sob a camada de turfa. (Entre 7,3 e 9,5 metros na zona sul);
  - Areias lodosas com 1 metro de espessura média;
  - Areias e cascalhos com 2,6 a 7,6 metros de espessura;
  - Substrato margoso
- Nível freático: +1,4 NGF (terreno natural +1,5 NGF).

PANTANO DE LA VIRVÉE. SOLUÇÃO DE MELHORAMENTO DE SOLOS COM INCLUSÕES RÍGIDAS

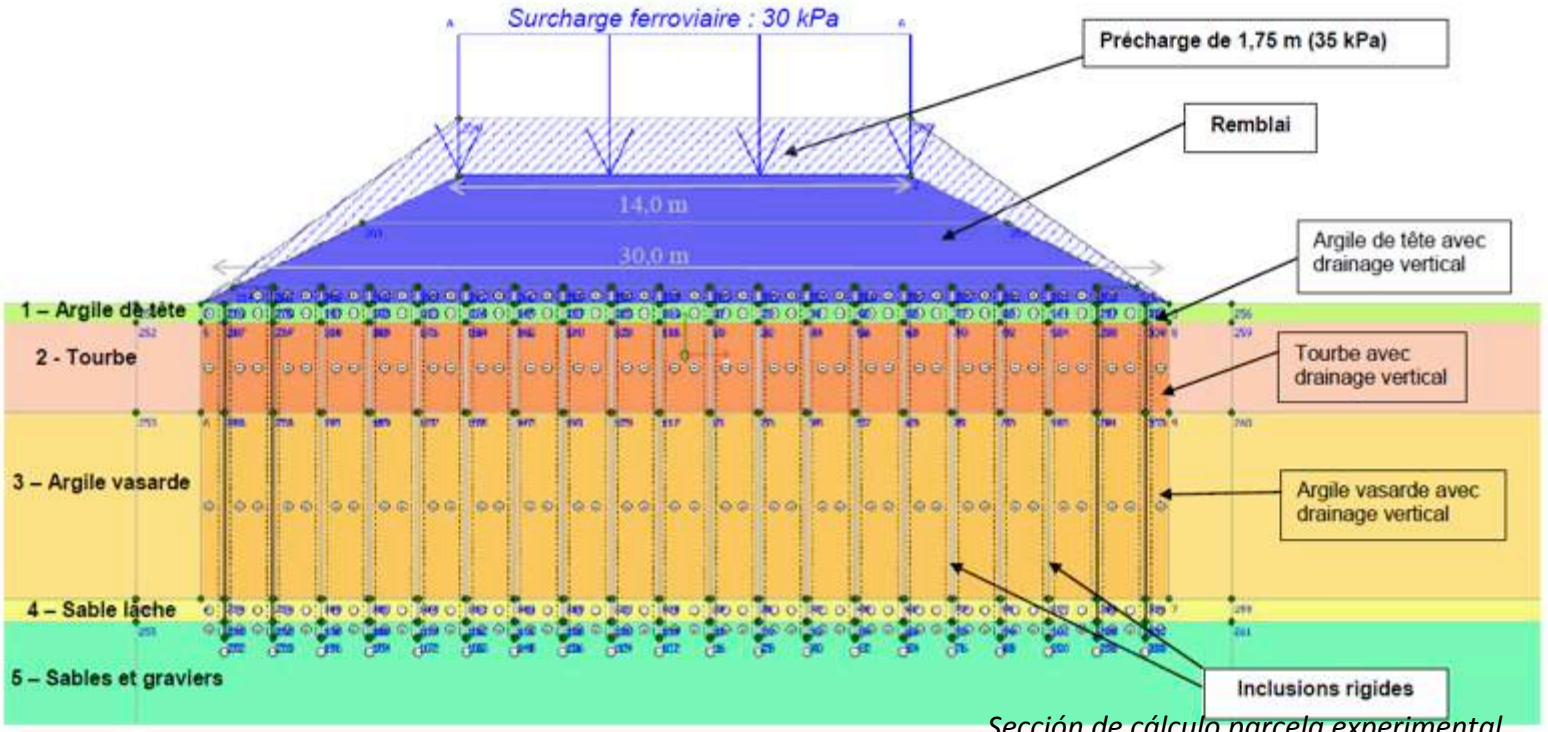

Sección de cálculo parcela experimental

- Soluções estudadas
  - Eliminação das turfas e substituição;
  - Drenagem vertical com pré-carga, inclusões rígidas e colunas de cimento e cal;
  - Drenagem vertical com pré-carga, inclusões rígidas e soil-mixing;

- Solução final:
  - Estacas pré-fabricadas de betão armado funcionando como inclusões rígidas associadas à drenagem vertical

PANTANO DE LA VIRVÉE. PRÉ-DIMENSIONAMENTO E ZONA EXPERIMENTAL

Fotografia aérea da zona experimental

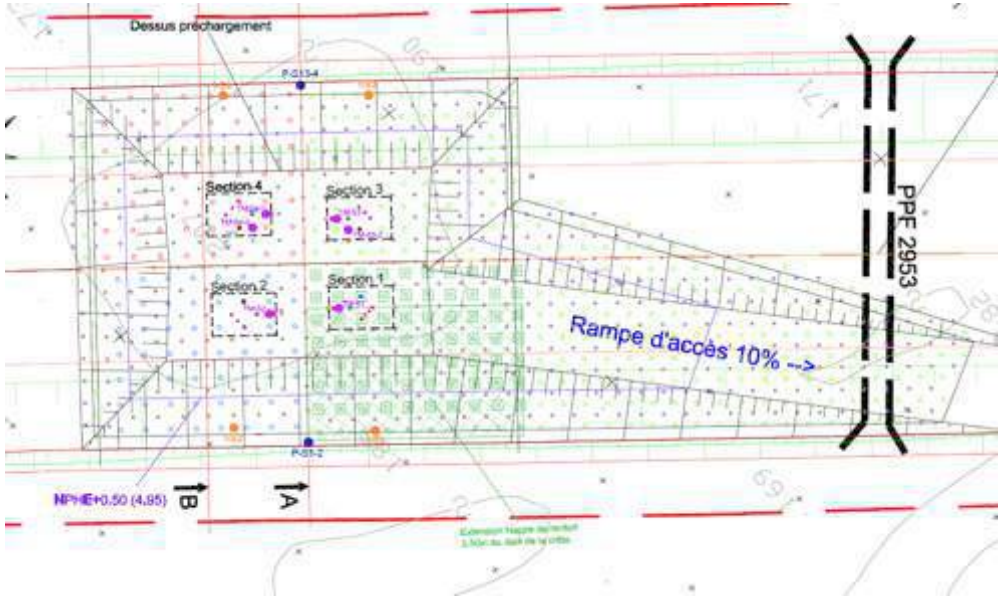

Planta geral da zona de ensaio

Sección	Malla	Elementos suplementarios de refuerzo
1	1,6 m × 1,6 m	Coronación con capiteles de 0,7 m × 0,7 m
2	1,7 m × 1,7 m	Refuerzo con dos geomallas
3	1,6 m × 1,6 m	Refuerzo con dos geomallas
4	1,8 m × 1,8 m	Refuerzo con dos geomallas

PANTANO DE LA VIRVÉE. PRÉ-DIMENSIONAMENTO E ZONA EXPERIMENTAL

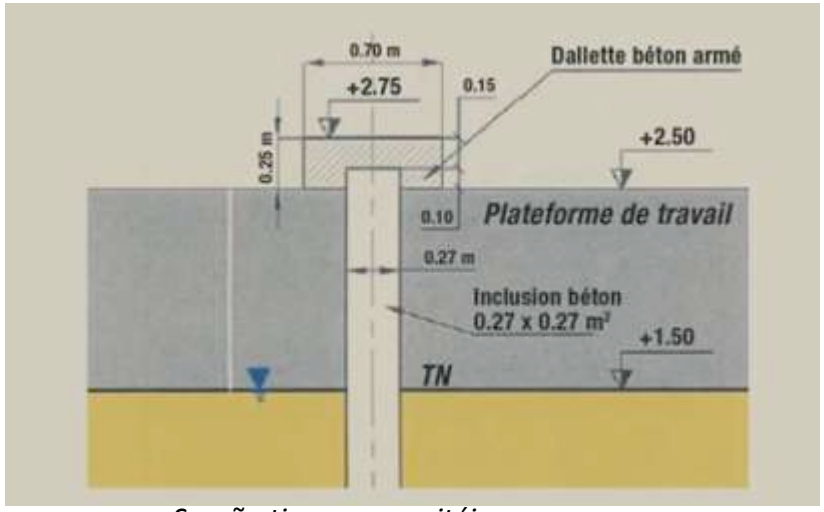

Secção tipo com capitéis

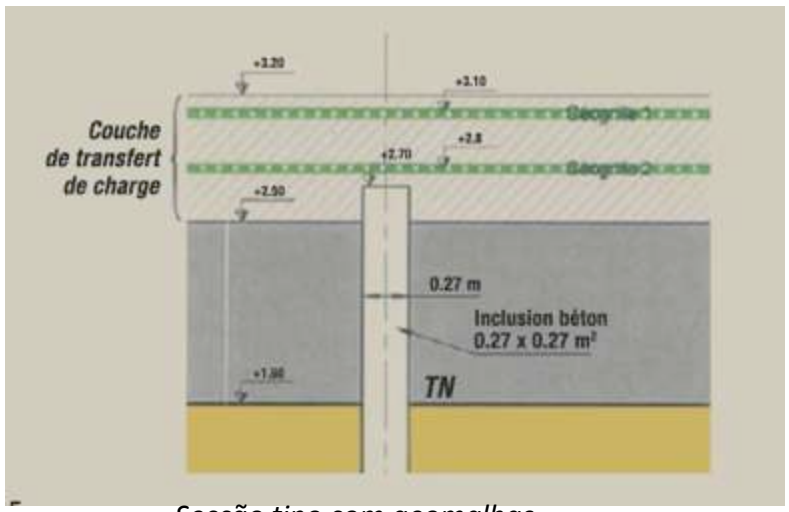

Secção tipo com geomalhas

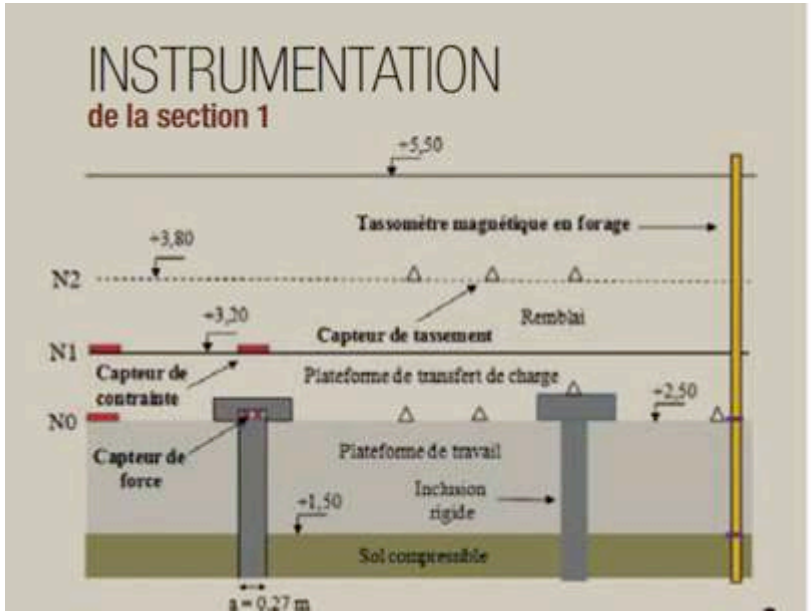

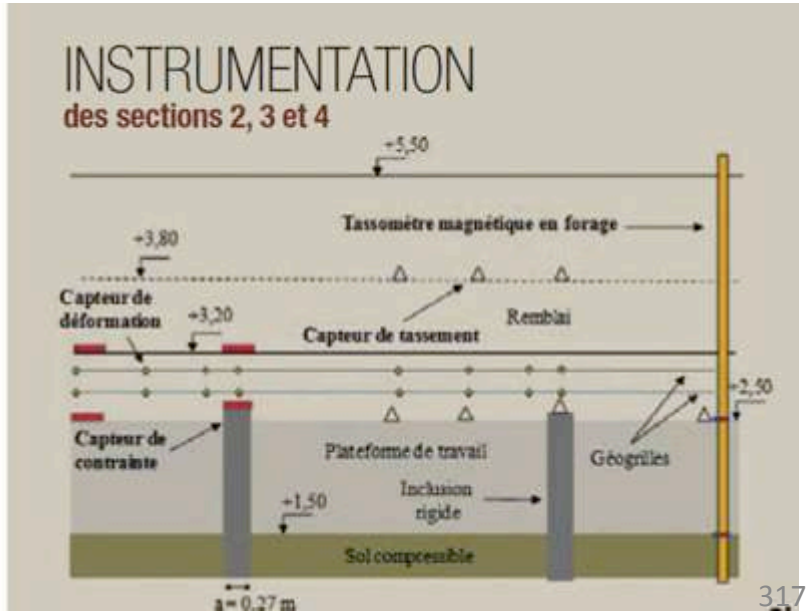

PANTANO DE LA VIRVÉE. PRÉ-DIMENSIONAMENTO E ZONA EXPERIMENTAL

Colocação de capitéis

Centrais de armazenamento de dados e pormenor das geomalhas

PANTANO DE LA VIRVÉE. PRÉ-DIMENSIONAMENTO E ZONA EXPERIMENTAL

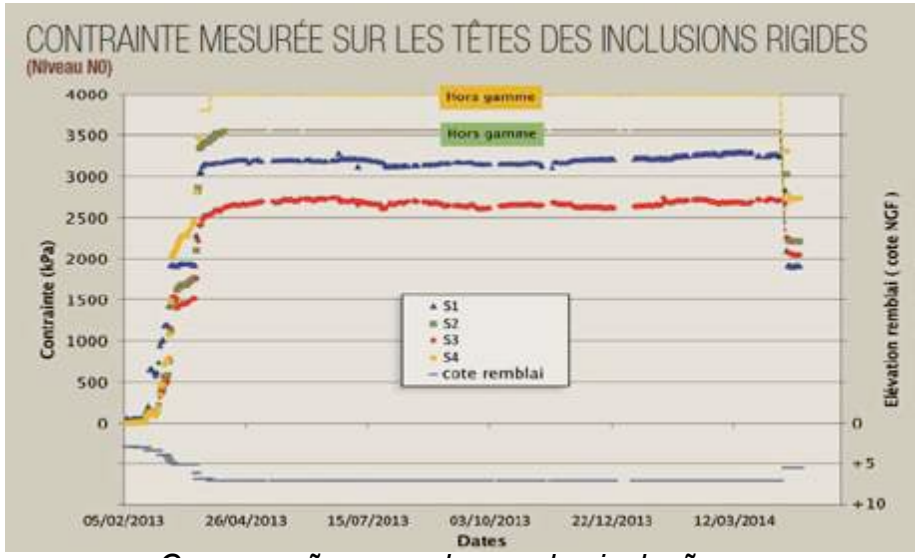

Compressões na cabeças das inclusões

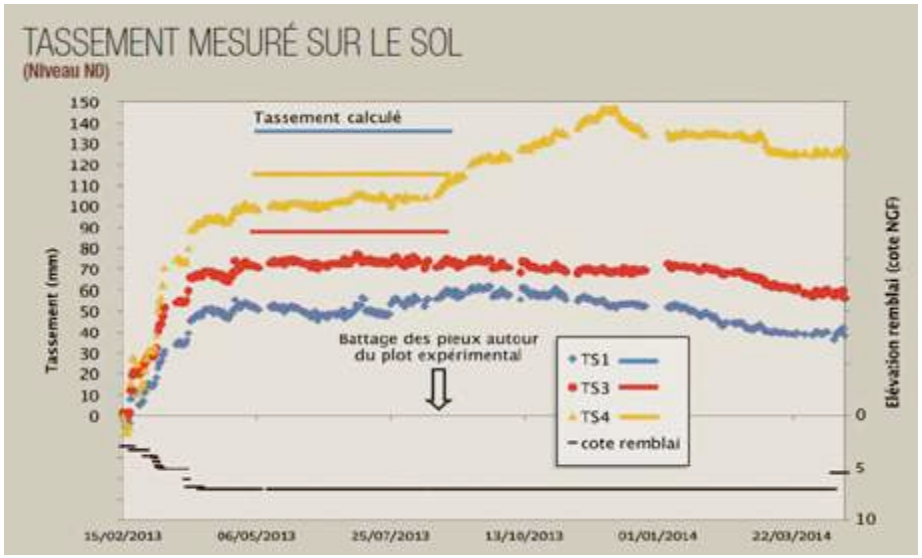

Assentamentos

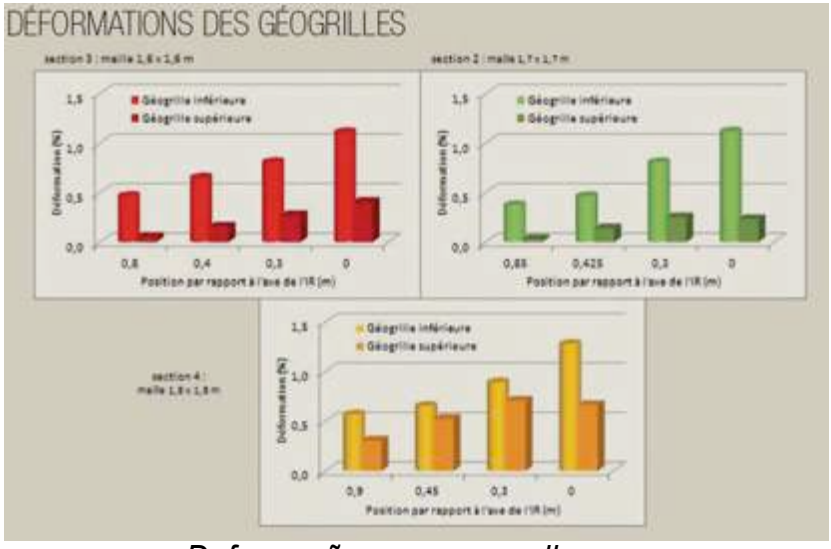

Deformações nas geomalhas

TABLEAU 1 : RÉSULTAT DU PRÉDIMENSIONNEMENT

	Plot avec dallettes	Plot avec géogrilles		Critères de dimensionnement
Maille (m x m)	1,6 x 1,6	1,6 x 1,6	1,8 x 1,8	-
Tassement en surface	13,6 cm*	8,8 cm*	11,2 cm*	< 10 cm **
Contrainte sur tête d'inclusion (Charge)	2,76 kPa (195 kN)	3,1 MPa (230 kN)	3,9 MPa (294 kN)	-
Contrainte moyenne sur le sol au niveau de la tête des inclusions	14,4 kPa	1 kPa	2 kPa	-
Contrainte maximale dans l'inclusion (Charge)	3,7 MPa (281 kN)	3,8 MPa (287 kN)	4,7 MPa (356 kN)	< 7,8 MPa (< 585 kN)
Sécurité vis-à-vis de la charge de fluage du sol Qc*** : Qc / Qmax	1,29	1,28	1,26	> 1,1
Sécurité vis-à-vis de la charge limite du sol Ql***: Ql / Qmax	1,85	1,83	1,8	> 1,4
Traction maximale dans les géogrilles (déformation)	-	146 kN/ml (1,1 %)	189 kN/ml (1,5 %)	< 284 kN/ml (< 2,2 %)

* calculé à partir du début des travaux de remblaiement, ** donné à partir de la mise en place de la couche de ballast, *** évaluée sous le plan neutre

PANTANO DE LA VIRVÉE. EXECUÇÃO DA OBRA

- Estaca CK-270 com 13 a 14 metros de comprimento total
- Características do betão:
  - Cimento CEM IV/B (P-V) 32,5 (ião NH4+ > 100 mg/l).
  - Classe de Resistência C45/55, determinada a partir das análises de cravação;
  - Resistência mínima > 25 MPa após a descofragem e transporte;
  - Consistência entre 140 y 210 mm;.
  - Rastreabilidade do processo de fabrico
  - Betão vibrado em moldes de cofragem

- Quantidades totais:
  - 8400 estacas
  - 115.920 ml

- Prespectiva orçamental:
  - 8.000.000 €

Malha de estacas do aterro experimental

Ensaio de carga estático executado com equipamento de cravação como estrutura de reacção

Verificação da cota final das estacas

Fotografia da obra em execução

CONCLUSÕES

- As estacas pré-fabricadas, funcionando como inclusões rígidas destinadas à fundação dos aterros sobre as zonas aluvionares, são uma solução que se adapta aos condicionamentos geotécnicos e estruturais da obra.
- A produção das estacas em fábrica permite a completa rastreabilidade do seu processo de fabrico e o cumprimento das elevadas exigências requeridas nos controles de qualidade.
- O uso da geomalha como elemento de reforço da plataforma de transferência de carga garante o bom comportamento do sistema.

OBRIGADO PELA VOSSA ATENÇÃO

Aterros sobre solos moles. Uma ou duas camadas de geogrelhas. Influência módulo de elasticidade da geogrelha. Casos de sucesso e insucesso

Jesús Ignacio Diego Pereda
Universidad de Navarra
Colaborador HUESKER

Organização
Sociedade Portuguesa de Geotecnia
Comissão Portuguesa de Geotecnia nos Transportes
Comissão Portuguesa de Geossintéticos
Apoios
LABORATÓRIO NACIONAL DE ENGENHARIA CIVIL
ORDEM DOS ENGENHEIROS

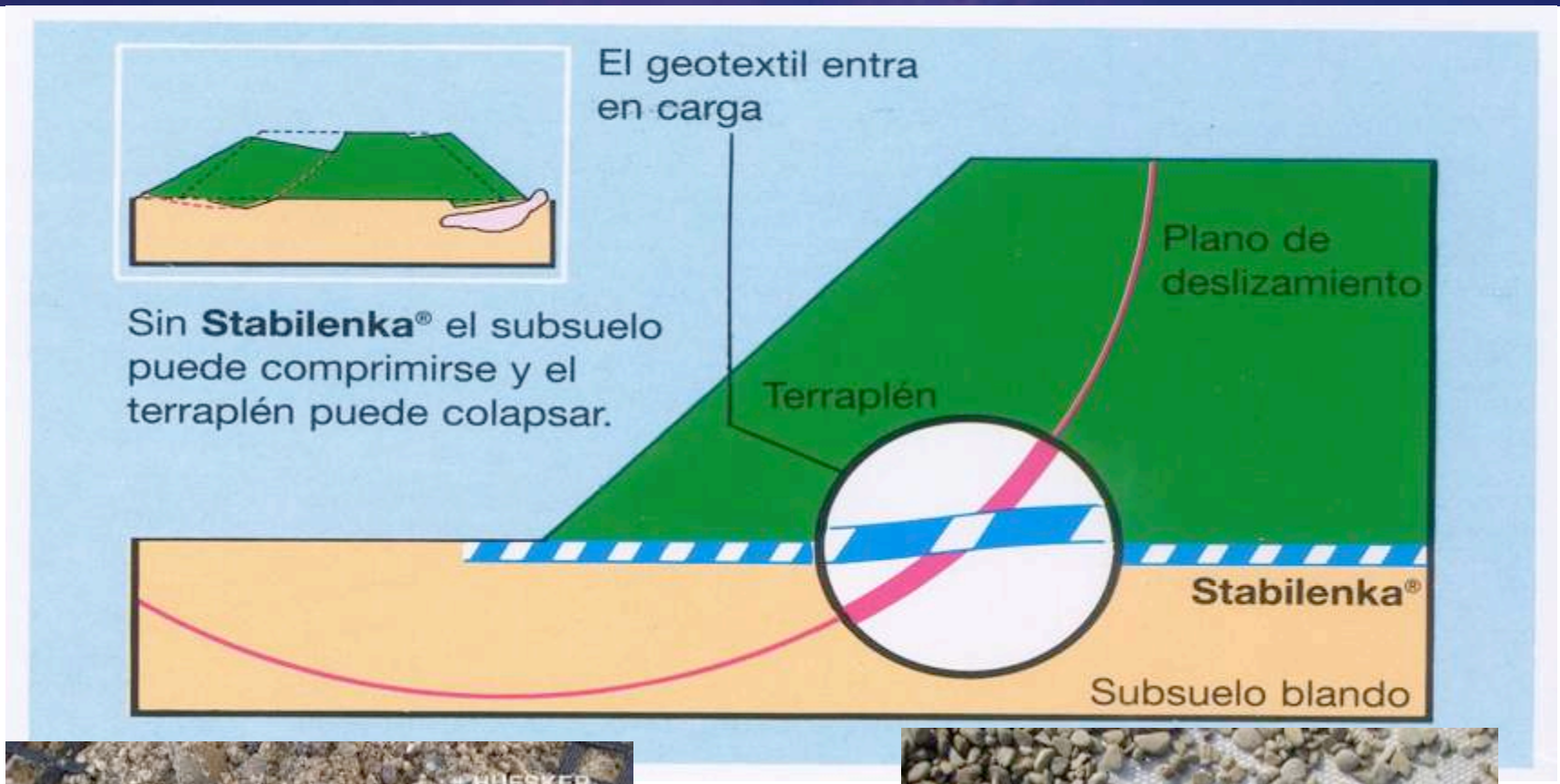
El geotextil entra en carga
Sin Stabilenka® el subsuelo puede comprimirse y el terraplén puede colapsar.
Plano de deslizamiento
Terraplén
Stabilenka®
Subsuelo blando


HUESKER

El diseño de los geosintéticos de refuerzo bajo terraplenes no sólo son útiles para aumentar la estabilidad del terraplén durante la construcción, Corto Plazo, y hasta el final del proceso de Consolidación, y que la durabilidad del mismo es menos importante. En situaciones a Largo Plazo también aumentan el Factor de Seguridad, y existen datos de grandes tensiones en geosinteticos bajo terraplenes después de **14 años**

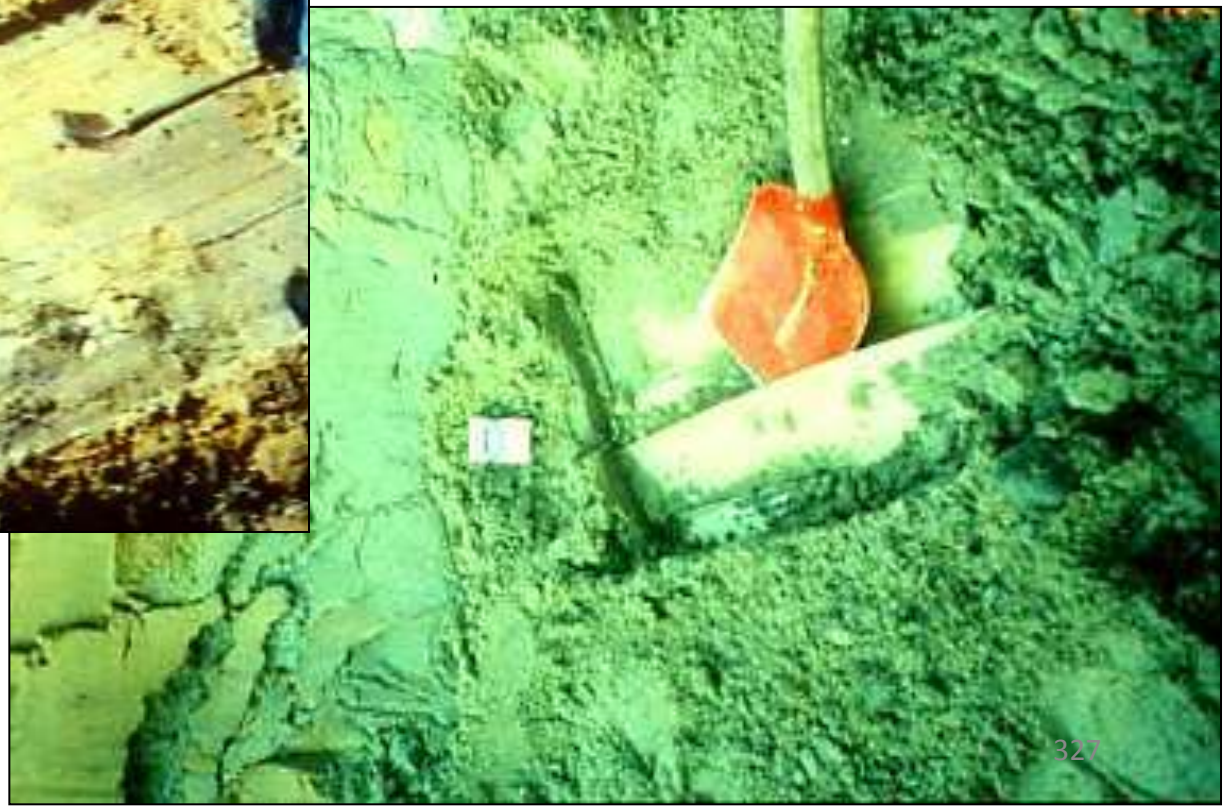

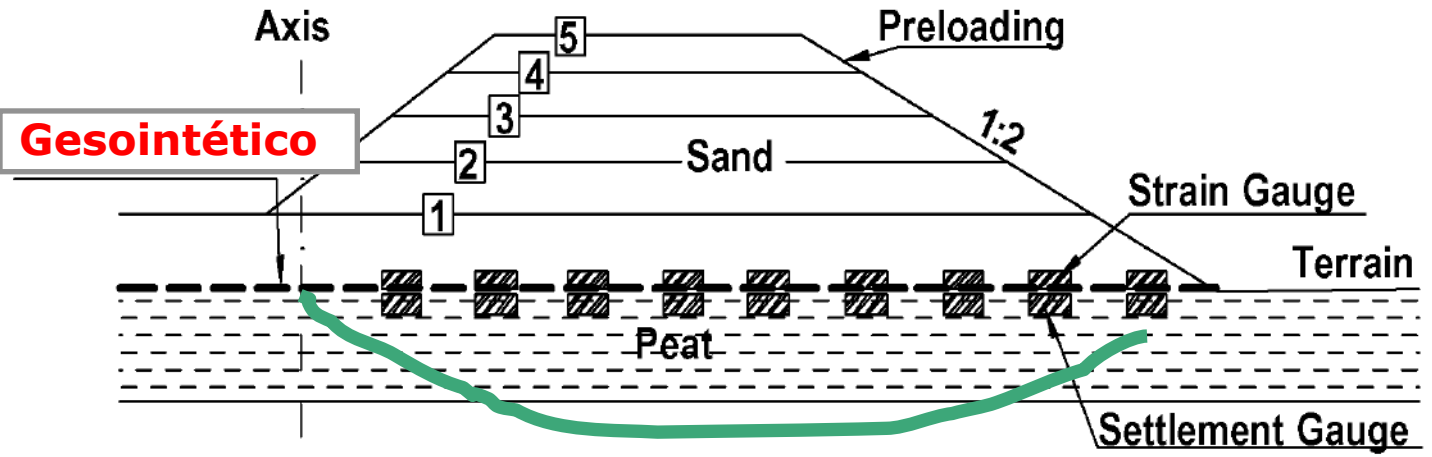

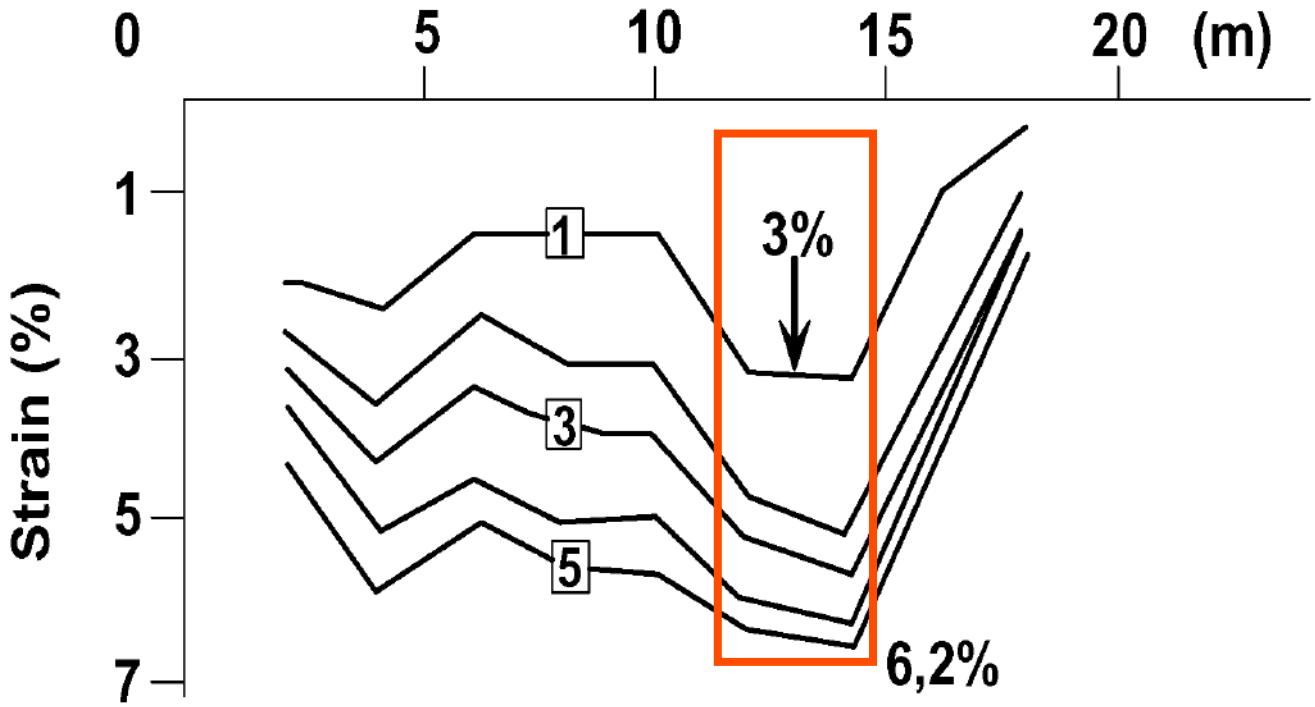

En los diseños usualmente se supone que el suelo blando es homogéneo, al menos, en la dirección transversal del terraplén. A menudo ese no el caso, siendo recomendable realizar este cálculo desde un punto de vista conservador

Dos metodos se usan habitualmente para analizar los terraplenes sobre suelos blandos

- Métodos de Equilibrio límite (Bishop, Janbu, Morgenstern-Price, etc) Estos consideran que la forma de rotura asumen un determinada geometría, plana, circular, etc, determinando el Factor de Seguridad con la forma de rotura que arroje el valor mínimo. (LEM) (ELU)

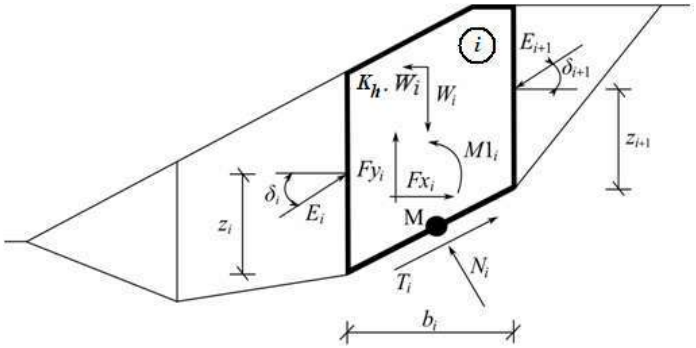

- Métodos de Elementos Finitos (FEM). Son métodos numéricos con el que obtenemos soluciones para las distintas condiciones de equilibrio, compatibilidad, comportamiento estructural y condiciones de contorno, tanto fuerzas como desplazamientos. Este programa genera una malla consistente en elemento finitos conectados entre sí por nodos. Cada uno de estos elementos de discretización se denomina elemento finitos. No se presupone a priori ninguna forma de rotura.(ELU y ELS)

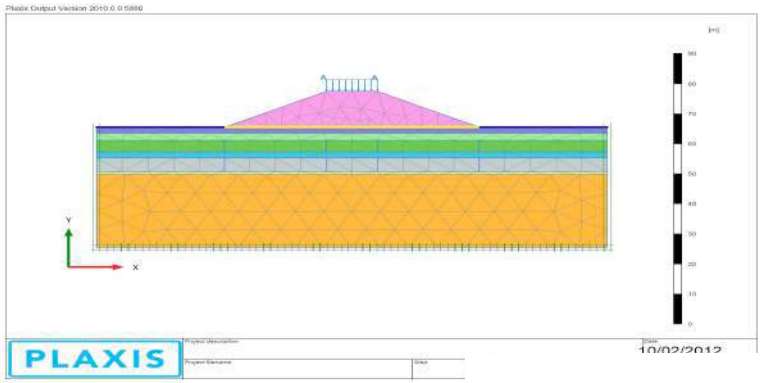

- Los cálculos de estbilidad , Estados límites Últimos, no están directamente acoplados con los cálculos de las deformaciones , Estados Límites de Servicio (LEM).

- Algunas normas basadas en la investigación y la experiencia recomiendan que para la tensión de diseño la deformación total correspondiente debería estar en el rango entre el 3 al 6%. La deformación total incluye la deformación inicial y la debida a la fluencia. Se recomienda limitar la deformación por fluencia a un máximo del 1% y en algunos casos de terraplenes especiales y/o para neutralizar posibles asientos por consolidación secundaría en los suelos blandos al 0.5%

Las deformaciones típicas en un suelo no cohesivo compactado para conseguir la mobilización del angulo de rozamiento pico estan entre **3 al 5%.** Para mayores deformaciones se debe considerar el angulo de rozamiento residual, y para deformaciones inferior el ángulo de rozamiento "pre-pico". Ambos ángulos de rozamiento son inferiores al pico. Estos es importante por que el geosintético va a trabajar mejor cuanto mayor sea el ángulo de rozamiento del suelo con el que ésta en contacto

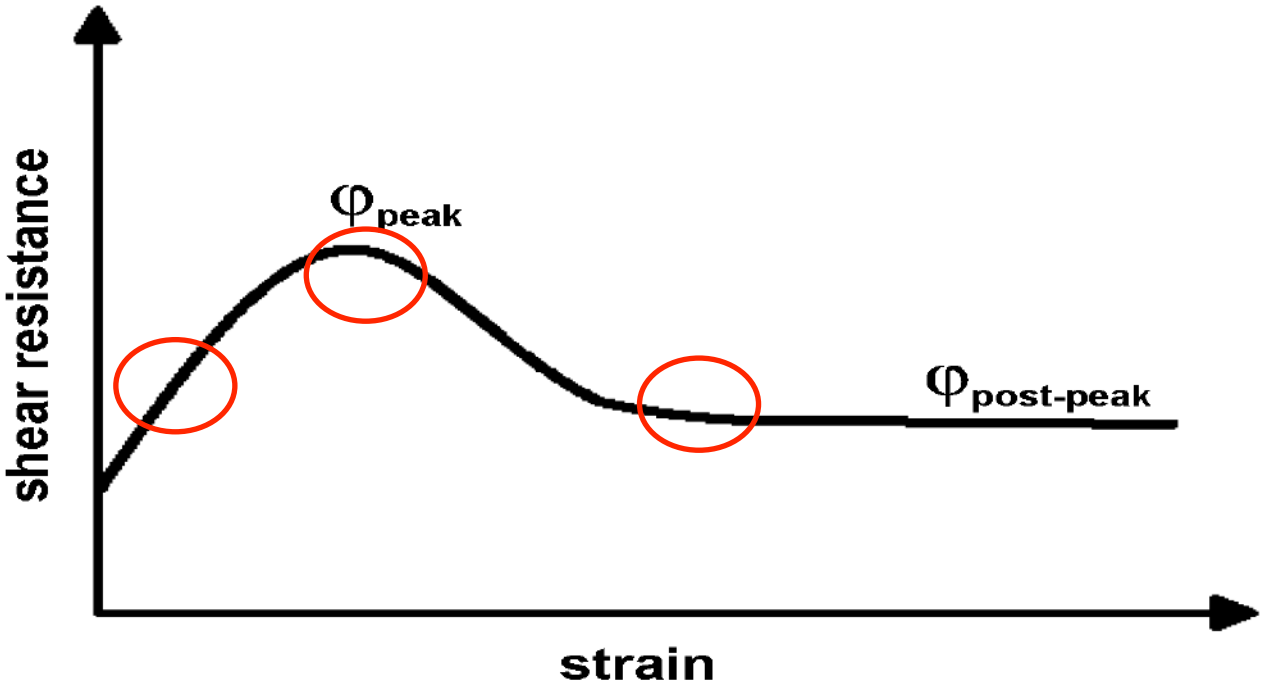

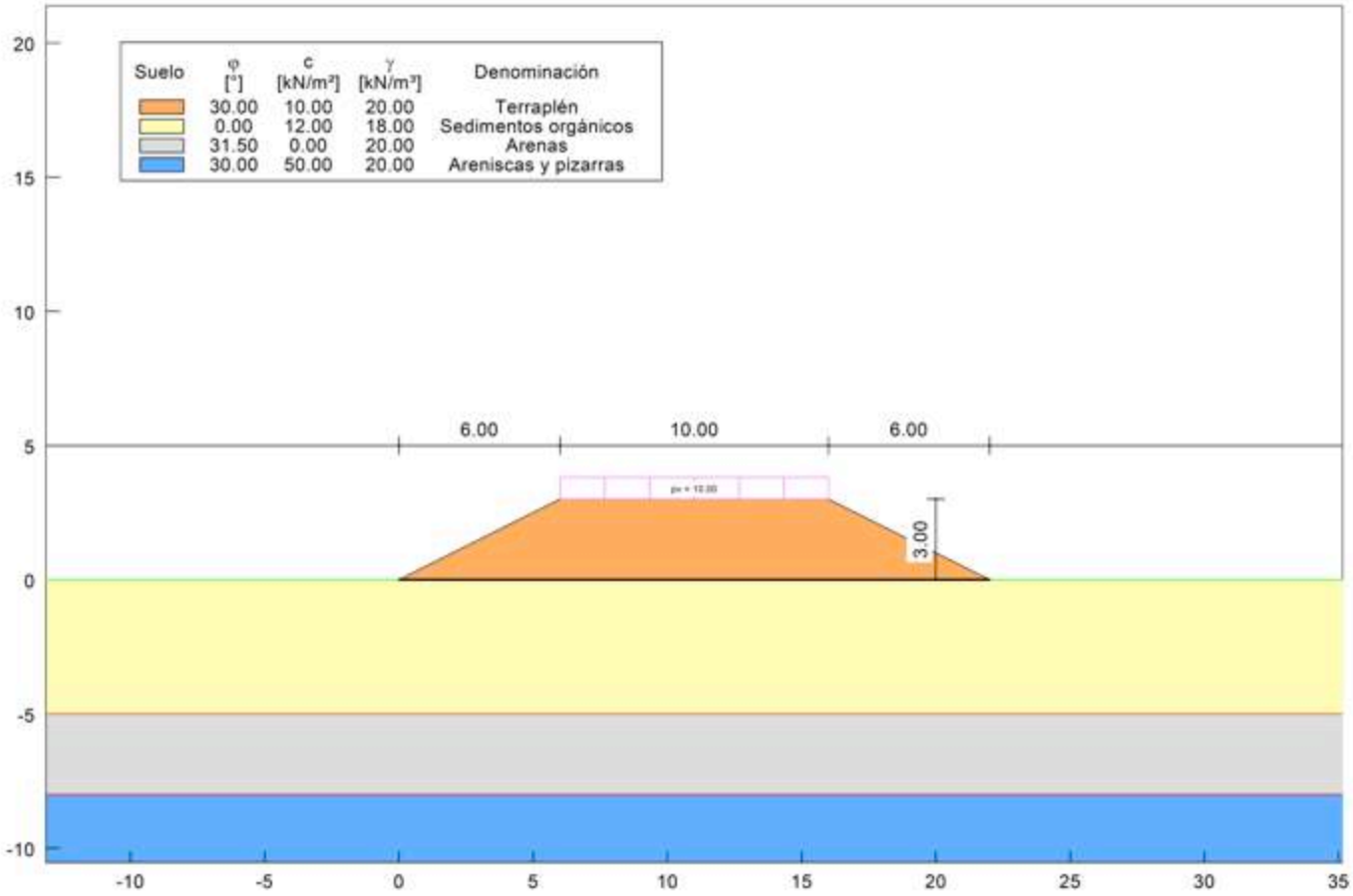

Ejemplo de terraplén sobre suelo blando. H= 3 m Taludes 2(H): 1(V) y 10 m de anchura en superficie con una sobrecarga de 10 kN/m2

Dos tipos materia prima usada en los geosintéticos de refuerzo.

- PET, Poliéster Deformación nominal 10-12 % Resistencia química 4<pH<9
- PVA. Polivinil Alcohol Deformación nominal 5-6% Resistencia química 2<pH<13

Case History: An experimental highway embankment (Matichard et al. 1994)

A highway by-pass in France involved the construction of a 5.8 m high experimental embankment on a peat bog over a period of 20 days. The foundation consisted of a 1.5 - 3 m peat layer overlaying a 1 - 2 m thick clay layer and 1 – 1.8 m clayey gravel layer underlain by bedrock. The water content ranged between 150% and 319% for the peat, and between 44% and 86% for the clay which had an undrained shear strength 40 - 60 kPa. Two layers of geotextile reinforcement with T_{ult} greater than 120 kN/m were used to prevent a rotational failure that

and this increased to 82 mm after 100 days. The maximum strain in the upper geotextile was 0.7% at the end of construction and 0.8% after 100 days; the maximum strain in the lower geotextile was 1.3% at the end of construction and 1.7% after 100 days.

Key findings:

There was a significant (factor of two) difference in strain between the upper and lower reinforcement layer.

Análisis mediante Método de Equilibrio Límite (Bishop). Sólo se considera la tensión del geosintético, ni la materia prima, ni la deformación.

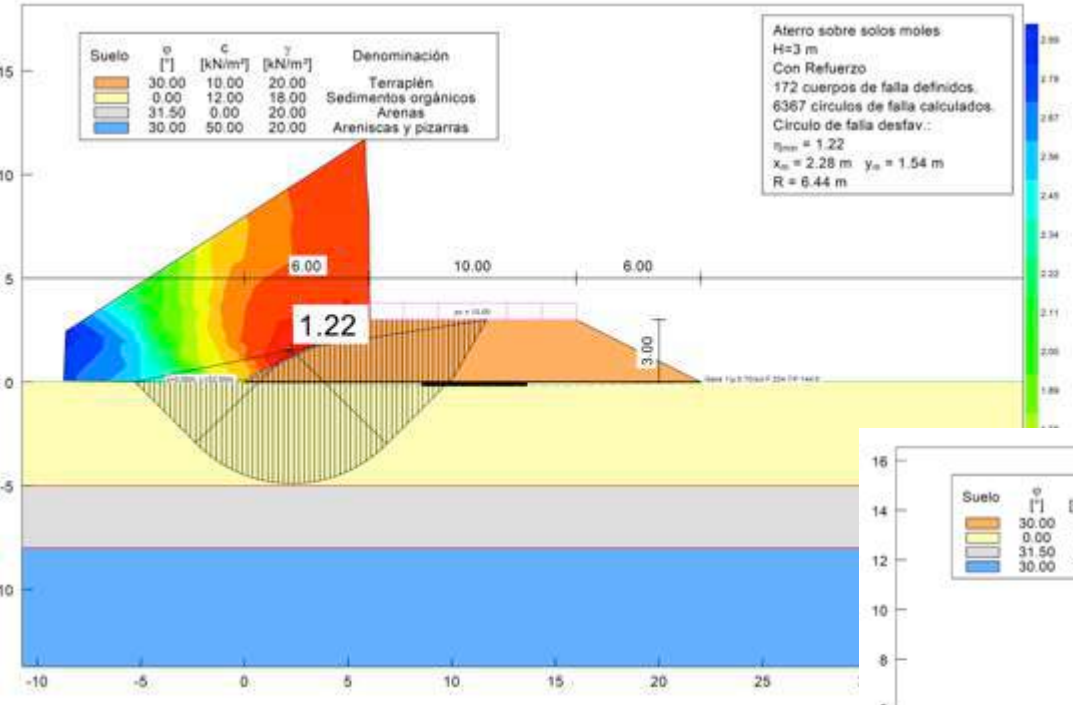

- Un geosintético de refuerzo con una tensión de diseño de 234,7 kN/m

- Dos geosintéticos de refuerzo con una separación entre ellos de 0,5 m con una tensión de diseño de 111,5 kN/m cada uno de ellos

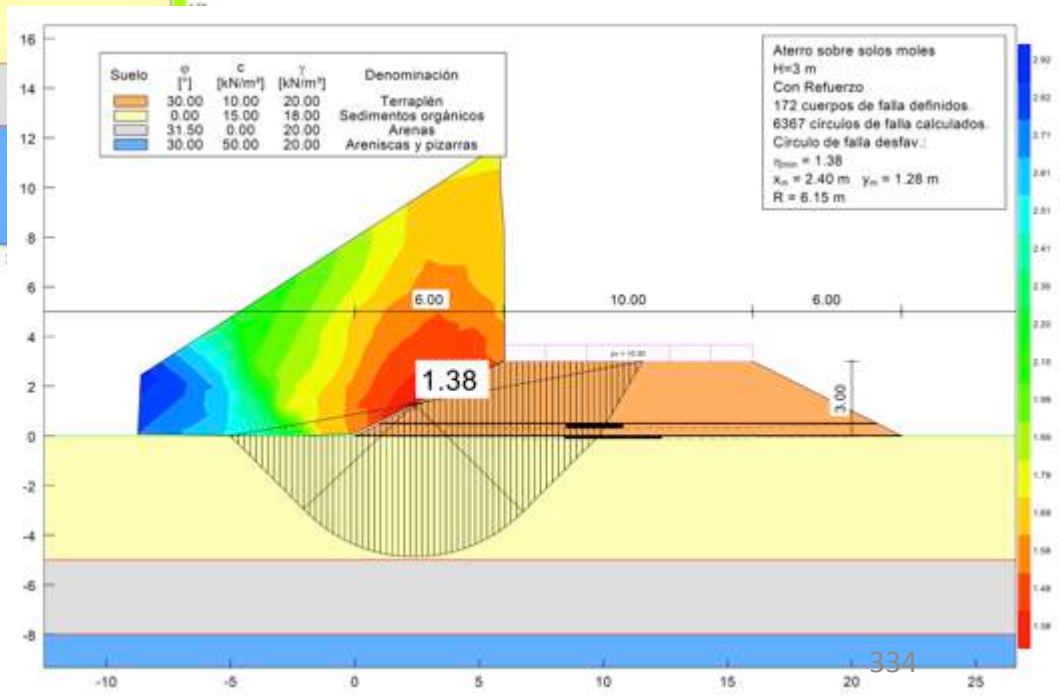

Análisis mediante Métdo de Elementos Finitos. Se considera la tensión del geosintético, la materia prima y la deformación, ya que estos dós ultimos determinan el Módulo de Elasticidad.

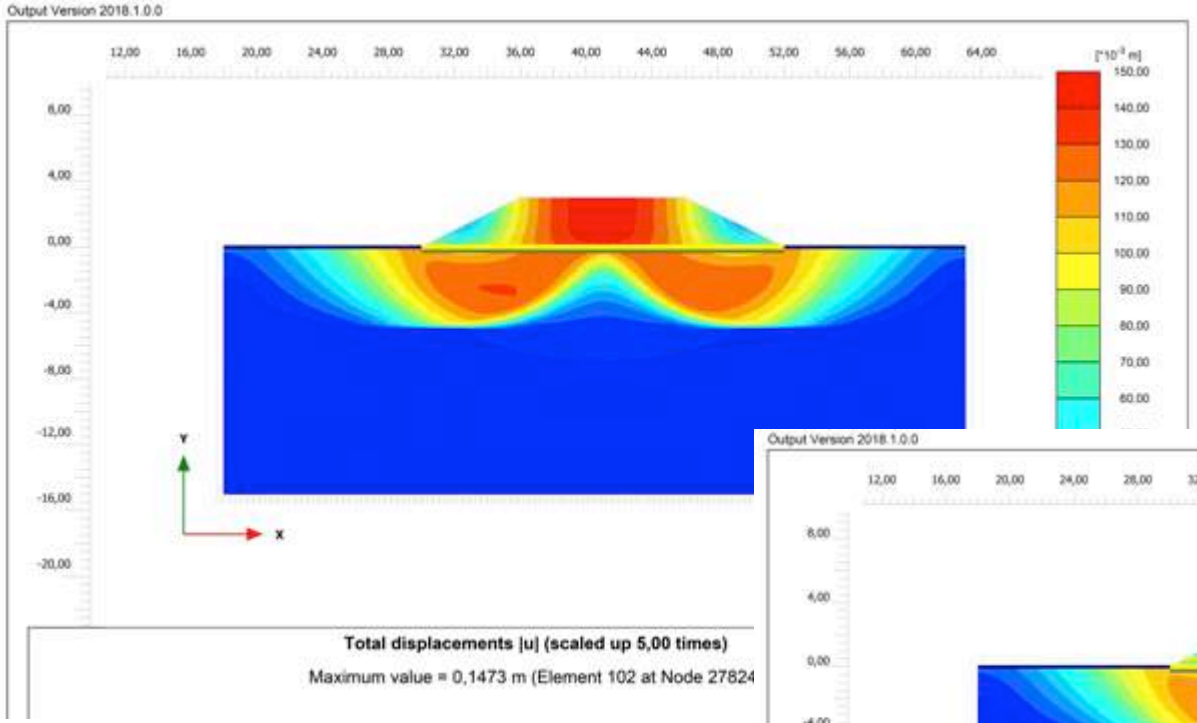

- Un geosintético de refuerzo de PET .Tensión de diseño de 234,7 kN/m y J=3400 kN/m

- Dos geosintéticos de refuerzo de PET con una separación entre ellos de 0,5 m. Tensión de diseño de 111,5 kN/m J=1700 kN/m cada uno de ellos.

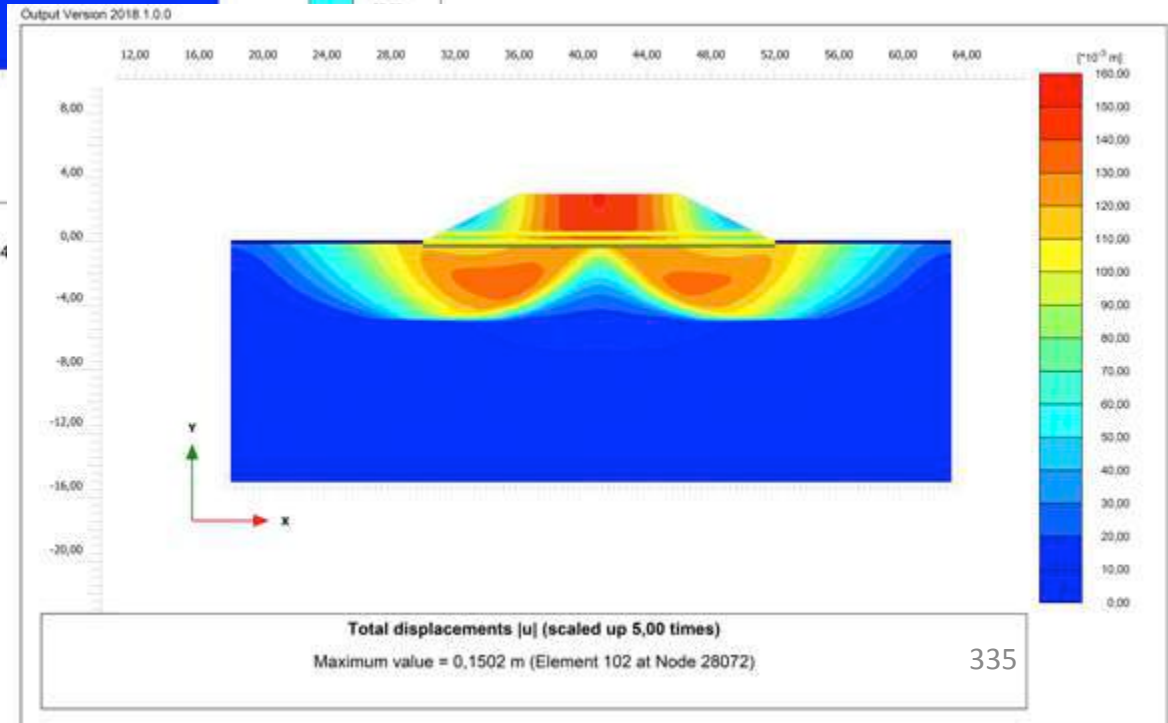

Análisis mediante Métdo de Elementos Finitos. Se considera la tensión del geosintético, la materia prima y la deformación, ya que estos dós ultimos determinan el Módulo de Elasticidad.

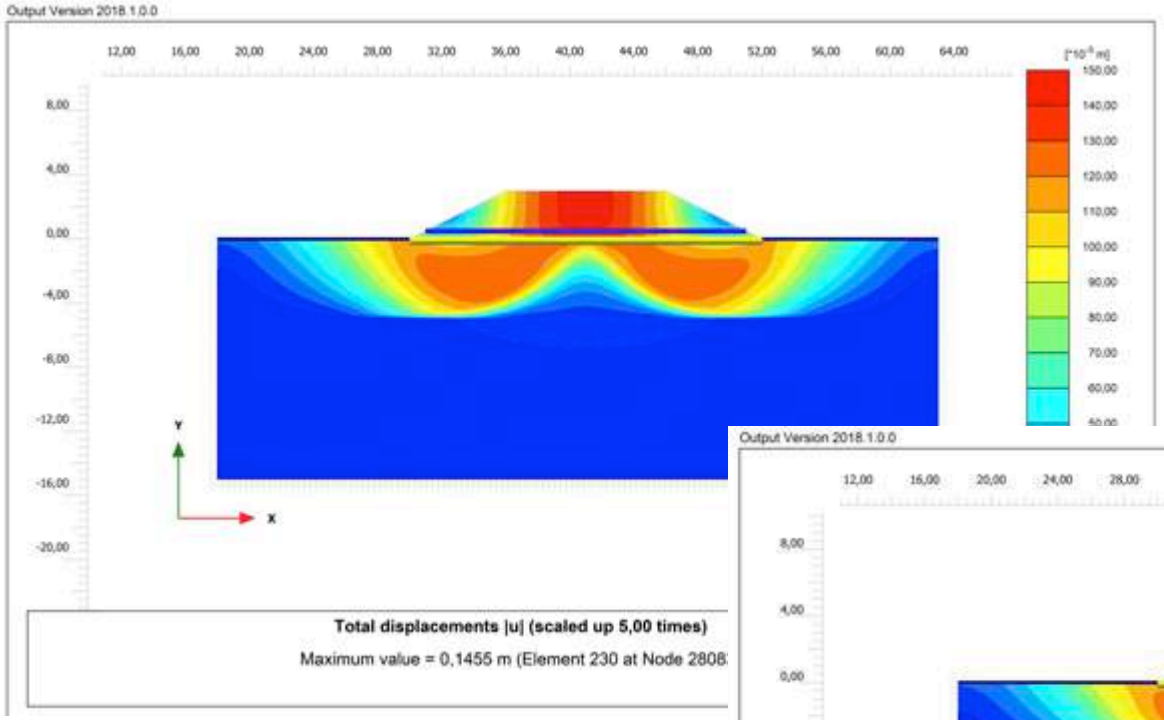

- Dos geosintético de refuerzo PET bajo el terraplén y a 0,5 m dentro del terraplén PVA .Tensión de diseño de 111,5 kN/m para ambos y J=1700 kN/m para PET y J=3400 kN/m para PVA

- Un geosintético de refuerzo de PVA. Tensión de diseño de 234,7 kN/m J=6800 kN/m

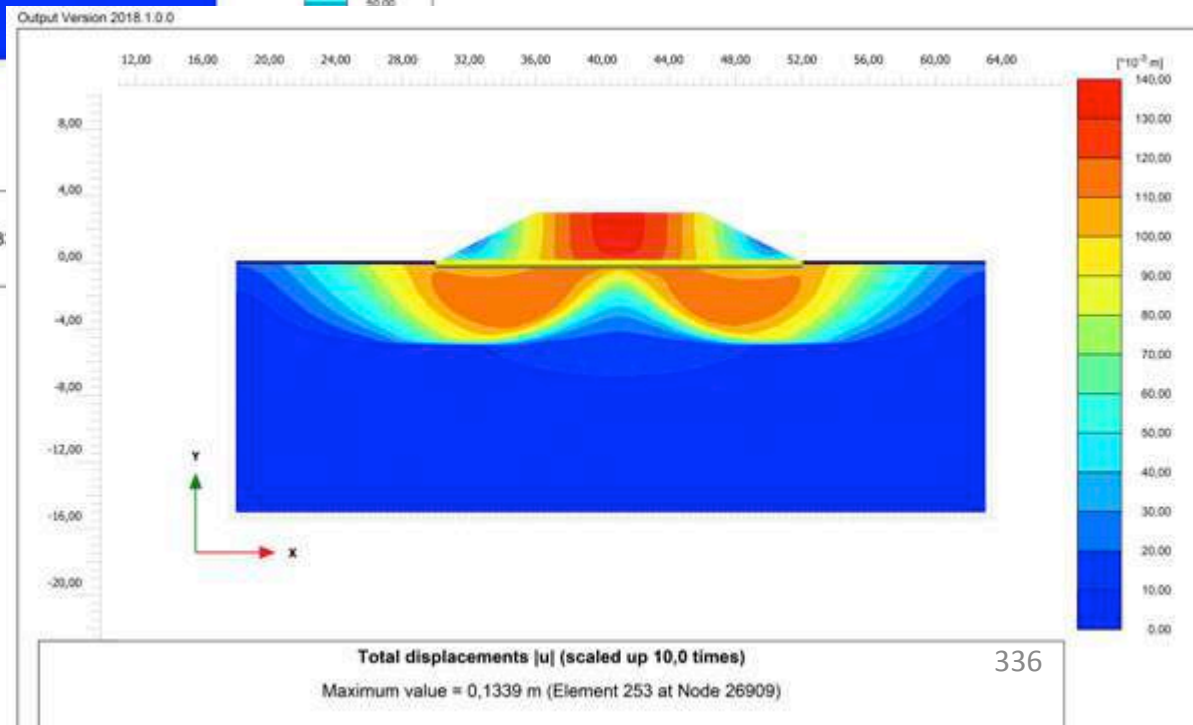

		UTS (kN/m)	J (kN/m)	Geogrid Tensile Strength from FEM Analysis (kN/m)	Settlement (m)	FS from FEM Analysis	FS from LEM Analysis
One PET Geogrid		234.7	3400	174.2	0.147	1.22	1.22
Two PET Geogrids		111.5	1700	Bottom 111.5 Top 78.54	0.15	1.21	1.38
Two Geogrids	Bottom PET	111.5	1700	92.66	0.145	1.21	1.38
	Top PVA	111.5	3400	111.5			
One PVA Geogrid		234.7	6800	178.7	0.133	1.22	1.22

- Conclusiones

- Factor de Seguridad para un único geosintético, de PVA o PET, para ambos métodos es el mismo 1.22.

- Existe una diferencia importante para el FS entre FEM y LEM en el caso de disponer dos geosintéticos. De esta manera el FS para LEM es de 1.38 y para FEM 1.21, tanto si se dispone dos geosintéticos de PET como si se dispone PET + PVA. La explicación a lo anterior radica en el hecho de que en los análisis con LEM hay que proporcionarles la tensión del geosintético, en cambio en los análisis con FEM la tensión que se desarrolla en el geosintético depende del módulo de elasticidad de éste y de la deformación del suelo a su alrededor.

		UTS (kN/m)	J (kN/m)	Geogrid Tensile Strength from FEM Analysis (kN/m)	Settlement (m)	FS from FEM Analysis	FS from LEM Analysis
One PET Geogrid		234.7	3400	174.2	0.147	1.22	1.22
Two PET Geogrids		111.5	1700	Bottom 111.5 Top 78.54	0.15	1.21	1.38
Two Geogrids	Bottom PET	111.5	1700	92.66	0.145	1.21	1.38
	Top PVA	111.5	3400	111.5			
One PVA Geogrid		234.7	6800	178.7	0.133	1.22	1.22

- Existe una diferencia importante en las tensiones de los geosintéticos de PET, ≈30%, que se obtienen en los análisis FEM cuando se disponen dos capas. De esta manera el geosintético inferior presenta una tensión de 111.5 kN/m y la superior de 78.54 kN/m. Esto se debe a la diferencia de módulos elásticos de los suelos con los que los geosintéticos están en contacto. En el caso del geosintético inferior está en contacto con un suelo blando, que permite una mayor deformación y como consecuencia una mayor tensión. Para el caso del geosintético dentro del terraplén, al tener este material un mayor módulo elástico, no le permite deformarse y por tanto alcanzar una mayor tensión. Parece claro que es totalmente recomendable disponer una sola capa de geosintético situada en la parte inferior en lugar de dos capas separadas. .
- En el caso de disponer un geomalla de PET en el fondo y una de PVA dentro del terraplén, al tener el PVA mayor módulo elástico, hace que está ultima tenga mayor tensión, 111.5 kN/m en PVA frente a 92.66 kN/m en PET.

		UTS (kN/m)	J (kN/m)	Geogrid Tensile Strength from FEM Analysis (kN/m)	Settlement (m)	FS from FEM Analysis	FS from LEM Analysis
One PET Geogrid		234.7	3400	174.2	0.147	1.22	1.22
Two PET Geogrids		111.5	1700	Bottom 111.5 Top 78.54	0.15	1.21	1.38
Two Geogrids	Bottom PET	111.5	1700	92.66	0.145	1.21	1.38
	Top PVA	111.5	3400	111.5			
One PVA Geogrid		234.7	6800	178.7	0.133	1.22	1.22

- Si se aumenta el módulo de elasticidad de las geomallas, usando PVA en lugar de PET, los asientos en los terraplenes disminuyen. En el caso de terraplenes de poca altura y donde los asientos sean un elemento limitante se recomienda el uso de materias primas con elevados módulos elásticos como el PVA.
- Hay que tener cuidado en los métodos LEM cuando se utilicen elementos de diferentes rigideces

- Autobahn A26 Hamburg-Stade: Dos capas de geosintético de refuerzo, como hemos visto no es la mejor solución, incluso es una solución bastante arriesgada

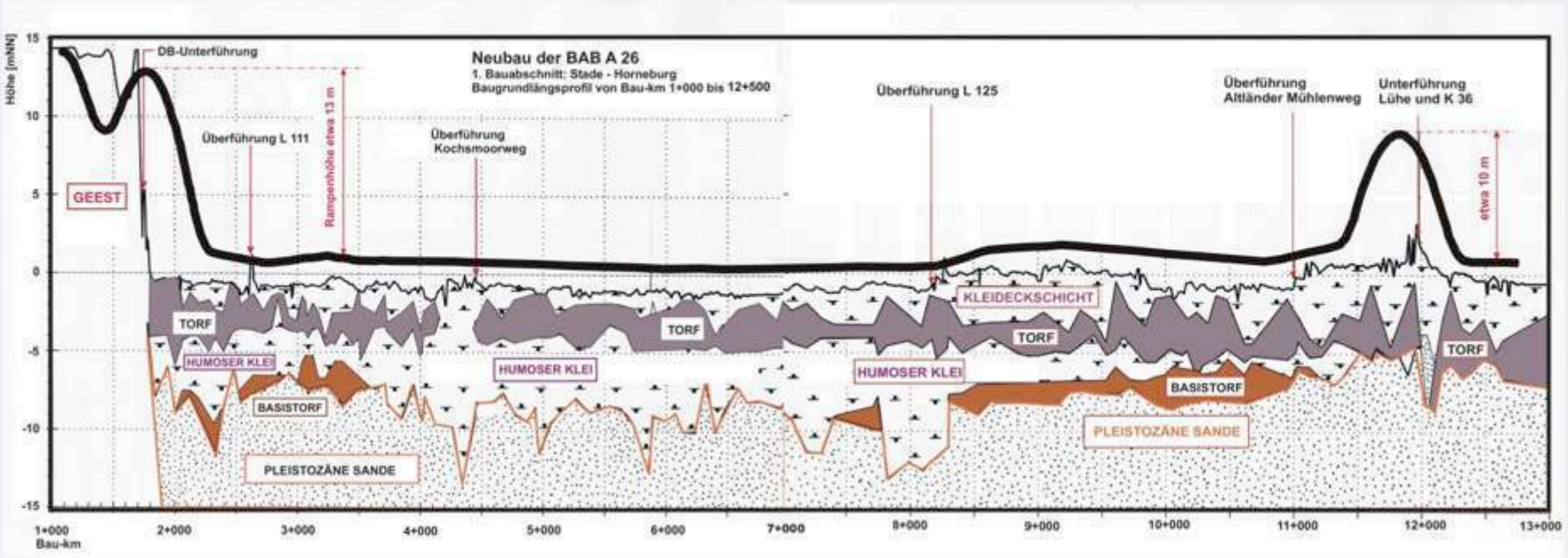
Neubau der BAB A 26
1. Bauabschnitt: Stade - Horneburg
Baugrundlängsprofil von Bau-km 1+000 bis 12+500
Höhe [mNN]
15
10
5
0
-5
-10
-15
DB-Unterführung
Überführung L 111
Rampenhöhe etwa 13 m
Überführung Kochsmoorweg
Überführung L 125
Überführung Altländer Mühlenweg
Unterführung Lühe und K 36
etwa 10 m
GEEST
TORF
HUMOSER KLEI
BASISTORF
PLEISTOZÄNE SANDE
TORF
HUMOSER KLEI
KLEIDECKSCHICHT
TORF
HUMOSER KLEI
BASISTORF
PLEISTOZÄNE SANDE
TORF
1+000
Bau-km
2+000
3+000
4+000
5+000
6+000
7+000
8+000
9+000
10+000
11+000
12+000
13+000

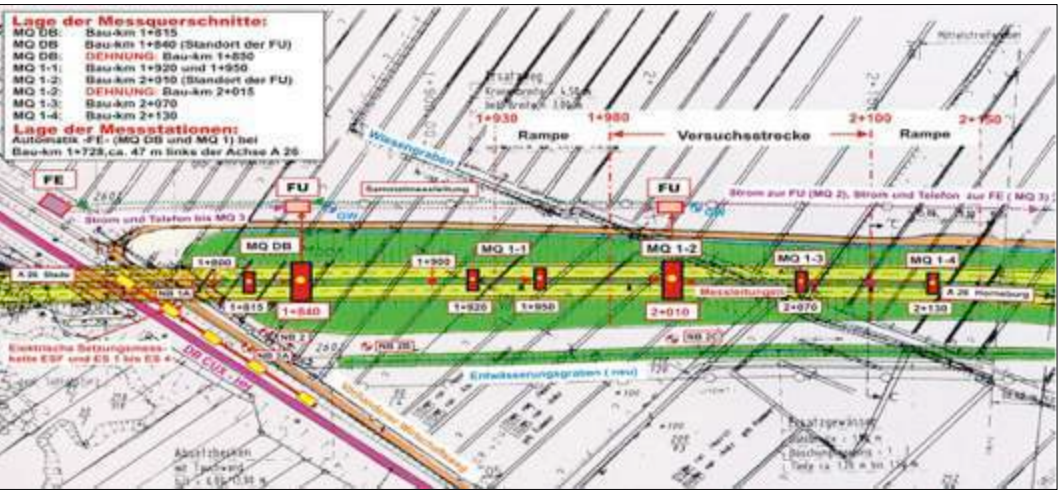
Lage der Messquerschnitte:
MQ DB: Bau-km 1+815
MQ DB: Bau-km 1+840 (Standort der FU)
MQ DB: DEHNUNG: Bau-km 1+830
MQ 1-1: Bau-km 1+920 und 1+950
MQ 1-2: Bau-km 2+010 (Standort der FU)
MQ 1-2: DEHNUNG: Bau-km 2+015
MQ 1-3: Bau-km 2+070
MQ 1-4: Bau-km 2+130
Lage der Messstationen:
Automatik -FE- (MQ DB und MQ 1) bei Bau-km 1+728,ca. 47 m links der Achse A 26
Rampe
Versuchsstrecke
Rampe
FE
FU
FU
MQ DB
MQ 1-1
MQ 1-2
MQ 1-3
MQ 1-4


Dehnungsmessgerät
mit 30 mm Messweg

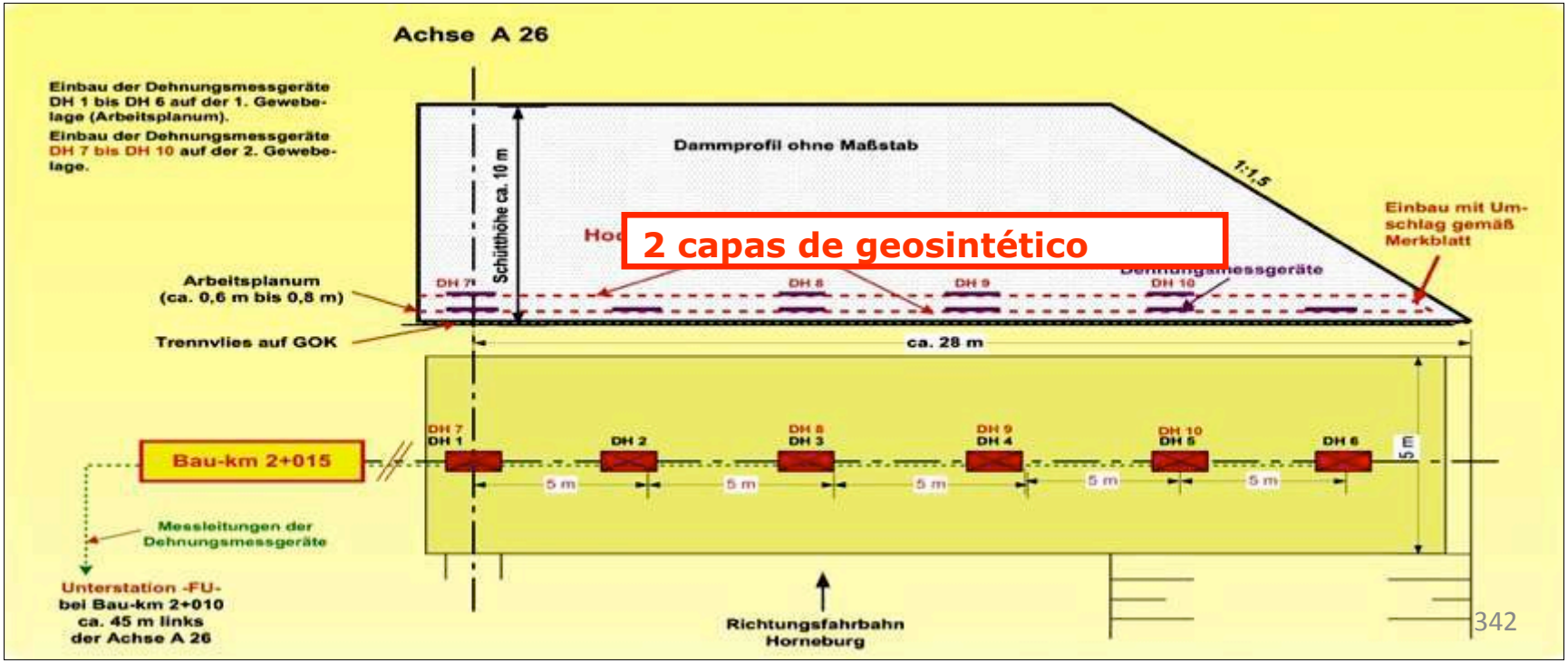
Achse A 26
Einbau der Dehnungsmessgeräte DH 1 bis DH 6 auf der 1. Gewebe-lage (Arbeitsplanum).
Einbau der Dehnungsmessgeräte DH 7 bis DH 10 auf der 2. Gewebe-lage.
Dammprofil ohne Maßstab
Schütthöhe ca. 10 m
1:1,5
2 capas de geosintético
Einbau mit Um-schlag gemäß Merkblatt
Arbeitsplanum (ca. 0,6 m bis 0,8 m)
Trennvlies auf GOK
DH 8
DH 9
DH 10
ca. 28 m
Bau-km 2+015
DH 7
DH 1
DH 2
DH 8
DH 3
DH 9
DH 4
DH 10
DH 5
DH 6
5 m
Messleitungen der Dehnungsmessgeräte
Unterstation -FU- bei Bau-km 2+010 ca. 45 m links der Achse A 26
Richtungsfahrbahn Horneburg

Doble capa geosintético separada 0.5 m

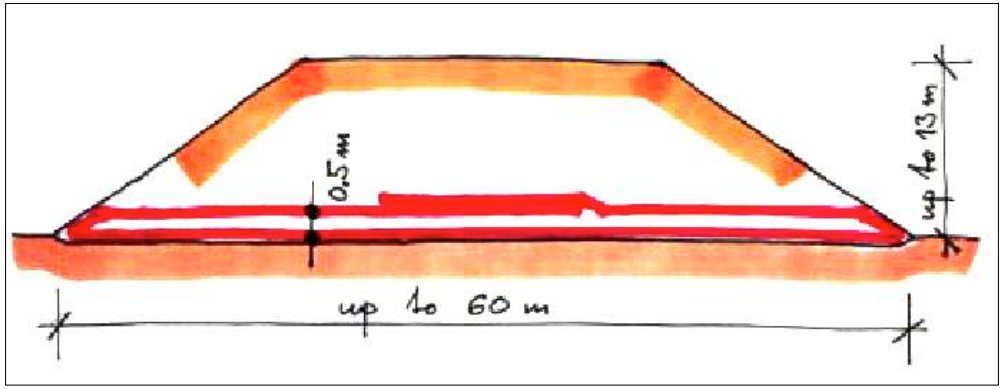

Doble capa geosintético separada 0.5 m

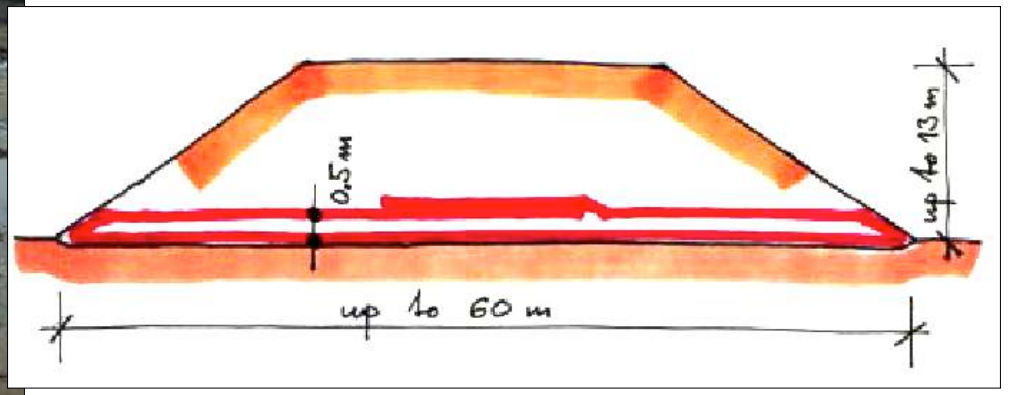

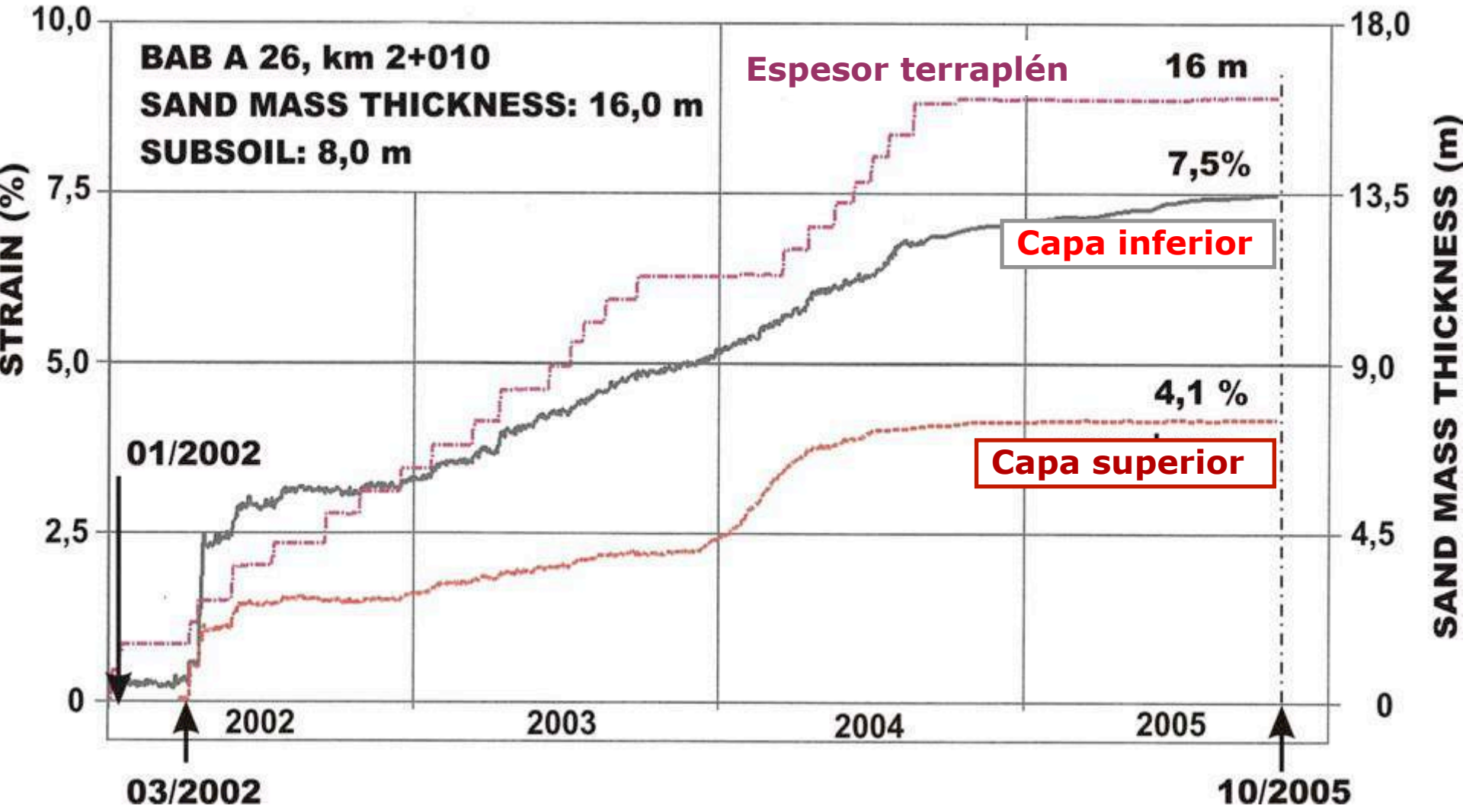
BAB A 26, km 2+010
SAND MASS THICKNESS: 16,0 m
SUBSOIL: 8,0 m
Espesor terraplén
16 m
7,5%
Capa inferior
4,1 %
Capa superior
01/2002
03/2002
10/2005
2002
2003
2004
2005
10,0
7,5
5,0
2,5
0
18,0
13,5
9,0
4,5
0
STRAIN (%)
SAND MASS THICKNESS (m)

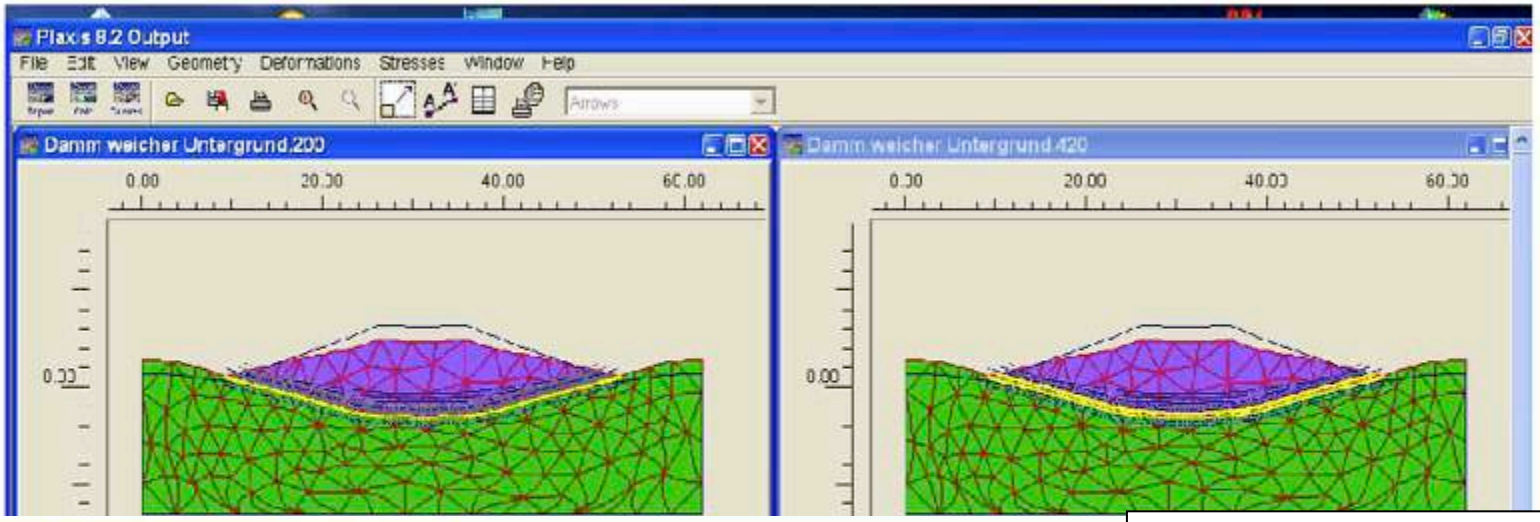

J = 1x6000 kN/m

J = 2x3000 kN/m 0.5 m distancia

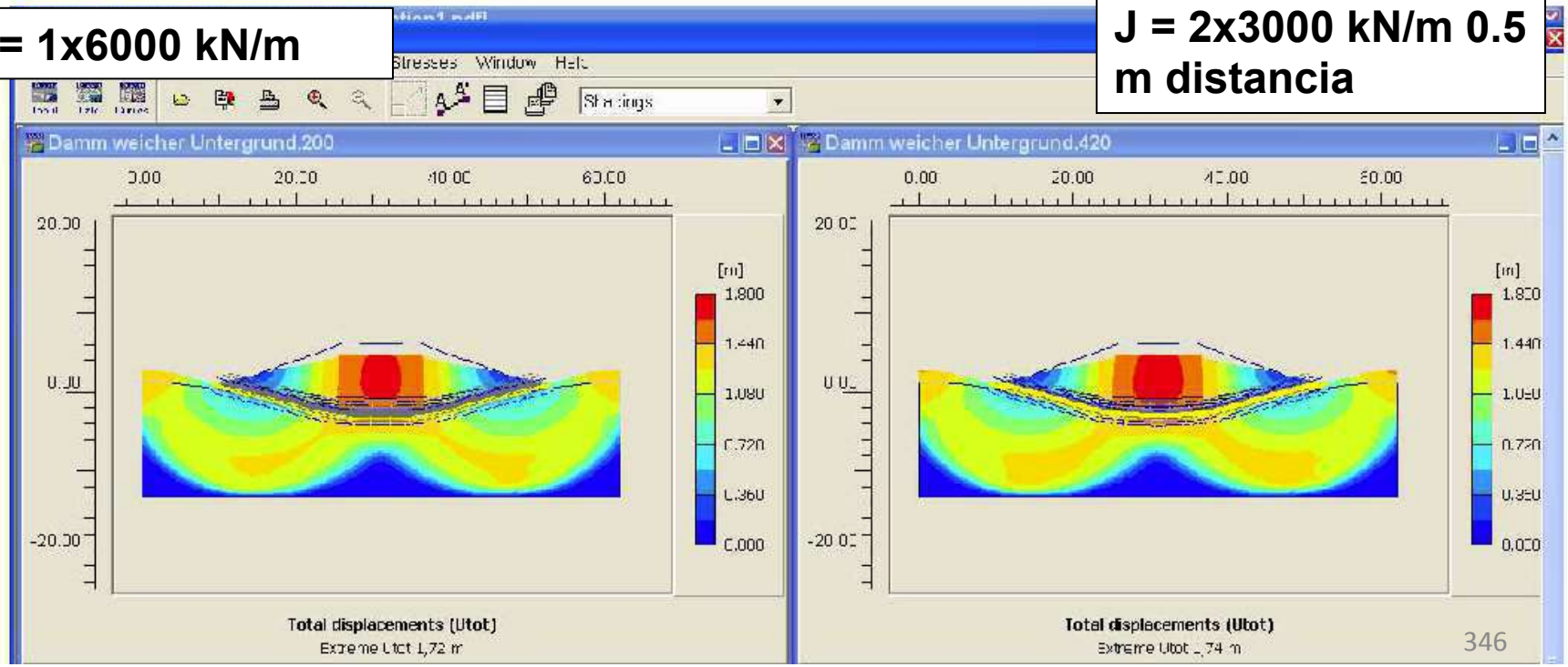

La diferencia medida In Situ entre la capa de geosintético inferior y superior del doble, no es detectada ni por los análisis numéricos, que dejan esa diferencia entre el 10-30 %. Mejor fiarnos en las medidas realizadas y sobre todo disponer una sola capa de refuerzo bajo el terraplén

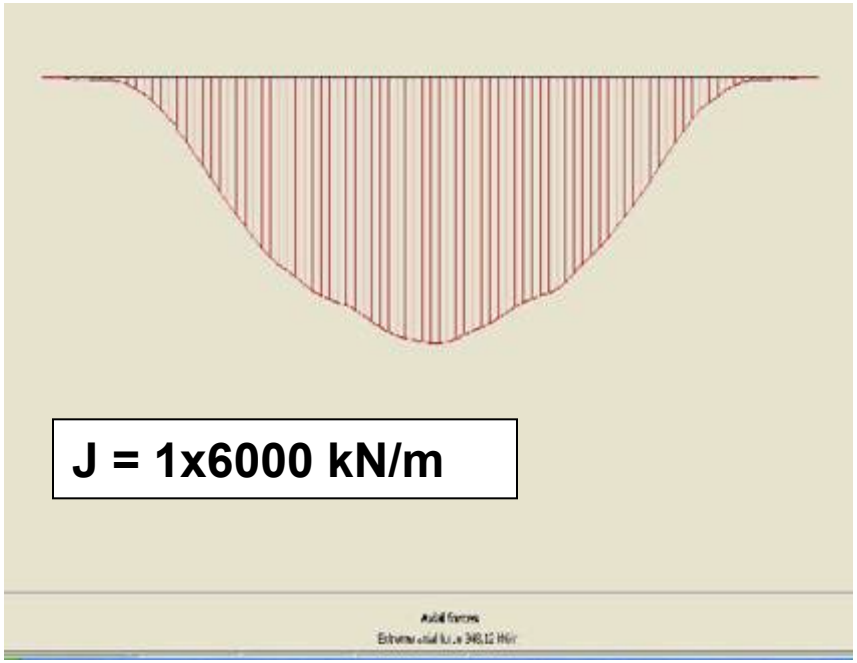

J = 1x6000 kN/m

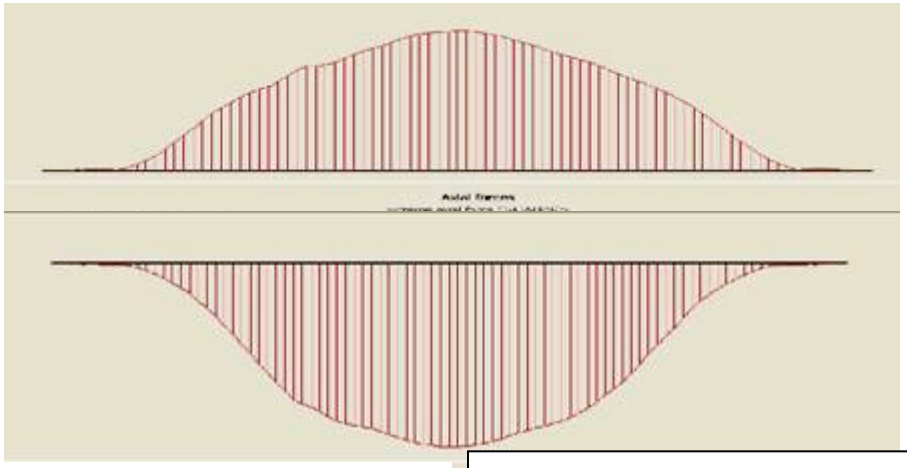

J = 2x3000 kN/m
0.5 m distancia

10- 30%… de diferencia, pero no x2

Muito Obrigado